Application of Cardiac Imaging in Hypertensive Patients

by

Ha Quang Vo

MSc

Submitted in fulfilment of the requirements for the Degree of Doctor of Philosophy (Medical Research)

Menzies Institute for Medical Research Tasmania

University of Tasmania

March 2019

Supervisors

Professor Kazuaki Negishi

Professor Thomas H. Marwick

Professor James E. Sharman

Declaration of originality

This thesis contains no material which has been accepted for a degree or diploma by the University or any other institution, except by way of background information and duly acknowledged in the thesis, and to the best of my knowledge and belief no material previously published or written by another person except where due acknowledgement is made in the text of the thesis, nor does the thesis contain any material that infringes copyright. The thesis was only proofread by http://experteditor.com.au/. The proofreading service did not contribute to the content of this thesis.

Name: Ha Quang Vo (Alex Vo)

Signed: Date: 18/08/2019

Statement of authority of access

The publishers of the papers comprising Chapters 2 and 3 hold the copyright for that content, and access to the material should be sought from the respective journals. The remaining unpublished content of this thesis may be made available for loan and limited copying in accordance with the *Copyright Act 1968 Australia*.

Name: Ha Quang Vo (Alex Vo)

Signed: Date: 18/08/2019

Statement of ethical conduct

The research related to this thesis complied with Australian codes for the Responsible Conduct of Research, National Statement of Ethical Conduct in Human Research, and the rulings of the Safety, Ethics and Institutional Biosafety Committees of the University

The Tasmania Human Research Ethics Committee (HREC) approved this project (Approval number H0012445, Targeted LOWering of Central Blood Pressure - LOWCBP). We obtained written participant informed consent from all participants

Name: Ha Quang Vo

Signed: Date: 18/08/2019

Statement of Co-Authorship

The following people and institutions contributed to the publication of work undertaken as part of this thesis:

Candidate -- Quang Ha Vo - Menzies Institute for Medical Research

Author 1 -- Thomas H. Marwick - Baker Heart and Diabetes Institute

Author 2 -- Kazuaki Negishi - Menzies Institute for Medical Research

Contribution of work by co-authors for each paper:

PAPER 1: Located in Chapter 2

Vo, H. Q., Marwick, T. H., & Negishi, K. (2019). Pooled summary of native T1 value and extracellular volume with MOLLI variant sequences in normal subjects and patients with cardiovascular disease. The international journal of cardiovascular imaging, 1-12.

Author contributions: Performed the experiments: Candidate and Author 2; Analysed the data: Candidate; Wrote the manuscript: Candidate, Author 1 and Author 2

PAPER 2: Located in Chapter 3

Vo, H. Q., Marwick, T. H., & Negishi, K. (2018). MRI-derived myocardial strain measures in normal subjects. JACC: Cardiovascular Imaging, 11(2 Part 1), 196-205.

Author contributions: Performed the experiments: Candidate and Author 2; Analysed the data: Candidate; Wrote the manuscript: Candidate, Author 1 and Author 2

Statement of Co-Authorship

We, the undersigned, endorse the above stated contribution of work undertaken for each of the published (or submitted) peer-reviewed manuscripts contributing to this thesis:

Signed:

	Quang Ha Vo Candidate Menzies Institute for medical research University of Tasmania	Adjunct Prof. Kazuaki Negishi Primary Supervisor Menzies Institute for medical research University of Tasmania	Prof. Alison Venn Head of School Menzies Institute for medical research University of Tasmania
Date:	01/07/2020	04/07/2020	08/07/2020

ABSTRACT

Introduction

Hypertension (HTN) is the most common modifiable cause of death from cardiovascular disease (CVD), afflicting an estimated 30% of the world's population, half of whom are unaware they have the disease. In the USA, the overall cost for HTN was $90.5 million in 2010. In Australia in 2011–13 one-third of adults had HTN, two-thirds of whom had uncontrolled high blood pressure.

HTN may lead to structural changes in the heart, which is called hypertensive heart disease (HHD). According to the American College of Cardiology (ACC) guideline for the management of chronic heart failure, HHD is classified into stage B heart failure. HTN causes left ventricular hypertrophy (LVH), a decrease of cardiac function, and may lead to fibrosis. However, the main focus of current cardiac clinical imaging is on left ventricular (LV) mass and left atrial (LA) dilatation, which reflect only macro changes of cardiac muscle. Functional diagnosis and tissue characteristics have not been mentioned in the latest guidelines for HTN diagnosis and there is still a gap in the literature that requires filling with high-quality studies. There are at least three reasons for this gap: (1) the sensitivity of conventional techniques is low and cannot follow the microscopic progression of the disease (sensibility); (2) conventional techniques may be affected by a number of factors and artefacts (reduced reliability); and (3) some advanced techniques require extra technical tasks (applicability).

Abstract

In this thesis, I am going to introduce several recent advanced validated imaging techniques which have high sensitivity and reliability but are still promisingly applicable to routine diagnosis of HHD. This thesis will combine three main focuses: (1) reviewing current states of the techniques; (2) evaluating the reproducibility of new techniques; and (3) applying these techniques to HHD.

Aims

This thesis aims to: (1) review and assess the usage of T1 mapping in HHD; (2) review and define normal ranges of feature tracking; (3) compare reproducibility of strain by tissue motion tracking in MRI (magnetic resonance imaging) and echocardiography; (4) assess the accuracy of volumes by strain analyses; (5) assess if LA function is independent of LV function in HHD; and finally, (6) identify which afterload is more strongly associated with LV anatomy and function.

Methods

Two systematic reviews and meta-analyses were performed to identify normal ranges in the literature and assess the applicability of the two techniques, T1 mapping and tissue motion tracking, in HHD. An important study platform for this research was LOWCBP. This is a multi-centre, randomised, open-label, blinded endpoint trial involving 308 patients being treated for uncomplicated HTN with controlled office blood pressure (OBP) (< 140/90 mmHg) but elevated central BP (≥ 0.5SD above age- and sex-specific normal values). Participants were randomised for intervention with spironolactone (25 mg/d) or usual care and are being followed over 24 months, with the primary outcome being LV mass index (using cardiac magnetic resonance

imaging). Office and central BP is measured in the clinic and at home over seven days and by 24-hour ambulatory monitoring. Firstly, 54 patients were selected to assess the reproducibility of novel techniques. Secondly, 100 patients were selected to evaluate a new method for volume measurement. Thirdly, 72 appropriate patients were included in a study that used advanced methods to assess the association between LA and LV function in HHD. Finally, 108 patients were eligible for a study on the association of afterload with cardiac activities.

Results

The first meta-analysis showed that T1 mapping can categorise cardiac diseases into three groups: those readily identified (i.e. amyloidosis and hypertrophic cardiomyopathy); those difficult to distinguish from normal (i.e. HTN); and remaining disease entities that can be separated from the normal, but with significant overlap with other cardiac diseases. In addition, abnormal native T1 values can be shorter time (e.g. Fabry, Iron overload) or pronounced prolongation (e.g. amyloid), while extra-cellular volume was only increased irrespective of the underlying pathophysiology.

In the second meta-analysis on normal ranges of strains by tissue motion tracking, 659 healthy subjects were included from 18 papers for MRI feature tracking. Pooled means of LV global longitudinal strain (LVGLS), LV global radial strain (LVGRS), and right ventricular global longitudinal strain (RVGLS) were determined. Meta-regression showed that variation of LVGCS was associated with field strength. Variations of LVGLS, LVGRS, and RVGLS were not associated with any of age, sex, software, field strength, sequence, LV ejection fraction, or LV size. LVGCS appeared

as the most robust in MRI feature tracking (FT). Among the MRI-derived strain techniques, the normal ranges were mostly concordant in LVGLS and LVGCS but varied substantially in LVGRS and RVGLS.

In the third study, the results have shown that LVGLS and RVGLS in echocardiography were more reproducible than those in MRI. This would be because echocardiographic images have higher temporal resolution, and software can follow minor motion of cardiac tissues.

In the fourth study, the volumes by strain analyses showed a great agreement with gold standard MRI volumes. In addition, the volumes by speckle tracking and FT showed a closer agreement with the gold standard compared to the conventional Simpson's biplane method. This method may also provide an opportunity to reduce the time taken for image analysis.

In the fifth study, strain analyses proved that LA function is not simply another side of the same coin with LV function. In fact, LA contractile strain is independent of LVGLS in both MRI and echocardiography. Therefore, LA function assessment should be required in further studies about HHD.

Finally, in the last study, I have pointed out the stronger association between 24-hour BP and LV mass, compared to OBP. OBP was associated with instantaneous parameters such as LV function.

Conclusion

This thesis has introduced novel advanced cardiac imaging techniques that may apply to HTN. Although T1 mapping was not applicable to HTN, tissue motion tracking appeared to be beneficial for high accurate cardiac diagnosis in hypertensive end-organ damage. In addition, volumes derived by the technique deviated less from the gold standard and the technique was less time-consuming, compared to the biplane method of disks on echocardiography; however, it requires further improvement. From the results of this study, this technique was reproducible and ready for clinical application. Thanks to the technique, additional independent variables were identified and allowed to assess cardiac function during hypertensive progression. Finally, combined with current imaging methods, the association between different components of BP and cardiac anatomy and function were represented. Unlike several assumptions about BP, each BP was found to have its own merits and was associated with different parameters of cardiac activity.

Accordingly, advanced cardiac imaging gives us more profound insights into cardiac activities with more sensitive, qualitative, reproducible parameters and fewer assumptions. These parameters have made clear the association between different components of BP and different aspects of cardiac activity. The 24-hour BP measure would be preferable because it reflects the accumulated effects of HTN.

Acknowledgements

It has been a privilege and a great honour to work under supervision of Professor Kazuaki Negishi for their guidance, encouragement and patience. He has been tirelessly working with me over 4 years. He is not only a supervisor, but also a mentor who has shaped my research pathway.

Kaz, although you are very busy, your door has not been closed whenever I am in trouble throughout my PhD. I appreciate your patience enthusiastic instruction on medical knowledge although many times I make you disappointed and get angry because of my careless. Your altitude has inspired me and helps me to know where I am, as well as to define my goal on a long run of my career. I always remember valuable lessons: 1) be careful in every single step 2) All formatting must be made on a purpose 3) Meet you weekly even twice a week in your busy timetable 4) Logically structure a manuscript with a balance between result and discussion 5) efficient methods to persuade reviewers in a rebuttal and 6) valuable statistics lessons over years of my PhD. They would be priceless knowledge for my research road ahead. I am very honoured to work under you, a world class cardiology. Without you, this thesis would only have the first page completed.

I also highly appreciate Professor Thomas E. Marwick, who were also my second mentor during my PhD. I believe not many people would have the privilege to work under your supervision. Although the time I work with you was very limited, your suggestions were keys for my decision in manuscript submission. I witnessed how a strong a team was when you were here. It was tremendously regretful when you moved to Melbourne, weekly seminar of our team was always in my mind.

My deep appreciation also goes to Professor James E. Sharman. Jim, thank you for your permission to allow me to be a part of the LOWCBP project. Despite many misunderstandings between us, you always welcome me to work with you. There were many challenges in collecting and analysing data in LOWCBP study. However, the way you deal with them was valuable experience for my career. It was a great honour to work and to be supervised by you.

I would like to say thank to Eswararaj Sivaraj. Eswar, apart from supervisors, I believed you have a great contribution to my PhD. You are not only my friend, but also my teacher. You are the one who laid the foundation for my skills in analysing echocardiographic images. Your contributions are uncountable. Chat and discussion with you were not only a kind of fun but also a way to enrich my knowledge. In addition, your story and advice also inspired me, motivated me during my PhD whenever I am in trouble. I hope you are always well-being and best luck for your coming PhD. I am always ready if you need any assistance.

I believe it would be a big mistake if I do not acknowledge Dr Hong Yang (Hilda). Hilda, thanks for being my friend, my advisor, and my accompany along my PhD. You are among the first persons I think of when I need an advice. Your helps were countlessly and cannot be described in few words. Although you are always busy, I have never seen you missing in any farewell. That is the reason why you are loved by everybody.

I also would like to spend one of my last paragraphs to my closest and beloved Chinese friend – Dr Bing Zhao. Bing, you are my friend, but not only this, but rather

than my soulmate who I can share everything with without hesitate. Apart from academic discussion, chats on movies music, food, and history with you comfort me and make me feel relax. I wish I would attend your graduation ceremony. Not sure if it is true or not, you were my best friend during my PhD, and will be in coming years. Please keep in touch, very sad to say goodbye to you.

Scientific presentations

Presentations at international conferences

- American College of Cardiology 2016 (Poster Presentation)
- Cardiac Society of Australia and New Zealand Conference 2016 (Poster Presentation)
- European Society of Cardiology 2016 (2 poster presentation)
- American Heart Association 2017 (Poster presentation)
- American Heart Association 2018 (Poster presentation)

Presentations at domestic conferences

• Menzies Student Showcase, Research week, 2017, UTAS (Poster presentation)

List of Abbreviation

2D 2-Dimension

3D 3-Dimension

ABP Ambulatory blood pressure

ALMS: Alström Syndrom

AS Aortic stenosis

BP Blood Pressure

CAD Coronary artery disease

CI: Confidence interval

CV Coefficient of varriation

CMR: Cardiac magnetic resonance

CTO: Chronic Total Occlusion

DB: Diabetes

DBP Diastolic Blood Pressure

DCM: Dilated cardiomyopathy

DENSE Displacement Encoding with Stimulated Echoes

DMD: Duchenne muscular dystrophy

ECV extracellular volume fraction

List of Abbreviation

EDV End diastolic volume

EF Ejection fraction

ESV End systolic volume

FT Feature Tracking

HCM: Hypertrophy cardiomyopathy

HLP: Hyperlipidaemia

HTN: Hypertension

LVEDVi: Left ventricular end-diastolic ejection fraction indexed

LVEF: Left ventricular ejection fraction

GLS Global Longitudinal Strain

HFpEF Heart Failure Preserved Ejection Fraction

ICC Intra-class correlation

ICM: ischemic cardiomyopathy

IHD: Ischemic heart disease

LA Left Atrium/ Atrial

LOWCBP LOwering Central Blood Pressure

LV Left Ventricle/ Ventricular

LVGCS left ventricular global circumferential strain

List of Abbreviation

LVGLS left ventricular global longitudinal strain

LVGRS left ventricular global radial strain

MAP: Mean arterial pressure

MI: Myocardial Infarction

MRI Magnetic Resonance Imaging

MT Myocardial Tagging

MOLLI Modified look-locker imaging

OBP Office blood pressure

PRISMA Systematic reviews and Meta-Analysisv

PP: Pulse pressure

RA: Rheumatoid Arthritis

RVGLS right ventricular global longitudinal strain

SBP Systolic Blood Pressure

SCLS: systemic capillary leak syndrome

SD Standard Deviation

SENC Strain-encoding

SLE: Systemic sclerosis

ShMOLLI Shortened modified look-locker imaging

List of Abbreviation

SSFP steady-state free precession

STE Speckle Tracking Echocardiography

List of Tables

List of Tables

List of Tables

List of Figures

List of Figures

Funnel plot of native T1 using MOLLI 3, 3, 5 with flip angle 35^{o} at 3T, Egger's test: p=0.04

Supplementary figure 2.8: Funnel plot of MOLLI T1 3 3 5 FA=50^{o} at 3T.

Funnel plot of native T1 using MOLLI 3, 3, 5 with flip angle 50^{o} at 3T, Egger's test: p=0.4

Supplementary figure 2.9: Funnel plot of MOLLI ECV 3 3 5 FA=35^{o} at 1.5T.

Funnel plot of ECV using MOLLI 3, 3, 5 with flip angle 35^{o} at 1.5T, Egger's test: p=0.36

Supplementary figure 2.10: Funnel plot of MOLLI ECV 3 3 5 FA=50^{o} at 3T.

Funnel plot of ECV using MOLLI 3, 3, 5 with flip angle 50^{o} at 3T, Egger's test: p=0.02

Supplementary figure 3.1: Funnel plots with Trim and Fill plots for meta-analysis of strains by MRI-FT

For assessment of publication bias, funnel plots of each FT strain parameter is shown with their trim and fill plots.

Supplementary figure 3.2: Cumulative plot of GCS by sample size

The papers, which reported LV GCS are aligned, based on their sample size from the smallest (n=10) to the largest (n=150). Each of articles has been added to previous one in a cumulative manner.

Supplementary figure 3.3: Global strains in Normal Subjects by different sample sizes.

List of Figures

List of Figures

Table of Contents

Table of Contents

Table of Contents

Chapter 1

Introduction

I. Background:

1. Definition and burden of hypertensive heart disease (HHD):

High blood pressure (BP) is the most common modifiable cause of death from cardiovascular disease (CVD), despite the availability of several effective pharmacological therapies. Hypertension (HTN) is currently defined as a resting systolic BP (SBP) >140 mmHg or diastolic BP (DBP) >90 or receiving therapy for the indication of lowering BP. HTN afflicts an estimated 30% of the world's population, half of whom are unaware they have the disease [1]. The World Health Organization reported 9.4 million deaths (40%) worldwide that involved HTN [2]. In the United States, the overall cost of HTN in 2010 was $90.5 million, reflecting the combined cost of healthcare services, medications, and missed days at work [3].

HHD is one of the target organ responses to arterial HTN. In addition, there is a link between HHD and atrial/ventricular arrhythmias, such as atrial fibrillation, which likely increases by 40–50% in the presence of HTN [4]. Ventricular arrhythmias occurs more frequently in HHD [5]. Myocardial infarction is another common end point of HTN. Increased susceptibility to ischemic heart disease rounds out the cardiovascular sequelae of HHD: compared to normotensive patients, hypertensive patients have six times higher risk of infarction [6].

Left ventricle hypertrophy (LVH) is the most common phenotype of cardiovascular target organ damage in patients with HHD. LVH has been demonstrated to negatively impact on left ventricle (LV) function and may lead to congestive heart failure [7]. High BP in vessels forces the heart to work harder, causing cardiomyocytes hypertrophy and an increase in wall thickness. The mechanism is not only a

compensatory mechanism to minimise wall stress but also the impacts of neurohormones, growth factors, and cytokines [8]. Pathological alterations in HHD patients are (1) cardiomyocytes hypertrophy leading to changes in microcirculation, causing myocardial ischemia; (2) stimulation of fibroblasts and collagen formation, which causes an accumulation of fibrosis and alterations in extra-cellular matrix; and (3) abnormalities of the intramyocardial coronary vasculature, including medial hypertrophy and perivascular fibrosis. Progressive LV systolic and diastolic dysfunction can be seen along with the progression of HHD because contractility and filling function are impaired due to cardiomyocytes hypertrophy. At the end stage of HHD, there are increases in volume and sphericity, and decreases in stroke volume and ejection fraction.

This end-organ damage would have been avoided by using an appropriate method for controlling BP. The literature gives many methods to estimate afterload BP. The invasive BP method has been accepted as the gold standard and is highly correlated to cardiac function in animal models. However, due to its nature, its use is limited in both research and clinical practice. Office blood pressure (OBP) is the most widely used method, which is assumed to be the 'standard' for high BP diagnosis in many institutions [9]. The majority of studies in epidemiology [10, 11] use BP measured by OBP in their studies as a risk factor. However, recently, 24-hour ambulatory BP (ABP) has been reported to be a better predictor for prognosis of hypertensive organ damage [12, 13], cardiovascular events [14-16], and all-cause mortality [17].

The benefits of OBP are that it is quick and easy to use. However, it has drawbacks. The main drawbacks are the influence of measurement error and inappropriate

measurement methods [18, 19]. These factors would, in turn, impact on decision-making about medication and therapy. Nevertheless, whether ABP should replace OBP in clinical settings, and the association of each BP index to cardiac anatomy and function, are still contentious issues. This thesis is going to answer the question by comparing the associations between different BPs with cardiac indexes.

Imaging is the most popular method for cardiac assessment. Several technical limitations require the measurements to go along with a number of assumptions. Novel techniques enable us to have an entire picture of cardiac activity including systolic function and cardiac characterisation. The next section outlines available indexes, including novel techniques, that can be utilised for cardiac assessment in HHD

2. Imaging in HHD

2.1 Imaging in Cardiac anatomy and function:

2.1.1 Left ventricular mass (LVM)

In clinical settings, LVH is defined as an increase in LVM, which is theoretically qualified by the weight of the heart. However, it is not feasible to weigh the heart in living patients. Therefore, LVM is usually estimated noninvasively, by echocardiography or cardiac magnetic resonance (CMR).

2.1.1.1 2D echocardiography for LVH assessment

Early echocardiographic studies set the cut off value of LVM to define LVH at 250g [20]. EACVI and ASE [21] recommends a formula to estimate LVM from linear

dimensions based on the assumption of the LV as a prolate ellipsoid with a 2:1 long/short axis ratio and symmetric distribution of hypertrophy:

$$LVM = 0.8(1.04[(LVIDD + PWTD + IVSD)^3 - (LVIDD)^3]) + 0.6g$$

Linear measurements of inter-ventricular septal wall thickness (IVST), as well as LV internal diameter (LVID) and posterior wall thickness (PWT), should be done from the parasternal acoustic window at end-diastole at the level of the LV minor axis (mitral valve leaflet tips) using 2D- targeted M-mode or directly from 2D images[22]. Although M-mode is the first method to be validated for LVM assessment [23], 2D echo derived measures were proven to be more accurate [24, 25]. Note that this formula is not applicable for patients with major cardiac geometry distortions such as LV aneurysm. LVM is usually indexed to body surface area (BSA) as a correction of obesity-related LVM or height. Indexing is also important because it influences the classification of LVH [25-30]. The normal range of LVM is also stratified by age and gender, and the LVM is affected by obesity, diabetes, and ethnicity [30-32]. The major problem in the 2D echocardiographic assessment of LVM is accurate identification of the endocardial border as well as the interface between the epicardium and pericardium. In obese patients, the image quality of a 2D echo is usually poor, which limits the accuracy of the LVM assessment.

2.1.1.2 3D echocardiography for LVH assessment

The main limitation of 2D echocardiography for LVH assessment is the dependence on geometric assumptions and imaging plane positioning [33]. In fact, 3D echocardiography has been proven to have a better intra- and inter-observer

reproducibility than 2D echo and a higher correlation with CMR, which is considered the clinical gold standard for LVH assessment [34]. However, the accuracy of 3D echocardiography is still uncertain. A meta-analysis has shown that the accuracy of this technique has been improving over time [35]. However, analogous to any ultrasound techniques, 3D echocardiography depends on adequate acoustic windows and the skill of practitioners. In addition, difficulties in tracing the epicardial border of patients with cardiac disease, particularly a dilated ventricle, were reported. There is still a tendency to underestimate LVM in 3D echocardiography, compared to CMR [36, 37].

2.1.1.3 CMR for LVH assessment

CMR is the gold standard for LVM quantification, allowing 3D modelling of LV free from geometric assumptions and acoustic window. Although black blood techniques were first used to estimate LVM, bright blood using steady-state free precession (SSFP) sequence is superior to the black blood technique due to high signal-to-noise ratio, contrast-to-noise, and shorter acquisition time. Both of these techniques have demonstrated high reproducibility [38]. There has been disagreement about whether papillary muscle should be included in LVM quantification by CMR [39, 40]. Recently, a study with a large sample size suggested that excluding papillary muscle showed better reproducibility [41]. However, among different functional measures by CMR, LVM appears to be the least reproducible and most variable parameter [42].

In general, LVM can be obtained in MRI by manually tracing the endocardial and epicardial borders of the heart on a stack of short axis slices. It does not require many assumptions but is a time-consuming task. Nevertheless, quantifying the mass by MRI

is much more reliable than by echocardiography.

2.1.2 Diastolic function in HHD

Diastolic function is one of the earliest markers of HHD. Normal diastolic function allows an adequate filling of LV at rest or during exercise without an increase in pressure. Abnormalities in pressure gradient can be a marker for diastolic dysfunction. In echocardiography, a combination of mitral valve inflow velocities and mitral annular velocities is used for diastolic function assessment. Mitral inflow velocity reflects changes in the transmitral pressure gradient during the diastolic phase. At the moment the mitral valve is opened, the mitral inflow velocity starts increasing and reaches its peak (E) in the early rapid-filling phase. Atrial contraction will cause a second peak in the late filling phase (A). How rapidly the flow velocities fall from the peak E to its baseline in early filling of LV is characterised by deceleration time (Dt). In addition to mitral valve inflow velocities, the early diastolic velocities of mitral anulus (E') is assessed by tissue doppler imaging (TDI). E/E' has shown to vary with LV filling pressure and would be a prognostic indicator for HHD. Although an alteration in E wave by changes in preload or left atrial (LA) pressure was found [43], E' at the lateral LV base does not change significantly, and effects of preload can be corrected by a ratio of E/E' [44]. These echographic parameters provide a pictorial information of diastolic function. Based on information obtained from echocardiographic examinations, a grading system similar to that of the New York Heart Association Functional Classification can be established.

2.1.2.1 Grading diastolic dysfunction [45]

Below is a common grading of diastolic dysfunction:

- Grade 0 = normal diastolic function
- Grade 1= impaired relaxation pattern with normal filling pressure
- Grade 1a= impaired relaxation pattern with increased filling pressure
- Grade 2= pseudo-normallised pattern
- Grade 3= reversible restrictive pattern
- Grade 4= irreversible restrictive pattern

2.1.2.1.1 Normal diastolic function

Filling patterns slightly vary in different age groups. In young healthy subjects, the filling process lasts within early diastole and requires less atrial contribution. Therefore, E/A >1.5, 160 msec < Dt < 230 msec, E'>10 cm/s, E/E' < 8 and Vp>50 cm/s.

2.1.2.1.2 Impaired myocardial relaxation (Grade 1-1a diastolic dysfunction):

In the majority of diseases, diastolic dysfunction begins with a reduction of E value. As an acute response, velocity in active mitral inflow (A) is increased, generating E/A less than 1 with prolonged Dt. E' is usually reduced below 7 cm/s and Vp also falls below 50 cm/s.

2.1.2.1.3 Pseudonormalized pattern (Grade 2 diastolic dysfunction) :

Due to the deterioration of diastolic function, LA pressure is increased to superimpose on relaxation abnormality. As a result, the E/A ratio lies in the range 1 to 1.5 and 160

msec < Dt < 220 msec. These parameters are quite similar to normal range (therefore this condition is referred to as pseudo-normal). There are several strategies to distinguish this condition from normal:

1. Demonstrate an impaired mycardial relaxation by E' < 7cm/s and E/E'>15.
2. In case of patients with an abnormal size of LV, or systolic dysfunction, or an increase in wall thickness, a normal E/A ratio suggests this condition.
3. Perform a Valsalva manoeuvre leading to a reduction in the E/A ratio by 0.5 or more and reversal of E/A ratio.

2.1.2.1.4 Restricted filling (Grade 3-4 diastolic dysfunction):

In this condition, the LA pressure is increased, leading to an early opening of the mitral valve, shortened iso-volumetric relaxation time (IVRT) and Dt, and an increase in E value. Therefore, E/A >2, Dt <160 msec, IVRT <70msec. The myocardial relaxation is also impaired in this condition, which means E<7cm/s, E/E' >15.

2.1.2.2 Echocardiographic LA size for HHD:

Filling LV includes two subsequent phases: early rapid filling (passive filling) and atrial contraction (active filling). In the first phase, the predominant driving force is the elastic recoil and normal relaxation. The role of LA pressure in this phase is likely to be less important. However, in the active filling phase, atrial contraction is the main factor creating a positive driving force from the LA to the LV. Any abnormality in the passive filling phase demands the LA works harder, which may lead to alterations in LA size as a response mechanism. Therefore, changes in LA size may be an independent prognosis factor for structural or functional changes

in HHD patients. In fact, enlargement of LA volumes has been demonstrated to be associated with patients with HHD [46]. Hypertensive patients with larger LA diameter are at a higher risk of ischemic stroke [47, 48] and have increased morbidity and mortality [49, 50]. However, the relation between LA and LV functions are not yet fully understood. Further studies are required to decide whether changes in LA sizes are a marker of chronic status of diastolic function.

2.1.3 Systolic function in HHD:

Systolic function is characterised by the extent of LV contractility and is associated with LV stiffness. Quantification of systolic function is one of the essential parts of cardiac imaging examinations. Traditional qualitative assessment of systolic function in clinical practice is primarily based on the changes in volume of the LV.

2.1.3.1 LV ejection fraction (LVEF):

LVEF is the most common expression of global systolic function in clinical settings. The LVEF is calculated as the alteration in volume between diastolic and systolic phases, which reflects how much of LV end diastolic volume (LVEDV) is pumped out of the LV after each contraction. However, the LVEF is only useful in a relatively advanced state [51]. Craig et al. demonstrated hypertensive patients who had abnormal systolic function but normal LVEF [52]. In general, subtle changes in systolic function cannot be detected by the LVEF. Other techniques are required to detect systolic dysfunction early. The development of technology allows quantitative assessment of myocardial deformation, which could be superior to the LVEF in early detection of abnormalities of systolic function in HHD.

2.1.3.2 Myocardial strain & strain rate:

Myocardial strain is an important measure, usually expressed in percentage of change, compared with original myocardial fibre length, so-called Lagrangian strain. The change of strain per unit of time is referred to as the strain rate. Strain provides information about the ventricular contractile function. Strain abnormality could be an accurate predictor in clinical practice of a variety of cardiac diseases. Strain is proven to be superior to LVEF in distinguishing between HHD, HCM, and athlete's heart [53]. Therefore, strain encapsulates the basic mechanical function of the myocardium and has the potential to become an important clinical index of regional ventricular function. There are several methods to estimate strain invasively and non-invasively. Among them, echocardiography is the most commonly used modality in clinical settings due to its acceptable accuracy, as well its convenience. In general, there are two methods for strain measurement in echocardiography: tissue Doppler imaging and 2D speckle-tracking.

2.1.3.2.1 Tissue Doppler imaging (TDI)

Historically, TDI was the first method for echo-derived myocardial strain. Strain values in TDI are derived from instantaneous velocity of tissue. However, velocity in TDI is angle dependent, so is strain. In other words, only if the movement of cardiac tissue is in the direction of the incoming ultrasound beam can strain be measured accurately. TDI underestimates strain values of cardiac tissue moving in the other direction. Recently, speckle-tracking echography (STE) has replaced TDI in strain measurement due to being easier to use and having minimum angle dependency, and therefore high

accuracy and robustness.

2.1.3.2.2 2D-speckle tracking (STE)

STE was first introduced by Reisner, Leitman, Friedman, and Lysyansky in 2004 [54-56]. The algorithm tracks speckle patterns which are generated from random reflection, refraction, and scattering of ultrasound beams. Because these speckles patterns move together with tissue, the software follows these speckles from frame to frame, which allows direct calculation of the Langrangian strain. In HHD patients, STE is shown to be more sensitive than LVEF to subtle changes in LV function, particularly during physical stress echocardiography. However, there is still disagreement over its ability to differentiate between a hypertensive patient and a normal healthy subject. Several studies have revealed that LVH predominantly impacts on longitudinal strain while LVEF is unchanged [57]. Galderisi suggested GLS is an independent parameter to differentiate hypertensive patients from athletes or normal subjects [53]. However, Narayanan found that the strain of hypertensive patients with normal LVEF was similar to healthy groups while E', E and peak myocardial systolic velocity were reduced [58].

2.1.3.2.3 CMR feature tracking

Although STE overcomes some of the drawbacks of TDI, limited acoustic window and poor image quality are still concerns in echocardiographic strain measurement. MRI could be a good option to overcome these concerns. In MRI, strains could be derived by using typical sequences such as myocardial tagging (MT), phase contrast velocity imaging, displacement encoding (DENSE), and strain encoding (SENC) [59, 60]. However, these methods require additional sequences, which extends the time of

acquisition. Recently, a number of authors have attempted to apply speckle-tracking algorithm to MRI cine images, which allows retrospective analyses and widely applies in routine diagnosis. Moreover, MRI-based feature tracking (FT) also allows assessing right ventricle (RV) [61, 62] and LA strains [63-78] and would be a promising technique in HHD assessment.

2.2 Tissue characterisation by T1 mapping

The fundamental principle of routine MRI is that the signal intensity of every pixel is based on the relaxation of hydrogen nuclei protons in a static field. Depending on the environment where the hydrogen nuclei protons are placed, the magnetic characteristics are different. T1 relaxation is one of the parameters that expresses magnetic features of the environment. T1 relaxation times between different types of tissues vary considerably, which means they allow tissue characterisation. A parametric image in which each pixel reflects the T1 relaxation of tissues at that position is referred to T1 mapping. T1 mapping plays an increasingly important role in research and clinical settings due to its ability to detect both focal[79] and diffuse [80] fibrosis non-invasively which was not detectable by conventional LGE images. Of note, T1 mapping might be better for diffuse than focal fibrosis quantification[79]. However, ability to detect focal fibrosis of T1 mapping was still limited, compared to conventional LGE [79]. Meanwhile, the detection of diffuse fibrosis, which is beyond the capabilities of LGE, is the primary strength of T1 mapping. This technique highlights vascular abnormalities which not only causes vasodilation and micro circulation but also contribute to the accumulation of extracellular collagen[81].

Native T1 images had a higher sensitivity than the late gadolinium enhancement (LGE) technique and T2 mappings in differentiating normal healthy subjects from myocarditis and dilated cardiomyopathy [82]. Sources of variation of native T1 are still controversial [83-85]. T1 was insensible to age and gender [83, 84] but varied with wall thickness [86], LV mass/ LV mass index, and severity of disease[87, 88]. An intermediate to good correlation between T1 values and strains [89-91] indicates the relation between tissue characteristics and cardiac functions. In addition, recent progress in CMR permits non-invasive quantification of myocardial extracellular volume (ECV) by using pre and post contrast T1 mappings and then adjusting for haematocrit. ECV by CMR has been validated against histopathology. However, ECV seemed to be altered with dose of contrast and well correlated with gender and LVEF [88, 92-94].

II. Potential novel techniques in HHD

The novel imaging technique enables us to non-invasively understand cardiac function and better describes the association between BP and cardiac functions. For example, T1 mapping may provide microscopic changes in myocardium during hypertensive progression or, compared to conventional LVEF, strain by tissue tracking can provide more information on the systolic function of the heart. This thesis will define several potential techniques that may be used in hypertensive diagnoses. Two systematic review and meta analyses on strain analyses and T1 mapping were conducted to define the possibility to apply these techniques in HHD. These studies are contained in **Chapters 2 and 3**.

Despite their superiority, the use of these techniques has been very limited in HHD. One of the main reasons preventing their application in HHD is their reliability. In fact, lack of systematic and large studies on reliability of these methods causes difficulty in multi-institutional studies or in definition of normal ranges. Among strain by tissue tracking values, the reproducibility of the LV strain has been the most widely studied, followed by that of FT, but only in small-sized studies. To the best of my knowledge, reproducibility of LA strains had not been conducted at the time of starting my research. See **Chapter 5** for a systematic study of the reproducibility of LA, LV, and RV strains on multi-modality.

By obtaining the reliability of LA strains, we would be more confident in assessing LA function and LV diastolic function based on LA strain analysis.

LA function in HHD has not attracted attention from researchers because the LA wall is thin, causing difficulty in accurate assessments. So far, only LA volumes and LA diameters have mainly been used in the literature, which provides little information on LA function and LV diastolic function. LA strains would be appropriate to study the association between LV and LA phasic function. **Chapter 7** of this thesis shows which phasic strain contains addition information on LV diastolic function.

In addition to strain analyses, tissue tracking has the ability to quantify volume. The popularity of established techniques has prevented this technique from attracting the attention of current researchers. A validation of this technique in **Chapter 6** demonstrates the superiority of this method over the conventional one.

III. Gaps in the literature

Although HTN has been established as the major risk factor of cardiovascular events, the majority of epidemiological studies have focused only on OBP. There have been few studies on the association between 24-hour ABP and cardiac function and hypertensive progression. Several studies have reported closer correlations and association between ABP and LV mass index or LV function compared to OBP [95]. However, those studies had several limitations: (1) only SBP and DBP were focused on; (2) they used LV mass derived from echocardiography with many assumptions and skill dependency-errors as small as a few millimetres can result in large errors in calculated LVM by echocardiography; (3) they concentrated only on the association between different BP values and LV anatomy or LV function; and (4) they only used limited established imaging techniques to study cardiac function. These gaps will be filled in **Chapter 7**. In this chapter, all validated techniques from chapter 1 to chapter 6 were taken into account to detect the association between BP from different aspects of the heart.

IV. Aims of this thesis

The aims of this thesis are based on the following facts:

1) HTN is the major risk factor of cardio-vascular events.

2) Most of epidemiology studies used only OBP as a risk factor.

3) Several pilot studies have found the superiority of 24h ABP over normal. OBP in HTN management.

4) Most of studies on HTN included only established variables or sensitive variables with high variability and less accurate such as LV mass by echocardiography.

5) advanced imaging modalities are able to identify early damage and show excellent prognosis values in HHD.

Therefore, my aims are to 1) define potential advanced techniques in HHD 2) validate these techniques and evaluate their reliability, and 3) evaluate the associations of different BPs with advanced parameters as a suggestion for future guidelines on HTN management.

Chapter 2

Pooled Summary of Native T1 value and Extracellular Volume with MOLLI Variant Sequences in Normal Subjects and Patients with Cardiovascular Disease

Abstract

Aims: T1 mapping by cardiac magnetic resonance (CMR) allows detection of abnormal myocardium. A number of myocardial abnormalities affects the signal captured in T1 mapping. We performed a systematic review and meta-analysis of native T1 and extracellular volume (ECV) in subjects with and without cardiac disease 1) to determine the normal ranges of T1 values and ECV by sequences as well as parameters influencing them, and 2) to summarize the differences in T1 values and ECV of the diseases relative to the normal ranges.

Methods: Three databases (EMBASE, SCOPUS, and MEDLINE) were systematically searched for native T1 time and ECV. Only human studies with a sample size of $\geq$20 subjects were included. A random effect model was used to pool data.

Results: The 69 selected articles included 1954 healthy subjects and 3186 with disease. T1 of normal healthy was different among MOLLI variants: in 1.5T sequences, ShMOLLI had the shortest (944 msec [95% confidence interval 925, 963]), followed by MOLLI 3(3)3(3)5 flip-angle 50º, 967 [959, 975] and flip-angle 35º, 969 [951, 988]. 3T had longer T1 than 1.5T by approximately 100-200 msec. ECV of the normal healthy was consistent among the studies (ranging from 25% to 27%), irrespective of subjects' factors, sequences, vendors, and contrast type. Many diseases demonstrated longer native T1 than normal subjects, but T1 was shorter in Fabry disease and iron overload. In contrast, all disease states showed either normal or increased ECV. Diagnostic accuracy of native T1 time was minimally affected by the difference in the sequences.

Conclusion: ECV is less influenced by methodology than T1 time among normal subjects. Different myocardial diseases are associated with shorter or longer T1 times, whereas ECV is consistently increased independent of the underlying pathophysiology.

I. Introduction

The unmatched ability of cardiac magnetic resonance (CMR) in providing myocardial tissue characterization has been strengthened by the development of T1 mapping [96, 97]. Unlike gadolinium enhancement, which images scar by comparison with a reference segment, this technique permits non-invasive quantification of diffuse myocardial fibrosis. T1 relaxation is a parameter that expresses the behavior of hydrogen nuclei in a magnetic environment. These protons release energy as they realign after exposure to an external field, and the time taken to realign is dependent on the nature of the tissue. T1 reflects the relaxation time in each pixel measured from its intensity in sequential images, often shown in a parametric display. T1 values obtained before and after contrast, together with hematocrit can be used to estimate the extracellular volume fraction (ECV) of tissue [96, 97].

The evolution of these methods from research to clinical use has met several barriers. Most reports have derived from single centers, with a variety of normal ranges, influenced by different sequences and field strengths. The magnitude of these variations relative to the changes associated with different disease entities is important in relation to possible clinical use.

Accordingly, we conducted a systematic review and meta-analysis 1) to determine the normal ranges of T1 values and ECV by sequences as well as parameters influencing on the pooled estimate, and 2) to summarize the differences in T1 values and ECV of the diseases relative to the pooled normal ranges. As the most widely used methods have been variants of modified look-locker imaging (MOLLI) including MOLLI within

17 heartbeats [3(3)3(3)5] and MOLLI within 9 heartbeats [5(1)1(1)1] (i.e. shortened modified look-locker imaging [ShMOLLI]), we focused on these widely used sequences.

II. Methods

Search Strategy: We followed the preferred Reporting Items for Systematic reviews and Meta-Analysis (PRISMA) Guideline [98] when performing our systematic review and meta-analysis. Last search was performed on 15th September 2017. Three academic databases (EMBASE, MEDLINE, SCOPUS) were systematically searched for native T1 values and ECV in human studies by two co-authors (HV and KN) under the guidance of our university librarian trained in systematic review. The key terms were: "shortened modified look locker inversion recovery", "shortened MOLLI", "ShMOLLI", "modified look-locker inversion recovery", "MOLLI", "extra cellular matrix", "extra cellular volume", "ECV", "extra cellular fraction", "ECF", "cardiac magnetic resonance", "CMR", and "cardiac MR". The reference lists of these articles were also scrutinized to identify some additional appropriate studies. Search hedges created are listed in the online supplementary material (**Appendix 2A**). The study was prospectively registered with the PROSPERO database of systematic reviews (registration number: CRD42016035488).

Study selection: The two authors included studies according to the following criteria; 1) written in English, 2) sample size 20 or more, and 3) use MOLLI or ShMOLLI. All discrepancies were reviewed and resolved by consensus of all authors.

Study exclusion: Our exclusion criteria were as follows: 1) animal studies, 2) studies which did not use MOLLI or ShMOLLI sequences, 3) Studies without native T1 or ECV by CMR, 4) reviews, technical notes, conference presentations, and meeting posters, 5) studies reporting groups that could not be subdivided (e.g. a study of volunteers where some had HTN), or 6) studies reporting data as median only.

Data collation and extraction: Data of native T1 and ECV were collected from texts, tables, and graphs in individual studies and entered into an electronic database. In case multiple articles came from a single dataset, the largest study was selected. All demographic, clinical characteristics and technical parameters were also extracted from texts, graphs and tables.

Outcomes of interest: In this meta-analysis, our outcomes of interest were ranges of native T1 using MOLLI within 17 heartbeats and MOLLI within 9 heartbeats (i.e. ShMOLLI) in normal participants and patients with different medical conditions.

Statistical analysis: The means and 95% confidence intervals (CI) of native T1 and ECV were computed using random effect models weighted by the inverse of variance. Cohen's D was used to measure standardized differences in mean values of healthy and diseased myocardium[99]. Funnel plots were constructed, and Egger's test was used to assess potential publication bias. Heterogeneity between subgroups or between studies was assessed by Cochran Q's test and the inconsistency factor (I^2). Meta-regressions were performed for each confounder to examine possible study factors associated with heterogeneity. Beta coefficient and its CIs were derived using least-mean square fitting method. Statistical analysis was performed using R version 3.2.2 (The R Foundation for

Statistical Computing, Vienna, Austria) with the "metafor" package and Microsoft Excel for Mac 2011 version 14.5.4 (Microsoft Corporation, Washington, United States). Two-tailed p values were applied, and the threshold of statistical significance was 0.05 except for Egger's test, where 0.1 was used.

III. Results

Study selection: From the 3 databases, 562 matched titles with the key terms were found (EMBASE [217], MEDLINE [298], Scopus [47]), and 356 records were identified through other sources (**Figure 2.1**). Of the 917 titles, 69 were eligible for this meta-analysis[83, 85, 86, 88-94, 100-158]. Most of the included studies were conducted in Europe (UK, Germany, Switzerland, and Austria) using MRI machines from Philips and Siemens (only two studies utilized equipment from GE [115, 116]). A variety of software was used to analyze T1 mapping (**Appendix 2E**). Most healthy participants were in middle age and had LVEF >55%.

T1 values and ECV in normal subjects: In general, T1 among normal subjects from 1.5T scanners were shorter than that from 3T (**Table 2.1**), where heterogeneity among the sequences were observed. On contrary, ECV among the normal subjects were almost the same irrespective of sequences and magnet strengths.

Native T1 value by ShMOLLI was the shortest among MOLLI scheme, followed by MOLLI 3(3)3(3)5 with flip angle (FA) of 35^{o} and FA 50^{o} : ShMOLLI at 1.5 T, 944 msec [95%CI 925, 963] (10 articles, **Table 2.1** and **Supplementary Figure 2.1**); MOLLI 3(3)3(3)5 FA 50^{o} at 1.5T 967 [959, 975](1 article); MOLLI 3-3-5 FA 35^{o} at 1.5T 969 [951, 988] (7 articles); as well as at 3T, MOLLI 3(3)3(3)5 FA 50^{o} 1097[1016,

1177] (6 articles), and MOLLI 3(3)3(3)5 FA 35° 1214[1161 1267] (3 articles). Of note, the pooled range of native T1 by MOLLI 17 heartbeat at 1.5T (by combining FA 35 and 50) was 970 [961, 981], and at 3T was 1127 [1084, 1169].

ECV in ShMOLLI at 1.5 T, 25.9% [95%CI 24.9, 26.8] (4 articles, **Table 2.1 and Supplementary Figure 2.2**); MOLLI 3(3)3(3)5 FA 50° at 1.5T 26.7% [25.6, 27.8] (1 article); MOLLI 3(3)3(3)5 FA 35° at 1.5T 25.2% [24, 26.4] (5 articles); MOLLI 3(3)3(3)5 FA 50° at 3T 25.1%[23, 27.3] (3 articles); and MOLLI 3(3)3(3)5 FA 35° 27.7% [26.1, 29.3] (1 article). The pooled range of ECV of all included studies was 25.9 [25.3, 26.4].

Univariable meta-regression analyses found factors contributing to the heterogeneity of the pooled T1 time but none for ECV (**Tables 2.2**). Field strength was associated with the heterogeneity in native T1 but neither of age, gender, LVEF, type of contrast, MRI vendor, contrast dose, type of sequence, or flip angle, affected pooled native T1 value when the all studies were included. When divided by field strength, significant vendor difference was observed in native T1 value in 3T (β=105, p=0.0005) and in ShMOLLI 1.5T (β=-62, p=0.004).

Comparison of native T1 times among diseases: Native T1 values among diseases and the normal ranges by sequences are illustrated in **Figure 2.2b.** Then, to outline the standardized differences of native T1 times to discriminate diseased from normal myocardium, Cohen's D (standardized difference between normal and disease) was calculated for each of the articles which reported T1 values of both healthy normal and diseased group and then pooled when possible (**Supplementary Figure 2.3**). In most

of the diseases (eg. myocarditis, hypertrophic cardiomyopathy, and diated cardiomyopathy), all methods demonstrated similar standardized differences, but several conditions showed discrepancies. In systemic lupus erythematosus, Studies using MOLLI sequences within 17 heartbeats at 3T had significant discrimination but those at 1.5T did not. Also, MOLLI 3T failed to distinguish hypertensive patients from normal using T1 values but MOLLI at 1.5T showed statistically significant discrimination, but the lower limit of 95% CI was very close to zero.

Comparison ECV among diseases*:* The standardized differences of ECV were also summarized in the same manner (**Figure 2.2b and Supplemental Figure 2.4**). All of the diseases had similar or larger ECV than normal. As in the case of native T1 time, it was difficult to distinguish hypertensive patients from normal using ECV.

Native T1 and ECV: To compare the standardized differences of native T1 time and ECV, diseases that had both T1 times and ECV were selected and represented in **Figure 2.3a** (Cohen's D) and **2.3b** (actual values). This summary of existing literature divided these conditions into three groups: diseases that are difficult to distinguish from normal (i.e. HTN); ones that are readily identified (i.e. amyloidosis and HCM) and remaining disease entities that can be separated from the normal, but with significant overlap with other diseases. For example, the standardized differences (i.e. Cohen's D) for HTN were in vicinity of zero in all sequences or field strengths, supporting that either native T1 value or ECV has limited ability to distinguish patients with HTN from the normal. On contrary, there were several diseases, whose point estimates far from zero. The farthest one was amyloidosis. Although Cohen's D from both native T1 value and ECV were

>2, that of native T1 was larger. We observed similar findings in HCM, SLE and myocarditis. Intriguingly, some diseases have better discrimination by T1 value and some by ECV. Plots for myocarditis from all three sequences were located close to the X-axis, reflecting larger Cohen's D in T1 time [1 to 2.7] than that of ECV [0.3 to 1.6]. Whereas, HFpEF had larger Cohen's D in ECV than that of native T1. Those from other conditions sit in between. Using MOLLI at 1.5T, the remaining disease entities overlap each other, with similar levels of standardized difference of T1 time and ECV (i.e. Cohen's D) [0.5 to 1.9].

Figure 2.3b shows pooled ranges of actual native T1 and ECV values in various diseases, which illustrates native T1 values can be higher or lower than normal ranges but no diseases have smaller ECV (i.e. only greater or equal ECV levels than normal ranges). Normal ranges from 1.5T magnet data were narrower than that of 3T. This could be partly because of less number of reports as it is newer than 1.5T. ECV from most of the diseases were between 27 and 40%. Only amyloidosis had the greatest difference than others. At 3T, DCM had longer T1 time and greater proportion of ECV. Of interest, myocarditis had greater ECVs than normal in all MOLLI sequences at 1.5T but MOLLI with 17 heartbeats showed longer native T1 value but shorter in ShMOLLI. Another discrepancy between 1.5T sequences was in HTN.

To assess whether different MOLLI schemes affect the diagnostic accuracy, diseases with both native T1 value and Cohen's D were selected and plotted in **Figure 2.3c**. In general, although native T1 values vary among the MOLLI sequences, their Cohen's D were overlapped, suggesting similar level of diagnostic accuracy. For example, Cohen's

D for myocarditis were approximately from 1.5 to 2 but no overlap was observed in their native T1 times.

IV. Discussion

In this systematic review and meta-analysis of pooled means of T1 values and ECV in normal subjects and patients, we found ECV was almost the same among normal subjects, whereas there was heterogeneity of reported T1 values. We also confirmed that many diseases demonstrated longer native T1 than normal subjects, but T1 was shorter in Fabry disease and iron overload. In contrast, all disease states showed either normal or increased ECV.

Pooled analyses among normal subjects showed significant discrepancies in T1 time between different field strengths. T1 time at 3T was longer than that at 1.5T by approximately 100-200 msec. Among the 1.5T scanners, native T1 values had limited overlaps among different versions of MOLLI. Meta-regression showed that heterogeneity in native T1 among normal subjects could be explained by the magnet strength (**Table 2.2**). Only 35^{o} and 50^{o} flip angles were used where majority of included studies used 35^{o} flip angle. 50^{o} flip angle were originally used by Messroghli who first introduced MOLLI in 2004 [159]. However, 35^{o} was chosen to maximize the signal intensity from myocardial tissue [160]. Association between flip angle and native T1 was not significant at 1.5T but significant at 3T. For example, in 1.5T normal native T1 at 35 ^{o} and 50^{o} flip angle were 969 and 967 msec, whereas in 3T they were 1214 and 1097 (**Table 2.1 and Supplementary figure 2.1**). This supports the advice for new

laboratories to establish their own sequence-specific normal ranges for native T1 using their healthy volunteers.

On contrary, ECV seems to be less sensitive to differences in field strengths or sequences, suggesting this method may be more robust than T1. However, ECV calculation, based on pre- and post-contrast T1 of both myocardial tissue and blood pool, does not necessarily eliminate all errors made in the measurement of any of these components. The calculation assumes similar additive errors in measurements in pre- and post-contrast images. Of course, this is not guaranteed; errors would not be cancelled by subtraction if they were multiplicative, unpredictable, or caused by motion. While Gd is restricted to the extracellular space, there is also transfer of magnetization as well as transfer of magnetized water between the extra- and intracellular space [130]. In addition, the ECV does not purely reflect Gd concentration in the extracellular space because estimated T1 with MOLLI variants are influenced by T2 relaxation.

One might argue that ECV can be used to assess progression or regression of fibrosis with follow up imaging. We consider that it is too early because of the following reasons: little is known on test re-test variability of ECV, and ideally biopsy-proven data for the changes in ECV would become available because of above multiple and unpredictable factors contributed to ECV.

T1 value in disease state: T1 relaxation depends on several factors, including field strength, temperature, micro-viscosity, and the presence of large molecules or paramagnetic substances. The T1 relaxation times of macro-molecules such as protein or fat are long [161] because of viscosity and molecular size. Fabry disease and iron

overload showed consistently shorter native T1 values, a reflection of the properties of the infiltrated material. Regretfully, the ECV in these conditions was not reported in the papers included in this study.

T1 mapping also appears to be a good option to distinguish many conditions, such as amyloidosis, hypertrophic cardiomyopathy, myocarditis and dilated cardiomyopathy from normal because the results were consistent between native T1 and ECV. Of these, amyloidosis would be one of the most beneficial targets from T1 mapping based on their longest native T1 and largest ECV. In addition, the combined plots of ECV and native T1 in **Figures 2.3a and 2.3b** demonstrate further insights. Although the patients with amyloidosis had the longest native T1 as well as the highest ECV, the CI of Cohen's D of native T1 time was greater than that of ECV, suggesting better discrimination of native T1. In addition, ECVs from the diseases had overlapped each other so it would be difficult to distinguish one disease from the others solely based on the ECV. On contrary, some diseases demonstrated greater differences in native T1 values from other diseases, such as, DCM at 3T.

Diseases with similar native T1 values to normal: In this study, HTN yielded native T1 and ECV values quite similar to normal subjects. Thus, it could be difficult to discriminate HHD from the normal.

Impact of types of MOLLI and field strengths on the Precision of T1: ShMOLLI seemed to generate the shortest T1 compared to other variants of MOLLI. However, the Cohen's D of T1 was similar among different MOLLI schemes at the same field strength, although T1 of sequence using 35^{o} is somewhat higher than 50^{o}.

Utility of T1 mapping for the differentiation of LVH etiology: This study suggested multi-parametric mapping is too early for assessing HTN. Nevertheless, it should not ignore the utility of T1 mapping for improved risk stratification in HTN patients. Native T1 of hypertensive patients with LVH was agreed to be longer than that of the control and patients without LVH [122, 156]. It has been widely accepted that abnormal fibrosis in myocardial interstitium plays an important role in LVH, which is characterised by longer T1 or and higher ECV. This emphasized the potential utility of this technique in LVH etiology and improving risk stratification in HTN patients. Further studies are required to confirm the direct proportionality between native T1 and severity of HTN.

V. Limitation:

Several factors merit consideration in the interpretation of our results. First, like all meta-analyses, this work is limited by variations in the original studies and publication bias, although we followed standard approaches to detect this. Likewise, the constituent observational studies may be limited by biases in the recruitment process. Second, we have assumed that all the measurements were performed by experts, but the levels of expertise among individuals who actually measured native T1 and ECV are uncertain. Third, significant heterogeneities among studies were identified. The meta-regression analyses and stratifications to elucidate the sources of variations did not show our hypothesized confounding factors to be fully explanatory. Variations could be additionally explained by differences in native T1 and ECV among different populations, and inter-observer variability related to differences in defining the region of interest. Fourth, because T1 mapping remains a relatively novel technique and variety

of non-commercial software were used in the included studies, underlying technical differences may have caused heterogeneity between studies.

VI. Conclusion:

ECV seems less influenced by methodology than T1 time among normal subjects. Native T1 shows narrower ranges of normal values for specific sequences with larger differences between normal and disease for some entities (HCM, myocarditis). In addition, native T1 shows a wider range of abnormalities starting from shortening in some infiltrative diseases (Fabry, Iron overload) to pronounced prolongation (e.g. amyloid), while ECV is greater in the disease than the normal. Type of MOLLI scheme did not impact on the precision.

Acknowledgements The authors thank Ms Elizabeth Seymour, for her support in systematic review.

Figure 2.1: PRISMA Flow Chart

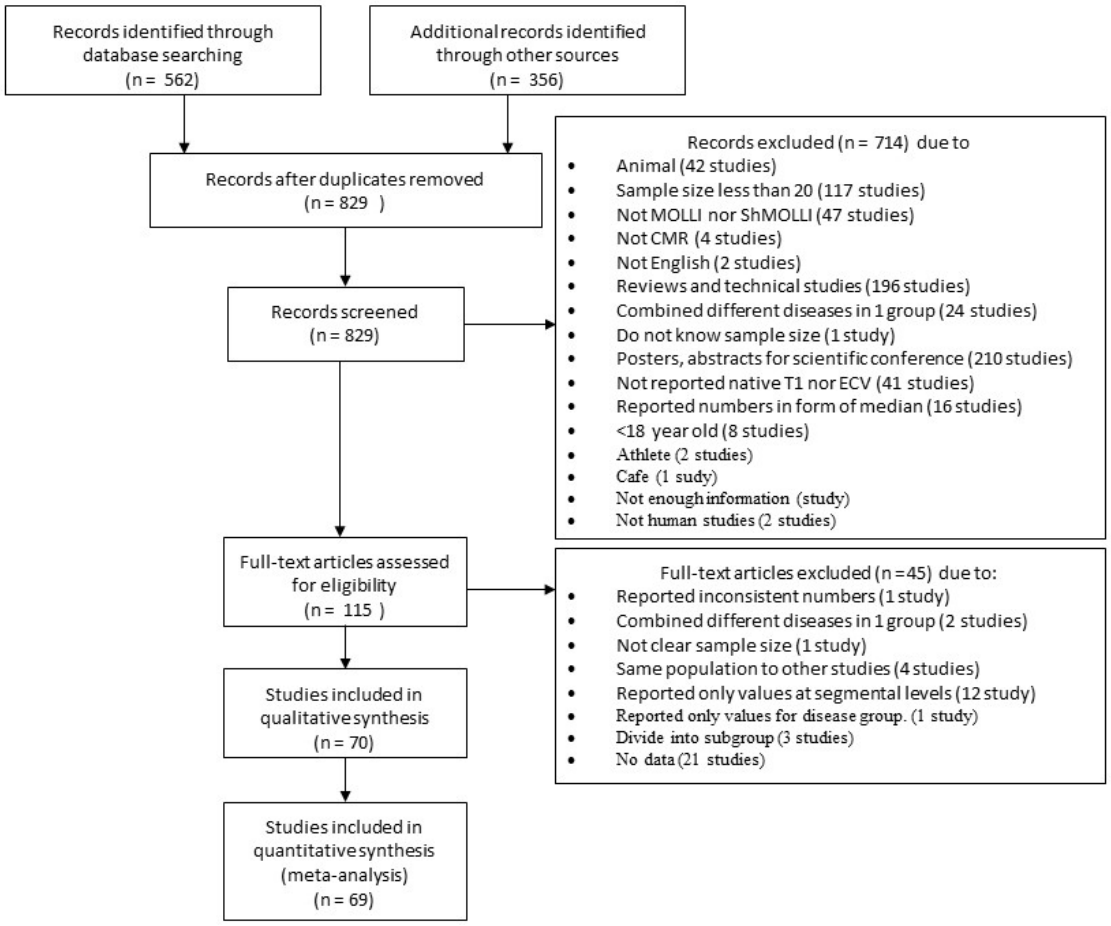

Figure 2.2a: Native T1 among diseases

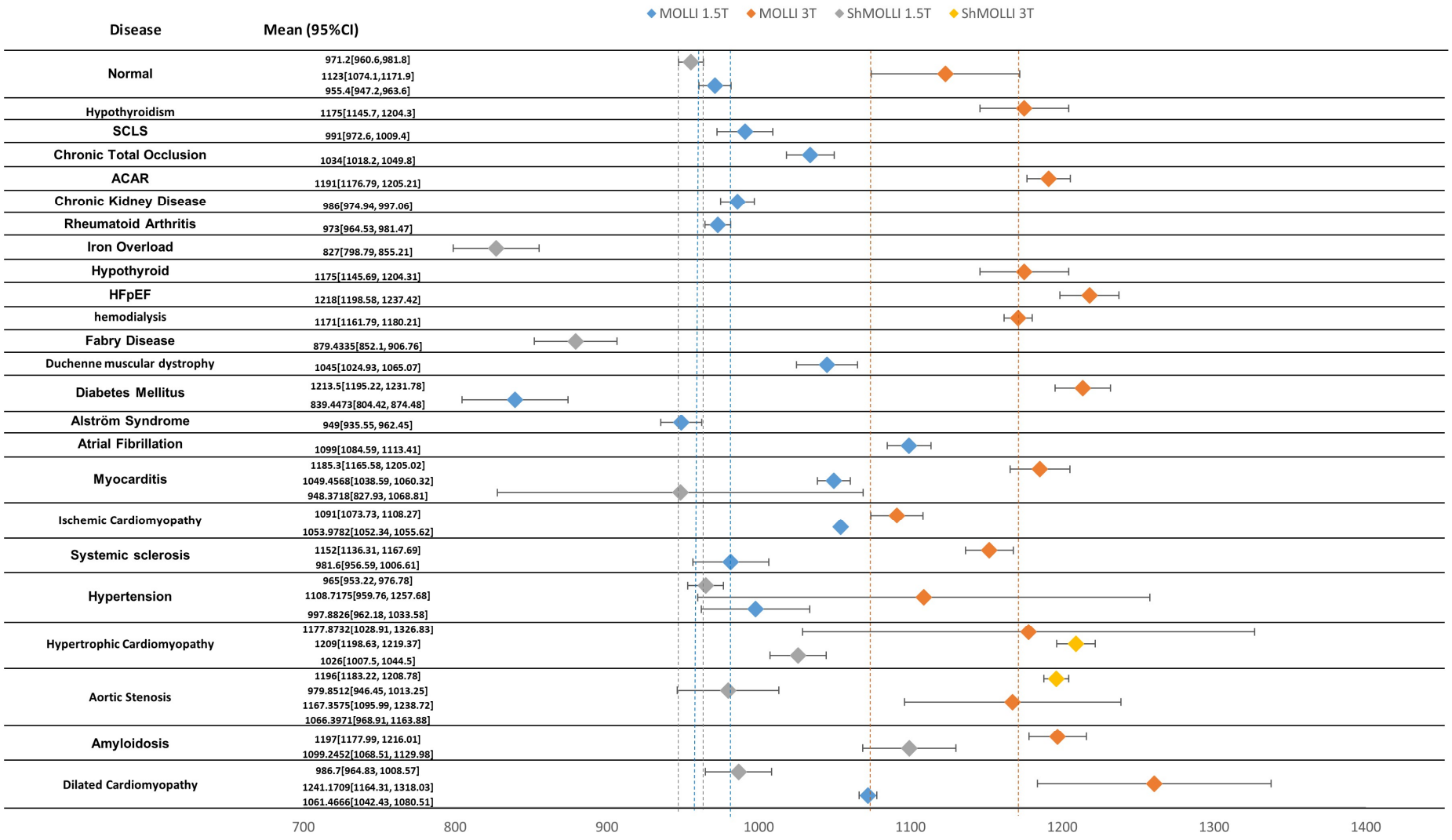

Figure 2.2b: ECV among diseases

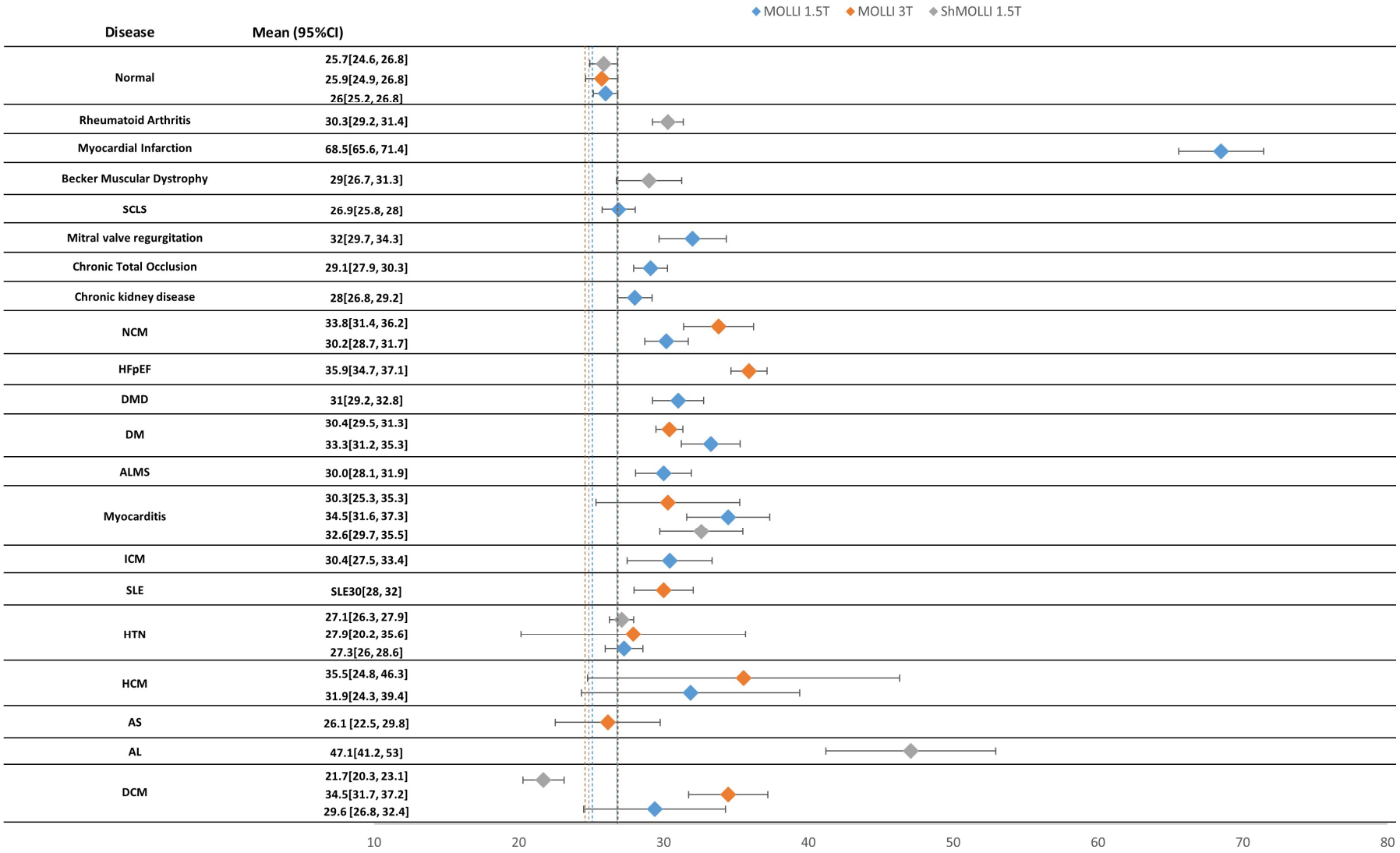

Figure 2.3a: ECV Cohen D vs T1 Cohen D

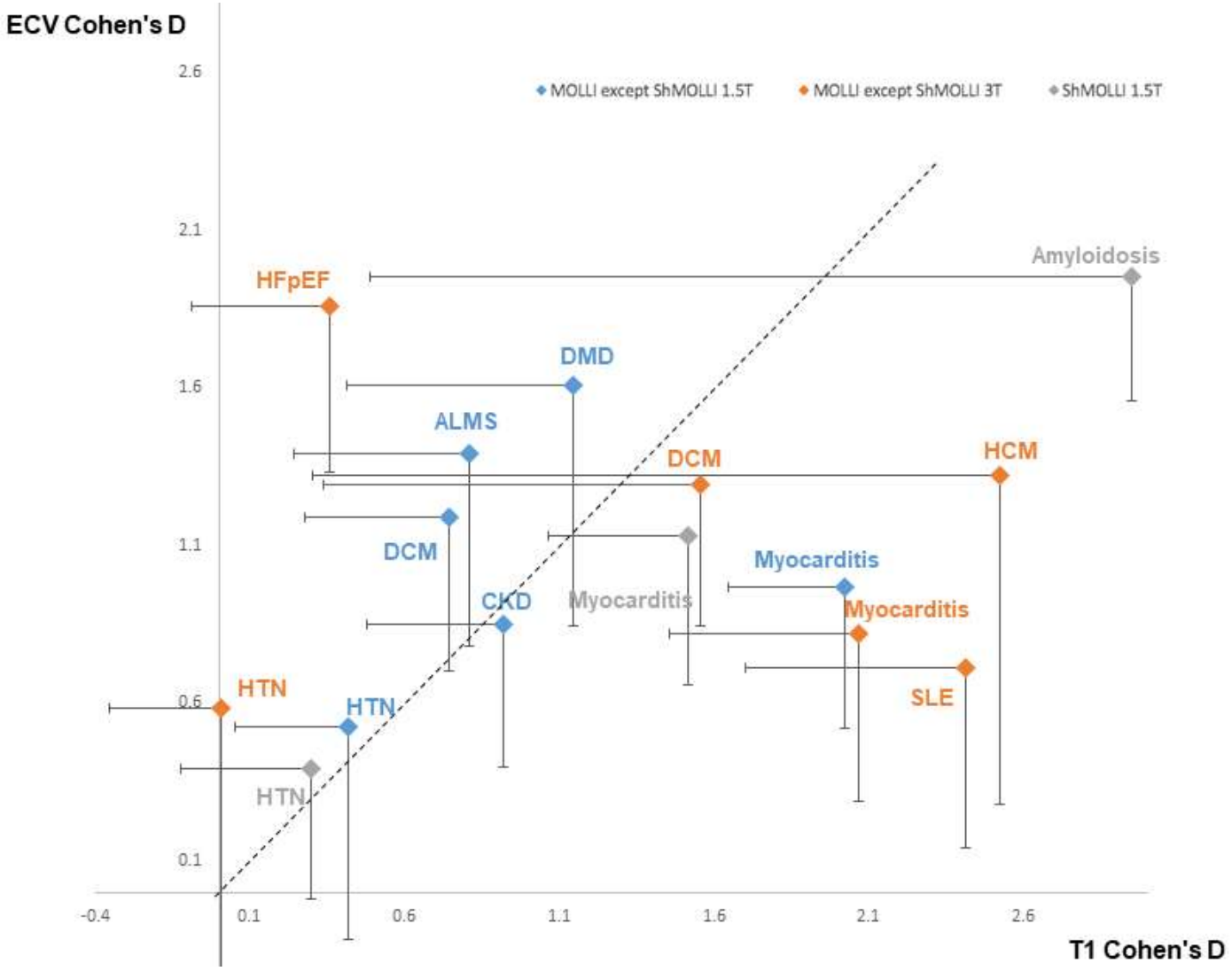

Figure 2.3b: ECV vs native T1

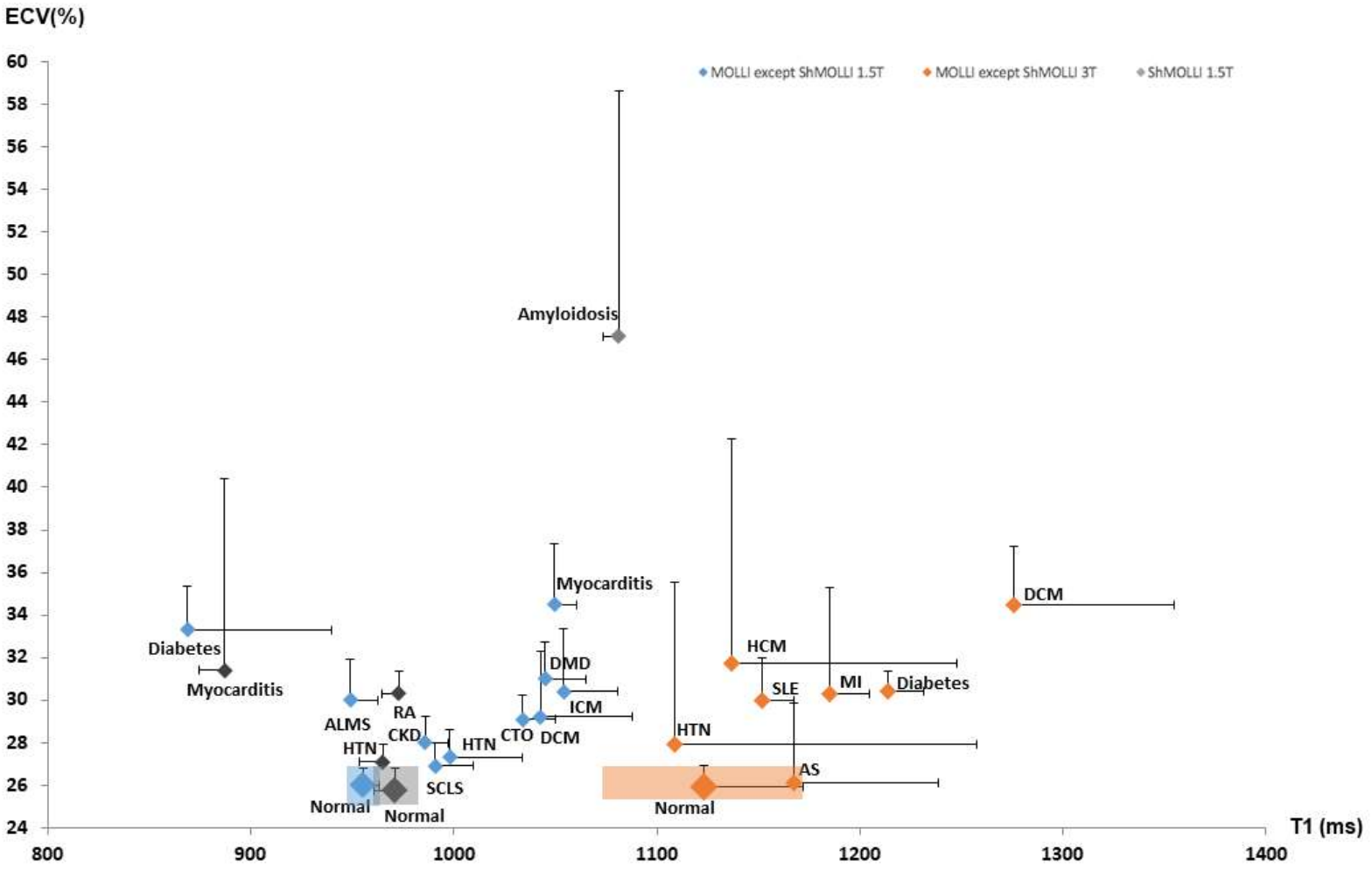

Figure 2.4c: T1 Cohen D vs T1

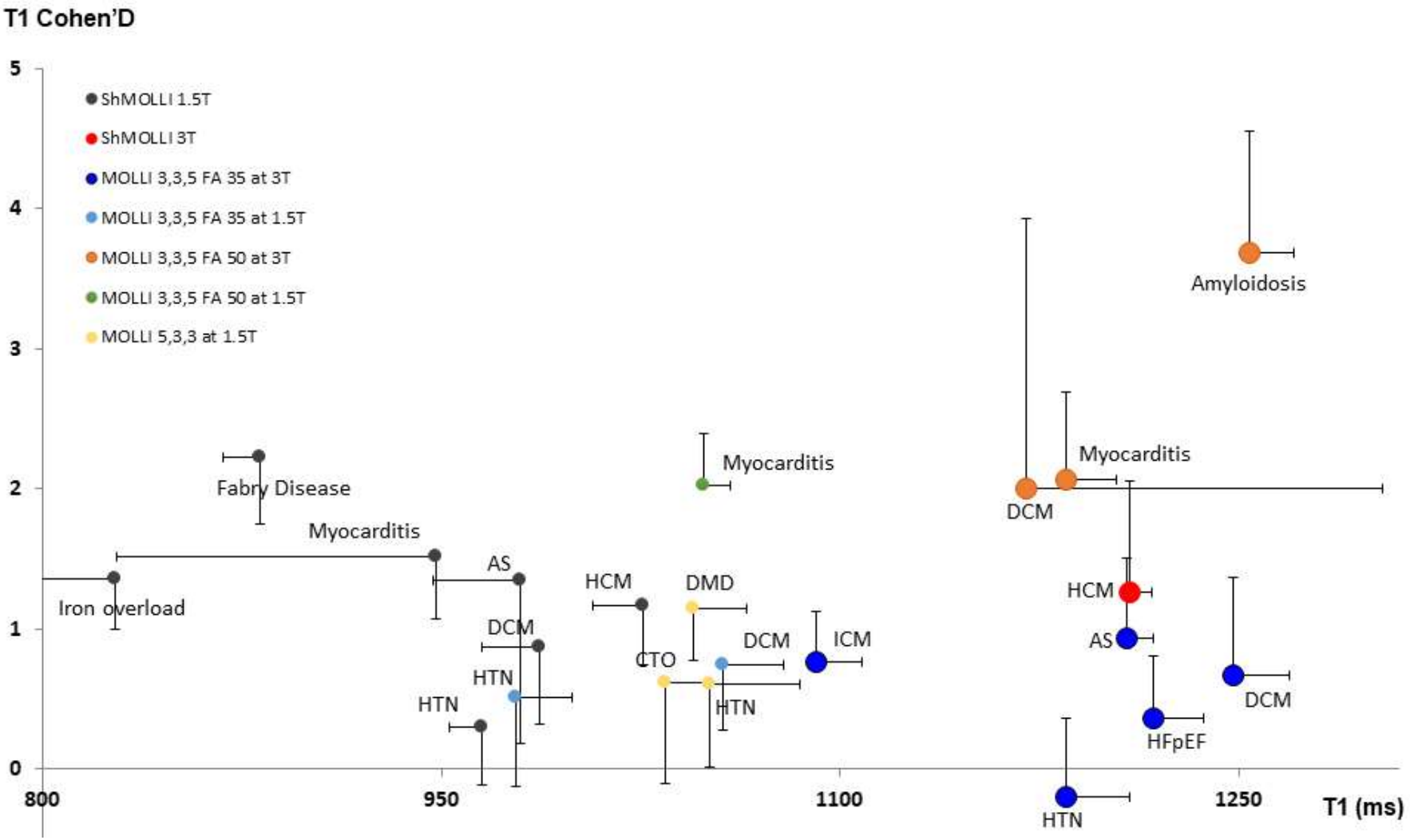

Supplementary Figure 2.1: T1 among the normal

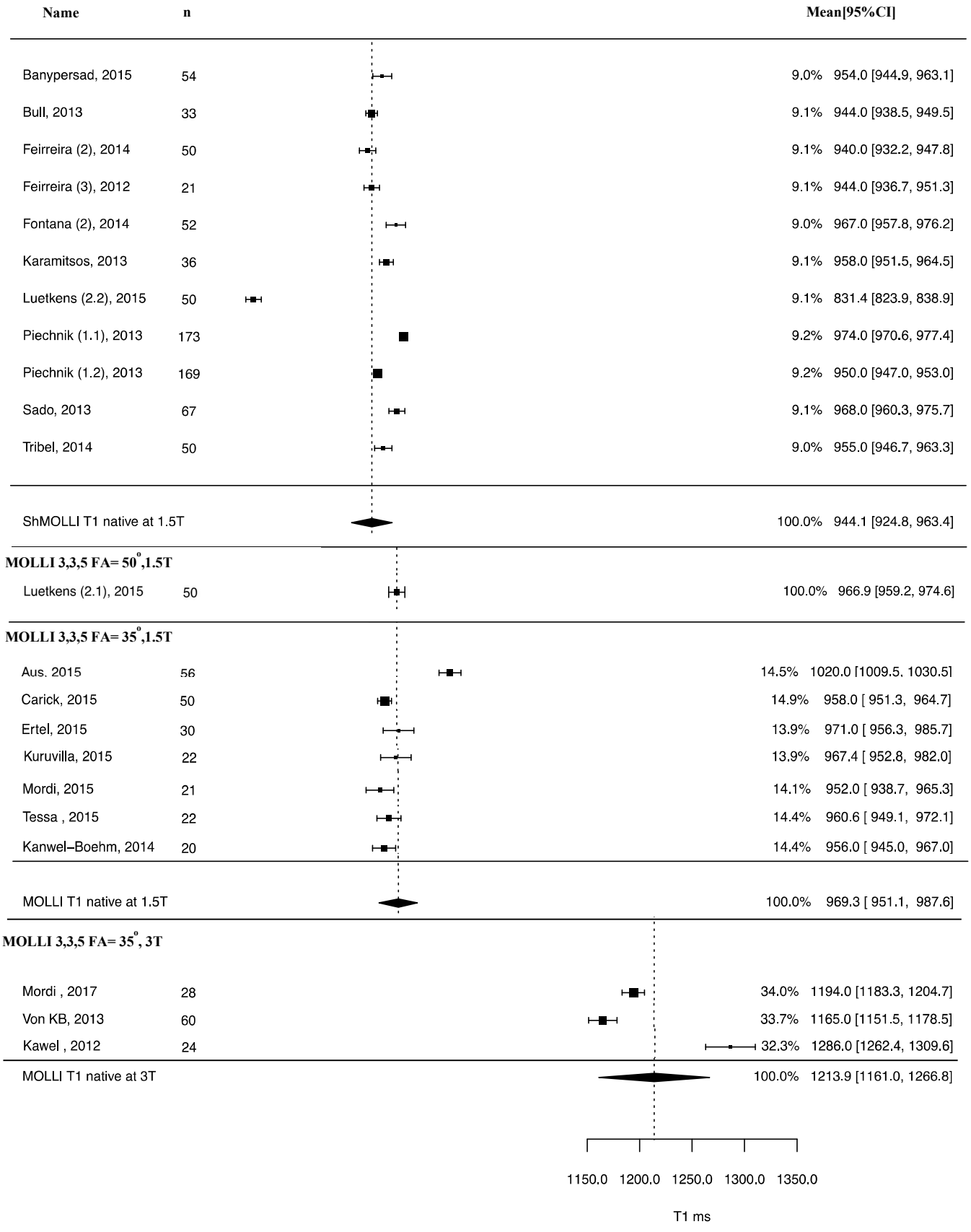

Supplementary Figure 2.2: ECV among the normal

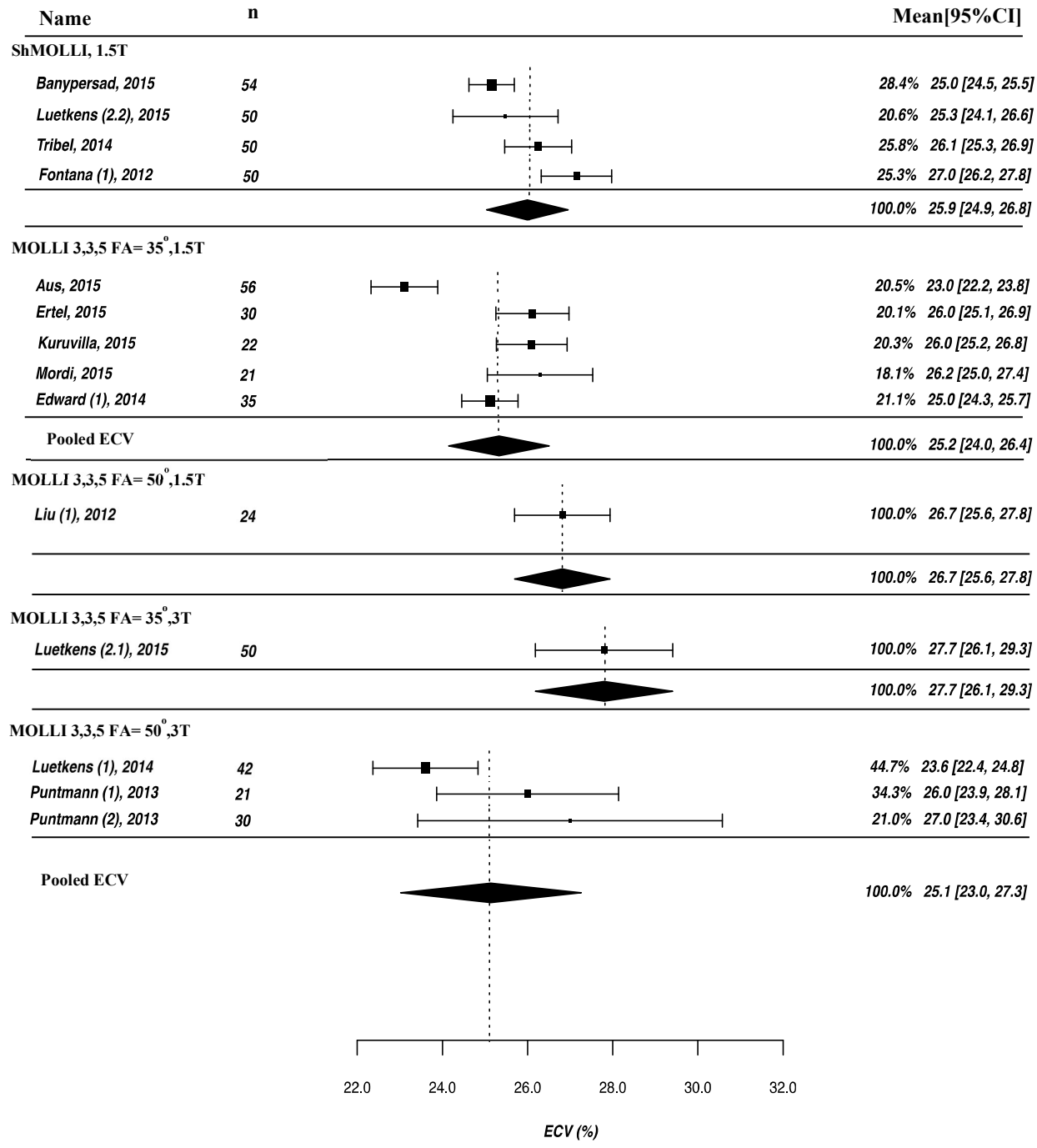

Supplementary figure 2.3: Pooled Cohen's D for differences in native T1 between normal and diseased group

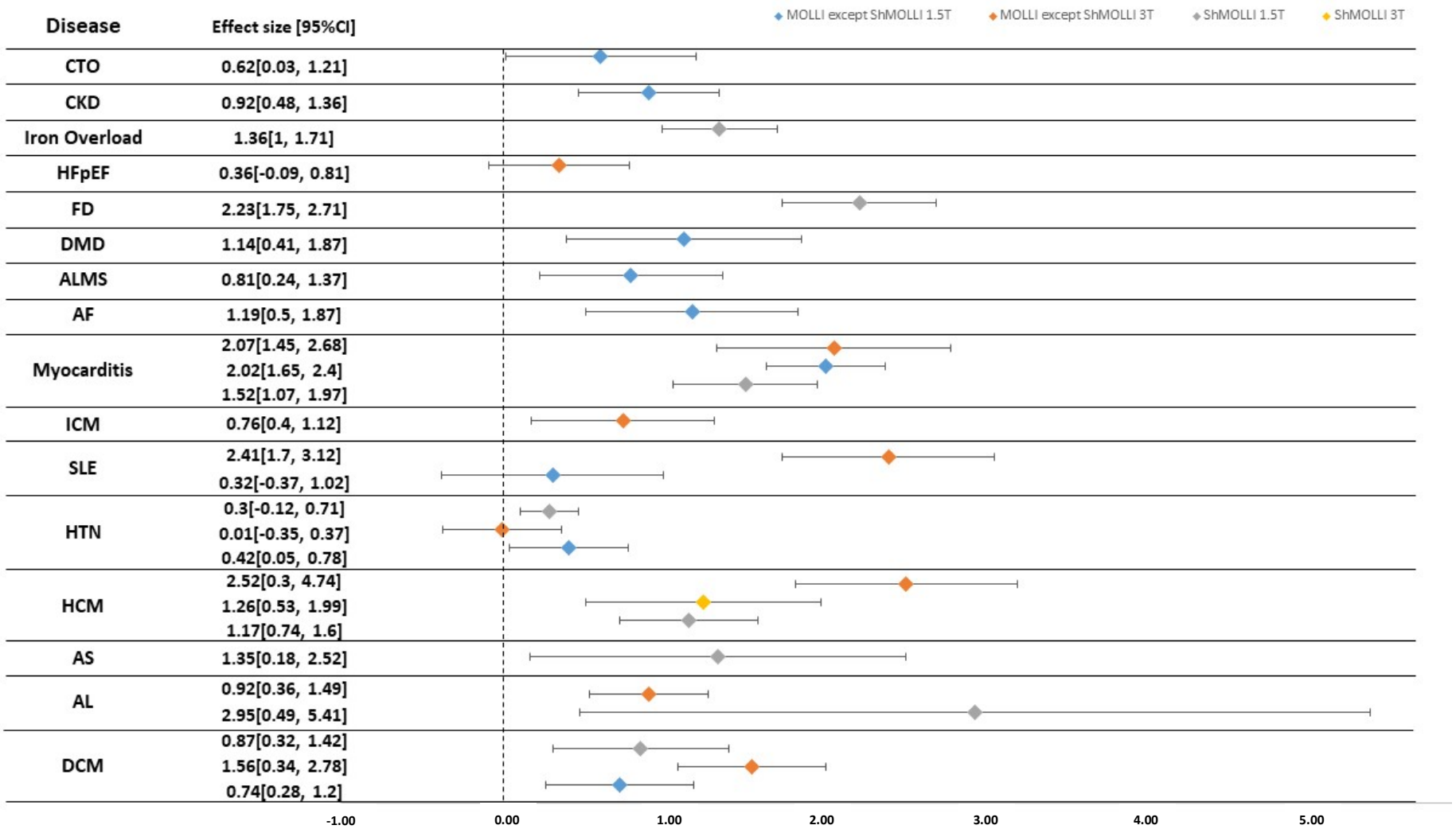

Supplementary figure 2.4: Pooled Cohen's D for differences in native T1 between normal and diseased group

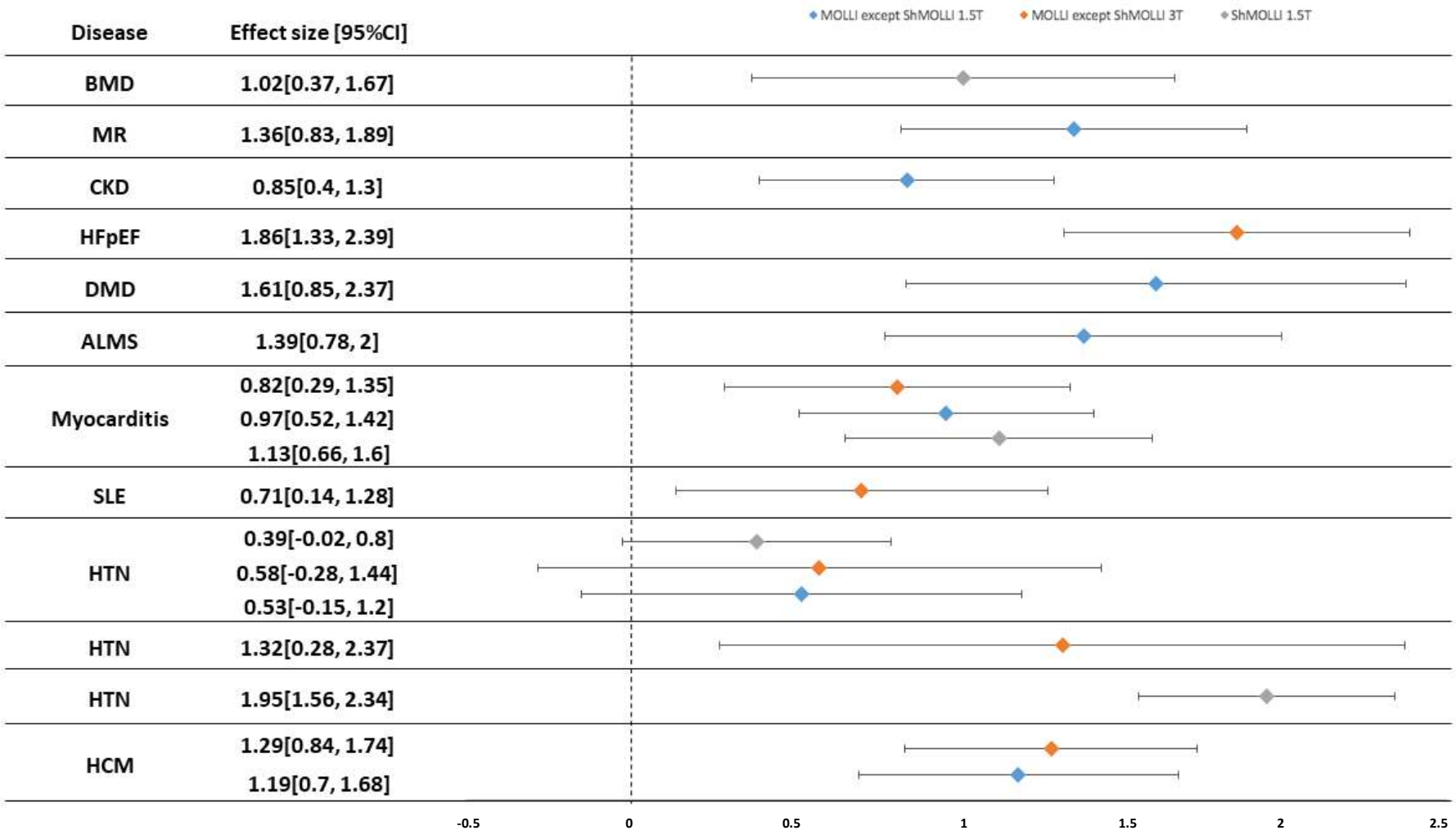

Supplementary figure 2.5: Funnel plot of MOLLI T1

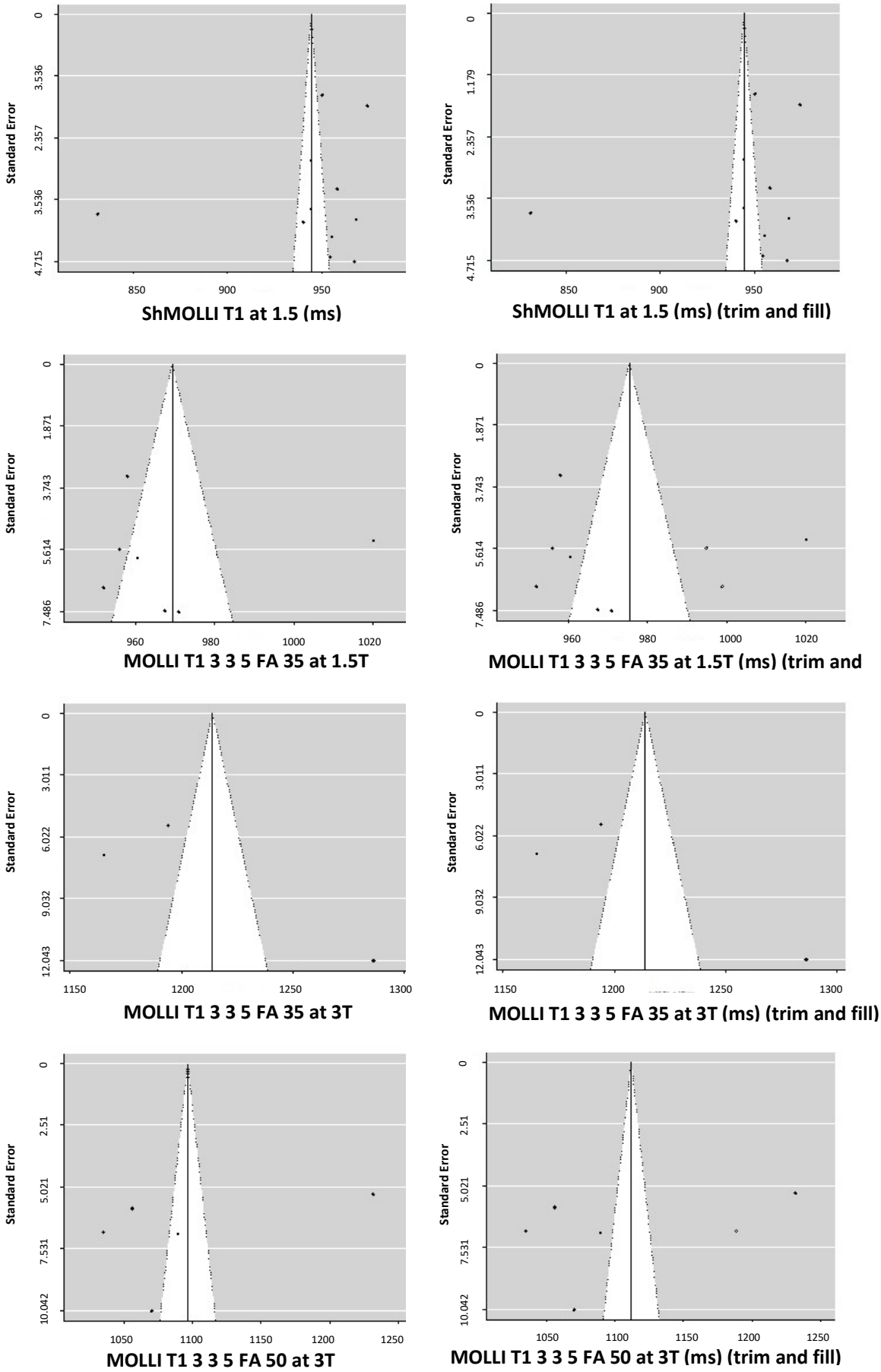

Supplementary figure 2.6: Funnel plot of MOLLI ECV

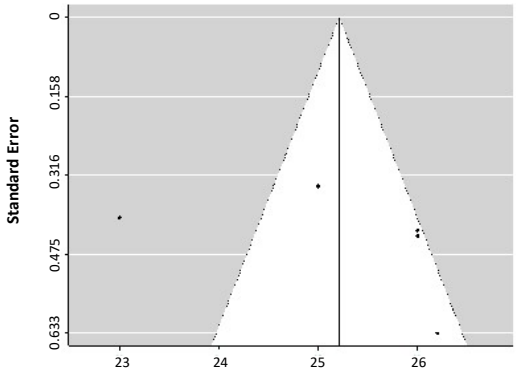

ECV MOLLI 3 3 5 FA 35 at 1.5 T (%)

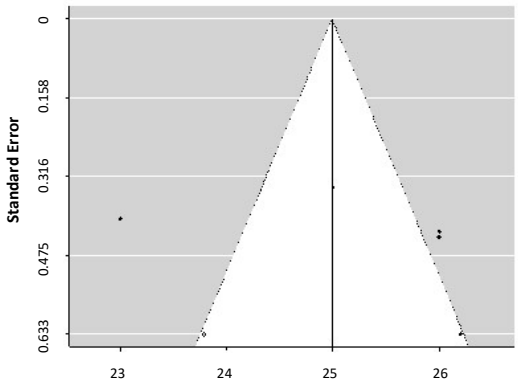

ECV MOLLI 3 3 5 FA 35 at 1.5 T (%) trim and fill

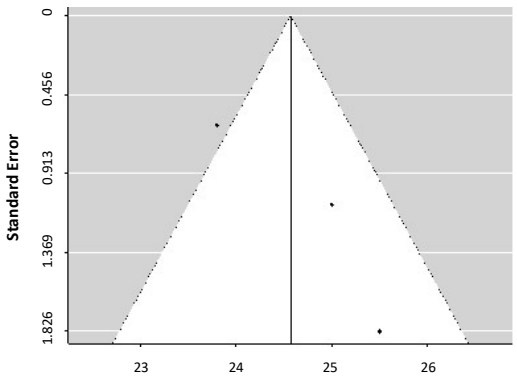

ECV MOLLI 3 3 5 FA 50 at 3T

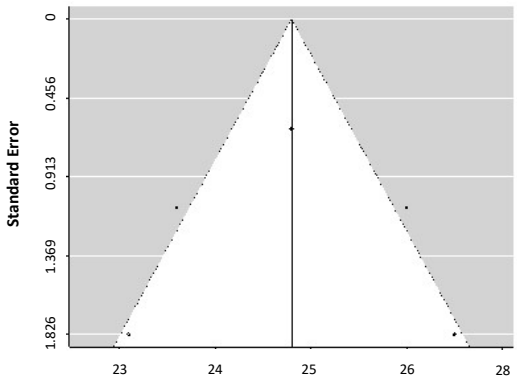

ECV MOLLI 3 3 5 FA 50 at 3T (%) trim and fill

Appendix 2A: Search criteria

I. PUBMED:

Keywords: ((((((shmolli) OR "shortened modified look locker inversion recovery") OR "shortened molli")) OR ((MOLLI) OR "Modified Look-Locker inversion recovery"))) AND (((((((("ECV") OR "extra cellular matrix") OR "ECF") OR "Extra cellular fraction") OR "extra cellular volume"))))) OR T1 map*) AND ((((("CMR") OR "cardiac magnetic resonance") OR "cardiac MR"))))

Results: 298 articles

II. SCOPUS:

1. (TITLE-ABS-KEY ("shmolli") OR TITLE-ABS-KEY ("shortened modified look locker inversion recovery") OR TITLE-ABS-KEY ("molli") OR TITLE-ABS-KEY ("modified look-locker inversion recovery"))
2. (TITLE-ABS-KEY ("cardiac mr") OR TITLE-ABS-KEY ("cmr") OR TITLE-ABS-KEY ("cardiac magnetic resonance"))
3. TITLE-ABS-KEY ("ECV") OR TITLE-ABS-KEY ("extra cellular matrix") OR TITLE-ABS-KEY ("ECF") OR TITLE-ABS-KEY ("Extra cellular fraction") OR TITLE-ABS-KEY ("extra cellular volume") TITLE-ABS-KEY (t1 map*)
4. #1 AND #2 AND #3

Results: 47 articles

III. EMBASE:

1 'cmr' OR 'cardiac magnetic resonance' OR 'cardiac mr'

2 'ecv' OR 'extra cellular matrix' OR 'ecf' OR 'extra cellular fraction' OR (t1 AND map*)

3 shmolli OR 'shortened modified look locker inversion recovery' OR 'shortened molli' OR molli OR 'modified look-locker inversion recovery'

4 #1 AND #2 AND #3

Results: 217 articles

Last search: 15 Sep 2017

Appendix 2B: Participant characteristics of subjects in included studies

Supplementary table 2.1: Included studies in normal healthy group

Study	Year	n	Age	Males (%)	LVEF (%)	FS (T)	Seq	Vendor	Agent contrast	Type of contrast	Bolus /Infusion	Commercial SW	T1n	T1p	ECV
Aus[100]	2015	56	52±9	66	62±3	1.5	M	P	DPTA	Linear		✗	✓	✓	✓
Banypersad[88]	2015	54	46±15	46	67±6	1.5	S	S	Dotarem	Macrocyclic	0.1mmol/kg bonlus+0.011 mmol/kg Infusion	-	✓	✗	✓
Bull [101]	2013	33	62±7	64		1.5	S	S	NA	NA	NA	✗	✓	✗	✗
Carick[102]	2015	50	53±13	52	-	1.5	M	S	NA	NA	NA	-	✓	✗	✗
Dabir (1.1)[104]	2014	34	-	-	-	1.5	M	P	Gadavis (Gadobutrol)	Macrocyclic	Bolus 0.1/0.15/0.2 mmol/kg	✓	✓	✓	✓
Dabir (1.2)[104]	2014	32	-	-	-	3	M	P	Gadobutrol	Macrocyclic	Bolus 0.1/0.15/0.2 mmol/kg	✓	✓	✓	✓

Dabir (1.3)[104]	2014	58	-	-	-	1.5	M	P	Gadobutrol	Macrocyclic	Bolus 0.1/0.15/0.2 mmol/kg	✓	✓	✓	✓
Dabir (1.4)[104]	2014	55	-	-	-	3	M	P	Gadobutrol	Macrocyclic	Bolus 0.1/0.15/0.2 mmol/kg	✓	✓	✓	✓
Edward (1)[91]	2014	35	59±13	63	74±6	1.5	M	S	Gadobutrol	Macrocyclic	Bolus 0.15 mmol/kg	✓	✗	✗	✓
Edward (2)[106]	2015	43	57±10	56	73±6	1.5	M	S	Gadobutrol	Macrocyclic	NA	✓	✓	✗	✓
Ertel[107]	2015	30	52	47	64±5	1.5	M	S	Gadopentate/ Gadobutrol	Linear	NA	-	✓	✗	✗
Feirreira (2)[108]	2014	50	41±13	74	-	1.5	S	S	NA	NA	NA	✓	✓	✗	✗
Feirreira (1)[109]	2012	21	55±13	38	-	1.5	S	S	Gadodiamide	Linear	NA	✗	✓	✗	✗
Fontana (1)[112]	2012	50	47±17	54	-	1.5	S	S	Gadobutrol	Macrocyclic	NA	-	✗	✗	✓
Fontana (2)[110]	2014	52	46±15	33	67±6	1.5	S	S	Dotarem	Macrocyclic	Bolus 0.1mmol/kg	-	✓	✗	✗
Kawel-Boehm[120]	2014	20	33±8	55	-	1.5	M	S	NA	NA	NA	✓	✓	✗	✗

Karamitsos[117]	2013	36	59±4	61	74±5	1.5	S	P	NA	NA	NA	✗		✓	✗	✗
Kawel [119]	2012	24	28±6	33	-	3	M	S	DPTA/BOPTA	Linear	Bolus	✗		✓	✗	✗
Kuruvilla[122]	2015	22	54 (48-61)	32	-	1.5	M	S	DPTA	Linear	Bolus 0.15mmol/kg	✗		✓	✓	✓
Liu (1)[124]	2012	24	27±6	33	62±4	3	M	S	NA	NA	NA	✓		✗	✗	✓
Liu (2)[125]	2014	92	37 (27-44)	-	55 (52-59)	3	M	S	NA	NA	NA	✓		✓	✗	✗
Luetkens (1) [126]	2014	42	39±10	64	63±7	3	M	P	Gadobutrol	Macrocyclic	Bolus 0.2mmol/kg	✗		✓	✗	✓
Luetkens (2.1) [127]	2015	50	39±17	60	73±13	1.5	M	P	Gadobutrol	Macrocyclic	Bolus 0.15mmol/kg	-		✓	✗	✓
Luetkens (2.2) [127]	2015	50	39±17	60	73±13	1.5	S	P	Gadobutrol	Macrocyclic	Bolus 0.15mmol/kg	-		✓	✗	✓
Mordi [128]	2015	21	48±16	100	65±4	1.5	M	S	Gadobutrol	Macrocyclic	Bolus	✓		✓	✗	✓

Piechnik (1.1)[85]	2013	173	39±14	0	-	1.5	S	S	NA	NA	NA	✗	✓	✗	✗
Piechnik (1.2)[85]	2013	169	37±15	100	-	1.5	S	S	NA	NA	NA	✗	✓	✗	✗
Puntmann (1)[130]	2013	21	38±6	24	61±5	3	M	P	Gadobutrol	Macrocyclic	NA	✓	✓	✓	✓
Puntmann (2)[132]	2013	30	43±9	63	63±6	3	M	P	Gadobutrol	Macrocyclic	NA	✓	✓	✓	✓
Puntmann (3)[131]	2014	47	51±15	52	61±6	3	M	P	Gadobutrol	Macrocyclic	NA	✓	✓	✗	✗
Rodrigues[156]	2017	25	46±14	60	64	1.5	M	S	NA	NA	NA	✓	✓	✗	✗
Mordi [154]	2017	28	67.7±11.2	50	64.2	3	M	P	Gadobutrol	Macrocyclic	NA	✓	✓	✗	✓
Homsi [149]	2017	20	63.2±10.5			1.5	M	P	NA	NA	NA	✓	✓	✗	✓
Luetkens [162]	2017	35	41.1±17.2		61	1.5	M	P	Gadobutrol	Macrocyclic	Bolus	✓	✓	✗	✓
Mazurkiewicza[153]	2017	30	33.1±5.2	66.6	65.1	1.5	S	S	NA	NA	NA	✓	✓	✗	✗
Homsi [149]	2017	20	63.2±10.5	50		1.5	M	P	Gadobutrol	Macrocyclic	NA	✓	✓	✗	✓
Gao[147]	2017	23	35.4±8	0	63	3	M	S	NA	NA	NA	✓	✓	✗	✗
Rutherford[157]	2017	28	60	57.1	63.3	3	M	S	NA	NA	NA	✓	✓	✗	✗
Shang[158]	2017	32	51.4±13.6	46.9		3	M	S	Gadobutrol	Macrocyclic	NA	✓	✓	✗	✗

Reiter [133]	2014	40	23±3	50	69±7	1.5	M	S	NA	NA	NA	-	✓	✗	✗
Sado [134]	2013	67	46 (24-88)	45	-	1.5	S	S	NA	NA	NA	✗	✓	✗	✗
Tessa [137]	2015	22	42±10	86	-	1.5	M	S	NA	NA	NA	✓	✓	✗	✗
Tribel [138]	2014	50	44 (32-55)	52	67±6	1.5	S	S	Dotarem	Macrocyclic	Bolus 0.1mmol/kg+0.011 infusion	-	✓	✓	✓
Von KB [140]	2013	60	48±17	50	64±5	3	M	S	Gadobutrol	Macrocyclic	NA	✓	✓	✓	✗

Commercial SW, commercially available software; **N,** sample size; **FS,** Field Strength; **M,** MOLLI; **S,** ShMOLLI; **T1n,** native T1; **T1p,** post-contrast T1; **ECV,** extra-cellular matrix; **P,** Philips; **S,** Siemens; **Seq,** Sequence

Supplementary table 2.2: Included studies in diseases group

Study	Year	N	Age	Males(%)	FT	Seq	Diseases	T1n	ECV	Risk Factors			
										DM	HTN	HLP	CAD
Aus [100]	2015	29	58±12	69	1.5	M	DCM	✓	✓	✗	✗	✗	✗
Banypersad[88]	2015	100	62±10	67	1.5	S	AL	✓	✓	✗	✗	✗	✗
Bull S (1.1)[101]	2015	22	68±19	59	3	S	AS	✓	✗	0	✓	✗	✗
Bull S (1.2)[101]	2015	24	70±10	67	3	S	AS	✓	✗	✓	✗	✓	✗
Bull S (1.3)[101]	2015	63	68±13	75	3	S	AS	✓	✗	✓	✗	✓	✗
Chen (1)[93]	2015	50	59±11	80	1.5	M	CTO	✓	✓	✓	✓	✓	✗
Chen (2.1)[94]	2015	27	68±9	78	1.5	M	ICM	✓	✓	✓	✓	✗	✗
Chen (2.2)[94]	2015	21	64±14	90	1.5	M	DCM	✓	✓	✓	✓	✗	✗
Chin (1)[103]	2014	122	71(65-77)	67	3	M	AS	✗	✓	✓	✓	✗	✓
Chin (2)[103]	2014	20	71(53-75)	50	3	M	AS	✓	✓	✓	✓	✗	✓
Dass[89]	2012	28	48±13	18	1.5	S	HCM	✓	✗	0	✓	✗	✗

Doltra[105]	2014	23	67±9	61	1.5	M	HTN	✓	✓	✓	✗	✓	✓
Edward (1)[91]	2014	35	59±13	63	1.5	M	MR	✓	✓	✓	✗	✗	✗
Edwards (2.1)[106]	2015	43	57±10	56	1.5	M	KD	✓	✓	✗	✗	✗	✗
Edwards (2.2)[106]	2015	43	57±10	56	1.5	M	HTN	✓	✓	✗	✓	✗	✗
Edwards (3)[90]	2015	26	27±9	65	1.5	M	DCM	✓	✓	✓	✓	✗	✗
Ertel[107]	2015	20	51(40-70)	65	1.5	M	SCLS	✓	✓	✗	✗	✗	✗
Ferreira[108]	2013	50	42±16	78	1.5	S	MI	✓	✗	✓	✓	✓	✗
Florian[92]	2014	27	35±12	100	1.5	S	MD	✗	✓	✗	✗	✗	✗
Fontana (1)[110]	2014	46	50±13	74	1.5	S	HCM	✓	✗	✗	✗	✗	✗
Fontana (2)[111]	2015	250	67±12	71	1.5	S	AL	✓	✓	✗	✓	✗	✗
Hinojar (1.2)[113]	2015	95	55±14	68	3	M	HCM	✓	✓	✗	✗	✗	✗
Hinojar (1.3)[113]	2015	69	54±13	65	3	M	HTN	✓	✓	✗	✗	✗	✗
Hong[114]	2015	41	56.2±20	63	3	M	HTN	✓	✓	✓	✓	✗	✗
Jellis (1)[115]	2011	67	60±10	-	1.5	M	DCM	✓	✗	✓	✓	✗	✗

Jellis (2.1)[116]	2014	25	60±9	40	1.5	M	DB	✓	✓	✓	✗	✗	✗
Jellis (2.2)[116]	2014	24	59±11	63	1.5	M	DB	✓	✓	✓	✗	✗	✗
Karamitsos[117]	2013	28	63±10	71	1.5	S	DB	✓	✗	✗	✗	✗	✗
Kato[118]	2016	50	60±8	74	1.5	M	AF	✓	✗	✓	✓	✓	✗
Kellman (1.1)[121]	2012	33	51±14	73	1.5	M	AL	✗	✓	✗	✗	✗	✗
Kellman (1.2)[121]	2012	33	57±10	82	1.5	M	HCM	✗	✓	✗	✗	✗	✗
Kuruvilla (1.1)[122]	2015	23	64(56-71)	43	1.5	M	MI	✓	✓	✗	✗	✗	✗
Kuruvilla (1.2)[122]	2015	20	55(44-66)	30	1.5	M	HTN	✓	✓	✗	✗	✗	✗
Lee[123]	2015	80	67±10	-	3	M	HTN	✓	✗	✓	✓	✓	✗
Luetkens (1)[126]	2014	24	35±15	75	3	M	HF	✓	✓	✗	✗	✗	✗
Luetkens (2.1)[127]	2015	34	45±19	50	1.5	M	MI	✓	✓	✗	✗	✗	✗
Luetkens (2.2)[127]	2015	34	45±19	50	1.5	S	Myocarditis	✓	✓	✓	✗	✗	✗
Ntusi[129]	2015	39	50±12	28	1.5	S	ACAR	✓	✓	✓	✓	✓	✗
Puntmann (1)[130]	2012	33	40±8	21	3	M	SLE	✓	✓	✗	✗	✗	✗

Puntmann (2.1)[132]	2013	25	44±11	64	3	M	HCM	✓	✓	✗	✗	✗	✗
Puntmann (2.2)[132]	2013	27	45±14	67	3	M	DCM	✓	✓	✗	✗	✗	✗
Puntmann (3.1)[131]	2014	82	52±16	53	3	M	DCM	✓	✗	✓	✓	✗	✗
Puntmann (3.2)[131]	2014	91	56±13	56	3	M	IHD	✓	✗	✓	✓	✓	✗
Sado (1)[86]	2012	44	49	39	1.5	S	FD	✓	✗	✗	✗	✗	✗
Sado (2)[134]	2015	88	34(13-72)	55	1.5	S	Iron overload	✓	✗	✗	✗	✗	✗
Singh[135]	2015	50	66±13	78	3	M	AS	✓	✓	✓	✓	✓	✓
Soslow[136]	2016	31	13±5	100	1.5	M	DMD	✓	✓	✗	✗	✗	✗
Tribel[138]	2015	40	59	53	1.5	S	HTN	✓	✓	✗	✓	✗	✗
Zhang[141]	2015	24	54±9	21	1.5	M	SLE	✓	✗	✗	✗	✗	✗
Ooji[139]	2015	35	54±15	71	1.5	M	HCM	✗	✓	✗	✗	✗	✗
Mahmod[152]	2014	26	67.8	73	3	S	AS	✓	✗	✓	✓	✗	✗
Shang[158]	2017	38	54.6	52.6	3	M	DB	✓	✓	✓	0	✗	✗
Rutherford[157]	2017	33	56	57.6	3	M	HD	✓	✗	✗	✗	✗	✗

Rodrigues[156]	2017	80	49	55	1.5	M	HTN	✓	✓	✓	✓	✗	✗
Rodrigues[156]	2017	20	55	70	1.5	M	HTN	✓	✓	✓	✓		✗✗
Nakamori[163]	2017	36	56	86	3	M	DCM	✓	✓	✓	✓	✓	✗
Mordi[154]	2017	62	70.8	32.3	3	M	HFpEF	✓	✓	✓	✓	✗	✗
Mordi[154]	2017	22	66.9	77.2	3	M	HTN	✓	✓	✓	✓	✗	✗
Gallego-Degado[146]	2016	31	49	61	3	M	AL	✓	✗	✓	✓	✗	✗
Gao[147]	2016	30	36.6	0	3	M	HP	✓	✗	✗	✗	✗	✗
Gormeli[148]	2017	37	43.5	46	3	M	DCM	✓	✓	✗	✗	✗	✗
Luetkens [162]	2017	48	43.6	56	1.5	M	Myocarditis	✓	✗	✗	✗	✗	✗
Mazurkiewicza[153]	2017	26	34.4	57.6	1.5	S	DCM	✓	✓	✓	✗	✗	✗
Claridge[144]	2017	72	72	80.6	1.5	M	ICM	✓	✓	✓	✓	✗	✗
Claridge[144]		58	58.5	79.3	1.5	M	NCM	✓	✓	✓	✓	✗	✗
Inui [164]		22	61.5	95	3	M	NCM	✓	✓	✗	✗	✗	✗
Mahmod[152]	2014	26	67.8	73	3	S	AS	✓	✓	✓	✓	✗	✗

Chapter 2: Pooled Summary of Native T1 value and Extracellular Volume with MOLLI Variant Sequences in Normal Subjects and Patients

N: sample size, **FS**: Field Strength, **M**: MOLLI, **S**: ShMOLLI, **T1n**: native T1, **T1p**: post-contrast T1, **ECV**: extra-cellular matrix, **Seq:** Sequence

ALMS: Alström Syndrom; **CAD:** Coronary artery disease; **CTO**: Chronic Total Occlusion; **DB**: Diabetes; **DCM**: Dilated cardiomyopathy; **DMD:** Duchenne muscular dystrophy; **HCM**: Hypertrophic cardiomyopathy; **HLP:** Hyperlipidaemia; **HTN**: Hypertension; **MI**: Myocardial Infarction; **CTO**: Chronic Total Occlusion; **ICM**: ischemic cardiomyopathy; **IHD:** Ischemic heart disease; **RA**: Rheumatoid Arthritis, **SCLS:** systemic capillary leak syndrome, **SLE:** Systemic sclerosis.

Supplementary table 2.3: Inclusion criteria of control groups

Study	Year	Inclusion criteria for control groups
Aus	2015	Subjects without systemic disease or history of cardiovascular events and with normal clinical examination served as a 'control', all underwent the following diagnostic procedures: 12 lead electrocardiogram (ECG), echocardiography oral glucose tolerance test and high-dose dobutamine stress CMR as well as subsequent contrast-enhanced CMR using a T1-weighted inversion recovery-prepared fast gradient echo sequence with an optimized inversion time 15 min after injection of a contrast agent revealed no pathological findings. Controls also showed no elevation of NT-pro-BNP as well as high- sensitive Troponin-T values
Banypersad	2015	Healthy volunteer
Bull	2013	Thirty-three age- and sex-matched normal volunteers were also recruited from both centres; comorbidities and symptoms of cardiac disease were excluded before inclusion in the study
Carick	2015	A total of 343 STEMI patients provided written informed consent. The eligibility criteria included an indication for primary percutaneous coronary intervention (PCI) or thrombolysis for STEMI . Exclusion criteria represented standard contraindications to contrast CMR.
Dabir (1.1) and Dabir (1.2)	2014	Healthy subjects with no significant medical history, no evidence of CVD (normal ECG, normal cardiac dimensions and function by cine CMR, normal tissue characterization) or taking any regular medication, were included
Dabir (1.3) and Dabir (1.4)	2014	An independent group of normotensive subjects referred for clinical CMR with a low pretest probability of cardiomyopathy or cardiac disease, taking no medication, and with subsequently normal findings on routine CMR, were used.
Edward (1)	2014	Healthy controls
Edward (2)	2015	Healthy controls with no history of cardiac disease, identified from convenience sampling, which is a nonprobability method of drawing representative data by selecting people because of the ease of their volunteering, availability, or easy access.
Ertel	2015	Control subjects were defined as individuals undergoing clinically-indicated contrast-enhanced CMR scans for suspected CVD, whose studies demonstrated normal ventricular size and systolic function, no significant valvular abnormalities, normal vasodilator perfusion

		imaging (for patients in whom stress testing was performed) and an absence of myocardial enhancement on late gadolinium enhancement imaging.
Feirreira (2)	2014	Healthy volunteers of similar age and gender distribution with no cardiac history or known cardiac risk factors, not on cardiovascular medications and with a normal electrocardiogram underwent CMR as controls.
Feirreira (3)	2012	Healthy volunteers with no prior cardiac history or known cardiac risk factors, not on cardiovascular medications and with a normal ECG underwent CMR, including cine, ShMOLLI T1-mapping, STIR and ACUT2E imaging.
Fontana (1)	2012	Normal subjects were recruited through advertising within the hospital, university and general practitioner surgeries. All normal subjects had no history or symptoms of CVD or diabetes. Four subjects had been prescribed statin therapy for hypercholesterolaemia (primary cardiovascular prevention), but no other normal subject was taking any cardiovascular medication. All subjects had a normal BP, 12 lead electrocardiogram and clinical CMR scan.
Fontana (2)	2014	Healthy volunteers were recruited through advertising in hospitals, universities, and general practitioner surgeries. All had no history or symptoms of CVD or diabetes mellitus, and all had normal 12-lead ECG and normal CMR scan.
Kawel-Boehm	2014	Healthy volunteers
Karamitsos	2013	Thirty-six normal volunteers were also recruited. All healthy controls had no history or symptoms of CVD and no risk factors (diabetes mellitus, HTN).
Kawel	2012	24 healthy subjects were imaged in two separate sessions using a 3T scanner and a 32-channel cardiac coil. Volunteers were recruited via the Volunteer Recruitment Office of the National Institutes of Health.
Kuruvilla	2015	Healthy volunteers who were normotensive and did not have a history of HTN were enrolled in the control arm
Liu (1)	2012	Twenty-four healthy volunteers without a history of cardiovascular or systemic disease were enrolled. The ECG obtained prior to the CMR exam did not show any abnormality and the physical exam performed by a physician did not reveal any pathologic finding. Normal LV and RV volumes and systolic functions were confirmed by CMR
Liu (2)	2014	Inclusion criteria were age >21 years and African American. Exclusion criteria were (1) any evidence of ischemic heart disease as indicated by clinical history, previous hospitalization for myocardial infarction, angina pectoris, or evidence of valve disease or HTN; (2)

		any symptoms believed to be related to CVD; (3) HTN and/or diabetes; (4) a positive urine test for illegal drugs; (5) HIV infection; (6) pregnancy; and (7) history of magnetic reso- nance imaging (MRI) claustrophobia.
Luetkens (1)	2014	The control group consisted of healthy volunteers and outpatients referred for nonspecific thoracic pain who did not show structural abnormality at cardiac MR imaging. All control subjects had no medical history of cardiac or vascular disease, no cardiac risk factors, and normal electrocardiographic results. In outpatients referred for nonspecific thoracic pain, a detailed diagnostic workup was performed (including Holter electrocardiography, assessment of cardiac enzymes, echocardiography, and cardiac stress test) and clinical follow-up was unremarkable, without signs of cardiac disease.
Luetkens (2)	2015	Healthy volunteers and outpatients referred for non-specific thoracic pain underwent CMR as controls. All control subjects had un-remarkable CMR results without structural abnormalities, no medical history of cardiac disease, no cardiac risk factors, and normal ECG results. In outpatients referred for non-specific thoracic pain, a detailed
Mordi	2015	21 healthy control patients without any his- tory of CVD, on no medications, and normal resting electrocardiograms
Piechnik	2013	All subjects were recruited through advertising as control cases for research studies. None had evidence of CVD or cardiac risk factors including HTN or diabetes, based on medical history. None were referred as patients for a clinical cardiovascular MR (CMR) scan which then turned out to be normal. In majority of cases the 12 lead ECG, BP or selected blood tests were confirmed normal on the day of scan. There were no pathological findings identified in the available cine images.
Puntmann (1)	2013	cardiomyopathy served as controls. Additional exclusion criteria for both the groups included a history of cardiac events or known coronary artery disease or any general contraindication to contrast- enhanced CMR or adenosine stress and subsequently evidence of regional hypoperfusion on adenosine testing or ischemia-like LGE
Puntmann (2)	2013	Thirty normotensive subjects with low pre-test likelihood for LV cardiomyopathy, not taking any regular medications and, consequently, with normal CMR findings including normal LV mass indexes, served as the control group. Additional exclusion criteria for all subjects were the generally accepted contraindications to CMR (implantable devices, cerebral aneurysm clips, cochlear implants, severe claustrophobia) or a history of renal disease with a current estimated glomerular filtration rate >30 ml/min/1.73 m^2.
Puntmann (3)	2014	Asymptomatic and normotensive subjects taking no regular medication and with no significant medical history (and consequently normal CMR findings, including volumes and mass) served as controls. Exclusion criteria for all subjects were the generally accepted contraindications to CMR (implantable devices, cerebral aneurysm clips, cochlear implants, severe claustrophobia) or a history of renal

		disease with a current estimated glomerular filtration rate <30 mL/min per 1.73 m^2
Reiter	2014	Forty healthy subjects without any history of cardiovascular or pulmonary disease were included in this prospective study. To reduce the influence of age-related differences in myocardial T1 values associated with myocardial changes during aging, the age limit was set to 35 years
Sado	2013	Healthy volunteers recruited from local hospitals, university, and general practice. All volunteers underwent cardiovascular history, examination, 12-lead EKG, and MRI of the heart (including contrast administration), to ensure no evidence of CVD
Tessa	2015	Population of the first part of this study constituted of 22 consecutive healthy asymptomatic subjects without contraindication to MR imaging. All subjects were recruited as control cases for research studies. None were referred as patients for a clinical CMRI scan which then turned out to be normal. None had evidence of CVD or cardiac risk factors including HTN or diabetes. They showed no abnormalities at physical examination, 12-lead ECG and echocardiography.
Tribel	2014	A control group of healthy, normotensive volunteers were recruited from hospital, university, community and general practice settings in Greater London, UK. None were referred as patients for a clinical CMR scan that then turned out to be normal. All normal subjects had no history or symptoms of CVD or diabetes. All subjects had a normal BP (defined as ≤140/90 mmHg), 12-lead ECG and clinical CMR scan. Exclusion criteria for both groups included diabetes mellitus, known ischaemic heart disease, contraindication to CMR (pacemakers) or gadolinium administration (glomerular filtration rate <30 mL/min/m2). Healthy volunteers were excluded if they had a history of cardiovascular symptoms, an abnormal ECG or abnormal CMR
Von KB	2013	The status “healthy” was based on: i) uneventful medical history, ii) absence of any symptoms indicating cardiovascular dysfunction, iii) normal ECG, iv) normal cardiac dimensions and function proven by cine CMR. v) normal myocardial tissue assessed by late enhancement (LGE).

Supplementary table 2.4: Inclusion criteria of disease groups

Study	Year	Inclusion criteria for disease groups
Aus	2015	Patients with symptoms of heart failure underwent clinical examination, blood analysis, and echocardiography and received the suspected diagnosis DCM at the University Hospital Heidelberg between July 2011 and December 2012. For further evaluation CMR was performed in these patients. Twenty-nine patients had increased LVEDV and LVEDD compared with an age- and gender-matched reference group and a reduced LVEF (EF ≤45%; 'DCM'). Significant coronary artery disease was excluded by means of coronary angiography.
Banypersad	2015	One hundred consecutive patients with systemic AL amyloidosis who were assessed between 2010 and 2012 at the National Amyloidosis Centre (Royal Free Hospital, London, UK) and in whom there were no contraindications to CMR (presence of non-MR compatible devices) or contrast administration (GFR < 30 mLs/min) or potential confounders to T1 measurement (known atrial fibrillation at first visit) were recruited. These 100 patients include all 60 patients studied previously in the baseline study.13 Approximately 25% of patients with systemic AL amyloidosis seen at the centre during this period had an eGFR of <30 mL/min/1.73 m2 and were therefore excluded. Six patients who were found to have atrial fibrillation/ flutter once in the scanner after they had consented were not excluded. All patients had histological proof of systemic AL amyloidosis except 2 (2%), who died before biopsy could be undertaken, but in whom monoclonal gammopathies were present and the organ distribution of amyloid on SAP scintigraphy was characteristic of AL type.
Bull S	2015	Patients with moderate or severe AS (based on Doppler echocardiographic demonstration of peak aortic valve gradient ≥36 mm Hg or valve area <1.5 cm2, according to established criteria) were recruited prospectively from cardiology clinics at the John Radcliffe Hospital in Oxford, UK. Exclusion criteria were contraindications to CMR (including defibrillators and pacemakers), more than mild aortic or mitral

		regurgitation, significant LV dysfunction (LVEF <40%), uncontrolled HTN or severe renal failure (serum creatinine >200mmol/l), which could in itself increase myocardial fibrosis
Chen (1)	2015	The inclusion criteria included known CTO confirmed at initial coronary angiography or suspected CTO disclosed by coronary CT angiography indicating coronary artery occlusion. In all instances, patients were excluded if they suffered from claustrophobia, uncontrolled tachyarrhythmias, or had clinical history of renal dysfunction, allergy to contrast media and metallic prosthetic implant. Patients with an estimated or known occlusion duration of 3 months, undergoing previous revascularization were also excluded.
Chen (2)	2015	In a prospective study of 48 consecutive patients (27 ischemic cardiomyopathy, 21 dilated cardiomyopathy) LV scar burdens were quantified (scar core and gray zone using late gadolinium enhancement LGE CMR; interstitial fibrosis using T1 mapping) before CRT implant.
Chin (1)	2014	Patients with mild to severe aortic stenosis were recruited prospectively. Patients who had other significant (moderate or severe) valvular heart disease or cardiomyopathies (acquired or inherited) were excluded. Presence of coronary artery disease was defined by previous infarction, clinical symptoms of angina (in those with mild or moderate aortic stenosis), evidence of myocardial ischaemia, or .50% luminal stenosis in a major epicardial vessel
Chin (2)	2014	Twenty asymptomatic patients with mild-to-severe aortic stenosis were recruited from outpatient clinics at the Edinburgh Heart Centre. The exclusion criteria for patients with aortic stenosis were as follows: (i) other significant valvular heart disease (moderate to severe in nature), (ii) acquired or inherited cardiomyopathies, (iii) previous myocarditis and (iv) the presence of focal LGE.
Dass	2012	Twenty-eight patients with HCM were recruited from the University of Oxford Inherited Cardiomyopathy clinic. The diagnosis of HCM was based on a genetic determination of a pathogenic mutation (14 MYBPC3 mutations; 6 MYH7 mutations), or in the absence of an identified mutation (8 subjects), HCM was defined as the presence of LVH not originating from other causes (≥15 or ≥12 mm in documented familial disease). All patients had a full Bruce protocol exercise tolerance test, and patients were excluded if there was evidence of epicardial

		coronary artery disease based on this test
Doltra	2014	Patients with resistant HTN referred to our institution for RD between January 2012 and October 2013, and those for whom complete clinical and CMR data were available were enrolled. "Resistant HTN" was defined as an office SBP above the target (≥140 mm Hg) or mean ambulatory 24-hour SBP >135 mm Hg despite the use of ≥3 antihypertensive agents of different classes, including a diuretic at maximum or highest tolerated doses. A stable antihypertensive medication regimen (>3-month treatment on stable dosing) was necessary before inclusion. Twenty-three patients who met these criteria and underwent renal denervation were included, and they constituted our RD group. One patient with multiple allergies to antihypertensive preparations was also included.
Edward (1)	2014	35 consecutive patients with asymptomatic chronic, moderate or severe primary degenerative MR without a class I indication for surgery were prospectively identified from the valve clinic at the Queen Elizabeth Hospital Birmingham, UK. Additional inclusion criteria were LVEF ≥60% calculated using the modified Simpsons rule and linear LV internal dimension in systole ≤40 mm measured from the parasternal long axis view on transthoracic echocardiography (TTE). The pathogenesis, lesion, and severity of MR were defined by echocardiography as part of routine care. Exclusion criteria included history of previous myocardial infarction or symptomatic coronary disease; history or evidence on echocardiography or at surgery of rheumatic heart disease history of uncontrolled HTN (>160/100 mm Hg); and known contraindication to MRI. Coronary angiography was performed if patients were considered for surgery on the basis of a class IIa indication (atrial fibrillation, pulmonary HTN, high likelihood of durable repair).
Edwards (2.1)	2015	treated patients who are hypertensive referred to a dedicated HTN clinic.
Edwards (2.2)	2015	Patients were prospectively recruited from renal clinics at the Queen Elizabeth Hospital Birmingham, England, from 2012 to 2014. Inclusion criteria were CKD stage 2 (eGFR 60 to 89 ml/min/1.73 m2 with other evidence of kidney disease: proteinuria/hematuria/structural

		abnormality/genetic), stage 3 (eGFR 30 to 59 ml/min/1.73 m2), and stage 4 (15 to 29 ml/min/ 1.73 m2) with no history or symptoms of CV disease or diabetes. Estimated GFR was measured by the 4-Variable Modification of Diet in Renal Disease formula.
Edwards (3)	2015	In total, 26 consecutive adults with genetically proven ALMS attending the National Centre for Rare Disease at the Queen Elizabeth Hospital Birmingham, England were studied prospectively as part of standard clinical care. Two other patients were seen at the National Centre during this time period but did not proceed with CMR due to contra-indications (one permanent pacemaker; one with a cochlear implant).
Ertel	2015	Patients were classified with acute intermittent systemic capillary leak syndrome on the basis of having one or more episodes associated with the diagnostic clinical triad of 1) hypotension, 2) elevated hematocrit, and 3) hypoalbuminemia, using established criteria
Ferreira	2013	This was a prospective study enrolling consecutive patients with suspected myocarditis from 2 hospitals (1 tertiary care center The John Radcliffe Hospital, Oxford, United Kingdom and 1 medium-sized district general hospital Milton Keynes Hospital, Milton Keynes, United Kingdom). Patients underwent CMR scanning at the John Radcliffe Hospital between January 2010 and March 2012. All patients had: 1) acute chest pain; 2) elevation in cardiac troponin I level (>0.04 mg/l); and 3) history of recent systemic viral disease or absence of significant (>50%) obstructive coronary artery disease on coronary angiography or absence of risk factors for coronary artery disease or age <35 years. Exclusion criteria included contraindications to CMR, previous myocardial infarction, previous myocarditis, or any chronic cardiac conditions. Patients who demonstrated myocardial infarction as evidenced by an ischemic pattern of LGE (i.e., an isolated area involving the sub- endocardium) or an obvious alternative diagnosis on CMR (such as Takotsubo or hypertrophic cardiomyopathy) were also excluded
Florian	2014	Twenty-nine patients with known BMD were prospectively enrolled between July 2012 and May 2013 and underwent comprehensive CMR studies. BMD had been previously diagnosed in a specialized Neurology Centre based on clinical data, skeletal muscle pathology with dystrophin analyses and/or genetic testing. From this population, two patients were excluded due to impossibility of giving contrast and thus, the final study group (BMD group) consisted of 27 patients

Fontana (1)	2014	20 patients with cardiac AL amyloidosis with disease proven by non-cardiac biopsy and cardiac involvement ascertained through echocardiography, sup- ported by a Mayo clinic classification score of 2 or 3 (average age: 60±10, 75% male). Patients with atrial fibrillation or a contraindication to contrast CMR examination were excluded from the study.
Fontana (2)	2015	Subjects were recruited at the National Amyloidosis Centre, Royal Free Hospital, London, United Kingdom, from 2010 to 2014.
Hinojar (1.2)	2015	Patients with HCM (n=95), by demonstration of an LVH (>15 mm) associated with a non-dilated LV in the absence of increased LV wall stress or another cardiac or systemic disease that could result in a similar magnitude of hypertrophy. All patients with HCM had an expressed phenotype with typically asymmetrical septal hypertrophy of increased LVWT, permitting unequivocal clinical diagnoses. HCM patients with previous septal ablation or myectomy were not included.
Hinojar (1.3)	2015	Evidence of treated essential HTN (n=69; SBP of >140 mmHg; diastolic BP of >95 mmHg) and the presence of concentric LVH defined as >12 mm in the basal septal and infero-lateral segments and without evidence of dilated LV cavity (end-diastolic diameter≤5.4 cm for women and ≤5.9 cm for men) on transthoracic echocardiography.
Hong	2015	From March 2010 through November 2013, 123 patients who were suspected to have cardiomyopathy were referred to our hospital. The inclusion criteria for the patient group were as follows: (1) left-ventricular chamber dilatation and LV end diastolic diameter (LVEDD) on short-axis view ≥6 cm and (2) systolic dysfunction with or without right ventricle (RV) dysfunction and LVEF (LVEF) ≥ 40%. Sixty-three patients fit the inclusion criteria. The exclusion criteria were (1) ischemic cardiomyopathy (n=21) and (2) restrictive cardiomyopathy (n = 1). In total, 41 patients were enrolled in this study.
Jellis (1)	2011	We prospectively recruited 67 apparently healthy subjects with T2DM from the hospital clinic and community. Subjects were excluded if they were pregnant or had preexisting microvascular or macrovascular complications of diabetes, known valvular, congenital or ischemic heart disease, or other significant comorbidities, including malignancy, renal failure, or significant psychiatric illness. Valvular disease was defined as greater than mild valvular regurgitation or stenosis or a past history of valve surgery. Additional exclusion criteria were a history

		of HHD manifesting as LVH on echocardiography and contraindications to CMR, such as claustrophobia or metallic implants. Subjects were analyzed as an entire study population and then stratified according to evidence of subclinical myocardial dysfunction (septal E_m >1 SD below normal for age) into predetermined normal and abnormal E_m groups for further assessment.
Jellis (2.1)	2014	Apparently healthy subjects with T2DM were consecutively recruited from the hospital clinic and community, based on an a priori protocol and independent of indications for echocardiographic exam. All subjects were screened for the presence of diastolic dysfunction. Candidates were excluded if they were pregnant, had a self-reported history of symptomatic micro- or macrovascular complications of diabetes (including nephropathy, neuropathy, retinopathy, peripheral vascular disease, ischaemic heart disease, and stroke) or other significant comorbidities including malignancy, renal failure, or significant psychiatric illness. Absence of valvular, congenital, hypertensive, or ischaemic heart disease was confirmed echocardiographically.
Karamitsos	2013	Fifty-three patients with systemic (primary) AL amyloidosis and no contraindications for CMR were recruited from the United Kingdom National Amyloidosis Centre (Royal Free Hospital, London, UK) between 2010 and 2011. All patients had histological confirmation of systemic AL amyloidosis by Congo red and immunhistochemical staining, which was obtained through specimens of kidney, bone marrow, soft tissues, fat, rectum, endomyocardium liver, lymph node, upper gastrointestinal tract, lung, bladder, and peritoneum. Participants were required to have glomerular filtration rate >30 ml/min since LGE was performed. On the basis of a combination of clinical and echocardiographic features, amyloid patients were categorized definite cardiac involvement. The categorization into definite or no cardiac involvement was based on international consensus criteria. An additional category of possible involvement was created for patients with cardiac abnormalities in whom there were confounding features. The categorization was defined as follows: definite cardiac involvement includes either of the following: 1) LV wall thickness of ≥12 mm in the absence of any other known cause; or 2) RV free wall thickening coexisting with LV thickening in the absence of systemic or pulmonary HTN.
Kato	2016	Inclusion criteria of this prospective study included a history of paroxysmal AF patients referred for their first pulmonary vein isolation.

		Exclusion criteria included patients in AF during MRI scan, reduced LV systolic function (LVEF < 50%), cardiomyopathy (HCM, DCM), cardiac sarcoidosis and amyloidosis, severe valvular heart disease, prior myocardial infarction and contraindication to MRI examination (claustrophobia, pacemaker implantation etc.).
Kellman (1.1)	2012	Chronic myocardial infarction was defined as a region of increased signal intensity on LGE that included the subendocardium that was within a coronary territory, and occurring in a patient with a clinical syndrome consistent with an acute coronary syndrome at least 6 months prior to the scan.
Kellman (1.2)	2012	The diagnosis of hypertrophic cardiomyopathy was supported by LVH (wall thickness >15 mm) in the absence of a clinical condition known to cause hypertrophy. If wall thickness was 10-15 mm, one or more additional criteria were required: (1) hypertrophy in a recognizable pattern like that of apical-variant HCM; (2) systolic anterior motion of the mitral valve with mitral regurgitation; and (3) resting LV outflow tract obstruction.
Kuruvilla	2015	Twenty subjects with HTN LVH , 23 subjects with HTN non-LVH were enrolled between November 2010 and October 2013 under an institutional review board–approved protocol. Patients with any other causes of LVH, known coronary disease, significant valvular disease, renal impairment with glomerular filtration rate <45 ml/min/1.73 m2 or reduced systolic function (ejection fraction [EF] <45%) were excluded. Subjects with a history of HTN with SBP >140 mm Hg or diastolic blood. pressure >90 mm Hg on at least 2 office readings , or taking 1 or more medications for HTN, were included. Subjects were then classified as having LVH if their LVM indexed by body surface area (LVMI) as measured by cardiac magnetic resonance imaging was >81 g/m2 for men or >61 g/m2 in women as defined by Olivotto et al. (). Hypertensive subjects not meeting criteria for LVH as defined in the preceding text were included in the HTN non-LVH group.
Lee	2015	Eighty asymptomatic patients with moderate or severe AS capable of more than four metabolic equivalents of physical activity according to routine medical interview, were enrolled in this prospective cohort study from October 2011 to April 2014. Patients underwent echocardiography and cardiac MR imaging. Moderate to severe AS was defined with echocardiography as maximal trans-aortic velocity

		higher than 3 m/sec or mean transaortic pressure gradient of more than 30 mm Hg and aortic valve area of up to 1.5 cm2 . According to the current criteria of severe AS—that is, an aortic valve area index less than 0.6 cm2/m2—78% of the patients (62 patients) had severe AS. Exclusion criteria were more than a moderate degree of concomitant aortic regurgitation (n = 3) or more than a moderate degree of mitral valve disease (n = 3), a previous history of cardiac surgery or myocardial infarction (n = 8), and LVEF of less than 50% at cardiac MR imaging (*n* = 7). Furthermore, symptomatic patients with dyspnea or other symptoms of heart failure—class III or IV according to the New York Heart Association functional classification system—and patients with typical exertional chest pain or syncope (*n* = 11) were excluded.
Luetkens (1)	2014	myocarditis group if they showed clinical evidence of having acute myocarditis. The clinical evidence was the reference standard against which the diagnostic performance of cardiac MR parameters was tested. All patients with acute myocarditis presented with acute chest pain, a history of viral infection during the last few weeks (flulike illness with diarrhea and bronchitis or pneumonia), and elevated serum markers indicating infectious disease (C-reactive protein). All patients had evidence of myocardial injury (electrocardiographic changes such as ST segment changes, atrio-ventricular block, supraventricular tachycardia) and/or elevated troponin, and did not have a medical history of cardiac disease. Coronary artery disease was ruled out before cardiac MR imaging by means of invasive cardiac catheterization. Exclusion criteria included contraindications for cardiac MR imaging, previous myocardial infarction, previous myocarditis, or other acute or chronic cardiac disease. The diagnosis of acute myocarditis was made on the basis of clinical observation only, and cardiac MR imaging results were not taken into consideration.
Luetkens (2)	2016	The study population of this prospective study consisted of patients with suspected acute myocarditis and control subjects. The diagnosis of acute myocarditis was made solely on the basis of clinical observation. This clinical evidence presented the reference standard against which the diagnostic performance of CMR parameters was tested. Patients with suspected myocarditis had: (i) acute chest pain, (ii) evidence of acute myocardial injury [electrocardiogram (ECG) changes and/or elevated troponin serum levels], and (iii) a history of viral infection during the last few weeks with elevated serum markers indicating infectious disease (e.g. C-reactive protein). Coronary artery disease was ruled out before CMR by means of invasive cardiac catheterization. Exclusion criteria included contraindications to CMR, previous myocardial

		infarction, previous myocarditis, and other medical history of cardiac disease. The diagnosis of acute myocarditis was made on the basis of clinical and laboratory observation only, and CMR results were not taken into consideration.
Ntusi	2015	This was a prospective study enrolling nonselected patients with Rheumatoid Arthritis (RA) with no known CVD. RA patients were recruited from 4 hospitals in the Thames Valley, United Kingdom. They underwent clinical assessment and CMR scanning between November 2010 and December 2012. Patients with RA included in the study were between 18 and 65 years of age and had a confirmed diagnosis of RA based on the 1987 American College of Rheumatology criteria (modified in 2010) (), as assessed by clinical consultant rheumatologists. Exclusion criteria included inability to tolerate CMR, contraindications to CMR, nonsinus rhythm, known heart disease (previous MI, previous myocarditis on history, heart failure, arrhythmia on 12-lead electrocardiography, or other chronic cardiac condition), renal impairment (estimated glomerular filtration rate <30 ml/min), impaired liver function (alanine aminotransferase level more than twice the upper limit of normal), and known hypersensitivity to gadolinium Female subjects who were pregnant, lactating, or planning a pregnancy were also excluded.
Puntmann (1)	2012	Thirty-three patients with an established diagnosis of SLE as per the American College of Rheumatology revised classification criteria and no history of previous cardiac symptoms were recruited from the Louise Coote Lupus Unit, St Thomas' Hospital, London. All patients were in clinical remission with stable blood results, and no change in medication was seen within the previous ≤8 weeks
Puntmann (2)	2013	Groups were based on CMR findings and consisted of subjects with known HCM and NIDCM. Diagnosis of HCM was based on the demonstration of a hypertrophied LVassociated with a non-dilated LV in the absence of increased LV wall stress or another cardiac or systemic disease that could result in a similar magnitude of hypertrophy. All patients with HCM had an expressed phenotype with typically asymmetric septal hypertrophy of increased LV wall thickness, permit- ting unequivocal clinical diagnoses. NIDCM was defined as an increase in LV volumes, a reduction in global systolic function, and absence of evidence of ischemic-like LGE
Puntmann (3)	2014	Patients were classified as ischemic heart disease (IHD) if they had at least 1 of the following: (1) significant documented coro- nary artery

		disease, (2) previous coronary revascularization, (3) pre- vious history of myocardial infarction, (4) evidence of ischemic-type LGE or significant inducible ischemia on CMR.[19] Diagnosis of non- ischemic DCM (NICM) was based on the evidence of (1) increased LV end-diastolic volume indexed to body surface aream, (2) reduced LVEF compared with published reference ranges nor- malized for age and sex, (3) absence of subendocardial LGE indica- tive of previous myocardial infarction, and (4) absence of any specific identifiable underlying cause (eg, aortic or valvular disease, myocar- ditis, amyloid, hypertrophic cardiomyopathy).[1]
Sado (1)	2012	Forty-four consecutive genetically proven Anderson Fabry Disease (AFD) patients were prospectively recruited from an inherited cardiac disease unit. Thirty-four patients (77%) had received enzyme replacement therapy for 78±40 months. Nine (90%) of those not on therapy were women. Six patients (14%, 5 women) had a clinical diagnosis of HTN and AFD. Twenty-four patients (55%), of whom 58% were men, had LVH, defined as an elevated LVMI calculated from cardiac magnetic resonance (CMR) steady-state free- precession cine images. All these patients also had a maximal LV wall thickness on CMR of >12 mm (which previous guidelines and publications have used to define the presence of LVH in AFD using echocardiography)
Sado (2)	2015	We prospectively recruited 88 consecutive patients with suspected iron overload referred for clinical MRI assessment of myocardial iron assessment at the Heart Hospital, London, UK. Most patients had an underlying diagnosis of beta thalassemia major, with the remainder split between genetic hemochromatosis, Diamond Blackfan anemia, beta thalassemia intermedia, sickle cell anemia, sideroblastic anemia, acute myeloid leukemia, aplastic anemia, PK deficiency, acute biphenotypic leukemia, pyropokilocytosis, myelodysplasia, congenital dyserythropoietic anemia, congenital erythropoietic porphyria, and a raised ferritin of uncertain etiology. No patients were excluded
Singh	2015	Patients participating in the 'Prognostic importance of microvascular dysfunction in AS' (PRIMID-AS) study. were prospectively recruited from a single centre. Inclusion criteria were (i) asymptomatic and (ii) moderate or severe AS (based on two or more echocardiographic criteria). Exclusion criteria were (i) contraindication to MRI, (ii) eGFR , 30, (iii) ejection fraction (EF) ,40%, (iv) other valve disease of

		more than moderate severity, and (v) recent myocardial infarction or previous coronary artery bypass grafting. The patient group was split into moderate and severe AS subgroups according to European Society of Cardiology (ESC) guidelines for further analysis
Soslow	2016	Participants in the DMD group were recruited from the multidisciplinary Neuromuscular-Cardiology Clinic and were over 7 years of age. The diagnosis of DMD was confirmed by either skeletal muscle biopsy or the presence of a dystrophin mutation and skeletal muscle weakness. Exclusion criteria were: requiring sedation for CMR, renal dysfunction or other contraindication to contrast-enhanced CMR
Tribel	2015	Hypertensive subjects were recruited prospectively from a specialist HTN clinic in a tertiary referral hospital. All patients had been investigated for secondary HTN as part of their clinical work-up in the specialist HTN clinic. Eligible patients were men and women between 18 and 80 years of age with essential HTN. In accordance with the 2011 UK HTN guidelines, ABP measurement (ABPM) was used to confirm diagnosis of recruited patients (clinic BP of ≥140/ 90 mmHg and daytime ABPM of ≥135/85 mmHg) and patients with “white coat” HTN (not on anti- hypertensive medications with a normal ABPM) were excluded. Comprehensive assessment on the day of the CMR consisted of clinical history, arterial stiffness and BP measurement following a period of rest, transthoracic echocardiography, electrocardiogram (ECG), blood tests (NT-pro-BNP, full blood count for the haematocrit, renal function, and lipid profile), 6- minute walk test (6MWT), and CMR (including equilibrium diffuse myocardial fibrosis protocol). ECG was analysed for LVH by Cornell product and Sokolow-Lyon voltage criteria
Zhang	2015	200 patients with SLE were prospectively enrolled at Johns Hopkins University for a previous imaging trial and underwent CT coronary angiography. From this population, randomly selected patients were recruited as part of a study to assess microvascular disease, edema, and fibrosis in SLE patients using cardiac MRI subjects with significant (70 %) coronary artery stenosis on prior cardiac CT or coronary revascularization were excluded. A total of 24 subjects with the diagnosis of SLE were enrolled. Diagnosis of SLE was based on American College of Rheumatology (ACR) criteria . Complete history and physical was performed in all patients at the time of enrollment. Disease activity was assessed by using the systemic lupus erythematosus disease activity index (SLEDAI) ()

Ooji	2015	Thirty-five patients with asymmetric basal-septal hypertrophy based on echocardiography were referred for cardiac MRI as part of HCM assessment.
Rodrigues	2017	Normotensive healthy volunteers
Mordi	2017	healthy volunteers were recruited from public advertising. Volunteers had no self-declared past medical history and were not taking any medication at the time of recruitment. Additionally, we performed a case record review to ensure there was no significant past medical history and that a resting electrocardiogram, echocardiogram, and BNP test were available. Volunteers were only recruited if all of these were normal
Homsi (1)	2017	Healthy age-matched and sex-matched outpatients (n=20) referred for nonspecific cardiac symptoms served as controls. All control subjects had unremarkable CMR results, no medical history of cardiac disease, and no risk factors for cardiac disease, and a detailed diagnostic workup including electrocardiogram showed no signs of cardiac disease.
Luetkens (3)	2017	The control group consisted of healthy volunteers and outpatients referred for nonspecific thoracic pain in which a detailed diagnostic workup and clinical follow-up were unremarkable and without signs of cardiac disease.
Mazurkiewicza	2017	healthy age- and sex-matched volunteers with no significant medical history and with normal physical examination and 12-lead ECG.
Homsi (2)	2017	Healthy age-matched and sex-matched outpatients (n=20) referred for nonspecific cardiac symptoms served as controls. All control subjects had unremarkable CMR results, no medical history of cardiac disease, and no risk factors for cardiac disease, and a detailed diagnostic workup including electrocardiogram showed no signs of cardiac disease
Gao	2016	healthy age-matched female controls.

Rutherford	2016	compared native myocardial global and septal T1 relaxation times as potential markers of diffuse myocardial fi brosis in incident HD patients with those of healthy volunteers (HVs).
Shang	2017	normal controls were recruited from the community population

Appendix 2C: Software used for analysing T1 mapping:

Variety of software was used to analyse T1 mapping. In brief, 9 commercial software has ability to analyse T1 mapping and ECV, which are: ARGUS (Siemens, Erlangen, Germany), ViewForum (Extended Workspace, Philips Healthcare, The Netherlands), Qmass (Medis Medical Image Systems), RelaxMaps in PRIDE environment (Philips Healthcare, The Netherlands), CVI42 and CMR42 (Circle Cardiovascular Imaging, Alberta, Canada), Prototype Vizpack software (General Electric Healthcare), MediaCare (Boston, Massachusetts) and OsiriX (Geneva, Switzerland). There are also free or open source software was reported in literature: ImageJ (National Institutes of Health, Bethesda, MD), Segment (http://segment.heiberg.se), MC-ROI (Interactive Data Language-IDL, ITT Exelis, McLean, Virginia), MRmap.

Chapter 3

MRI-derived myocardial strain measures in normal subjects

- a systematic review and meta-analysis

Abstract

Objectives: The aim of this study was to perform a systematic review and metaanalysis to estimate the normal ranges of MRI based MRI-FT and to identify sources of variations. Similar analyses were also performed for Strain-Encoding (SENC), Displacement Encoding with Stimulated Echoes (DENSE) and myocardial tagging (MT).

Background: MRI-FT is a novel technique for quantification of myocardial deformation using MRI cine images. However, the reported 95% confidence intervals (CIs) from the two largest studies have no overlaps.

Methods: Four databases (EMBASE, SCOPUS, PUBMED, and Web of Science) were systematically searched for MRI strains of LV and RV. The key terms for MRI-FT were: “tissue tracking”, “feature tracking”, “cardiac magnetic resonance”, “cardiac MRI”, “CMR” and “strain”. A random effect model was used to pool LV global longitudinal strain (GLS), global circumferential strain (GCS), global radial strain (GRS) and RVGLS. Meta-regressions were used to identify the sources of variations.

Results: 659 healthy subjects were included from 18 articles for MRI-FT. Pooled mean of LVGLS was 20.1% [95% CI: 20.9, 19.3], LVGCS 23% [24.3, 21.7], LVGRS 34.1% [28.5, 39.7], and RVGLS 21.8% [23.3, 20.2]. Although there were no publication biases except for LVGCS, significant heterogeneities were found. Meta-regression showed that variation of LVGCS was associated with field strength (β=3.2, p=0.041). Variations of LVGLS, LVGRS, and RVGLS were not associated with any of age, gender, software, field strength, sequence, LVEF, or LV size. LVGCS seems the most

robust in MRI-FT. Among the MRI-derived strain techniques, the normal ranges were mostly concordant in LVGLS and GCS but varied substantially in LVGRS and RVGLS.

Conclusion: The pooled means of 4 MRI-derived myocardial strain methods in normal subjects are demonstrated. Differences in field strength were attributed to variations of LVGCS.

.

I. Introduction

Cardiac wall motion analysis plays a central role for assessment of ventricular contractile function. Cardiovascular magnetic resonance (CMR) is a radiation-free, reference standard for assessment of cardiac anatomy and wall motion because of its excellent endocardial border definition due to high spatial and contrast resolution. However, the current assessment of wall motion is primarily subjective, and results are skill- and experience- dependent. The quantification of myocardial deformation provides further insights into cardiac function in a variety of subclinical cardiac diseases.[165, 166] Although several quantitative assessment techniques have been proposed, such as myocardial tagging (MT), phase contrast velocity imaging, displacement encoding (DENSE), and strain encoding (SENC) for strain analysis.[167, 168], these methods require additional sequences and time.

Recently, MRI FT has been introduced using cine images and provides a fast and accurate assessment of both ventricular [61, 169-175] and atrial strains [68, 72] with STE or MT[176]. To date, however, only a few data exist on MRI-FT normal reference values, and they are based on small or modest sample-size studies. The reported 95% confidence intervals (CIs) from the two largest MRI-FT studies have no overlaps[177, 178]. Therefore, in this study, we aimed 1) to perform a systematic review for studies that reported MRI-FT strain values from normal healthy population, 2) to estimate the pooled means of their myocardial strains by meta-analysis, and 3) to elucidate possible sources of variation affecting the strain values by meta-regression analyses. We also performed the same systematic review and meta-analysis for DENSE, SENC, and MT.

II. Methods

Search Strategy: We followed the Preferred Reporting Items for Systematic reviews and Meta-Analysis (PRISMA) guideline when performing our systematic review and meta-analysis[179]. The first search was performed on 4 August 2015, and the last search was performed on 21 October 2015. Four academic databases (EMBASE, PUBMED, Scopus and Web of Science) were systematically searched for the strain values of the left or right ventricle derived from MRI-FT technique by two co-authors (HQV and KN) under the guidance of a librarian trained in systematic review. The key terms were: "tissue tracking", "feature tracking", "cardiac magnetic resonance", "cardiac MRI", "CMR" and "strain". The reference lists of these articles were also scrutinized to identify some additional appropriate studies. Search hedges created are listed in the online supplementary material (**Appendix 3A**). The study was prospectively registered with the PROSPERO database of systematic reviews (registration: CRD42015025616). Methods for DENSE, SENC, and MT are reported in Appendix B and C.

Study selection: From these lists, studies were included if the articles reported strain values using cardiac MRI in healthy subjects. The two co-authors reviewed and chose studies if the studies met each of following criteria: (1) studies recruited extensively normal healthy subjects (2) studies included a control group, which was defined as normal and healthy. The definition of the normal healthy group varies with studies. In this meta-analysis, this group of subject was identified if subjects: (1) were not associated with any disease (diabetes, heart failure, etc.), or associated with overt symptoms or adverse outcomes, (2) did not have any history of heart disease, (3) were

not currently implanted with any cardiac devices, (4) were indicated as being healthy, and (5) had age >18 years old. The definitions of healthy subjects are shown in the supplementary Table 3.1. All discrepancies were reviewed and resolved by consensus of all authors.

Study exclusion: The search was uniquely concentrated on human studies, published in English. Animal studies and conference presentations were excluded.

Data Collation: Strain data were extracted from individual studies and entered into an electronic database. LVGLS, LVGCS, LVGRS and RVGLS were extracted from text, table and graphs. In cases where we believed that multiple articles to come from a single dataset, the largest study was selected.

Data extraction: All demographic, common clinical characteristics and strain information were extracted from texts and tables. In cases where the same subjects were measured several times in a day by using the same equipment[180] the first dataset was used. A study applied 2 different software to the same population [181]. Only one software data (TomTec) was selected and used because vast majority of the articles used the software.

Outcomes of Interest: In this meta-analysis, our outcomes of interest were normal ranges of left and strains (LV-GLS, -GCS, -GRS, and RVGLS) measured by MRI-FT.

Statistical analysis: The means and 95% confidence intervals (CI) of LVGLS, LVGCS, LVGRS, and RVGLS were computed using random effect models weighted by inverse variance. Funnel plots with and without the Duval and Tweedie's trim and fill were constructed and Egger's test was used to assess potential publication bias. The

heterogeneity between subgroups or between studies was assessed by Cochran Q's test and the inconsistency factor (I^2). Meta-regressions were performed for each risk factor to examine possible study factors associated with heterogeneity. Beta coefficient and its CIs were derived using the least-mean squares fitting method. Statistical analysis was performed using R version 3.2.2 (The R Foundation for Statistical Computing, Vienna, Austria) with the "metafor" package. Two-tailed p values were applied and the threshold of statistical significance was 0.05 except for Egger's test, where 0.1 was used.

III. Results:

Study selection: For MRI-FT, 416 titles were matched with the key terms from the 4 databases (EMBASE [218], PubMed [64], Scopus [59], and Web of Science [75]; Figure 1). Eighteen valid studies (659 normal participants) met the selection criteria and were included in this meta-analysis, where 17 were eligible for LVGCS, 12 for LVGLS and LVGRS, and 9 for RVGLS.

Most subjects were middle-aged (**Table 3.1**). Many studies (15/18 studies) had a small sample size (n ≤50) and only three studies had sample size ≥100 with a maximum of 150. Thus, sensitivity analyses were based on the sample size.

Software used for MRI-FT was also collected to find the association of software and the variation of strain. A majority of included studies used software from one vendor (Diogenes or 2D CPA, TomTec Imaging Systems, Unterschlessheim, Germany), the other software included Velocity Vector Imaging (Siemens Medical Solutions, Malvern, PA, USA), Circle (Circle Cardiovascular Imaging Inc., Calgary,

Canada)[181] and MTT (Toshiba Medical Systems, Tochigi, Japan)[171]. Further detailed information can be found in **Supplementary table 3.2.**

Normal Ranges of MRI-FT:

LVGLS: The pooled mean of LVGLS was -20.1% [95% CI: -20.9, -19.3] (**Figure 3.2**). Among 12 studies, 9 reported LVGLS from the apical 4-chamber view only and three from the three apical three views, where their values were quite similar. Although no significant publication bias was identified by the funnel plot (**Supplementary figure 3.1**) and Egger's test, there was a significant heterogeneity in LVGLS. A univariable meta-regression was performed to find factors that have significant contributions to the heterogeneity (Supplementary table 3.3). LVGLS was not associated with sex, field strength, sequence, scanner vendor and LVEF. All studies reported LV GLS used the same software.

LV GCS and GRS: The pooled means of LVGCS and LVGRS were -23.0% [-24.3, -21.7] and 34.1 [28.5, 39.7]. Among the 17 articles for LVGCS, 10 reported LVGCS from only one level of short-axis (the papillary muscle level) and the remaining 7 from three short axis levels. Their reported LVGCS values also overlapped (**Figure 3.3**). Similarly, 7 out of 12 reported LVGRS from one level only and the rest 5 from three levels, also showing significant overlap (**Figure 3.4**).

Egger's tests indicated a publication bias for LVGCS (p=0.07) (**Supplementary figure 3.1**) but not in LVGRS. Normal range in LVGCS from the Duval and Tweedie's trim and fill process was quite similar. Sample size was not associated with the LVGCS heterogeneity in both meta-regression, (β=-0.016, p=0.3) and cumulative forest plot

(**Supplementary figure 3.2**). Meta-regression analyses of LVGCS showed significant contributions of field strength (**Supplementary table 3.3**). Among our hypothesised confounding factors, there were no confounders that can significantly explain the heterogeneity of LVGRS.

RVGLS: All nine studies reported RVGLS from the 4-chamber view only and the pooled mean was -21.8 [-23.3; -20.2] (**Figure 3.5**). Although no publication bias was seen, there was a significant heterogeneity. In meta-regression analyses, none of age, sex, field strength, sequence, LVEF or software vendor was associated with the variability of RVGLS.

Additional analysis: Table 2 summarizes coefficient of variance of the included articles. LVGCS tends to show smallest inter- and intra-observer variability in MRI-FT strain.

Subsequent sensitivity analyses based on sample size (all, ≥20 or ≥100) revealed no obvious effect of sample size (**Supplementary figure 3.3**). Additional sensitivity analyses by limiting articles using TomTec software showed similar results (**Supplementary table 3.4**)

Similar investigations were performed for SENC, DENSE, and MT. Results are summarized in Table 3 and Online Supplementary materials (**Supplementary figures 3.4-3.7** and **Supplementary tables 3.5-3.8**). MRI-FT and SENC share similar LVGLS but MT showed smaller. MRI-FT demonstrated slightly larger LVGCS than the other MRI-strain techniques. There were substantial heterogeneities in normal ranges of LVGRS and RVGLS.

IV. Discussion

This is the first systematic review and meta-analysis of pooled mean of MRI-FT among normal subjects. Although MRI-FT has substantial potential, the normal ranges from the two largest studies have no overlaps. This really hampers wider use of this technique. Our results warrant the need for a larger-scale study determining normal rages for FT strains, preferably with some standardizations for the number of views used. In the meantime, estimated means (with 95%CI) would serve as a reasonable guide for end-users. We also performed similar analysis for other MRI-derived strains like MT, SENC, and DENSE as comparators.

Software. Software from one vendor dominated currently, and more than half of the studies measured LV strains from a single view - but this had a minimal impact on these measurements. Most articles used SSFP or b-SSFP cine images (**Supplementary table 3.1**). The main reasons for this are 1) a routine CMR technique, 2) high contrast to noise ratio (CNR) at the endocardial-blood interface, 3) little blood flow dependency, 4) higher temporal resolution, and 5) short acquisition time.[171] The other sequence used was fast gradient echo cine [171]. Their strain values were similar to those from SSFP but required a longer acquisition time.

Sample size. Most of studies included had a small sample size (n ≤50) and only three studies had sample size ≥100 with a maximum of 150 with limited overlap among their normal ranges. This may be because CMR requires more resources than other non-invasive cardiac modalities. LVGLS was minimally affected by the sample sizes. LVGCS from small-sized studies seemed to show smaller values, although this was not a significant determinant of LVGCS in the meta-regression.

Slices. More than a half of the studies derived LVGCS and LVGRS from a single slice at the papillary muscle level only and the rest used three short-axis planes although their normal ranges overlapped (**Figures 3.3 and 3.4**). Similarly, most of the LVGLS were calculated from the 4-chamber view only, while only three papers used three apical views. They are also overlapped (**Figure 3.2**). Nevertheless, the use of single plane method should depend on the underlying disease - if a heterogeneous distribution of disease process can be anticipated, three-level method would reflect more accurate deformation of the whole heart.

Observer variability. While the normal values of LVGLS and LVGCS fluctuated in a narrow range, LVGRS had a wider range of CIs. Supplementary figure also reflects this variation, where LVGRS for different sample sizes yielded an unpredictable pattern. Unfortunately, our meta-regression analyses did not identify the source of this variation. The same issue has been reported in STE [182] and its causes remain contentious. We speculate that through-plane motion could be a partial explanation for this problem.

Calculation of global strain. Another point to be mentioned is that there are two ways of global strain calculation: 1) global strain is an average of peaks of individual strain curve and 2) peak of the mean curve. Only one paper clarified which method they used to obtain global strains. Although a high correlation between the two methods was reported [177], this ambiguity caused difficulties and bias in this meta-analysis. In this context, only results from second method were included. In addition, a few studies measured LVGLS using apical three views and LVGCS and LVGRS from three short axis planes.

Heterogeneity among studies: In our meta-analysis, each of strain metrics had large I^2 values. The interpretation of I^2 was discussed in Appendix F (**supplementary materials**). Most of our hypothesised confounding factors were not fully explanatory for this. This problem could be further explained by three potential reasons: 1) Population. Normal strain values among different populations may slightly differ. 2) Inter-observer variability. Inter-observer variability could be another source of variation among studies. Differences defining myocardial contours may result in between-study heterogeneity. **Table 3.2** summarizes inter- and intra-observer variability of included studies. The CV of inter-observer variability ranged from 3.7% to 32.2%, while those of intra-observer were 2.7% to 43.5%. LV GCS seems to be the most robust. 3) Different software vendors also could be a source of heterogeneity. However, our sensitivity analysis including studies using TomTec only (**Supplementary tables 3.4a and b**) did not show substantial reduction in I^2.

Comparisons with normal ranges among various methods. Normal ranges of STE, MT, SENC, DENSE and MRI-FT are summarized in Table 3. Although MRI-FT derived LVGLS and LVGCS yield quite similar ranges to those of STE, there are discrepancies in LVGRS and RVGLS.

MT is an MRI technique that generates grid patterns or parallel lines on the magnitude-reconstructed images (SPAMM or CSPAMM), which are then analyzed, or by extracting information about myocardial tags in k-space (HARP). The strength of MT is its insensitivity to through-plane motion [178]. However, MT suffers a low temporal resolution, low signal-noise ratio, and requires some extra sequences, prolonged image acquisition, and a longer breath-hold. The agreement between MRI-

FT and MT still remains controversial. Some reported a poor agreement [183], others showed high correlations [178, 184]. In this study, LVGLS and GCS by MT were somewhat less negative than those by STE and MRI-FT. This could be due to its insensitivity to through-plane motion.

DENSE is another technique for strain calculation, first introduced in 1999 [185]. The phase-reconstructed images by DENSE have high temporal and spatial resolution and direct extraction of motion data [186, 187]. However, this technique required some specific sequences, which may prolong scan time. So far, applications of DENSE in clinical have been still limited with small sample size and only applied for short-axis images. The pooled normal ranges of DENSE were lower than MRI-FT. Due to a few study that reported LVGRS by DENSE, it varied in a very wide range of 95% CI.

SENC is developed on the concepts of myocardial MT, but it uses tag planes parallel to the image plane [188]. In other words, LVGLS is obtained from short-axis views and LVGCS from long-axis views. In general, normal ranges of SENC were similar to those by MRI-FT. Interestingly, SENC can provide RVGCS. Between-study variability of both LV and RVGCS by SENC could be explained by proportions of males. Additionally, that of RVGCS could be also explained by age, gender, and software vendors.

V. Limitation

Several factors merit consideration in the interpretation of our results. First, like all meta-analyses, this work is limited by variations in the original studies and publication bias, although we followed standard approaches to detect this. Likewise, the constituent

observational studies may be limited by biases in the recruitment process. Second, we have assumed that all of the measurements were performed by the experts, but the levels of expertise among individuals who have actually measured the strain are uncertain. Third, significant heterogeneities among studies were identified. Thus, we performed subsequent meta-regression analyses and stratifications to elucidate the sources of the variations. Fourth, as mentioned above, most papers had sample sizes of <50, and larger sample sized studies are needed for more accurate estimation of normal ranges in MRI-FT, especially in RVGLS. Fifth, our study may not have enough power to test vendor differences because only three studies reported non-TomTec software data. Only one MRI-FT study performed head-to-head comparison[175]. Further studies on this issue should be warranted because this could be a modifiable issue as shown in STE[189]. Sixth, the high intra-study and inter-study variability and the systematic differences between studies cause difficulties to derive clear normal ranges. Finally, strain is affected by loading conditions, but we had insufficient data to analyse this.

VI. Conclusion

The pooled means of MRI-FT strains are similar to those of STE. Differences in sequence and software were attributed to variations of LVGRS and LVGCS, respectively. LV and RV GLS variations seemed likely not to be attributed to any of age, gender, software, field strength or sequence.

Acknowledgements

The authors thank Ms Elizabeth Seymour, for her support in systematic review.

Figure 3.1: PRISMA flow chart

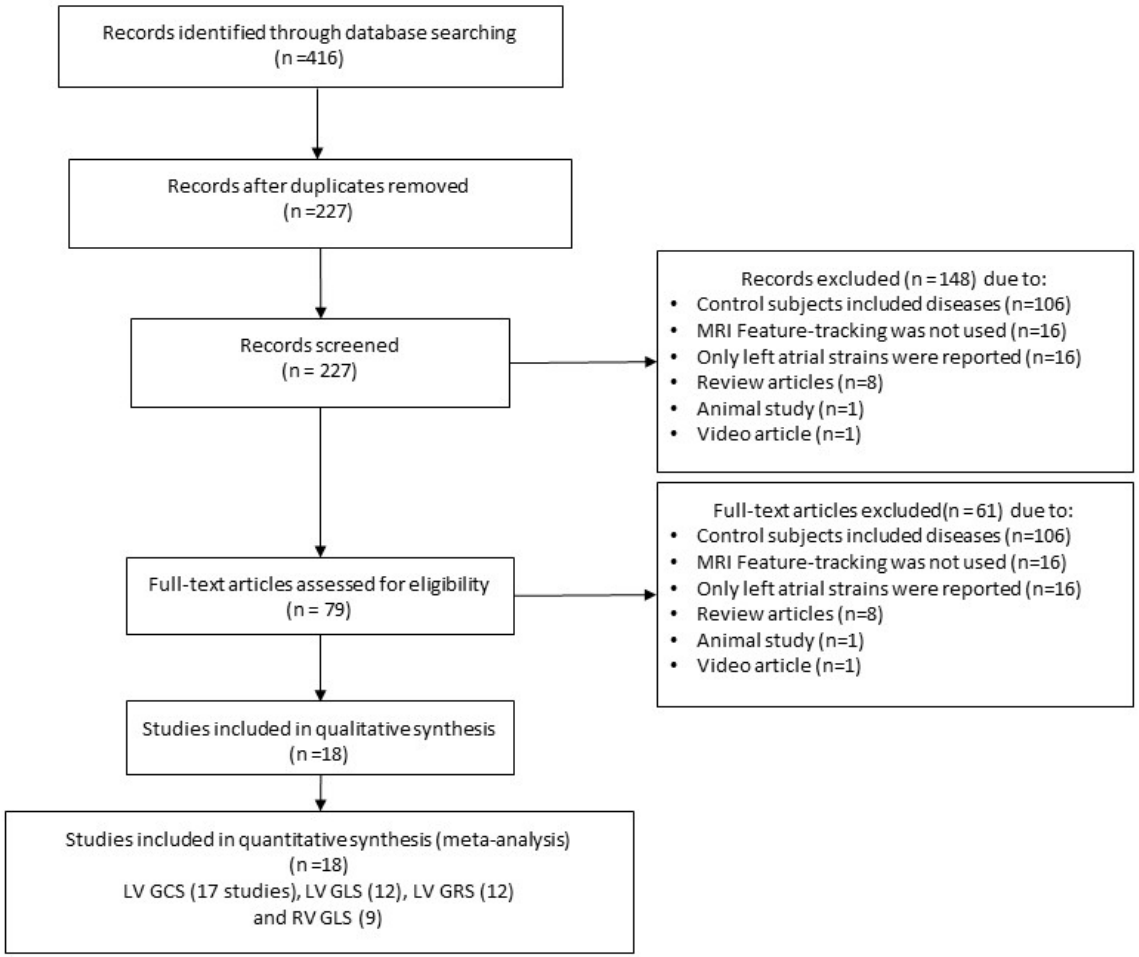

Figure 3.1: Normal value of LV GLS

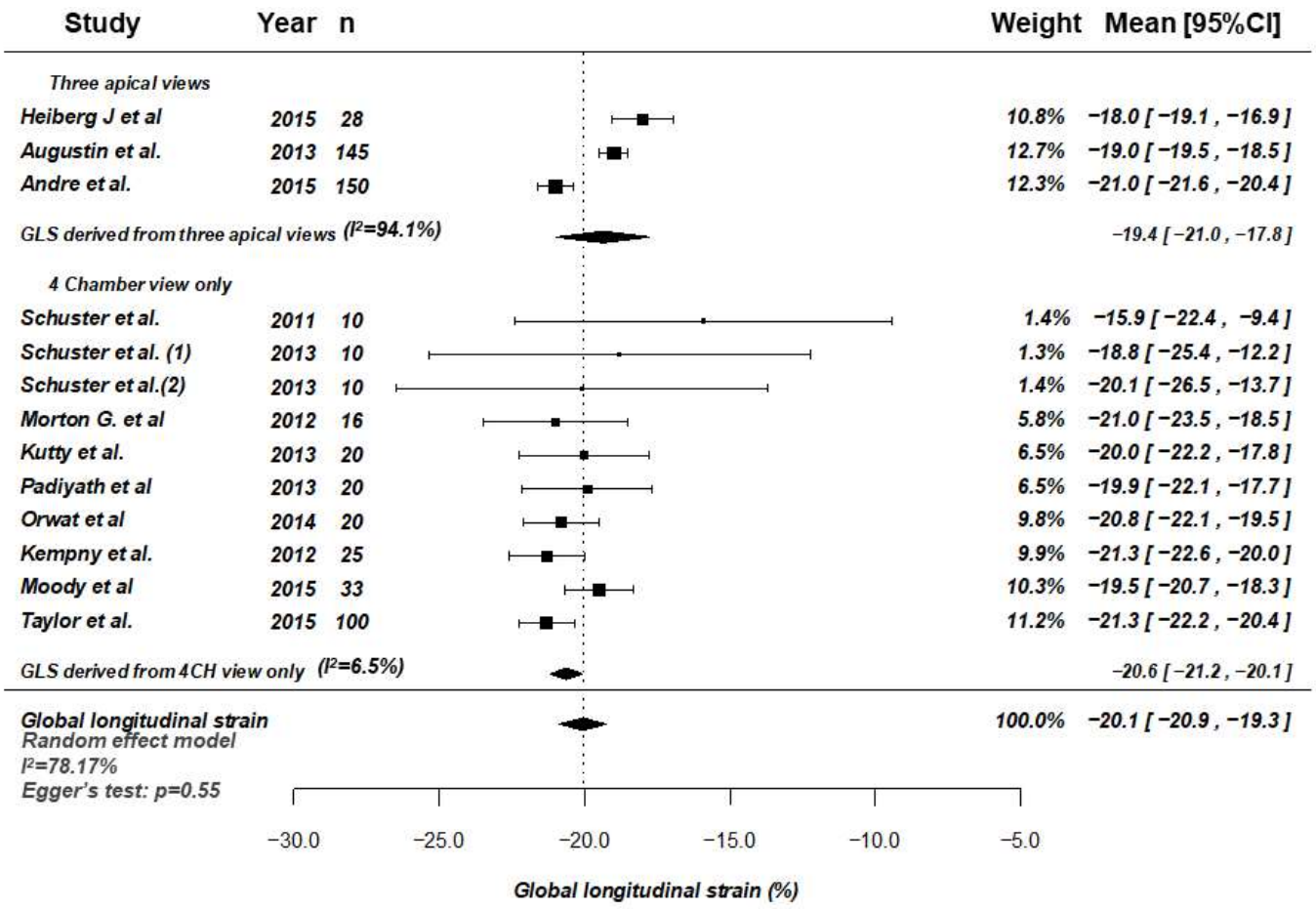

Figure 3.2: Normal value of LV GCS

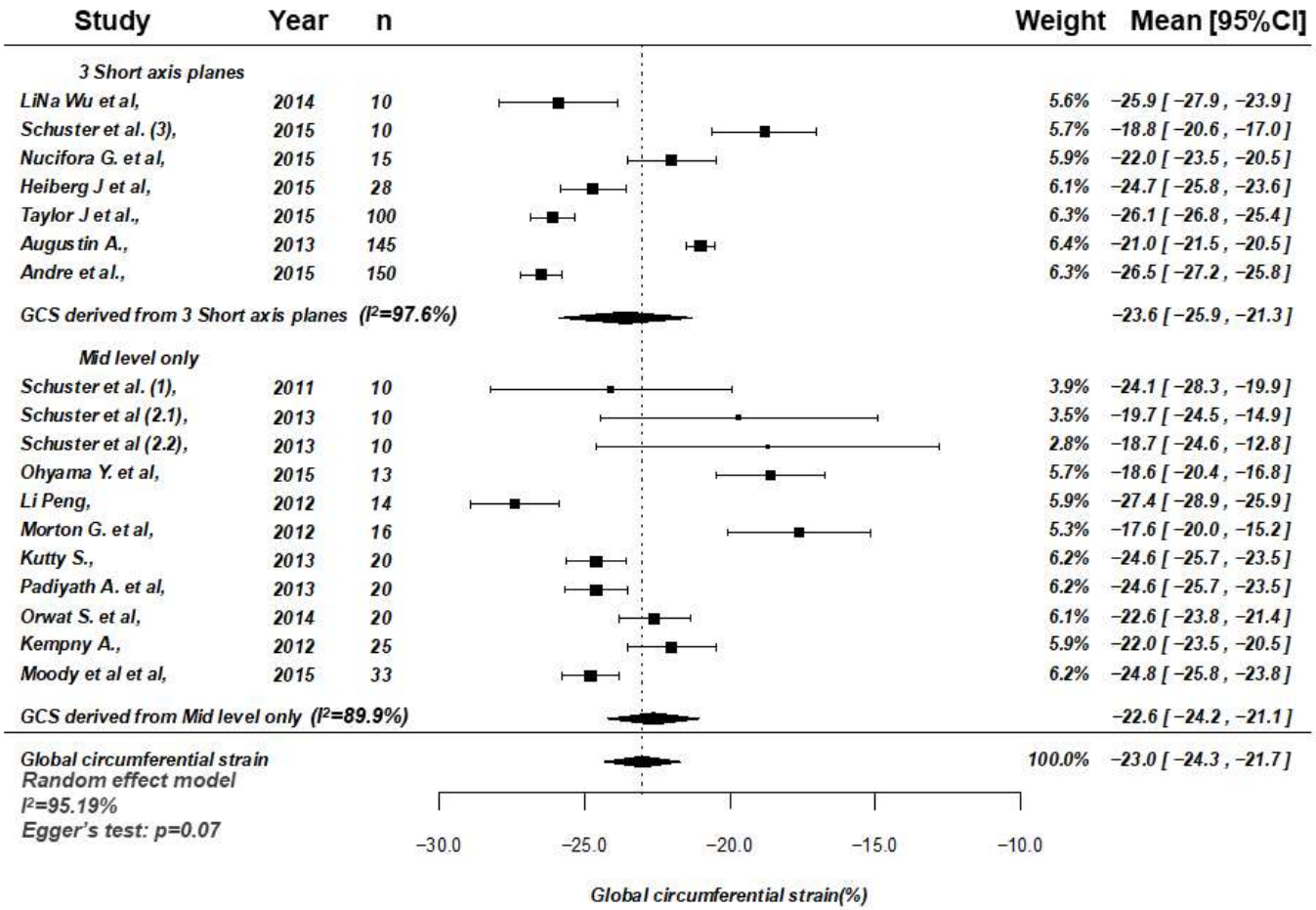

Figure 3.3: Normal value of LV GRS

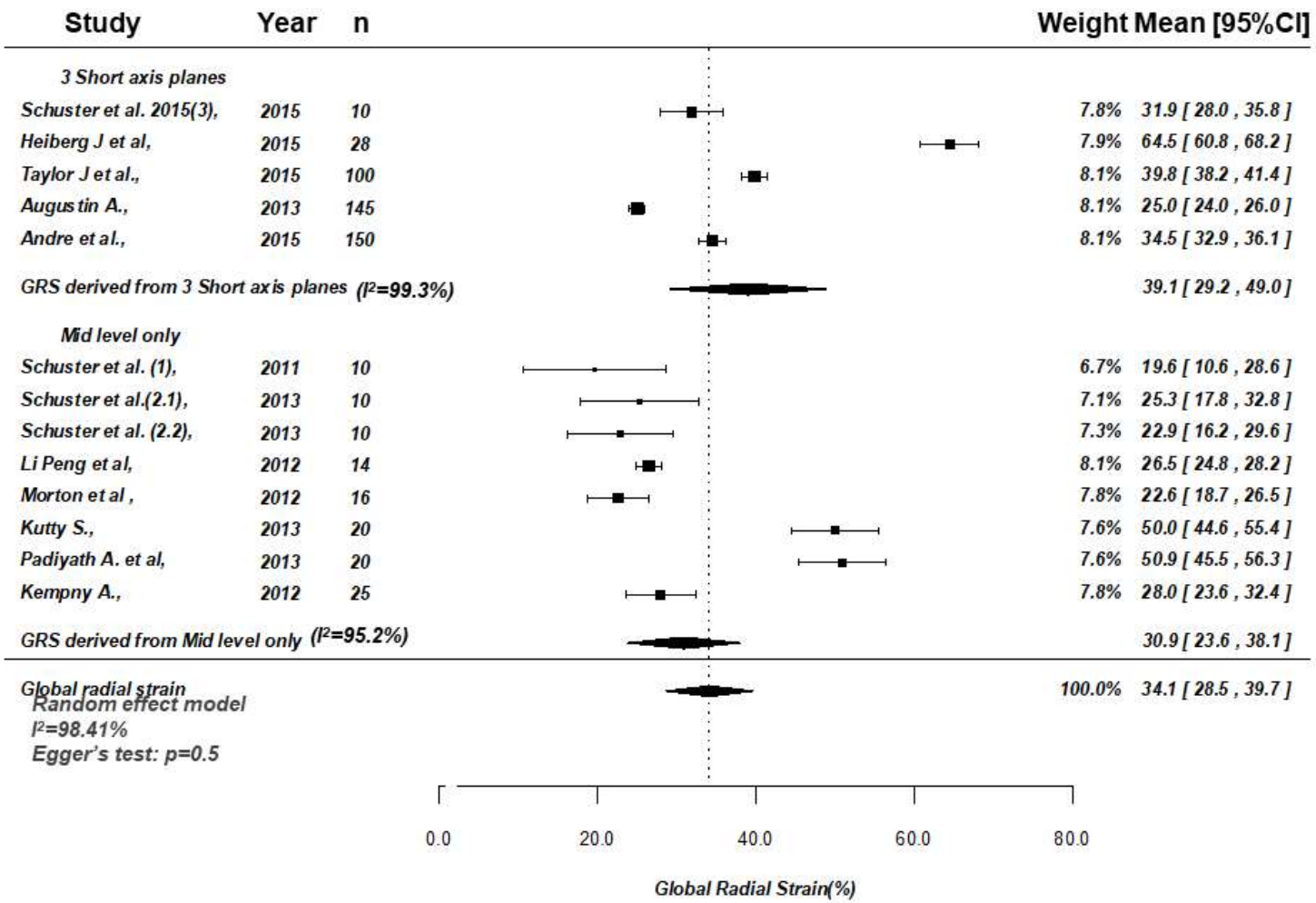

Figure 3.4: Normal value of RV GLS

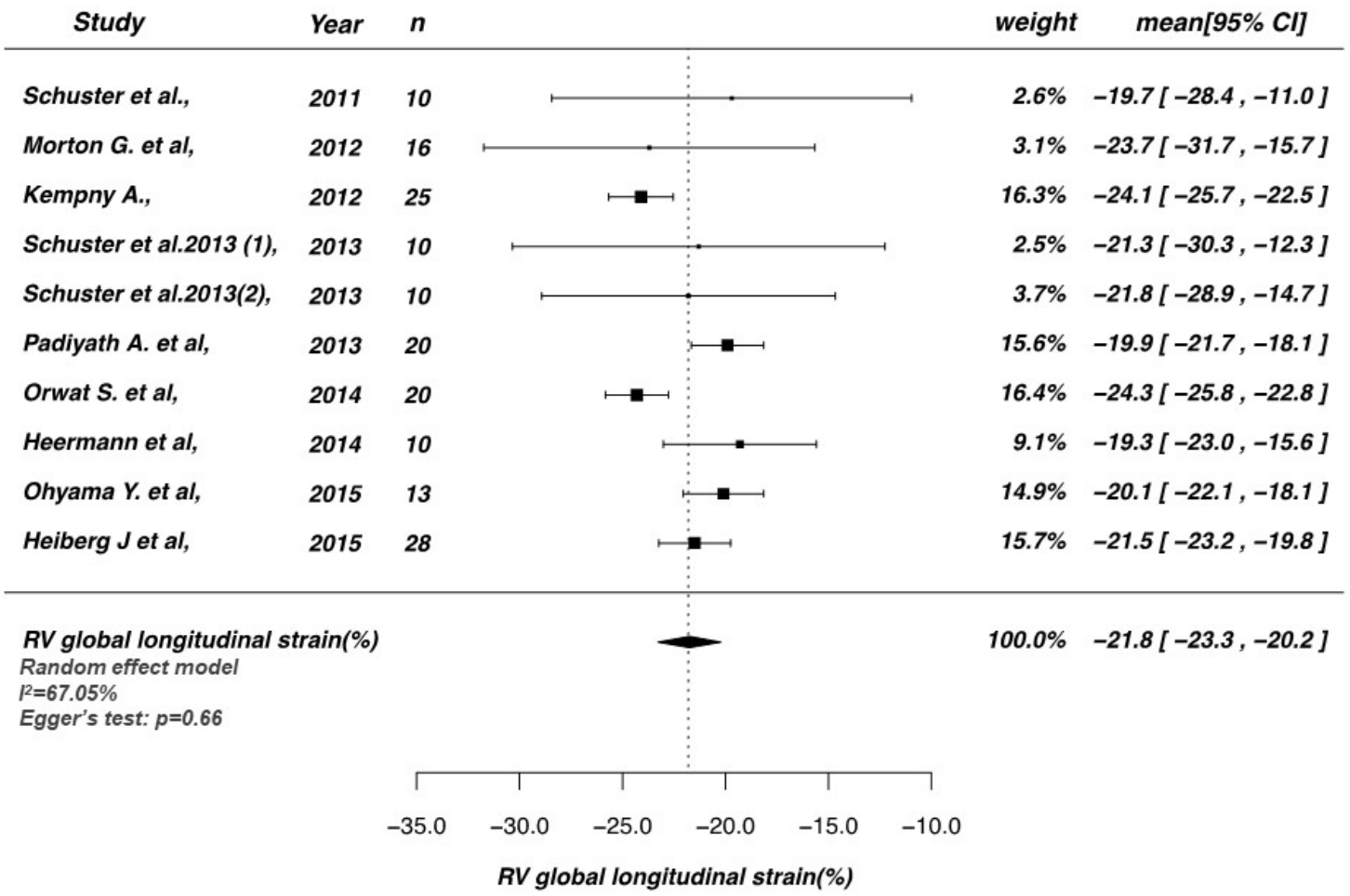

Supplementary figure 3.1: Funnel plots with and without Trim and Fill

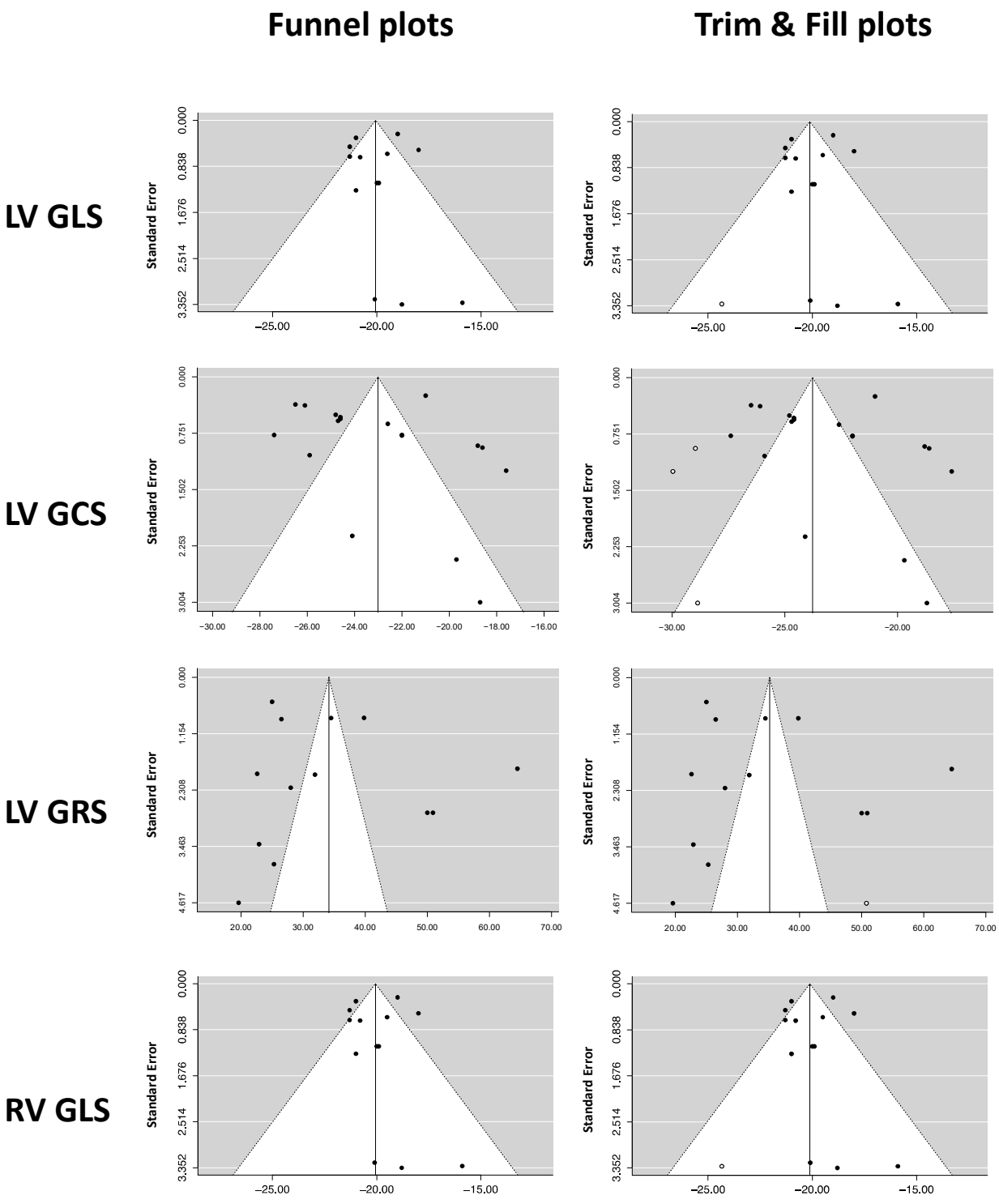

Supplementary figure 3.2: Cumulative plot of GCS by sample size (smallest to highest)

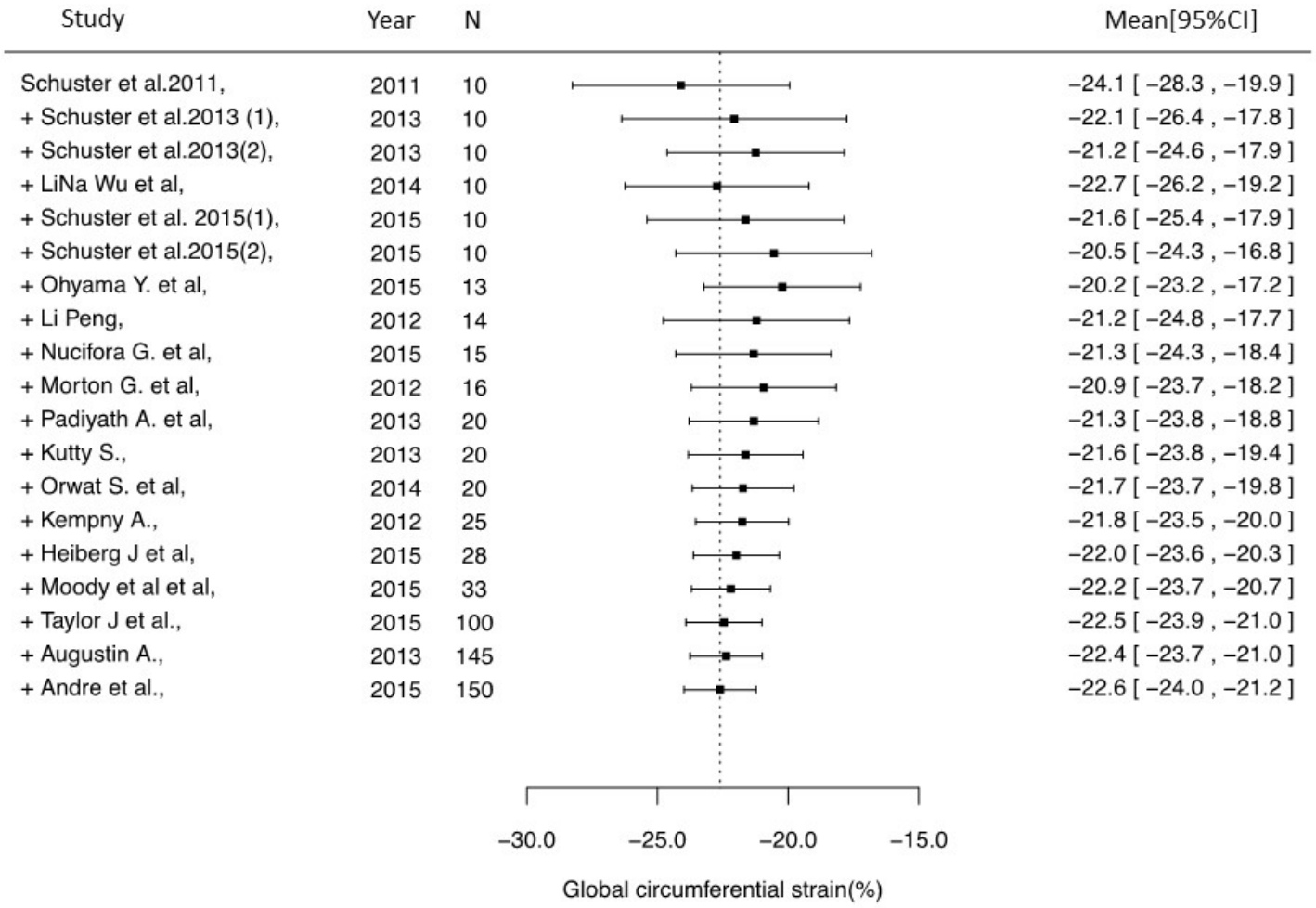

Supplementary figure 3.3: Normal ranges for global strains in different sample sizes

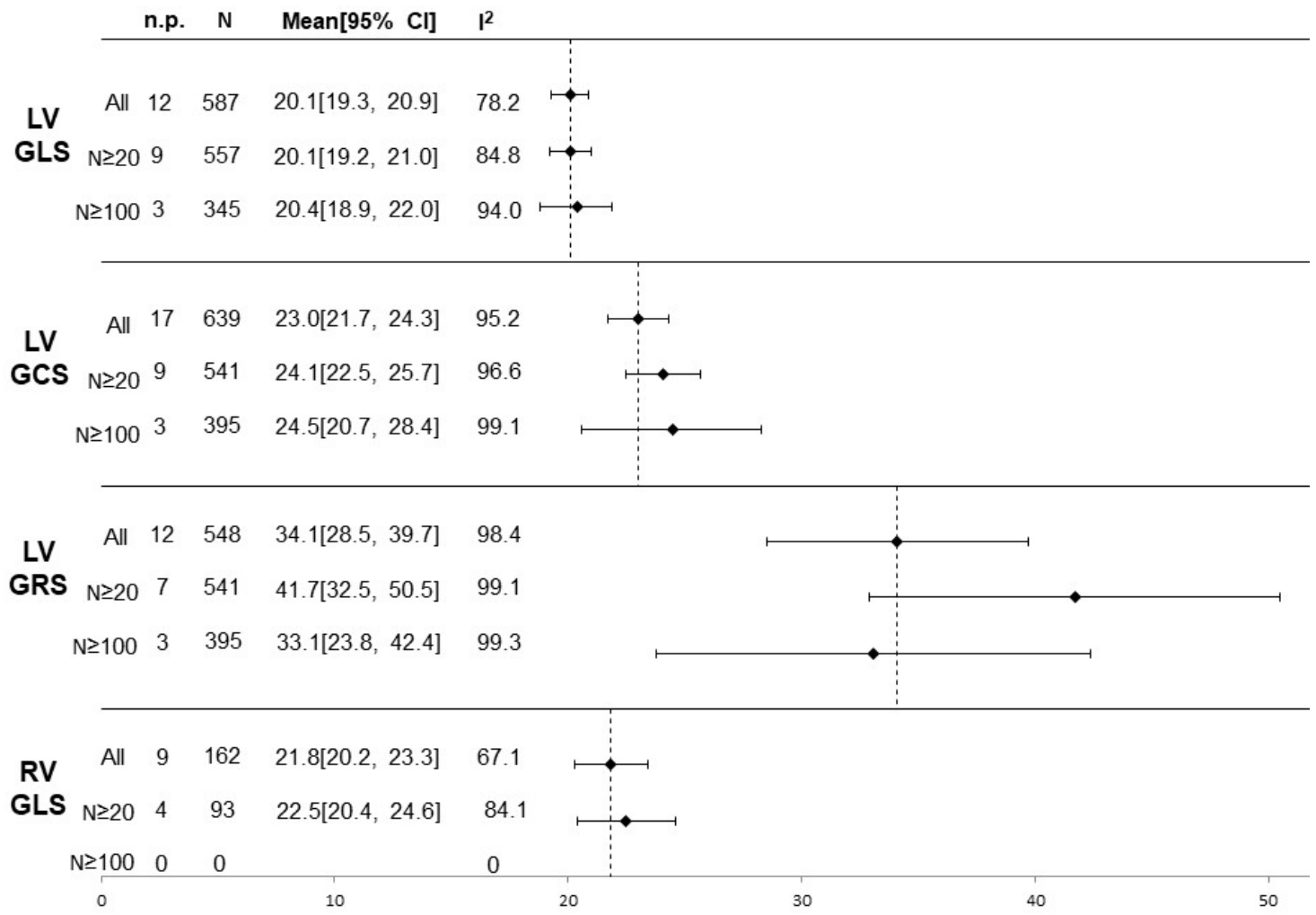

Supplementary figure 3.4: PRISMA flow chart for strain by DENSE, SENC, and MT

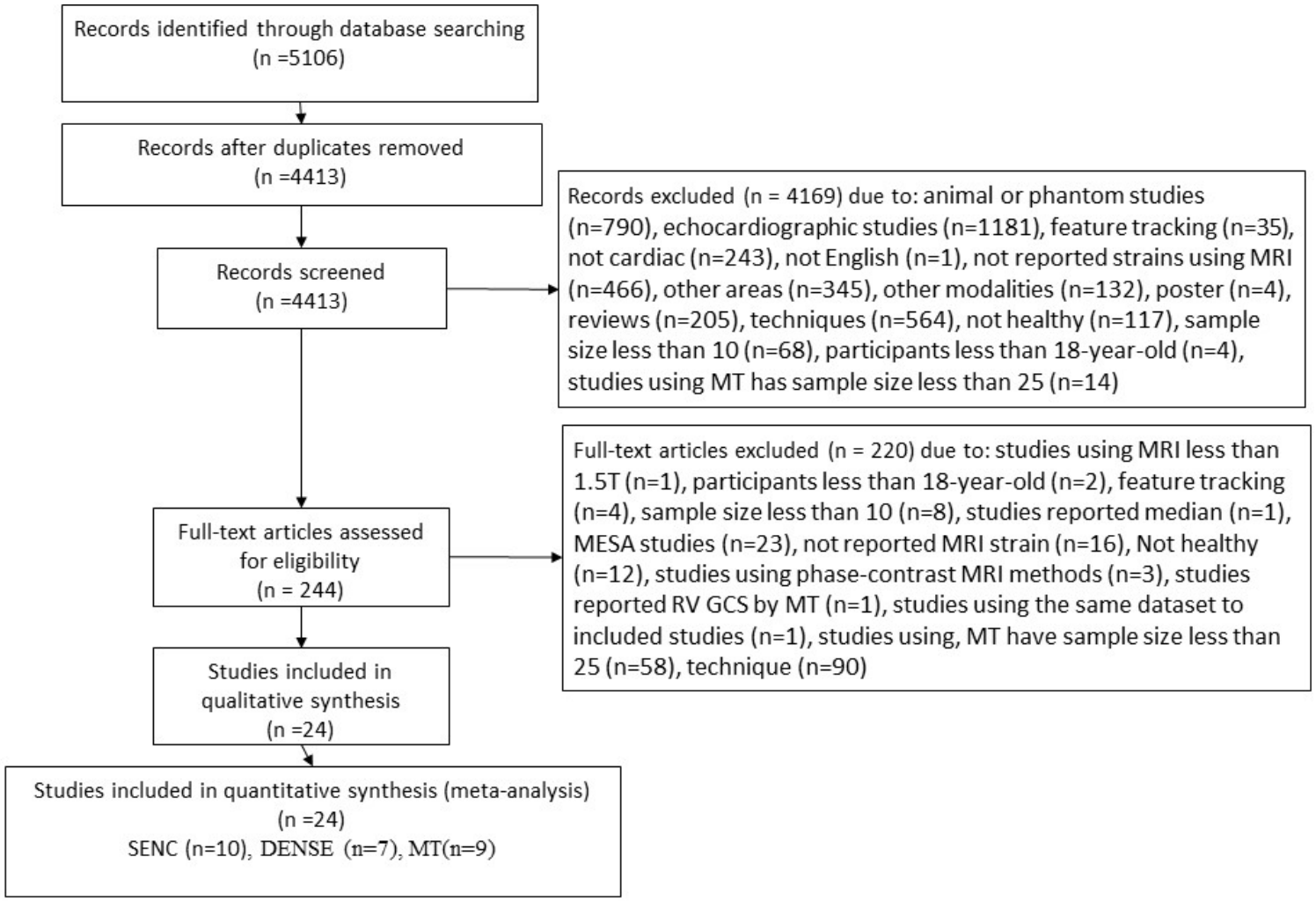

Supplementary figure 3.5: Forest plot for strains by SENC

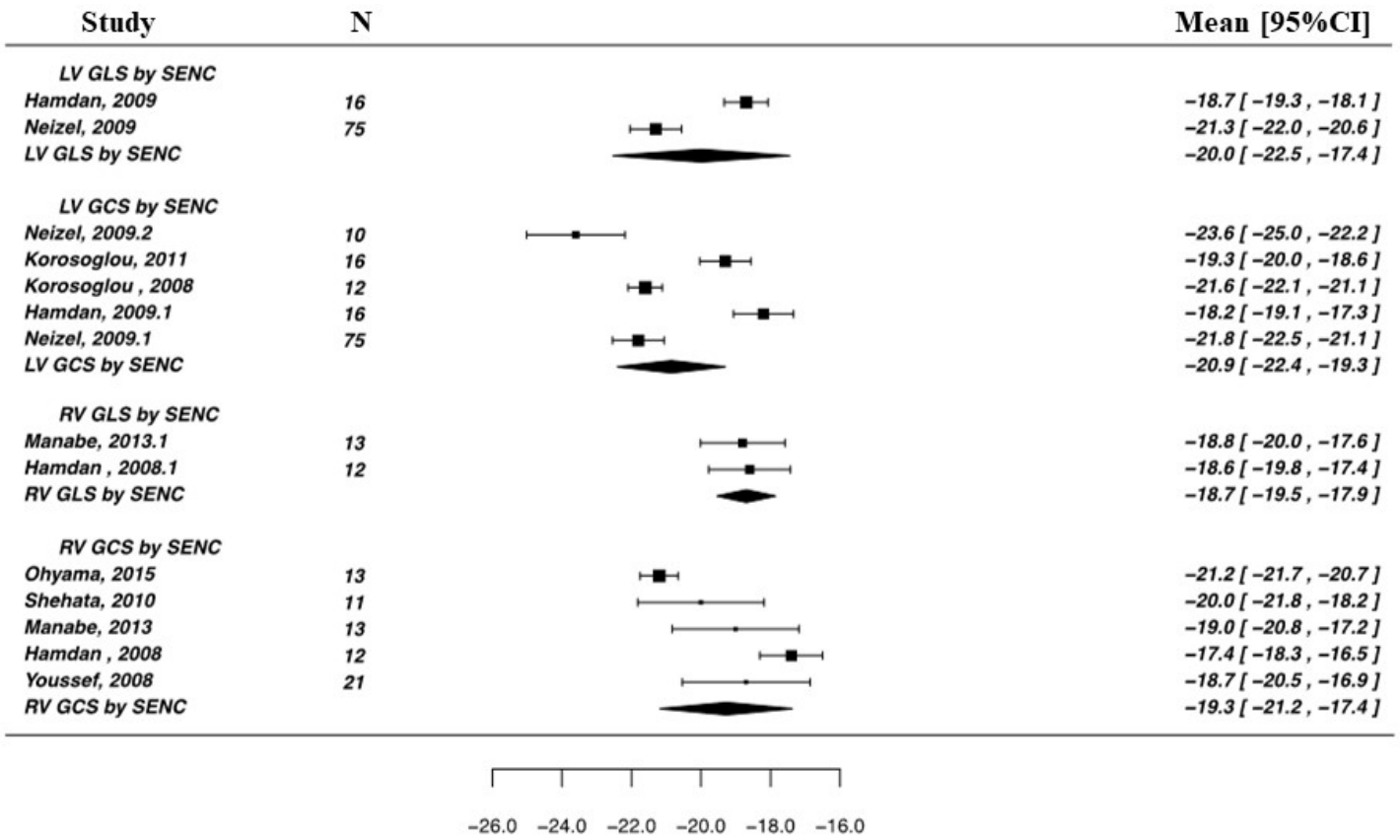

Supplementary figure 3.6: Forest plot for strains by DENSE and MT

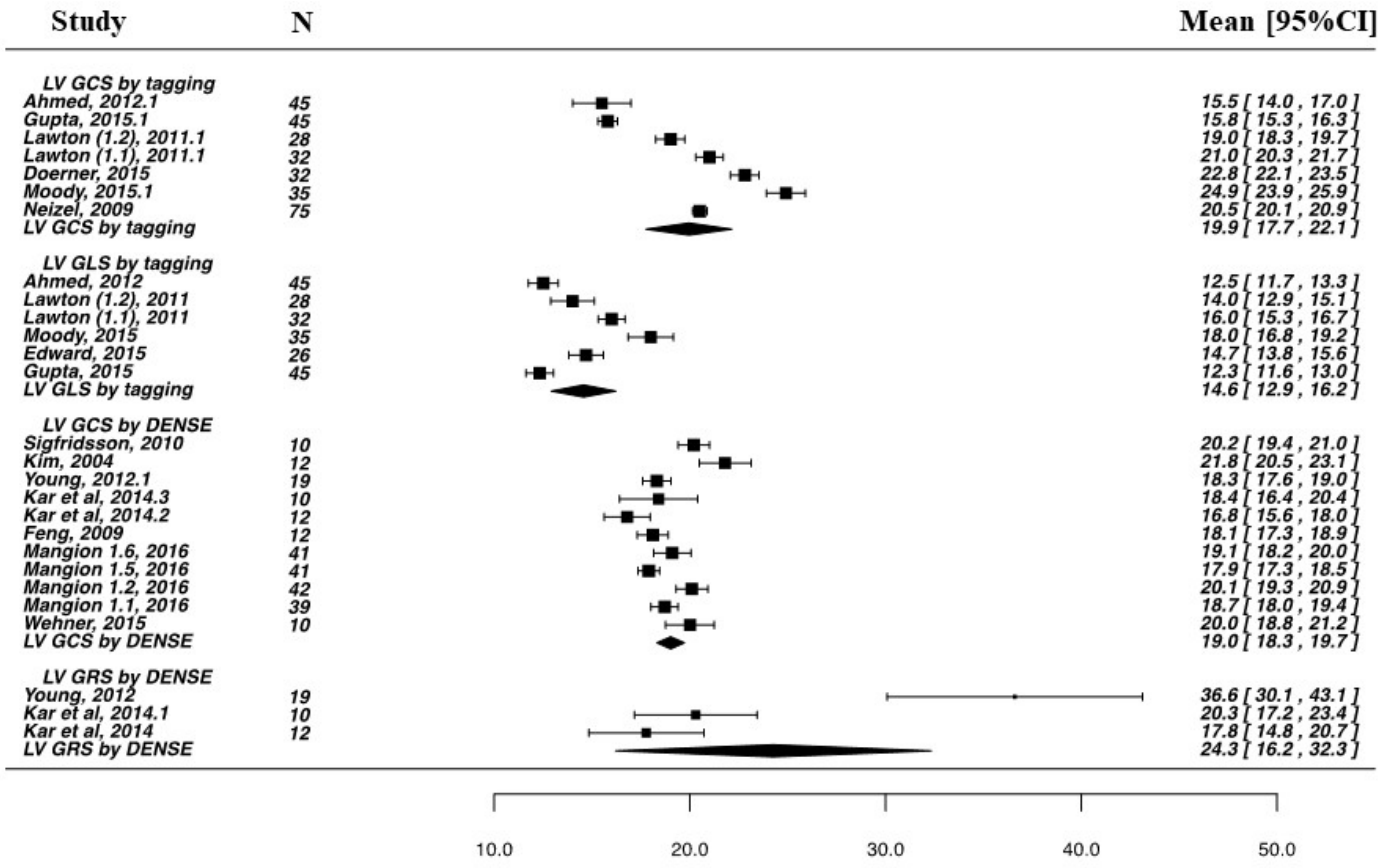

Supplementary figure 3.7: Funnel plot with and without Trim and Fill (DENSE, SENC, and MT)

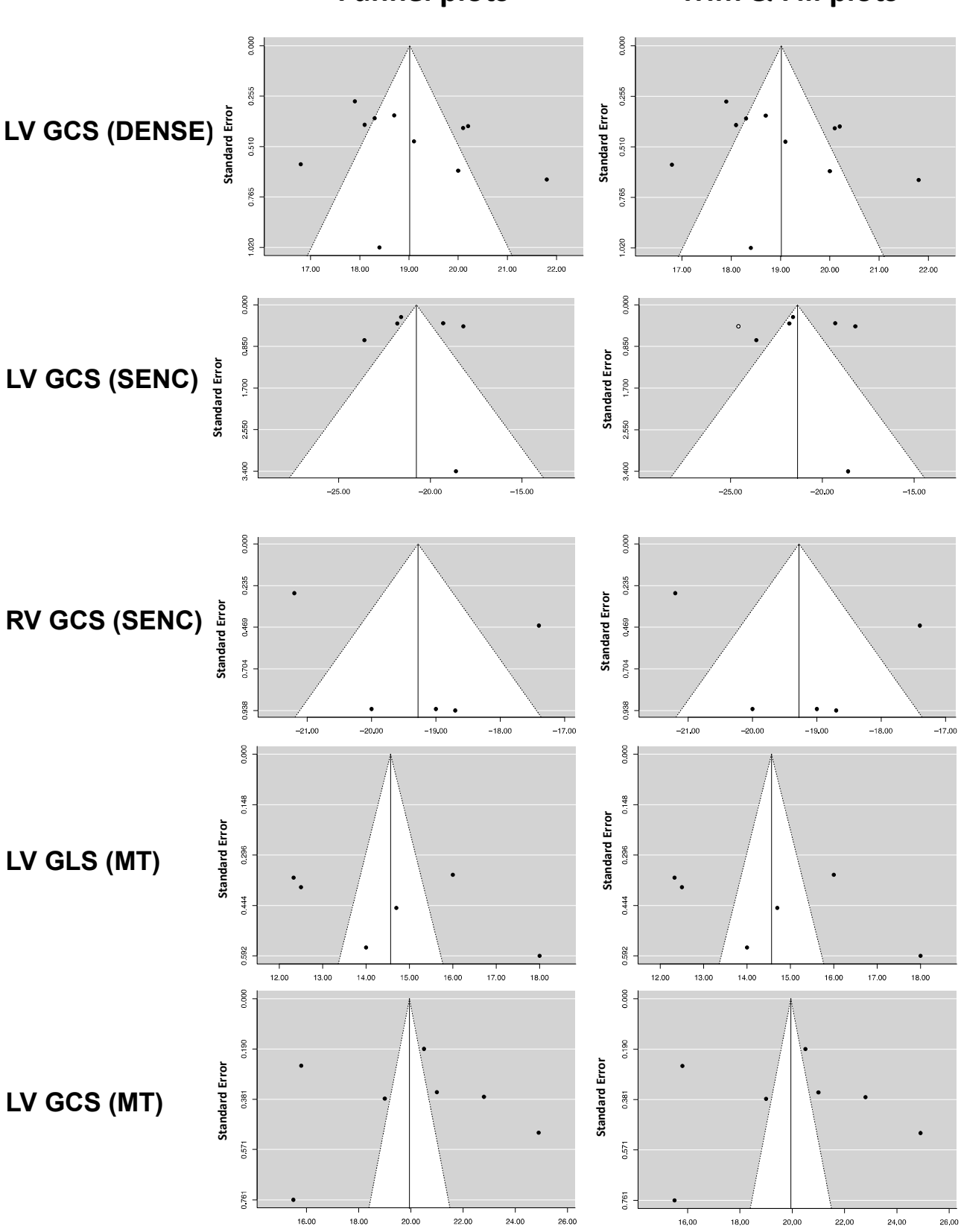

Table 3.1: Summary of included Studies

Study	Year	Age	N	Men	LVEF	Software	Vendor	Strain*	Chamber
Schuster [173]	2011	40.6(23.9-51.8)	10	5	56.9 ± 4.4	Diogenes	TomTec	L/C/R	LV, RV
Kempny [169]	2012	33.1 ± 15.7	25	15	63.6 ± 5.7	Diogenes	TomTec	L/C/R	LV, RV
Morton [170]	2012	27.9 ± 5.7	16	8	58.5 ± 3.2	Diogenes	TomTec	L/C/R	LV, RV
Li Peng [190]	2012	50 ± 9	14	11	-	VVI	Siemens	C/R	LV
Augustin [178]	2013	29.7 ± 7.6	145	54	-	2D CPA	TomTec	L/C/R	LV
Kutty [191]	2013	37.1 ± 7	20	10	57.5 ± 3	2D CPA	TomTec	L/C/R	LV
Padiyath [172]	2013	37 ± 8.5	20	-	-	2D CPA	TomTec	L/C/R	LV, RV
Schuster_1[#] [174]	2013	41(24-52)	10	5	61.3 ± 7.7	Diogenes	TomTec	L/C/R	LV, RV
Schuster_2[#] [174]	2013	31(26-39)	10	5	59 ± 3	Diogenes	TomTec	L/C/R	LV, RV
Orwat [192]	2014	24 ± 3	20	10	64.4 ± 5.3	2D CPA	TomTec	L/C	LV, RV

LiNa Wu [193]	2014	37 ± 11	10	9	61 ± 6	Diogenes	TomTec	C	LV
Heermann [61]	2014	24.3 ± 3	10	5	63.6 ± 4.2	Diogenes	TomTec	L	RV
Andre [177]	2015	45.8 ± 14	150	75	-	2D CPA	TomTec	L/C/R	LV
Moody [183]	2015	41 ± 12	33	26	71 ± 6	Diogenes	TomTec	C/R	LV
Nucifora [194]	2015	46 ± 12	15	11	68 ± 8	2D CPA	TomTec	C	LV
Ohyama [171]	2015	53.7 ± 7.5	13	4	66.2 ± 6.5	MTT	Toshiba	L/C	LV, RV
Schuster [181]	2015	40.6(23-51)	10	5	57.9 ± 5.6	2D CPA	TomTec/ Circle	C/R	LV
Taylor [195]	2015	44.5 ± 14	100	50	71.9 ± 6	Diogenes	TomTec	L/C/R	LV
Heiberg [62]	2015	21.3 ± 2.5	28	18	56.7 ± 6.2	2D CPA	TomTec	L/C/R	LV

More detailed information can be found in Online Supplemental Supplementary table 2

*L/C/R: Longitudinal /circumferential/ radial strain.

This paper reported data from two populations.

MTT, pixel-based Multimodality Tissue Tracking; VVI, Velocity Vector Imaging

Table 3.2: A summary of inter- and intra-observer variabilities of included studies, expressed as coefficient of variance

	Intra- observer				Inter- observer			
	LV GLS	**LV GCS**	**LV GRS**	**RV GLS**	**LV GLS**	**LV GCS**	**LV GRS**	**RV GLS**
Kempny[169]	10.8%	6.7%	21.4%	9.7%	9.6%	8.5%	21.4%	8.3%
Schuster 2011[173]	-	3.7%	9.9%	-	-	3.7%	9.9%	-
Augustine[178]	12.3%	2.8%	22.9%	-	10.9%	4.9%	32.2%	-
Schuster 2013, 1.5T [174]	17.3%	13.3%	16.4%	28.7%	-	-	-	-
Schuster 2013, 3T [174]	18.1%	17.2%	19.8%	43.5%	-	-	-	-
Orwat[196]	-	-	-	-	13.2%	11.1%	-	-
Andre[177]	4.3%	4.8%	7.9%	-	4.8%	5.7%	10%	-
Taylor[197]	7.68%	3.55%	8.9%	-	5.48%	4.95%	14.67%	-
Schuster 2015 (12)	-	2.69%	10.1%	-	-	4.4%	13.2%	-

Table 3.3: Comparison between DENSE, SENC, Myocardial Tagging, STE and MRI-FT in normal strain values

	SENC	DENSE	Tagging	Feature tracking	Speckle tracking*
LV GLS	-20 [-22.5, -17.4]	-	-14.6 [-16.2, -12.9]	-20.1 [-20.9, -19.3]	-19.7 [-20.4, -18.9]
LV GCS	-20.9 [-22.4, -19.3]	-19.0 [-19.7, -18.3]	-19.9 [-21.1, -17.7]	-23 [-24.3, -21.7]	-23.3 [-24.6, -22.1]
LV GRS	-	24.3 [16.2, 32.3]	-	34.1 [28.5, 39.7]	47.3 [43.6, 51]
RV GLS	-18.7 [-19.5, -17.9]	-	-	-21.8 [-23.3, -20.2]	-27 [-29, -24]
RV GCS	-19.3 [-21.2, -17.4]	-	-	-	-

*This is adapted from reference [182]

Appendix 3A: Search criteria for feature tracking meta-analysis

I. PUBMED:

Keywords: ((((“feature tracking") OR "tissue tracking")) AND ((("cardiac mr") OR "cmr") OR "cardiac magnetic resonance")) AND "strain"

Results: 64 articles

II. SCOPUS:

1. (TITLE-ABS-KEY ("feature tracking") OR TITLE-ABS-KEY ("tissue tracking"))
2. (TITLE-ABS-KEY ("cardiac mr") OR TITLE-ABS-KEY ("cmr") OR TITLE-ABS-KEY ("cardiac magnetic resonance"))
3. TITLE-ABS-KEY ("strain")
4. #1 AND #2 AND #3

Results: 59 articles

III. EMBASE:

1 'feature tracking' OR 'tissue tracking'

2 'cardiac mr' OR 'cmr' OR 'cardiac magnetic resonance'

3 'strain'

4 #1 AND #2 AND #3

Results: 59 articles

IV. WEB OF SCIENCE

1 TOPIC: ("feature tracking") OR TOPIC: ("tissue tracking") Indexes=SCI-EXPANDED, SSCI, A&HCI, CPCI-S, CPCI-SSH, BKCI-S, BKCI-SSH, CCR-EXPANDED, IC Timespan=All years

2. TOPIC: ("cardiac mr") OR TOPIC: ("cmr") OR TOPIC: ("cardiac magnetic resonance") Indexes=SCI-EXPANDED, SSCI, A&HCI, CPCI-S, CPCI-SSH, BKCI-S, BKCI-SSH, CCR-EXPANDED, IC Timespan=All years

3. TOPIC: ("strain") Indexes=SCI-EXPANDED, SSCI, A&HCI, CPCI-S, CPCI-SSH, BKCI-S, BKCI-SSH, CCR-EXPANDED, IC Timespan=All years

4. #3 AND #2 AND #1Indexes=SCI-EXPANDED, SSCI, A&HCI, CPCI-S, CPCI-SSH, BKCI-S, BKCI-SSH, CCR-EXPANDED, IC Timespan=All years

Results: 75 articles

Last search: 21 October 2015

Appendix 3B: Search criteria for strain by DENSE, SENC and MT

I. PUBMED:

Keywords:

((((((((((((((((((("harmonic phase"[All Fields] OR "HARP"[All Fields]) OR "zHARP"[All Fields]) OR (spatial[All Fields] AND modulation[All Fields] AND magnetisation[All Fields])) OR "SPAMM"[All Fields]) OR "CSPAMM"[All Fields]) OR "Displacement encoding with stimulated echoes"[All Fields]) OR "DENSE"[All Fields]) OR "SinMod"[All Fields]) OR (sine[All Fields] AND wave[All Fields] AND modelling[All Fields])) OR "strain encoding"[All Fields]) OR "SENC"[All Fields]) OR "phase contrast"[All Fields]) OR "PCMRI"[All Fields]) OR "velocity encoded"[All Fields]) OR "velocity encoding"[All Fields]) OR "strain encoded"[All Fields]) OR "VENC"[All Fields]) OR ((((("tag"[All Fields] OR "tagging"[All Fields]) OR "tagged"[All Fields]) OR "tags"[All Fields]) AND ((((((("myocardial"[All Fields] OR "myocardium"[All Fields]) OR "endocardial"[All Fields]) OR "endocardium"[All Fields]) OR "tissue"[All Fields]) OR "magnetic resonance"[All Fields]) OR "mr"[All Fields]))) OR "spatial modulation of magnetization"[All Fields]) AND ((((("cardiac"[All Fields] OR "cardiovascular"[All Fields]) OR "heart"[All Fields]) AND ("mr"[All Fields] OR "magnetic resonance"[All Fields])) OR "CMR"[All Fields])) AND (((((("cardiac"[All Fields] OR "heart"[All Fields]) OR "ventricle"[All Fields]) OR "ventricular"[All Fields]) AND "deformation"[All Fields]) OR "strain"[All Fields]) AND ("loattrfull text"[sb] AND ("1997/01/01"[PDAT] : "2016/12/31"[PDAT]) AND English[lang])

Results: 487

II. SCOPUS:

(((ALL ("harmonic phase") OR ALL ("HARP") OR ALL ("zHARP") OR ALL ("spatial modulation of magnetisation") OR ALL ("spatial modulation of magnetization") OR ALL ("SPAMM") OR ALL ("CSPAMM") OR ALL ("Displacement encoding with stimulated echoes") OR ALL ("DENSE") OR ALL ("SinMod") OR ALL ("sine wave modelling") OR ALL ("strain encoding") OR ALL ("strain encoded") OR ALL ("SENC") OR ALL ("phase contrast") OR ALL ("PCMRI") OR ALL ("velocity encoded") OR ALL ("velocity encoding") OR ALL ("VENC"))) OR (((ALL ("tag") OR ALL ("tags") OR ALL ("tagged") OR ALL ("tagging"))) AND ((ALL ("myocardial") OR ALL ("myocardium") OR ALL ("endocardial") OR ALL ("endocardium") OR ALL ("tissue") OR ALL ("magnetic resonance") OR ALL ("mr"))))) AND ((((ALL ("cardiac") OR ALL ("heart") OR ALL ("ventricle") OR ALL ("ventricular"))) AND (ALL ("deformation"))) OR (ALL ("strain"))) AND ((((ALL ("cardiac") OR ALL ("cardiovascular") OR ALL ("heart"))) AND ((ALL ("mr") OR ALL ("magnetic resonance"))))) OR (ALL ("cmr"))) AND (LIMIT-TO (DOCTYPE , "ar")) AND (LIMIT-TO (LANGUAGE , "English")) AND (LIMIT-

TO (SRCTYPE , "j")) AND (LIMIT-TO (PUBYEAR , 2016) OR LIMIT-TO (PUBYEAR , 2015) OR LIMIT-TO (PUBYEAR , 2014) OR LIMIT-TO (PUBYEAR , 2013) OR LIMIT-TO (PUBYEAR , 2012) OR LIMIT-TO (PUBYEAR , 2011) OR LIMIT-TO (PUBYEAR , 2010) OR LIMIT-TO (PUBYEAR , 2009) OR LIMIT-TO (PUBYEAR , 2008) OR LIMIT-TO (PUBYEAR , 2007) OR LIMIT-TO (PUBYEAR , 2006) OR LIMIT-TO (PUBYEAR , 2005) OR LIMIT-TO (PUBYEAR , 2004) OR LIMIT-TO (PUBYEAR , 2003) OR LIMIT-TO (PUBYEAR , 2002) OR LIMIT-TO (PUBYEAR , 2001) OR LIMIT-TO (PUBYEAR , 2000) OR LIMIT-TO (PUBYEAR , 1999) OR LIMIT-TO (PUBYEAR , 1998) OR LIMIT-TO (PUBYEAR , 1997))

Results: 4352

III. Embase:

'harmonic phase' OR 'harp' OR 'zharp' OR 'spatial modulation of magnetisation' OR 'spatial modulation of magnetization' OR 'spamm' OR 'cspamm' OR 'displacement encoding with stimulated echoes' OR 'dense' OR 'sinmod' OR 'sine wave modelling' OR 'strain encoding' OR 'senc' OR 'phase contrast' OR 'pcmri' OR 'velocity encoded' OR 'velocity encoding' OR 'strain encoded' OR 'venc' AND ('cardiac' OR 'cardiovascular' OR 'heart' AND ('mr' OR 'magnetic resonance') OR 'cmr') AND ('cardiac' OR 'heart' OR 'ventricle' OR 'ventricular' AND 'deformation' OR 'strain') AND (1997:py OR 1998:py OR 1999:py OR 2000:py OR 2001:py OR 2002:py OR 2003:py OR 2004:py OR 2005:py OR 2006:py OR 2007:py OR 2008:py OR 2009:py

OR 2010:py OR 2011:py OR 2012:py OR 2013:py OR 2014:py OR 2015:py OR 2016:py) AND 'article'/it

Results: 267

Appendix 3C – Method for systematic review of normal ranges of strains using DENSE, SENC, and MT

Search Strategy: We followed the Preferred Reporting Items for Systematic reviews and Meta-Analysis (PRISMA) guideline when performing our systematic review and meta-analysis[179]. The last search was performed on 01 May 2016. Three academic databases (EMBASE, PUBMED, and Scopus) were systematically searched for the strain values of the left or right ventricle derived from DENSE, SENC, and MT by two co-authors (HQV and KN) under the guidance of a librarian trained in systematic review. The reference lists of these articles were also scrutinized to identify some additional appropriate studies

Study selection: From these lists, studies were included if the articles reported strain values using cardiac MRI in healthy subjects. The two co-authors reviewed and chose studies if the studies met each of following criteria: (1) studies recruited extensively normal healthy subjects (2) studies included a control group, which was defined as normal and healthy (3) Participants had age >18 years old (4) reported bi-ventricular strains by DENSE, SENC, or MT (5) The cut-off sample size for studies reported strains by DENSE and SENC was 10 (6) The cut-off sample size for studies reported strains by MT (7) Field strength ≥1.5T (8) reported strains in form of mean and standard deviation (9) Only human studies. The definitions of healthy subjects are shown in the supplementary table 3.5. All discrepancies were reviewed and resolved by consensus of all authors.

Study exclusion: The search was uniquely concentrated on human studies, published in English. Animal studies and conference presentations were excluded.

Data Collation: Strain data were extracted from individual studies and entered into an electronic database. LVGLS, LVGCS, LVGRS, RV GLS, RV GCS were extracted from text, table and graphs. In cases where we believed that multiple articles to come from a single dataset, the largest study was selected.

Data extraction: All demographic, common clinical characteristics and strain information were extracted from texts and tables.

Outcomes of Interest: In this additional meta-analysis, our outcomes of interest were normal ranges of left and right ventricular strains (LVGLS, GCS, GRS, RVGLS, and RVGCS) measured by DENSE, SENC, and MT.

Statistical analysis: The means and 95% confidence intervals (CI) of LVGLS, LVGCS, LVGRS, and RVGLS were computed using random effect models weighted by inverse variance. Funnel plots with and without the Duval and Tweedie's trim and fill were constructed and Egger's test was used to assess potential publication bias. The heterogeneity between subgroups or between studies was assessed by Cochran Q's test and the inconsistency factor (I^2). Meta-regressions were performed for each risk factor to examine possible study factors associated with heterogeneity. Beta coefficient and its CIs were derived using the least-mean squares fitting method. Statistical analysis was performed using R version 3.2.2 (The R Foundation for Statistical Computing, Vienna, Austria) with the "metafor" package. Two-tailed p values were applied and the threshold of statistical significance was 0.05 except for Egger's test, where 0.1 was used.

Appendix 3D – Supplementary Tables

Supplementary table 3.1. The definitions of healthy subjects

Study	Year	Control selection	Disease studied
Schuster [173]	2011	Healthy volunteers	dobutamine stress
Kempny [169]	2012	Without CVD	Tetralogy of Fallot
Morton [170]	2012	Exclusion criteria were: known cardiac, respiratory or renal disease or a contraindication to MRI	Reproducibility of FT
Li Peng [190]	2012	Normal Volunteers	
Augustin [178]	2013	None of the subjects had documented cardiovascular risk factors, cardiac disease or other medical problems relevant to cardiac function	Global and regional LV cardiac deformation
Kutty [191]	2013	Not currently active in competitive sports, had no history of cardiac or any other chronic illness, and were normotensive on the day of the study	Aortic coarctation
Padiyath [172]	2013	Control subjects. Exclusion criteria were any residual intra-cardiac shunt, pulmonary atresia, pacemaker or defibrillator implantation, or claustrophobia	Tetralogy of Fallot

Schuster [174]	2013	Healthy volunteers	Intra-observer reproducibility of FT
Orwat [192]	2014	Healthy volunteers were recruited prospectively	LVH
Wu [193]	2014	No cardiovascular history, no risk factors nor used medication	Segmental strain vs tissue tagging
Heermann [61]	2014	Healthy volunteers	ARVC
Andre [177]	2015	No signs, symptoms or a history of any cardiac disease cardiovascular, cerebrovascular, relevant non-cardiac diseases, no diabetes; no regular medication except for contraceptives, chronic thyroid hormone substitution or vitamins; No abnormal blood test results	Age- , gender- related LV deformation
Moody [183]	2015	No diabetes mellitus, no history of cardiovascular or pulmonary disease, no evidence of hypertensive end organ damage, no LV systolic dysfunction, and no atrial fibrillation	Comparison with tagging
Nucifora [194]	2015	Control subjects, without evidence of structural heart disease and no history of HTN, diabetes mellitus, or any other systemic disease	hypertrophic cardiomyopathy
Ohyama [171]	2015	Exclusion criteria : any evidence suggestive of systemic HTN, diabetes mellitus, ischemic or non-	pulmonary HTN

		ischemic heart disease, chest disease, and history of smoking or contraindication to CMR studies	
Schuster [172]	2015	Healthy volunteers	Inter-vendor agreement in FT
Taylor [195]	2015	Exclusion criteria: any history of CVD, any history of diabetes or glucose intolerance, renal impairment, anemia or atrial fibrillation, first-degree relative with a proved or potentially inheritable cardiac condition, or a history of premature coronary artery disease, previous prescription of an anti- hypertensive medication. Inclusion: an OBP <140mmHg systolic or 90 mmHg diastolic had to have a 24-h ambulatory average of <135/ 85 mmHg	normal values of FT
Heiberg [62]	2015	Healthy control	

Supplementary table 3.2: Characteristics of healthy subjects in included studies (feature tracking)

Study	BMI	BSA	Body Weight	Body Height	HR	MRI vendor	Field strength	Software	Version
Schuster [173]	-	-	-	-	68.6 ± 11.9	Philips	1.5T	Diogenes	
Kempny [169]	-	-	70.1 ± 11.2	176.8 ± 8.9	-	Philips	1.5T	Diogenes	1.1.0.2
Morton [170]	26.2 ± 6.8	-	-	-	-	Philips	1.5T	Diogenes	
Li Peng [190]	-	-	-	-	-	Siemens	1.5T	VVI	3.702
Augustin [178]	24.1 ± 4.4	-	70.7 ± 13.6	171.2 ± 9.1	66.9 ± 9.3	Siemens	1.5T	2D CPA	
Kutty [191]	-	1.85 ± 0.3	72 ± 14.6	174.4 ± 7	-	Philips	1.5T	2D CPA	2011
Padiyath [172]	-	-	-	-	-	Philips	1.5T	2D CPA	1.1.0
Schuster_1 [174]	25 ± 3.3	-	-	-	71 ± 12	Philips	1.5T	Diogenes	
Schuster_2 [174]	26.1 ± 8.1	-	-	-	72 ± 10	Philips	3T	Diogenes	
Orwat [192]	-	-	-	-	-	Philips	1.5T	2D CPA	1.1.0

LiNa Wu [193]	-	-	-	-	-	Siemens	1.5T	Diogenes	
Heermann [61]	-	1.81 ± 0.17	66.4 ± 9.4	176.1 ± 9.1	-	Philips	1.5T	Diogenes	
Andre [177]	24.4 ± 3.1	1.9 ± 0.2	74 ± 12.8	174 ± 9.6	-	Philips	1.5T	2D CPA	
Moody [183]	-	-	77 ± 11	-	66 ± 10	Siemens	1.5T	Diogenes	
Nucifora [194]	-	1.87 ± 0.17	-	-	-	Siemens	1.5T	2D CPA	
Ohyama [171]	-	1.79 ± 0.17	-	-	-	Siemens	3T	MTT	
Schuster [172]	-	-	-	-	-	Philips	1.5T	2D CPA	1.1.2.36
Taylor [195]	-	1.85 ± 0.2	74.3 ± 12.4	170 ± 9.6	67.3 ± 11.2	Siemens	1.5T	Diogenes	
Heiberg [62]	-	1.83 ± 0.18	68 ± 11.1	176.6 ± 9.4	84 ± 14	Philips	1.5T	2D CPA	

Supplementary table 3.2 (cont.)

Study	RV MI	RV ESVi	RV EDVi	RV ESV	RV EDV	RVEF	RVSVi	RV CI	LV mass
Schuster [173]	-	32.1 ± 8.6	76.6 ± 14.3	-	-	58.5 ± 4.1	-	3 ± 0.6	-
Kempny [169]	-	34.7 ± 10	77.7 ± 9.9	-	-	55.3 ± 6.6	-	-	-
Morton [170]	-	-	-	-	-	-	-	-	-
Li Peng [190]	-	-	-	-	-	-	-	-	-
Augustin [178]	-	-	-	-	-	-	-	-	-
Kutty [191]	-	-	-	-	-	-	-	-	-
Padiyath [172]	-	-	-	-	-	-	-	-	-
Schuster_1 [174]	-	26.5 ± 9.8	71.6 ± 16.3	-	-	63.6 ± 8.2	45.1 ± 9.6	3.2 ± 0.7	-
Schuster_2 [174]	-	30.8 ± 5.1	84.5 ± 1.1	-	-	63.3 ± 6	53.7 ± 9.5	3.8 ± 0.7	-
Orwat [192]	-	-	-	-	-	-	-	-	-

LiNa Wu [193]	-	-	-	-	-	-	-	-	111 ± 28
Heermann [61]	-	36.7 ± 6.4	88.1 ± 12.8	-	-	58.3 ± 4.8	-	-	-
Andre [177]	-	-	-	-	-	-	-	-	-
Moody [183]	-	-	-	-	-	-	-	-	122 ± 27
Nucifora [194]	-	20 ± 7	71 ± 10	-	-	72 ± 7	-	-	-
Ohyama [171]	-	33.2 ± 11.8	76.1 ± 16	-	-	57.5 ± 7	42.9 ± 4.8	-	-
Schuster [172]	-	-	-	-	-	-	-	-	-
Taylor [195]	-	-	-	-	-	-	-	-	-
Heiberg [62]	6.2 ± 1.2	-	-	-	-	-	-	-	-
Schuster [173]	SSFP	-	33.4 ± 7.5	76.9 ± 12.5	-	-	3 ± 0.6	-	-
Kempny [169]	bSSFP	-	27.5 ± 5.1	78.8 ± 11.2	-	-	-	-	-
Morton [170]	SSFP	-	-	-	67.5 ± 17.3	161.7 ± 33.3	-	-	-
Li Peng [190]	-	-	-	-	-	-	-	-	-

Augustin [178]	SSFP	-	-	-	-	-	-	70.6 ± 8.2	116.3 ± 11.9
Kutty [191]	SSFP	-	-	75.8 ± 12.7	-	-	3.2 ± 0.6	-	-
Padiyath [172]	SSFP	-	-	-	-	-	-	-	-
Schuster_1 [174]	SSFP	-	29.7 ± 9.3	75.2 ± 13.7	-	-	3.2 ± 0.5	-	-
Schuster_2 [174]	SSFP	-	35±4.2	85.4 ± 8.5	-	-	3.6 ± 0.6	-	-
Orwat [192]	bSSFP	-	-	-	148 ± 27	52 ± 11	-	-	-
LiNa Wu [193]	bSSFP	-	-	-	69 ± 17	180 ± 33	-	-	-
Heermann [61]	bSSFP	-	28.8 ± 4.5	79 ± 8.2	-	-	-	-	-
Andre [177]	SSFP	-	-	-	-	-	-	75.7 ± 8.6	125.5 ± 11
Moody [183]	SSFP	64 ± 11	-	-	37 ± 13	124 ± 25	-	72 ± 6	120 ± 11
Nucifora [194]	SSFP	55 ± 9	25 ± 9	76 ± 14	-	-	-	-	-
Ohyama [171]	FGRE	-	22.7 ± 6.7	66.2 ± 10.1	-	-	-	-	-
Schuster [172]	SSFP	-	21.7 ± 5.1	51 ± 7.5	-	-	-	-	-

Taylor [195]	SSFP	58.8 ± 11.5	18.1 ± 5.9	63.1 ± 10.4	-	-	-	73.1 ± 7.1	122.6 ± 12.3
Heiberg [62]	bSSFP	10.2 ± 2	-	-	-	-	-	-	-

Supplementary table 3.3: Univariable meta-regression analyses between strains and Ages, Gender, Field Strength, Sequences, LVEF, and LVEDVi.

	LV GLS			**LV GCS**			**LV GRS**			**RV LS**		
	β	p	Q_E	**β**	p	Q_E	**β**	p	Q_E	**β**	p	Q_E
Age	-0.04	0.19	63.04	-0.08	0.14	307.8	-0.08	0.75	752.22	0.08	0.28	20.98
Gender	0.006	0.79	105.0	-0.04	0.26	365.3	0.11	0.42	660.3	-0.07	0.3	16.15
Field Strength (1.5T vs 3T)	-0.03**	0.99	55	**3.2****	**0.041**	**323.2**	-8.1**	0.27	750.7	1.08	0.4	22.6
Sequence*	-	-	-	4.4	0.11	301.5	-	-	-	1.9	0.4	22.43
LVEF	-0.11	0.17	18.3	-0.16	0.25	152.9	-0.29	0.78	490.8	-0.11	0.66	18.53
LVEDVi	-	-	-	-0.04	0.73	115.2	-0.27	0.41	87	-	-	-
Scanner vendor***	0.23	0.8	46.3	-1.5	0.32	389	-2.8	0.76	621	1.9	0.4	22.4

*SSFP vs. Fast Gradient Echo (FGRE), only 1 study reported strains using FGRE

**Only 1 study reported strains at 3T

***Philips is the reference

Q_E : Residual heterogeneity

Supplementary table 3.4a: Summary of pooled strain values derived from CMR-based feature tracking using software from TomTec only

	LV GLS	LV GCS	LV GRS	RV GLS
Mean [95%CIs]	-20.1 [-20.9, -19.3]	-23.0 [-24.4, -21.7]	34.8 [28.4, 41.2]	-22.0 [-23.7, -20.4]
Cochrane Q	55	301.5	726.7	22.4
I^2	78.2	95.0	98.5	64.3
Tau^2	1.26	6.4	121.3	3.0
Egger's test	0.55	0.08	0.4	0.56

Supplementary table 3.4b: Summary of pooled strain values derived from CMR-based feature tracking using software from TomTec only

	LV GLS			LV GCS			LV GRS			RV GLS		
	β	p	Q_E	**β**	p	Q_E	**β**	p	Q_E	**β**	p	Q_E
Age	-0.04	0.19	63.04	**-0.1**	**0.04**	**241.2**	-0.08	0.75	752.2	0.07	0.64	20.93
Gender	0.006	0.79	105.0	-0.04	0.26	365.3	0.11	0.42	660.3	0.002	0.99	11.0
Field Strength	-0.03	0.99	55	3.0	0.26	298.9	-8.6	0.29	720.3	0.16	0.95	22.4
LVEF	-0.11	0.17	18.3	-0.18	0.16	98.6	-0.15	0.78	490.8	**-0.4**	**0.005**	**7.8**

Supplementary table 3.5: Characteristics of healthy subjects in included studies (DENSE, SENC and MT)

Study	Year	Age	N	%Males	EF	SBP	DBP	FS	Vendor	technique	ROI	Strain
Neizel[198]	2009	44±13	75	53.3	-	127±11	77±9	1.5	Phillips	MT	LV	CS
Gupta[199]	2015	41±12.6	45	46.7	65±5	118±13	74±11	1.5	GE	MT	LV	LS, CS
Edward[90]	2015	27±6	26	65	68±5	119±9	72±7	1.5	Siemens	MT	LV	LS, CS
Moody[183]	2015	41±12	35	62	71±6	120±11	72±6	1.5	Siemens	MT	LV	LS, CS
Doerner[200]	2015	28±3.5	32	62.5	63.1±3.9	109±10	62±8	1.5	Phillips	MT	LV	LS, CS
Lawton (1.1)[201]	2011	34.8±10.4	32	0	-	117±10.4	73.7±7.9	1.5	Siemens	MT	LV	LS, CS
Lawton (1.2)[201]	2011	31.6±11.3	28	100	-	123.6±15	73.6±11.4	1.5	Siemens	MT	LV	LS, CS
Moore[202]	2000	37±11	31	51.6	-	-	-	1.5	GE	MT	LV	LS, CS
Ahmed[203]	2012	41±12.6	45	46.7	65±5.5	118±3	74±11	1.5	GE	MT	LV	LS, CS
Wehner[204]	2015	27±9	10	50	-	-	-	3	Siemens	DENSE	LV	CS
Kar [205]	2015	-	12	50	-	-	-	1.5	Siemens	DENSE	LV	CS, RS
Kar [205]	2015	-	10	40	-	-	-	1.5	Siemens	DENSE	LV	CS, RS
Feng[206]	2009	34.5±11	12	-	-	-	-	3	Siemens	DENSE	LV	CS

Young[207]	2012	-	19	-	-	-	-	1.5	Siemens	DENSE	LV	CS,RS
Mangion[187]	2016	44.8±18	89	50	-	-	-	*	Siemens	DENSE	LV	CS
Kim[186]	2004	32(24-40)	12	75	-	-	-	1.5	Siemens	DENSE	LV	CS
Sigfridsson[208]	2010	-	10	-	-	-	-	1.5	Phillips	DENSE	LV	CS
Neizel[198]	2009	44±13	75	53.3	-	-	-	1.5	Phillips	SENC	LV	LS, CS
Hamdan[209]	2009	34±2.1	16	87.5	-	-	-	3	Phillips	SENC	LV	LS, CS
Korosoglou [210]	2008	-	12	-	-	-	-	-	Phillips	SENC	LV	CS
Ohyama[171]	2015	53.7±7.5	13	30.8	66.2±6.5	119±5	72±4	3	Phillips	SENC	RV	CS
Korosoglou [211]	2011	62±3	16	63	67±2	-	-	1.5	Phillips	SENC	LV	CS
Neizel [198]	2009	55±9	10	-	-	-	-	1.5	Phillips	SENC	LV	CS
Youssef[212]	2008	35±7	21	33.3	-	-	-	3	Phillips	SENC	RV	CS
Hamdan[213]	2008	30±1.8	12	15	-	-	-	3	Phillips	SENC	RV	LS, CS
Manabe[214]	2013	44±7	13	8	-	-	-	1.5	Phillips	SENC	RV	LS, CS
Shehata[215]	2010	49.5±10.2	11	64	-	-	-	3	Phillips	SENC	RV	CS

DENSE, Displacement Encoding with Stimulated Echoes; MT, Myocardial Tagging; SENC, Strain-encoding

Supplementary table 3.6: Control selection (DENSE, SENC and MT)

Study	Year	Control selection
Neizel[198]	2009	Healthy volunteers
Gupta[199]	2015	healthy individuals
Edward[90]	2015	healthy controls with no history of cardiac disease
Moody[183]	2015	Normal healthy adults were identified from an ongoing prospective, observational research study examining the effects of living kidney donation on cardiovascular structure and function (REC: 10/H1207/70). The current UK exclusion criteria for living kidney donation include: diabetes mellitus, any history of cardiovascular or pulmonary disease, evidence of hypertensive end organ damage, LV systolic dysfunc tion, and atrial fibrillation. Prior to nephrectomy, all potential kidney donors who underwent normal base- line cardiac MR studies from March 2011 to June 2012 were included as healthy controls. Control sub- jects also had normal 12-lead electrocardiography, stress echocardiography, and routine hematology and biochemistry profiles
Doerner[200]	2015	Only healthy volunteers without an apparent medical history were enrolled
Lawton[201]	2011	no history of any cardiac disease

Moore[202]	2000	Thirty-one healthy volunteers who gave informed consent were examined; these individuals had no clinical history of CVD, diabetes mellitus, or potential cardiac symptoms such as chest pain or dyspnea.
Ahmed[203]	2010	control volunteers (age 40 11 years, median age 38 years, age range 21 to 62 years) who had no prior history of CVD and were not taking any cardiovascular medications.
Wehner[204]	2015	Ten healthy subjects (50 % female, age 27 ± 9) with no history of car- diovascular disease and ten subjects with a history of myo-cardial infarction or congestive heart failure
Kar [205]	2015	healthy subjects
Feng[206]	2009	healthy human subjects
Young[207]	2012	Healthy volunteers
Mangion[187]	2016	Healthy volunteers aged at least 18 years with no prior medical history (including cardiovascular health problems, medication, or systemic illness) were invited to participate by placing advertisements in public buildings (eg, hospital, university). The other exclusion criteria included standard contraindications to MR (eg, metallic implants and metallic foreign body) and known or suspected pregnancy. Written informed consent was subsequently obtained from prospective participants. A 12-lead electrocardiogram (ECG) was obtained in all subjects and a normal ECG was an inclusion criterion

Kim[186]	2004	healthy volunteers (nine men and three women; age range, 24 – 40 years; mean age, 32 years) with normal cardiac findings, including no history of heart disease and no risk factors for coronary artery disease
Korosoglou [210]	2008	Healthy volunteers were included in this study. Exclusion criteria were any evidence of systemic HTN or ischemic heart disease, on the basis of clinical history, previous hospitalization for myocardial infarction, angina pectoris, or electrocardiographic evidence of previous infarction
Neizel[198]	2009	Seventy-five healthy volunteers were examined. Volunteers with signs, symptoms, or a his- tory of any cardiac disease, including arterial HTN, cardiovascular, cerebrovascular, or noncardiac diseases, were excluded. We also excluded all volunteers on regular medication except for contraceptives or vitamins
Hamdan[209]	2009	16 healthy adult subjects (14 men, 34 2.1 years old) with an averaged Framingham risk score of 1%. Subjects were included if they showed no evi- dence of cardiac disease and if the clinical examination and electrocardiogram (ECG) were normal. None was taking medication known to influence cardiac function
Neizel[198]	2012	Sixteen age-matched healthy volunteers underwent CMR in order to acquire normal values for perfusion reserve and myocardial strain and strain rate values. All control subjects underwent laboratory testing before enrollment and exclusion criteria were any history, symptoms, electrocardiographic signs, or bio- chemical findings indicative of CVD (normal B-type natriuretic peptide and troponin T lev- els), evidence of systemic HTN (baseline blood pressure >140/85 mmHg), diabetes mellitus (HbA1c >5.9%), impaired fasting

		glucose (fasting glucose >110 mg/dL), or hyperlipidemia (LDL >130 mg/dL). Laboratory measurements were performed both in patients and in controls in the fasting state
Youssef[212]	2008	healthy volunteers
Hamdan[213]	2008	Healthy adult volunteers with no known history of cardiovascular dis- ease. Clinical examinations and electrocardiograms of the subjects were normal.
Manabe[214]	2013	healthy control subjects
Shehata[215]	2010	Healthy volunteers were included in the study. Exclusion criteria included any evidence suggestive of systemic HTN, diabetes mellitus, ischemic or nonischemic heart disease, chest disease, and history of smoking
Ohyama[171]	2015	healthy volunteers , exclusion criteria for healthy volunteers included any evidence suggestive of systemic HTN, diabetes mellitus, ischemic or non-ischemic heart disease, chest disease, and history of smoking, contraindication to CMR studies (e.g. presence of metallic implants and inability to follow instructions for breath holding).
Ahmed[203]	2012	Control group comprised volunteers who were healthy with no history of CVD and not using any prescription medication.
Sigfridsson[208]	2010	Healthy controls

Supplementary table 3.7a: Summary of pooled strain values by DENSE, SENC and myocardial tagging

	LV GLS By tagging	LV GCS By tagging	LV GCS by DENSE	LV GRS by DENSE	LV GLS by SENC	LV GCS by SENC	RV GLS by SENC	RV GCS by SENC
Mean [95%CIs]	-14.6 [-16.2, -12.9]	-19.9 [-22.1, -17.7]	-19.0 [-19.7, -18.3]	24.3 [16.2, 32.3]	-20.0 [-22.5, -17.4]	-20.9 [-22.4, -19.3]	-18.7 [-19.5, -17.9]	-19.3 [-21.2, -17.4]
Cochrane Q	114.1	476.8	71.7	26.7	27.4	83.2	0.05	53.7
I^2	95.6	98.7	86.1	92.5	96.35	95.2	0	92.6
Tau^2	4.1	8.7	1.20	45.9	3.3	3.0	0	4.2
Egger's test	0.22	0.67	0.51	<0.001	-	0.38	-	0.76

Supplementary table 3.7b: Uni-variable meta-regression by DENSE, SENC and myocardial tagging

	LV GLS by tagging			LV GCS by tagging			LV GCS by SENC			RV GLS by SENC			LV GCS DENSE		
	β	**p**	**Q_E**	**β**	**p**	**Q_E**	**β**	**p**	**Q_E**	**β**	**p**	**Q_E**	**β**	**p**	**Q_E**
Age	0.03	0.84	100.3	0.16	0.49	450.3	-0.06	0.62	51.8	**-0.16**	**<0.001**	**1.03**	-	-	-
Gender	0.008	0.79	105.6	-0.005	0.9	476.7	0.09	0.05	9.5	**-0.05**	**0.01**	**7.5**	0.01	0.46	57.0
Weight	0.026	0.4	68.1	0.05	0.24	337.9	-	-	-	-	-	-	-	-	-
SBP	-0.08	0.85	113.8	0.09	0.73	476.8	**-**	**-**	**-**	-	-	-	-	-	-
DBP	1.57	0.07	72.3	0.31	0.26	431.1	-	-	-	-	-	-	-	-	-
HR	-	-	-	**0.94**	**0.0007**	**96.2**	-	-	-	-	-	-	-	-	-
FS	-	-	-	-	-	-	2.1	0.15	28.3	-0.2	0.9	52.4	0.33	0.51	61.7

Supplementary table 3.8: Summary of pooled strain values by DENSE, SENC and myocardial tagging

	GE		Phillips		Q_E
LV GLS by Tagging	**3.2**	**0.002**	-	-	29.8
LV GCS by Tagging	**5.9**	**0.002**	-0.03	0.99	117.6
RV GCS by SENC	-	-	2.6	0.03	7.8
LV GCS by DENSE	-	-	1.3	0.26	58.4

Siemens was the reference

Appendix 3E – Interpretation of I^2

Although I^2 value is conventionally used to assess heterogeneity in meta-analysis, "an I^2 value near 100% means only that most of the observed variance is real, but does not imply that the effects are dispersed over a wide range (they could fall in a narrow range but be estimated precisely). Nor does a low value of I^2 imply that the effects are clustered in a narrow range (the observed effects could vary across a wide range, in studies with a lot of error). As such, I^2 is not meant to address the substantive implications of the dispersion" [216]. As Higgins et al defined I^2 as between-study variance divided by total variance x 100 (%) [217], this only reflects the extent of overlap among CIs. A good example is shown in Figure 3.2. Three studies which used three apical views for GLS have relatively narrower CIs than the below 10 studies using 4-chamber view only. However, the I^2 of the former was 94.1%, which is by far larger than that of the latter, only 6.5%. Indeed, obtained normal range for GLS [-21.2, -20.1] is narrower than each of reported ranges, suggesting better precision.

Chapter 4

Summary of methods used

I. Aim of this chapter

This chapter provides a summary of methods used in the following chapters (Chapters 5 to 8). This is because these chapters used the baseline data from an ongoing LOWCBP[218] study in order to avoid unnecessary repetition and gain a better understanding of methods used..

II. Population

The population was recruited from February 2013 to March 2016 in Tasmania. Recruitment was conducted through advertising in the general community as well as in clinics (including pharmacies, general practice, hospitals).

Inclusion criteria

- Aged 18 – 70 years on stable antihypertensive therapy (at least one month).
- Taking at least one, but no more than three, antihypertensive drugs to lower BP (rationale for ≤3 drugs is that this will rule out cases of complicated or resistant HTN which may require special attention beyond this study protocol).
- Seated OBP <140/90 mmHg (controlled OBP).
- Seated central SBP ≥ +0.5SD of age- and gender-specific normal values (uncontrolled central BP). See **table 4.1** for cut off central SBP values. For example, a 55-year-old male with central SBP of ≥120 mmHg will be eligible if OBP <140/90 mmHg.

Table 4.1. Age- and gender-specific central SBP cut off values for inclusion into trial

Age (years)		<20	20 - 29	30 - 39	40 - 49	50 - 59	60 - 69	70 - 79
Target central SBP (mmHg)	Male	≥107	≥109	≥114	≥118	≥120	≥122	≥122
	Female	≥103	≥106	≥111	≥115	≥121	≥123	≥124

Data from the largest normative central BP dataset published to date (n=4002).

Exclusion criteria

- Seated OBP ≥140/90 mmHg (uncontrolled OBP)
- Seated OBP <140/90 mmHg but central SBP below +0.5SD of age- and gender-specific normal values as per **table 4.1** (controlled central BP). For example, a 55-year-old male with central SBP of 119 mmHg or less).
- Women who were pregnant, breastfeeding or childbearing age with intending pregnancy.
- Concomitant therapy with both ACEi and ARB (due to risk of hyperkalaemia).
- Therapy with digoxin or lithium or non-depolarizing skeletal muscle relaxants (e.g. Tubocurarine).
- A clinical history of CVD, which may affect estimation of central BP or complicate therapeutic decisions. This included; established coronary artery disease, coronary artery bypass graft surgery, aortic valve stenosis (gradient >20 mmHg), systolic heart failure or ejection fraction <50% or other serious cardiovascular event within six months of enrolment.

- Chronic use of sex hormone therapy or non-steroidal anti-inflammatory drugs
- Using any aldosterone inhibitor (eplereone, spironolactone) within 30 days of enrolment.
- Contraindication to spironolactone including; anuria, acute renal insufficiency, significant impairment of renal excretory function (creatinine clearance ≤50 mL/min [Cockcroft-Gault formula]) or hyperkalemia (plasma potassium >5.0 mmol/l at initiation).
- Using potassium supplements or potassium-sparing diuretics (e.g. amiloride or triamterene).

III. Imaging protocol

1. CMR acquisition protocol

CMR images were obtained with a 1.5-T MRI scanner with a phased array cardiac coil. An electrocardiogram (ECG)-gated breath-hold vertical long axis (2 chamber) LV and horizontal long axis (4 chamber) image were used to identify the cardiac short axis. The whole heart was imaged in the short axis plane, from ventricular apex to base including both atria, using 14 to 20, 10-mm slice SSFP cines without interslice gap, matrix 256x256, and field of view 350-400. All images were acquired during 10- to 15-second breath holds and stored digitally for offline analysis of cardiac volumes, mass and function. All CMR scans were performed by the same experienced operator.

For the local ascending aortic strain measurements, an axial dataset was positioned perpendicularly to the axis of the aorta at the level of the bifurcation of the pulmonary trunk (between 2 and 4 cm above the aortic junction) to ensure optimal imaging quality and to avoid distortion due to the aortic valve movement. An axial dataset was acquired according to the SSFP sequence using the following average scan parameters: field-of-view = 370 mm × 370 mm, repetition time = 3.2 msec, echo time = 1.4 msec, flip angle = 50°, slice thickness = 8 mm, pixel size = 1.65 mm × 1.92 mm, and inter phase duration = 33 msec. For further evaluation of the aortic geometry, axial and coronal sequences covering the whole aortic arch were acquired using the same protocol.

For the aortic arch pulse wave velocity estimation, the phase contrast (PC) slice was set at the level used for ascending aortic strain measurement. Hence, the ascending and descending aorta could be studied simultaneously. The PC data were acquired using a retrospective ECG-gated breath-hold gradient sequence with a velocity-encoding gradient in the through-plane direction, which provided phase-related pairs of modulus and velocity-encoded images. The scan parameters were repetition time = 9 msec, echo time = 3.5 msec, flip angle = 20°, views per segment = 2, rectangular field-of-view = 50%, acquisition matrix = 256 × 128, pixel size = 1.58 mm × 1.58 mm, slice thickness = 8 mm, and encoding velocity = 200 cm/s. View sharing was used resulting in an effective temporal resolution of 18 msec.

2. Echocardiography protocol

LV structure and function were measured using 2D and 3D echocardiography as per guidelines [46] (Vivid E9, GE Medical, Milwaukee, WI, USA).

IV. Blood pressure measurement

1. Office and central blood pressure

OBP were recorded with SphygmoCor XCEL (AtCor Medical, Sydney, NSW). Radial applanation tonometry was also used to estimate central BP with validated [4,34,35] and reproducible [36] device (SphygmoCor 8.1, AtCor Medical, Sydney, NSW). For eligibility assessment, the radial pressure waveform was calibrated using two methods; 1) with average office SBP and diastolic BP (DBP) from the XCEL measurements and; 2) from the average mean arterial pressure (calculated by office DBP + 0.4* office pulse pressure) and DBP from the XCEL measurements. This approach gives a closer approximation of the true mean arterial pressure compared with the one third rule [37] and is currently regarded as the preferred method to calibrate radial pressure waveforms [38–40]. All measures were taken with a correct sized cuff, feet flat on floor, back supported and without talking (as per recommendations) [41]. After a five-minute rest, measures were acquired in duplicate using SphygmoCor 8.1, immediately after the BP recordings with SphygmoCor XCEL. A second and a third set of duplicate measures (1 minute apart) were taken after 10 and 15 minute rests, and the average of any two consecutive measurements from either SphygmoCor XCEL or SphygmoCor 8.1 were used to assess eligibility using the calibration methods mentioned above. We have recently found that this is the optimal, and most clinically relevant, time to acquire brachial.

2. 24-hour ambulatory blood pressure

A Mobil-O-Graph (I.E.M. Industrielle Entwicklung Medizintechnik GmbH) validated [43,44] BP monitor was used to record central and OBP over 24 hours (every 20 mins during the day and 30 mins overnight) according to a recommended protocol [45]. Night-time was defined from patient diaries of sleep and awake times.

V. A summary of the method used in the following chapters

In summary, participants with normal OBP with elevated CBP were recruited from February 2013 to March 2016 in Tasmania. During the two-year study period, each participant was scanned with echocardiography (3 times, 1st, 12th, and 24th of month, including both standard and advanced assessments) and MRI (2 times, 1st and 24th of month) techniques including myocardial strain. OBP, 24-hour ABP, and CBP were also recorded. All images were then anonymised and analysed by the author (HV). For chapters that assessed inter-observer variability, other experts were also involved (Mr Eswararaj Sivaraj for echocardiography and Prof Kazuaki Negishi for MRI). The main aims of the following chapters are to: 1) validate novel with standard imaging methods; and 2) seek associations between different components of blood pressure and cardiac functions measured by advanced methods.

Chapter 5

Robustness of MRI and echocardiographic myocardial strains of the ventricles and left atrium

Abstract

Aims. This study aimed to evaluate and compare the reproducibility of atrial and ventricular strains on both MRI and echocardiography.

Background. Myocardial strain is a relatively novel and sensitive measure of systolic function. Speckle tracking echocardiography (STE) has been used widely in research community, but more and more in clinical settings. The use of feature tracking (FT) from MRI is also increasing. Before the full clinical application, the reproducibility of this technique should be clarified. Although several studies have been conducted, majority of studies had small sample size (<20) and using single modality.

Methods. Strain analyses were performed on two apical views using dedicated software. Images were assessed twice by the same observer for intra-observer evaluation and by another operator for inter-observer evaluation. Intra- and Inter-observer variability were also conducted in LVEDV measurement

Results. MRI LVEDV had the highest reproducibility among the measures. Regarding strain analysis, MRI FT strain had similar inter- and intra-observer variability, compared to STE. LVGLS was most robust, followed by RVGLS in both modalities. LA strains had the least agreement, especially LA conduit strain.

Conclusion. Although various elements may affect on reproducibility, STE and FT shared similar robustness in LV, RV and LA strains. This study suggests ventricular strains and LA reservoir strain have sufficient robustness for clinical use in both modalities.

I. Introduction

Myocardial strain is a sensitive and robust measure of systolic function and has incremental prognostic information beyond conventional left ventricular ejection fraction (LVEF) [219-222]. Speckle tracking echocardiography (STE) has been used widely in research community and become more and more utilized in clinical setting. Besides, MRI feature tracking (FT) has been applied with normal values being determined recently[223]. One of the main barriers for clinical application is attributed to limited data on the reproducibility of this technique. Currently, there are three gaps in literature. 1) Majority of studies on the reproducibility have focused on LV longitudinal deformation. Less attention has been paid on right ventricular (RV) and left atrial (LA) strains. 2) The assessment of STE reproducibility was small in size [219, 224-227], so did FT. STE reproducibility has been assessed many studies, but majority had <20 cases[219, 228]. MRI strain reproducibility has been assessed in smaller extent as it is newer but also <20 cases.[229] 3) Few studies compared the reliability of MRI FT and STE[228]. In other words, a full picture of reproducibility of STE and FT has not been drawn. Therefore, this study aimed to evaluate the reproducibility of atrial and ventricular strain on both MRI and Echocardiography to elucidate the differences if any.

II. Method

Study Population: This study is a sub-study of an ongoing LOwering Central Blood Pressure (LOWCBP) study [218]. Briefly, the inclusion criteria were 1) adult participants on stable antihypertensive therapy; 2) 1-3 hypertensive drugs to lower blood pressure; 3) seated brachial blood pressure being ≤ 140/90 mmHg; and 4) seated

central systolic blood pressure ≥ +0.5SD of age- and gender-specific normal values. This sub study used the population recruited in Royal Hobart Hospital, Tasmania, Australia.

Echocardiography: Transthoracic echocardiograms were performed using commercially available ultrasound systems (Vivid E9, GE Medical, Milwaukee, WI, USA). Each participant first underwent an extensive standard assessment of cardiac anatomy and cardiac function according to clinical protocol with one ultrasound system. Acquisition was obtained at the highest possible frame rate with optimization of image depth and sector width. Multiple consecutive cardiac cycles of the three standard apical views were acquired and digitally stored as raw data for offline analysis. LV end-diastolic and end-systolic volumes were performed using the biplane method of disks, according to American Society of Echocardiography Guidelines [230].

Magnetic Resonance Imaging: Cardiac magnetic resonance (CMR) images were obtained with a 1.5-T MRI scanner with a phased array cardiac coil. An electrocardiogram-gated breath-hold vertical long axis (2-chamber [2C]) LV and horizontal long axis (4-chamber [4C]) image were used to identify the cardiac short axis according to the recommendation[231]. The whole heart was imaged in the short axis plane, from ventricular apex to base including both atria, using 14 to 20, 10-mm slice SSFP cines without interslice gap, matrix 256 x 256, and field of view 350-400. All images were acquired during 10- to 15-second breath holds and stored digitally for offline analysis of cardiac volumes, mass and function. All CMR scans performed by the same experienced operator.

Measurement of myocardial strain Echocardiographic strain was analysed on EchoPAC PC (software version 112, GE Medical, Milwaukee, WI) and MRI FT strain was analysed on Qstrain (Medis, Leiden, The Netherlands). 2-dimensional images from 2 apical views (4 and 2 chamber views) were used. Readings were obtained by averaging 6 segments in each view. LVGLS was determined from the average of 12 segments. After tracing of the endocardial border, the region of interest was adjusted to include the entire myocardial thickness and avoid the pericardium. LA strains were also estimated from the average of 12 segments. LA reservoir and contractile strain were selected manually from the strain-time curve. The region of interest includes only LA thin wall and avoids appendage. The quality of tracking was assessed manually. The cardiac cycle with the best tracking and visually most credible strain curves were selected for analysis. In segments with poor tracking, the border was readjusted manually until optimal tracking was achieved. After adjustment, segments with consistently poor tracking were excluded. Then, LV and LA strains were calculated as the averaged value of strains from each 2C and 4C view. RV strains were assessed from 4C views [232].

Statistical Analysis Continuous variables are presented as mean ± standard deviation (SD). Categorical variables are expressed as percentages. Normality was evaluated using the Kolmogorov-Smirnov test. Inter- and Intra-observer variability were studied using Bland-Altman analysis to quantify a systemic difference (bias) between two techniques and the spread of differences of mean bias (limits of agreement [LOA]). Intraclass correlation coefficients (ICCs) were also used for the assessment of agreement. The coefficient of variation (CV) was calculated for all measurements. To

assess intra-observer variability, the same operator performed measurements after an interval of at least two weeks, blinded to previous measurements. For the assessment of inter observer variability, a second operator blindly measured the same group of subjects. Intra-observer and inter-observer variability values were summarized as the absolute difference, CV, ICC and Bland- Altman statistics and by calculating the coefficients of variation. Statistical analyses were performed using a standard statistical software package (SPSS software 22.0, SPSS Inc., Chicago, IL). Statistical significance was defined by $p< 0.05$.

III. Results

Study population: Patient demographics and imaging parameters are summarized in **Table 5.1**. Among the 54 patients (aged 54.7± 9.6), 50% of participants had family history of CAD and 13% of them smoked and diabetes. LVEF were normal in both Echocardiography (60.9 ±5.9 %) and MRI (56.3±5.8%) (**Table 5.2**). FT showed slightly larger ventricular strains value than ST (LVGLS, STE 18.2±2.2% versus FT 20.5±2.3%; RVGLS, 23.3±3.5% versus 26.0±3.7%). However, LA strains were larger in STE (LA Reservoir strain, 39.2±8.7% versus 33.1±5.4%; LA contractile strain, 17.4±4.3% versus 15.7±3.3%; LA conduit strain, 21.8±6.4% versus 16.3±6.3%)

Strain reproducibility: ICC and CV of LV, RV and LA strains are illustrated in **Figure 5.1**. In general, STE and FT shared similar concordance among the spectrum of strains. The spectrum of the reproducibility of strains (LVGLS, RVGLS and LA strains) spread from fair to excellent (ICC 0.78 ~ 0.9), slightly lower than those of LV end-diastolic volume (LVEDV). Among the all strains assessed, LVGLS had the best concordance

(ICC 0.83~0.86, CV 4.5%~6.5%) followed by RVGLS (ICC 0.78~0.83, CV 6.2~7.7%) and LA strains.

Bland-Altman analyses also indicated the excellent reproducibility of LV and RV GLS in both modalities **(Table 5.3)**. For LVGLS, STE and FT had similar reproducibility, where STE had slightly larger bias (1~2% vs 0.3%) but smaller LOA (3% vs 3.5%). The biases in RVGLS were approximately zero with almost twice as large LOA as LVGLS had (5~6%). Among the LA strains, LA reservoir strain had better concordance than contractile or conduit strains. Inter- and intra-observer ICC and CV of LA reservoir strain were (ICC 0.85~0.9, CV 6.4~10.0%), followed by LA contractile strain (ICC 0.77~0.81, CV 9.3~12.8%)

Volume by MRI is considered as a gold standard, widely being accepted both in academic and clinical community. The inter- and intra-reliability in this study also confirmed the robustness of this technique. All indices indicated an excellent reliability of the volume by MRI. Whereas, reproducibility of volume measurement by Echo were lower than those by MRI, especially assessed with CV.

IV. Discussion

The study has drawn a comprehensive picture on the reproducibility of both STE and FT strains. STE and FT had similar robustness among the spectrum of strains. Ventricular strains had comparable reproducibility, although both inter- and intra-observer variabilities of LVGLS were better than those of RVGLS. LA strains had lower reproducibility than ventricular strains with only LA reservoir strain being

satisfactory. From the best of our knowledge, this is the first paper that focused the reproducibility of all LV, RV, and LA strains with two different modalities. Besides, MRI has higher spatial resolution but lower temporal resolution than echocardiography has. Thus, this study also aimed to assess which resolution affects more on the robustness of myocardial strain. As demonstrated above, both resolutions affected similarly.

Reproducibility of LV and RV strains: Several comparisons have been performed in literature, but majority of them were limited because of small sample size (~20), the use of single modality, or only focusing on ventricular strains[233-235]. In literature, comparable robustness has been reported between the two ventricles with CV revolving around 10% in majority of studies. LVGLS has been reported as the most reliable measure [219, 236, 237], which is consistent with our results. Our study yielded CV between 4.5 and 6.5 for LVGLS, and between 6.2 and 7.6 for RVGLS. These are similar to the work of Cheng et al [219] but better than previous reports in 2011-2012, where CVs were approximately 16 ~25% [238, 239]. Possible reasons for this improvement would be due to better image quality (higher resolution) and better tracking algorithm.

Reproducibility of LA strains: One of the obstacles to apply LA strains by tissue tracking has been, compared with LVGLS, was because LA strain had high inter- and intra-variability [240, 241]. In general, LA reservoir strain was the most reproducible among LA strains. The reproducibility of LA conduit strain was the worst among all variables (**Figure 5.1**). It would be because it contained a combined error of LA reservoir and contractile strain.

Reproducibility of STE and FT: There were limited comparisons in reproducibility between strain by FT and STE. In this study, despite various influence and obvious differences, the reproducibility of ventricular deformation by FT provided comparable values to those measured by STE. Both STE and FT are rooted in pattern matching technologies. In general, a tracking method begins with identifying a small window covering the patterns on one frame and searching for the most similar neighbouring window of the same size in the subsequent frame. The major differences between STE and FT are inherently based on the tracked patterns: STE exploits the stochastic reflection of ultrasound beam from the cardiac structures, called speckle, which serves as unique fingerprints for pattern matching technology. Because speckle does not exist in MRI images, patterns in FT are inhomogeneity of tissue brightness, roughness at the border of different tissue types [242, 243]. As long as the patterns are unique, using different patterns have minimised effects on the difference in reproducibility between STE and MRI. Major differences stem from (1) special resolution (affects qualities of manual tracing and tracking) and (2) temporal resolution (e.g. frame rate). Manual trace depends on various variables including technician's expertise and image quality. As being known, CMR has higher special resolution than echocardiography, FT can be less dependent on technician's expertise, compared to STE. It should be borne in mind that ventricular walls are relatively thick, compared to LA, density of speckle patterns moving simultaneously with endocardial border of LV wall or RV wall is high, differences in manual trace less impact on the final results. RV strain was somewhat less reproducible than LV strain due to the thick trabeculations present within the RV.

Limitation: Our results should be interpreted in the context of following limitations. In most cases, echocardiograms and CMR were performed on different days, small changes in physiologic variables between the tests were unavoidable although the median difference was 16 days. However, the temporal difference should have minimal effects on the reproducibility. In addition, both FT and STE in our study applied on 2D method, through plane motion can be problematic, especially in patients with higher heart rate. Fortunately, heart rate during MRI of our patients lied between 47 to 88 bpm.

V. Conclusion

Although various elements may effect on reproducibility, STE and FT shared similar robustness in LV, RV and LA strains. This study suggests ventricular strains and LA reservoir strain have sufficient robustness for clinical use in both modalities.

Acknowledgement/sources of funding. This work was supported in part by a project grant from the National Health and Medical Research Council of Australia (reference 1044551). Dr Negishi is supported by a Fellowship (Award Reference No.101868) from the National Heart Foundation of Australia.

Table 5.1: Patient demographics

Variable	Value
N	54
Age, years	54.7±9.6
Male, %	53%
Height, cm	169.8±9.4
Weight, kg	87.1±14.8
BSA, kg/m^2	2.02± 0.21
Smoked, %	13%
Family History of CAD, %	50%
Diabetes, %	13%

Table 5.2: Imaging parameters

Variable	Echocardiography	MRI	p-value
LVEDV, ml	96.6±24.8	153.9±29.4	<0.01
LVEDVi, ml/m2	47.7±10.1	76.0 ± 11.0	<0.01
LVESV, ml	38.2±12.1	67.5±16.5	<0.01
LVESVi, ml/m2	18.8±5.1	33.2±6.5	<0.01
LVEF, %	60.9±5.9	56.3±5.8	<0.01
E, m/s	0.65±0.15	-	
A, m/s	0.58±0.14	-	
E/A	1.2±0.4	-	
Myocardial strains			
LVGLS, %	18.2 ± 2.2	20.5 ± 2.3	<0.01
RVGLS, %	23.3±3.5	26.0±3.7	<0.01
LA Reservoir strain, %	39.2±8.7	33.1±5.4	<0.01
LA Contractile strain, %	17.4±4.3	15.7±3.3	<0.01
LA Conduit strain, %	21.8±6.4	16.3±6.3	<0.01

Table 5.3: Reproducibility of strains by tissue tracking and volumes

		LV GLS		RV GLS		LA Reservoir strain		LA contractile strain		LA conduit strain		LV EDV	
		Bias	**LOA**	**Bias**	**LOA**	**Bias**	**LOA**	**Bias**	**LOA**	**Bias**	**LOA**	**Bias**	**LOA**
MRI	**Inter-Observer**	-0.3	3.3	-0.1	6.7	1.4	8.6	0.8	6.1	-7.1	13.2	-2.2	3.9
	Intra-Observer	0.3	3.5	0.0	6.2	0.1	8.5	-0.6	5.6	0.6	7.9	-1.3	2.3
Echo	**Inter-Observer**	2.5	2.9	0.9	5.6	-2.5	11.6	-0.8	7.9	-1.7	9.1	-9.6	27.8
	Intra-Observer	1.3	3.2	-0.2	5.4	-2.7	7.2	-1.5	8.3	-1.2	8.9	-0.7	27.7

Figure 5.1: Inter- and Intra- variability of MRI and Echo Strains

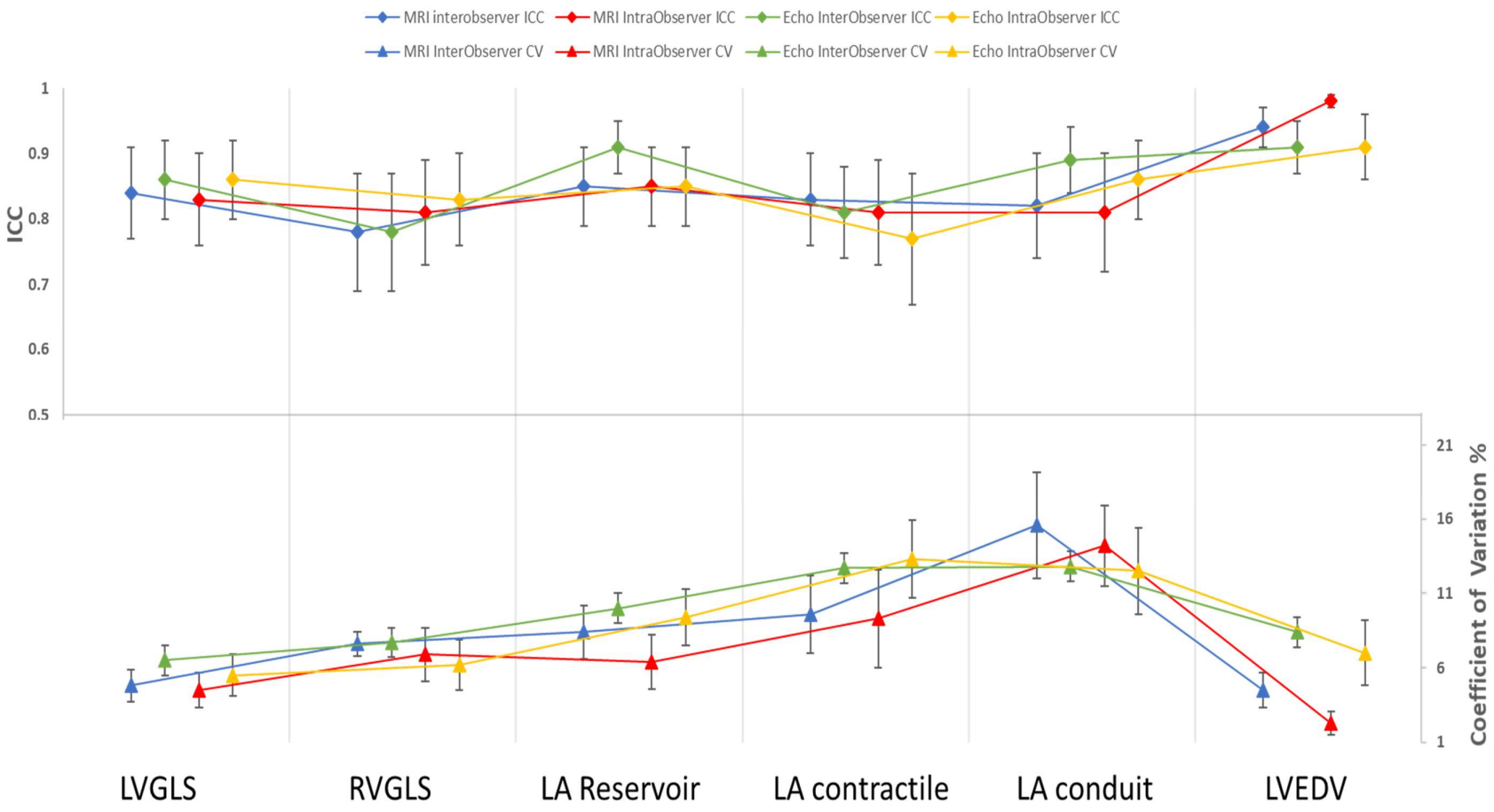

Chapter 6

Volume quantification derived from Speckle tracking and Feature tracking

a Head-to-Head comparison study

Abstract

Aim: This study aimed to evaluate the agreements between the volumes measured by strain analysis and those by conventional imaging methods.

Background: Speckle tracking echocardiography (STE) and MRI feature tracking (FT) are robust and sensitive methods to assess cardiac function. These methods can also provide cardiac chamber volumes. However, little is known about the accuracy compared with gold standard MRI measurement.

Methods: We assessed 2-dimensional echocardiography (2DE) and MRI data from 100 patients with hypertension. The agreements between volumes (end-diastolic, EDV; end-systolic, ESV; and ejection fraction, EF) by different methods and modality were evaluated using Bland-Altman plots, coefficient of variance, inter-class correlation and Pearson's correlation coefficients.

Results: Compared with MRI-derived volumes, 2DE yielded the smallest volumes and the largest underestimation (ΔEDV, -45.7±17.5 ml; ΔESV, -23.7±12.6 ml; and ΔEF, 3.6±7.3 %), followed by volumes by STE (ΔEDV, -29.2±25.4 ml; ΔESV, 15.9±14.9 ml; and ΔEF, 2.6±7.7 %). Volumes by FT were the most concordant with the MRI-derived volumes with EF being almost identical (ΔEDV, -18.7±16.2 ml; ΔESV, -7.7±8.2 ml; and ΔEF, -0.3±7.65%). Among these three volume-related parameters, EF had the least discrepancy to MRI-derived one.

Conclusion: Volumes by strains were more concordant with MRI-derived volumes than those by conventional echocardiography. However, they still significantly underestimated the volumes.

I. Introduction

Left ventricular (LV) volumes are key indexes in clinical practice. Accurate estimation of end-diastolic (EDV) and end-systolic volume (ESV), and ejection fraction (EF) is essential for routine management of patients[230, 244]. MRI being gold standard of measurement. The measurement, however, is based on manual tracings of endocardial border on every slice in a stack of short axis views, which is time-consuming. Two-dimensional (2D) echocardiography (2DE) with method of discs, remains the most widely utilized technique for volume quantification [230, 245].

Speckle tracking echocardiography (STE) and MRI feature tracking (FT) allow semi-automatic measurement of strain and have caught the attention of many researchers and clinicians [21, 223, 246-248]. These methods can provide LV volumes curves for a cardiac cycle without additional effort. This could have potential to save time and resources. However, Limited studies with small samples size were conducted in literature to validate these methods[249, 250]. We aimed to elucidate the accuracy of the volumes from STE and FT against gold standard MRI volumes.

II. Method

Study Population: This is a sub-study of an ongoing Targeted LOWering of Central Blood Pressure (LOWCBP)[218]. This is a multi-centre, randomized, open-label, blinded endpoint trial. 100 adults with normal EF, aged 57.6± 8.8 were randomly selected among 144 recruited participants in an ongoing study at Royal Hobart Hospital, Tasmania Australia from February 2013.

Echocardiography: Standard assessment of cardiac anatomy and function by transthoracic echocardiograms were performed using Vivid E9 (GE Medical, and Milwaukee, WI, USA) at the highest possible frame rate with optimization of image depth and sector width. LV end-diastolic and end-systolic volumes were performed using the biplane method of discs. All measurements have followed ASE guidelines [230].

Magnetic Resonance Imaging CMR images were obtained with a 1.5-T MRI scanner with a phased array cardiac coil (GE Signa HDxt, Milwaukee, WI, USA). Full MRI protocol was found in [218]. All CMR scans were performed by experienced operators. Low-quality images were excluded from this study. Conventional volume measurement was performed on Medis Qmass (Medis Medical Imaging Systems, Leiden, the Netherlands). Endocardial border was drawn semi-automatically on a stack of short axis from base to apex at end-diastolic and end-systolic phase[231].

Measurement of volumes by strain analysis: Two commercially available software were used to evaluate volumes by strain analysis in STE (Tomtec, Tom-Tec Imaging Systems, Unterschleissheim, Germany) and FT (Medis Qstrain, Medis Medical Imaging Systems, Leiden, the Netherlands). The endocardial border was manually traced, and the region of interest was adjusted when necessary. The software then tracked motion on a frame-to- frame basis throughout the entire cardiac cycle and generate a volume-time curve. The quality of tracking was assessed manually. The cardiac cycle with the best tracking and visually most credible strain curves was selected for analysis. In segments with poor tracking, the border was readjusted

manually until optimal tracking was achieved. After adjustment, segments with consistently poor tracking were excluded. The final volumes were calculated as an average of volumes in two views. EDV and ESV were chosen manually from the curve. These volumes were then compared with gold standard MRI volumes. All measurement was performed by the same examiner (HV).

Statistical Analysis. Continuous variables are presented as mean ± standard deviation (SD). Categorical variables are expressed as percentages. Normality was evaluated using the Kolmogorov-Smirnov test. Agreement were studied using Bland-Altman analysis to quantify a systemic difference (bias) between two techniques and the spread of differences of mean bias (limits of agreement [LOA]). Intraclass correlation coefficients (ICCs) were also used for the assessment of agreement. The coefficient of variation (CV) was calculated for all measurements. Statistical analyses were performed using a standard statistical software package (SPSS software 22.0, SPSS Inc., Chicago, IL). Statistical significance was defined by $p< 0.05$.

III. Results

Patient characteristics

The study consisted of 100 participants with medically controlled hypertension, of whom 52% had family history of coronary artery disease (**Table 6.1**). This included 9% with diabetes and 35% smoked. Their age spread from 24 to 70 with average of 57.6±8.8 years. The median number of days between echocardiography and MRI acquisition was 16 days (25^{th} and 75^{th} percentile 11, 25).

Comparison with gold standard

The results of volume comparison are summarised in **Table 6.2.** Compared with MRI-derived gold standard volumes, 2DE yielded the smallest volumes and the largest difference from MRI volumes (Δ EDV, -45.7±17.5 ml. Δ ESV, -23.7±12.6 ml, Δ EF, 3.6±7.3 %), followed by volumes by STE (Δ EDV, -29.2±25.4 ml. Δ ESV, 15.9±14.9 ml, Δ EF, 2.6±7.7 %).

In Bland-Altman analyses (**Figures 6.1-6.3**), LOA of LVEDV between MRI and FT was the narrowest so as in LVESV. However, LOAs were similar among the three comparison (MRI vs volume by FT, MRI vs volume by STE, and MRI and 2DE).

Concordance of the volume assessment within the same modality:

The results of concordance are summarized in **Table 6.3**. Agreements in LVEDV and LVESV between MRI and FT were very good with ICC being 0.91 [95%CI 0.88, 0.95] and 0.88 [0.82, 0.92], which were higher than those between 2DE and STE (0.84 [0.76, 0.89] and 0.86 [0.79, 0.9], respectively. However, ICC of EF between 2DE and STE was higher than that between MRI methods (0.77 vs.0.57), probably because most of our population had normal EF with a narrow distribution.

Among the volumes measured, LVESV demonstrated the largest variability. CV were 15.4% in echocardiography and 13.6% in MRI, followed by LVEDV with 12.6% and 10.5%, respectively. LVEF had the lowest CV despite their lowest ICCs among the three parameters, 5.3% and 7.5%, in echocardiography and MRI, respectively.

IV. Discussion

The study investigated the accuracy of volumes assessments by strain methods. Basically, the method is a derivation from tissue tracking technology, where a manual tracing of endocardial border at end diastolic phase is tracked over cardiac cycles to define the volume curve. Although several studies assess the accuracy of STE or FT derived volumes against MRI volumes, this is the first study which compared all 2DE, STE, and FT with MRI volumes. Our results have shown a decent agreement between this method and the established volumes. Our data suggested that EDV and ESV, evaluated by FT, showed relatively small bias and close agreement with the gold standard MRI volumes. The volumes by STE were better than 2DE volumes in term of agreement with the gold standard. LVEF showed to be the least agreement among the three parameters in all comparisons.

Volume by STE: Our data demonstrated that volume by STE still significantly underestimate LV volumes. Previous animal and human studies showed that STE underestimates volumes with high variability in the comparison with gold standard (negative biases between 15 to 30 ml) [233, 249, 251]. One of the reasons would be because, like all 2DE, the accuracy of the endocardial border tracing is affected by trabeculation of the LV. Another reason would be that volume quantification by STE relies heavily on geometric assumption and is sometimes affected by the use of foreshortened apical views [249, 252]. An additional limitation of STE, which was inherent in 2D techniques, was through plane motion. Software only detects in-plane motion, out of plane motion was ignored or assumed to be noise and interfering with tracking [253, 254].

Volume by FT: Our data showed that FT yielded larger volumes than those from 2DE or STE but still underestimated compared with MRI, although these two shared the same signal-to-noise ratio. Similar results were reported by Di Bella et al. that EDV and ESV by FT underestimate by around 38-40 ml, compared with conventional MRI[255]. Those values were tripled values in our studies (10-14 ml). Technical improvement would be an explanation for the differences because their study was conducted ten years ago in 2009 when FT was still in its dawn. A recent study [233] demonstrated similar agreement in EDV with our results (bias 17.1 ml vs 18.7 ml and r=0.97 vs. 0.91). However, they had larger bias in ESV (bias 13.0 ml vs 8 ml) but stronger correlation (r=0.98 vs. 0.88). Probably these discrepancies are from the difference in population. They studied on population with a wider range of EF (10~80%), where 41% of their participants had EF <35%. In addition, a reason for the discrepancy between FT and MRI is the slices used. Standard MRI volume measurement uses a stack of short-axis images whereas FT uses apical long-axis images. In addition, the assumption of bullet shaped LV is not necessarily satisfied.

Ejection Fraction: Among indexes reported in our study, LVEF were always not only the least bias and variability but also the least correlations, highly agreed with the results of Nishikage et al.[250] It would be because LVEF in our study lied between narrowed and overlapped ranges, statistical parameters could not describe clearly the differences between different methods. Regrettably, ranges of LVEF were not reported in majority of study in this topic. A study with wide ranges of LVEF with different patient conditions would be more appropriate.

State-of-art volume analysis: Recently, several deep learning convolutional neural network (CNN) models have achieved state-of-the-art performances for LV segmentation from cine MRI, leading to simple volume analysis. CNN does not require physician's intervention and accelerate the diagnosis process. However, CNN is a data-hungry method with expensive computation for model training. In addition, accuracy and robustness are extremely crucial in medical domain. Further researches on vulnerability of deep learning methods must be conducted for the eventual use in patients. Prior to the maturity of LV volume by deep learning, that by strain analysis, as this study suggested, is far practical and ready for clinical use, compared with CNN. Firstly, this method is definitely faster than conventional LV volume quantification. Secondly, the quality of tracking can be visibly assessed to ensure the accuracy. Finally, the robustness of strain analysis, as described in chapter 5, is an advantage for further use.

Limitation: This study has several limitations. First, in majority of cases, MRI were taken in different days from echocardiography. However, the median difference was 16 days, where one can assume no significant changes in LV volumes and physiology because none had significant cardiovascular events between the two scans. Secondly, bsecause this is a single centre study, differences in ethnicity have not been considered. Thirdly, population in this study had a very narrow range of LVEF, which causes difficulties to assess the agreement between methods.

V. Conclusion

Although high variability of volume derived from tissue tracking with standard measurement has been found in this study, high correlations were also explored. It suggested the feasibility of these methodology in clinical. Normal ranges should be conducted in further studies.

Acknowledgement/sources of funding. This work was supported in part by a project grant from the National Health and Medical Research Council of Australia (reference 1044551). Dr Negishi is supported by a Fellowship (Award Reference No.101868) from the National Heart Foundation of Australia.

Table 6.1: Patient demographic

Variable	Value
N	100
Number of days between 2 scans (IQR)	16 (11-28)
Age, years	57.6±8.8
Male, %	54%
Height, cm	169.3±9.6
Weight, kg	84.3±15.3
BSA, kg/m^2	1.99± 0.22
Smoked, %	35%
Family History of CAD, %	52%
Diabetes, %	9%

Table 6.2: Imaging parameters

	MRI		Echocardiography		p-value
	Conventional	FT	STE	Conventional	
LVEDV, ml	153.1±28.9	134.4 ± 29.8 †	124.0±29.5 †	107.4±25.2 †	<0.01*
LVEDVi, ml/m^2	77.1±12.4	67.7±13.3†	62.3±13.2†	54±11.3†	<0.01*
LVESV, ml	66.8±19.0	59.0±17.4†	50.9±17.5†	41.8±23.8†	<0.01*
LVESVi, ml/m^2	33.5±8.6	29.6±8.2†	25.5±8.1†	21.6±6.6†	<0.01*
LVEF, %	56.8±7.2	56.5±6.7	59.3±6.8†	60.4±5.8†	<0.01*
Δ EDV	REF	-18.7±16.2#	-29.2±25.4#	-45.7±17.5	<0.01*
Δ ESV	REF	-7.7±8.2#	-15.9±14.9#	-23.7±12.6	<0.01*
Δ EF	REF	-0.3±7.65#	2.6±7.7	3.6±7.3	0.01

*repeated ANOVA

†P<0.05 (Bonferroni corrected), compared with conventional MRI

#P<0.05 compared with conventional Echocardiography

Table 6.3: Comparison of LV volumes by different methods

		LVEDV	LVESV	LVEF
2D Echo volume	r	0.8	0.75	0.42
	ICC	0.88 (0.83, 0.92)	0.84 (0.76, 0.89)	0.59 (0.39, 0.72)
vs				
	CV	25.4 ±1.02	31.4 ± 1.38	7.4 ± 5.02
MRI volume				
	Bland-Altman	-45.7 ± 34.2	-23.7 ± 24.6	3.6 ± 14.3
STE Volume	r	0.62	0.67	0.4
	ICC	0.77 (0.65, 0.84)	0.8 (0.7, 0.87)	0.57 (0.36, 0.71)
vs				
	CV	16.5 ± 10.4	21.4 ± 1.47	7.7 ± 5.32
MRI volume				
	Bland-Altman	-29.2 ± 49.8	-15.9 ±29.2	2.5 ±15
	r	0.85	0.78	0.4
FT Volume	ICC	0.91 (0.88, 0.95)	0.88 (0.82, 0.92)	0.57(0.36, 0.71)
vs	CV	10.5 ± 0.71	13.6 ± 0.97	7.5 ± 0.71
MRI volume	Bland-Altman	-18.7 ±31.7	- 7.7 ± 23.7	-0.3 ± 15
STE Volume	r	0.73	0.76	0.62
	ICC	0.84 (0.76, 0.89)	0.86 (0.79, 0.9)	0.77 (0.65, 0.84)
vs				
	CV	12.6 ± 0.92	15.4 ± 1.17	5.3 ± 0.46
2D Echo volume				
	Bland-Altman	16.6 ± 40.1	7.9 ± 22.3	- 1.1 ± 11.2

All $p < 0.05$

Figure 6.1 Comparison LVEDV measured by different methods

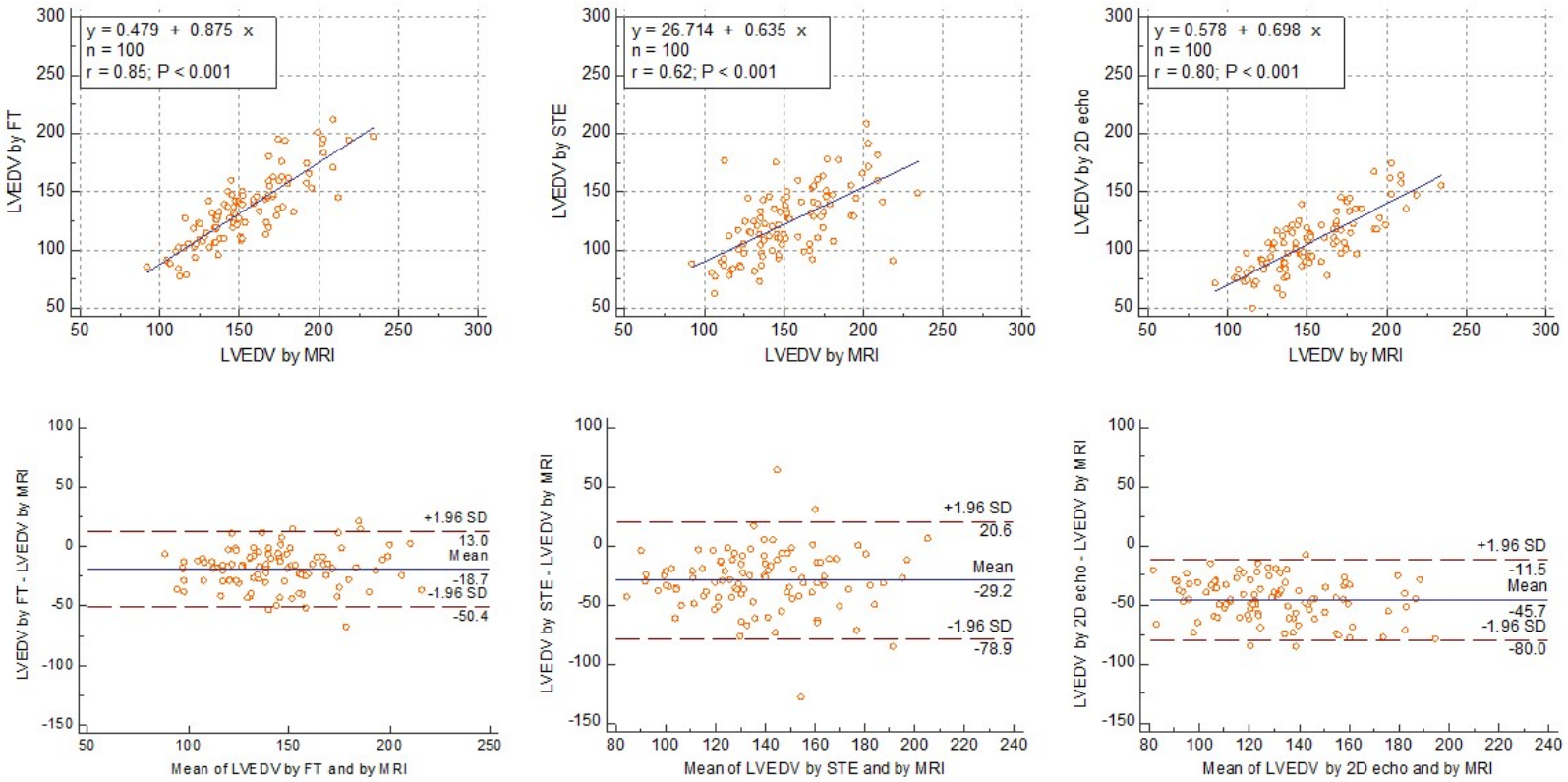

Figure 6.2 Comparison LVESV measured by different methods

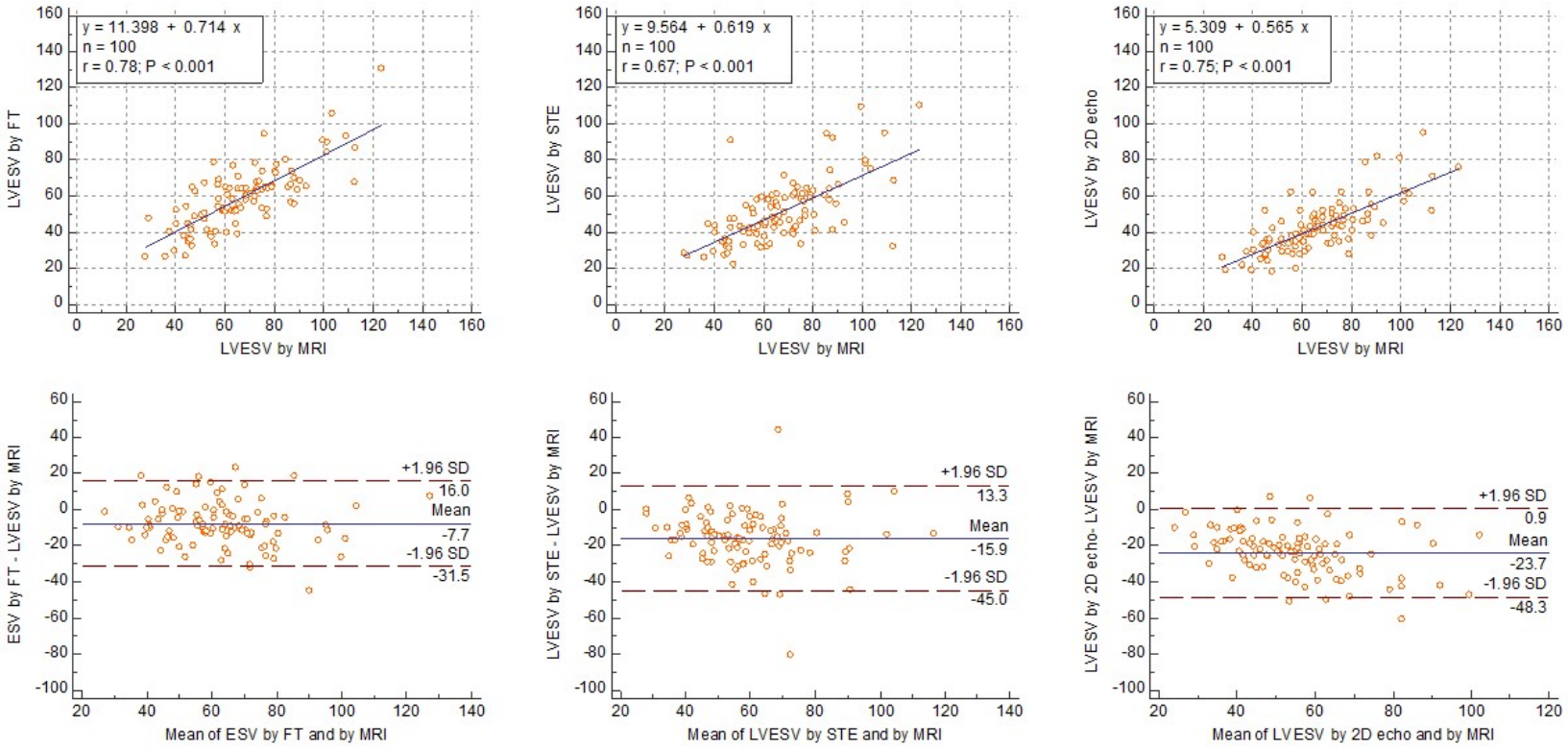

Figure 6.3 Comparison LVEF measured by different methods

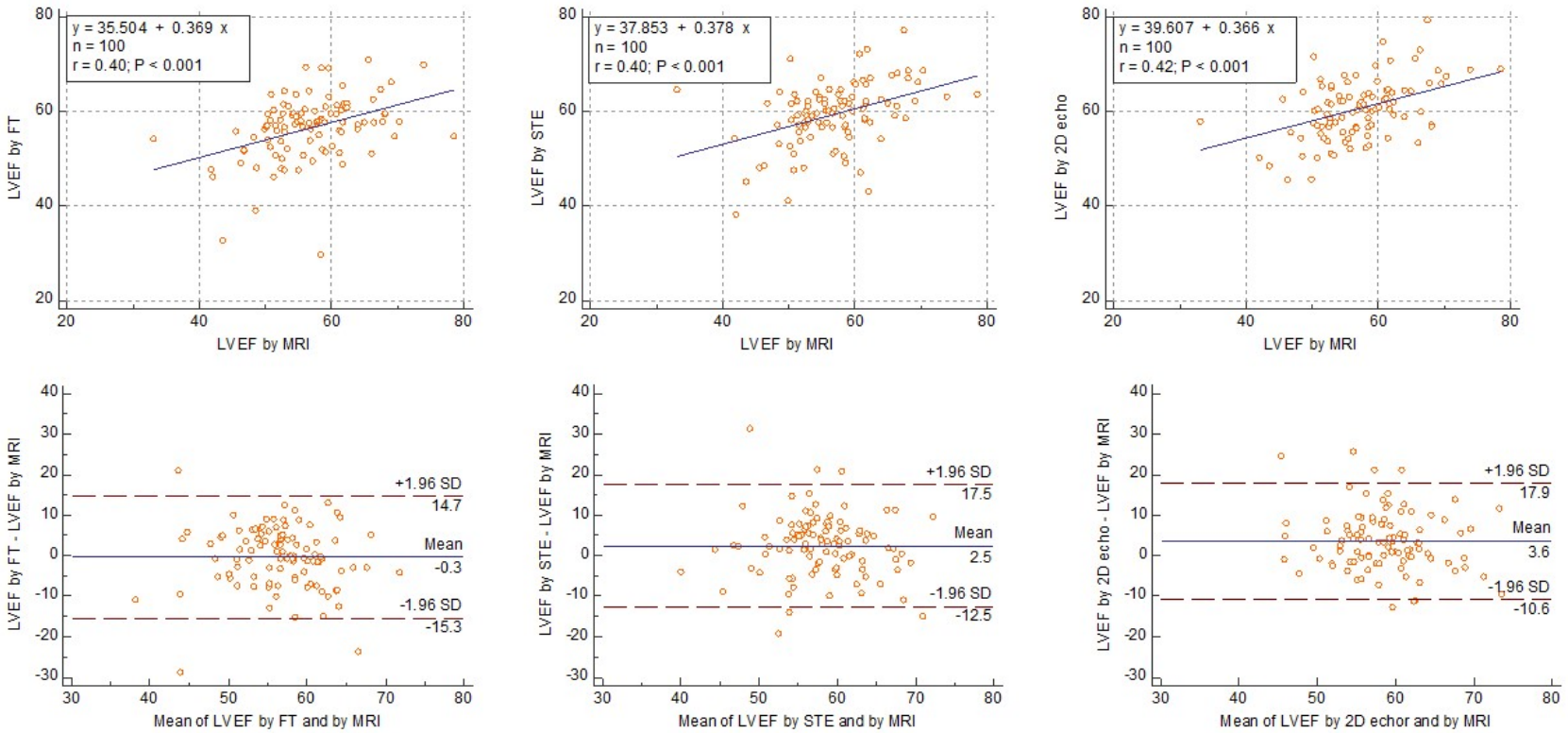

Chapter 7

Left atrial contractile strain is independent of left ventricular strain irrespective of modalities.

Abstract

Introduction: LA strain is a quantitative functional parameter of LA function with diagnostic and prognostic value. However, it may merely reflect the change in LV deformation because LA function reflects underlying LV longitudinal function. This study aimed to test our hypothesis that LA reservoir strain, but not LA contractile strain, is independently associated with LVGLS in both echocardiography and MRI strains.

Methods: Medically controlled hypertensive adults who had both echocardiography and MRI were used. Strain analyses were performed on 2CH and 4CH views using dedicated software. The association between LA reservoir, conduit, and contractile strains, as well as LVGLS and other LV standard parameters, were assessed in both univariable and multivariable linear regression models.

Results LVGLS, LA reservoir strain, and conduit strain were mutually correlated but not LA contractile strain in both modalities. Mild to moderate correlations between LA reservoir and contractile strains were identified (echocardiography: $r=0.64$, $p<0.01$; MRI: 0.28, $p=0.01$). The correlation coefficients between LVGLS and LA reservoir strain were greater than those between LVGLS and LA contractile in both STE and FT (both $p < 0.05$). In multivariable models, LVGLS were significantly associated with LA reservoir strain and LA conduit strain but not LA contractile strain in either of modalities.

Conclusion. The relationship between LV longitudinal function and LA strain varies according to the phases of LA function. LA reservoir strain is closely related to LV

longitudinal function. However, our MRI and echo findings both indicate that LA contractile strain is an intrinsic LA property.

Keywords: LA Contractile, LA pump strain, Atrial kick, LA function

I. Introduction

LA is far from a bystander collecting blood from the lungs and distributing it to the LV. It also plays a pivotal role in left-sided cardiac performance[256-258]. Dynamic and interactive associations between LA and LV functions have been reported in the literature [256, 259-263]. Recent advances in deformation analysis facilitate quantification of LA phasic strains STE [264, 265] or more recently with MRI FT [266]. LA strains are strong predictors of cardiac outcomes in various conditions [267, 268]. However, no incremental prognostic value of LA strain over LVGLS and LA volume has been reported in patients post myocardial infarction [269]. This has provoked scepticism that LV and LA strains might be merely a surrogate of LV longitudinal strain [264, 270, 271], particularly in the context of abnormal LV function [256, 272-274].

Recently, we showed that LA reservoir and conduit strains are independently determined by LVGLS, but no association was seen between LA contractile function and LVGLS. [260] However, this finding could be applicable to a single modality, transthoracic echocardiography (TTE) as little is known about the comparative effects of different imaging modalities on the relationship LA and LV strain analysis. Collectively, this study aimed to elucidate the relationships between LA and LV longitudinal functions using two different imaging modalities (TTE and MRI) and their strain parameters.

II. Method

Study Population: This is a sub-study of an ongoing LOWCBP study [218]. Briefly, the inclusion criteria were 1) adult participants on stable antihypertensive therapy; 2) 1-3 hypertensive drugs to lower BP; 3) OBP being ≤ 140/90 mmHg; and 4) seated central SBP (cSBP) ≥ +0.5SD of age- and gender-specific normal values. This sub-study used the baseline data from the population recruited in Royal Hobart Hospital, Tasmania, Australia.

Echocardiography: Transthoracic echocardiograms were performed using commercially available ultrasound systems from Vivid E9 (GE Medical, and Milwaukee, WI, USA). Each participant first underwent an extensive standard assessment of cardiac anatomy and function according to our protocol. The images were acquired at the highest possible frame rate with optimization of image depth and sector width. Multiple consecutive cardiac cycles of the three standard apical views (A4C, A2C, and ALAX views) were acquired and digitally stored as raw data for offline analysis. LV end-diastolic and end-systolic volumes were measured using the biplane method of disks. The baseline assessment included standard 2D, M-mode, color Doppler, pulse and continuous wave Doppler, and tissue Doppler imaging using standard parasternal, apical, subcostal and suprasternal windows [275].

Magnetic Resonance Imaging: CMR images were obtained with a 1.5-T MRI scanner with a phased array cardiac coil (GE Signa HDxt, Waukesha, WI). An ECG-gated breath-hold LV vertical long axis (2-chamber) and horizontal long axis (4-chamber) images were used to identify the cardiac short axis. The whole heart was imaged in the

short axis plane, from the LV apex to the roof of both atria, using 14 to 20, 10-mm slice SSFP cines without an interslice gap, with 50 frames per cardiac cycle, matrix 256x256, and field of view (FOV) 350-400. All image cine slices were acquired during 10- to 15-second breath holds and stored digitally for offline analysis of cardiac volumes, mass and function. All CMR scans performed by the same experienced operator.

Measurement of myocardial strain: All offline measurements were performed by the same observer (HV). STE strain was analysed on EchoPAC PC software (version 112, GE Medical, Milwaukee, WI) and MRI FT strain were analyzed on Qstrain (Version 2.0, Medis BV, Leiden, The Netherlands). 2-dimensional images from 2 apical views (A4C and A2C) were used for LA and LV strains for comparison purpose. Readings were obtained by averaging six segments in each view. LVGLS was determined from the average of all 12 segments. After tracing of the endocardial border, the region of interest was adjusted to include the entire myocardial thickness and avoid the pericardium [276]. The software then selected stable speckles within the myocardium and performed STE on a frame-to-frame basis throughout the entire cardiac cycle. LA strains were also estimated from the average of 12 segments. LA reservoir and contractile strain were selected manually from the line chart of LA strain. The region of interest includes only LA thin wall and avoids appendage. The quality of tracking was assessed manually. The cardiac cycle with the best tracking and visually most credible strain curves was selected for analysis. In segments with poor tracking, the border was readjusted manually until optimal tracking was achieved. After adjustment, segments with consistently poor tracking were excluded. Final LV and LA strains were calculated as the averaged value of strains from each of A4C and A2C views.

Statistical Analysis. Continuous variables are presented as mean ± standard deviation (SD). Categorical variables are expressed as percentages. Pearson's correlation was used to express the correlation coefficient between LA and LV strains. Normality was evaluated using the Kolmogorov-Smirnov test. Linear regression analysis was used to examine the associations between LA and LV strains and other echo variables. The same process of regression was applied for both echo and MRI strain. Statistical analyses were performed using a standard statistical software package (R Development Core Team. R: a language and environment for statistical computing. R Foundation for Statistical Computing, Vienna, Austria. http://www. R-project.org). Statistical significance was defined by two-sided $p< 0.05$.

III. Results

Patient demographics: Patient characteristics were summarized in **Table 7.1**. A total of 78 patients were included in this study (mean age, 56.1±9.2 years, 54% men). The majority of participants had normal LVEF (60.9±6.2% in TTE, 56.6±6.0%, $p<0.01$). Mean LVGLS was within normal limits and similar between the modalities (18.2±2.2%, 18.3±2.2%, respectively) (**Table 7.2**); whereas MRI FT yielded lower LA strains ($p<0.01$) than STE (LA Reservoir strain 38.4±8.0% in STE versus 32.3±6.5% in MRI FT; Contractile strain 17.5±4.0% versus 15.3±4.0%; Conduit strain 20.7±6.1% versus 17.0±6.6%).

Correlation analysis: In general, LVGLS, LA reservoir strain, and LA conduit strain were significantly correlated to each other but not with LA contractile strain in both modalities (**Figures 7.1 and 7.2**). LA reservoir strain had excellent correlations with

LA conduit strain (Echo: r=0.87, p<0.01; MRI: 0.81, p<0.01). In contrast, LA contractile strains were not correlated to LVGLS (p>0.15) in both modalities but had moderate correlations with LA reservoir strain (Echo: r=0.64, p<0.01; MRI: 0.28, p=0.01). Furthermore, the correlation coefficients between LVGLS and LA reservoir strain (i.e., r_1) were greater than those between LVGLS and LA contractile strain (i.e., r_5) in both STE and FT (both $p < 0.05$).

Determinants of LA strains: LVGLS was a significant determinant of LA reservoir and conduit strains in both uni- and multivariable models in both modalities, whereas it was not the case for LA contractile strain (**Tables 7.3 and 7.4**). Of note, their beta coefficients were similar between LA reservoir and contractile strains in both STE and MRI FT. Regarding LA contractile strain, no associations were found between LVGLS and LA contractile strain in both uni- and multivariable linear models. Only mitral A-wave velocity was an independent predictor for LA contractile strain in both STE and FT strains.

IV. Discussion

The results of our study demonstrated that, regardless of the imaging modality, LVGLS was associated with LA reservoir and conduit strains but not with LA contractile strain. These results indicate that the LA reservoir and conduit strains are influenced by LV longitudinal function to the extent that they reciprocate LV function. However, LA contractile strain was not influenced by LV longitudinal contraction, and thus it reflects an intrinsic LA property, a finding supported by the association between mitral A wave velocity and LA contractile strain in our population.

Current imaging assessments of LA function are primarily based on LA volumes (maximum and minimum), pulmonary venous velocity, mitral valve inflow velocity, and/or mitral annular velocity. Nonetheless, none of the above parameters provide an entire picture of LA phasic function, rather than the only snapshot of LA function at a specific time point of cardiac cycle [277]. Strain imaging describes the deformation of the LA wall relative to its initial length. Thus, it can quantify the three phases of the LA function: LA reservoir, conduit, and contractile.

LA strains, mainly LA reservoir strain, have been reported as an independent prognostic marker of CVD [278, 279]. However, a recent study showed that the LA reservoir function could not provide any additional information on adverse outcome over LVGLS and LA enlargement in myocardial infarction population [269]. A possible reason for this is that LA reservoir function is highly correlated with other measures of LV longitudinal function such as LVGLS.

LA reservoir function is determined by LA stiffness, LA volume, and LV longitudinal function [280-282]. LV base descent during LV systole causes more blood flows to the LA chamber from pulmonary veins. Therefore, it is not surprising that reservoir strain is closely related to LVGLS. The results are in line with previous reports showing that LA reservoir function is a predictor for LV diastolic dysfunction.

In this study, we identified the following unique aspects of LA contractile strain: 1) LA contractile strain was not associated with LVGLS but was independently associated with mitral A-wave in both STE and MRI FT; and 2) the correlation coefficient between LVGLS was significantly stronger than that between LVGLS and LA contractile strain

($r_1 > r_5$). These findings indicate that LA contractile strain contains intrinsic atrial property rather than simply mirroring LV function. These results are in line with previous reports that demonstrated the incremental predictive value of LA contractile strain over clinical information, LVEF, LA volume, and LA reservoir function to predict subsequent atrial fibrillation [283].

STE vs. MRI FT. Although STE and FT are theoretically similar techniques, the strain values may slightly differ due to advantages and disadvantages in image resolution. CMR images have a higher spatial resolution, but a lower temporal resolution (i.e., lower framerate) than echocardiographic images do. The higher spatial resolution makes our tracing of the LA wall easier and more accurate, improving the quality of wall tracking by distinguishing the wall from blood or pericardial interfaces. However, lower framerate of MRI FT would cause underestimation of the strain, as the framerate is known to affect strain values (**Figure 7.3**) [284]. This is more prominent near the end-diastolic phase when the mitral annulus moves a lot within a single MRI frame. When R-R gating is used, the end-diastolic phase is the end of one cardiac cycle when the tracking error is accumulated. Because of these positive and negative aspects, we used both modalities to avoid bias from a single modality.

Study limitation Our population was a heterogenous group of patients with high central blood pressure, regardless of the presence of LV remodelling. Accordingly, generalisability of our findings to a non-hypertensive population may be limited by the potential for sampling bias. MRI and echo strain were measured using different vendors However, it would not influence the association between LA and LV function because

no cross-modality comparison was made in our analyses. Although strain values were generated automatically by dedicated software, manual tracing of LA wall are required. Therefore, both STE and MRI FT are operator-dependent. In our study, because a single operator performed strain analysis, inter-variability did not impact on our results (**Table 7.5**). In addition, the association between LA volume and LA strains has not been assessed in this study because MRI and echo images in my study were not LA-focused and then inappropriate for LA volume quantification. Further studies are required to discover the relation between LA size and function.

V. Conclusion

Although LA function is affected by underlying LV longitudinal function, the influence of this varies according to the phases of LA function. Whereas LA reservoir strain is closely related to LV longitudinal function, it appears that LA contractile strain is an intrinsic marker of LA function.

Acknowledgement/sources of funding

This work was supported in part by a project grant from the National Health and Medical Research Council of Australia (reference 1044551)

Table 7.1: Patient demographics

Variable	Value
N	78
Age, years	56.1±9.2
Men, %	53.9%
Height, cm	169.4±9.6
Weight, kg	87.2±16.0
24h MAP, mmHg	94.9±7.6
BSA, kg/m^2	2.02±0.22
Smoked, %	33%
Currently smoking, %	4%
Family History of CAD, %	51%
Diabetes mellitus, %	12%

CAD = coronary artery disease.

Table 7.2: Imaging parameters

Variable	Echocardiography	MRI	p-value
LVEDV, ml	98.8 ± 24.9	156.1 ± 30.2	<0.01
LVEDVi, ml/m^2	48.9 ± 10.6	77.4 ± 12.3	<0.01
LVESV, ml	39.1 ± 12.7	68.31 ± 17.9	<0.01
LVESVi, ml/m^2	19.3 ± 5.6	33.8 ± 7.7	<0.01
LVEF, %	60.9 ± 6.2	56.6 ± 6.0	<0.01
LV Mass, g	175.8 ± 45.9	106.9 ± 26.8	<0.01
LV Mass Index, g/m^2	87.0 ± 20.7	52.7 ± 10.7	<0.01
E, m/s	0.64 ± 0.14	-	
Dec T, ms	197.2 ± 49.7	-	
A, m/s	0.59 ± 0.14	-	
E/A	1.14 ± 0.39	-	
e', cm/s	8.4 ± 1.8	-	
E/e'	8.0 ± 2.4	-	
Myocardial strains			
LVGLS, %	18.2 ± 2.2	20.5 ± 2.3	<0.01
LA Reservoir strain, %	38.4 ± 8.03	32.3 ± 6.5	<0.01
LA Contractile strain, %	17.5 ± 4.0	15.3 ± 4.0	<0.01
LA Conduit strain, %	20.7 ± 6.1	17.0 ± 6.6	<0.01

Table 7.3: Association between STE atrial strains and LV mechanics and diastolic function

	LA reservoir strain				LA contractile strain				LA conduit strain			
	Uni Variable		Multi Variable		Uni-Variable		Multi-Variable		Uni-Variable		Multi-Variable	
	β	P-Value	β	P-Value	β	P-Value	β	P-Value	β	P-Value	β	P-Value
Age	-0.18	0.08	-	-	0.08	0.11	-	-	-0.26	<0.01	-	-
Gender	0.97	0.62	-	-	1.18	0.22	1.6	0.09	-0.12	0.23	-	-
BSA	2.0	0.6	-	-	2.8	0.15	-	-	-0.78	0.83	-	-
24h MAP	-0.13	0.3	-	-	-0.01	0.8	-	-	-0.12	0.23	-	-
E	5.4	0.42	-	-	-7.9	0.01	-	-	11.2	0.03	9.1	0.07
A	-2	0.77	-	-	9.0	<0.01	8.9	<0.01	-10.9	0.04	1.6	<0.01
E'	1.76	<0.01	1.4	<0.01	-0.02	0.95	-	-	1.8	<0.01	-	-
LV EF	0.27	0.08	-	-	0.06	0.46	-	-	0.2	0.08	-	-
LVMI	-0.05	0.24	-	-	0.01	0.56	-	-	-0.07	0.05	-	-
LV GLS*	1.4	<0.01	1.2	<0.01	0.29	0.19	0.3	0.12	1.2	<0.01	0.7	0.02

*LVGLS from Speckle tracking echo

Table 7.4: Association between MRI feature tracking atrial strains and LV mechanics and diastolic function

	LA reservoir strain				LA contractile strain				LA conduit strain			
	Uni-Variable		Multi-Variable		Uni-Variable		Multi-Variable		Uni-Variable		Multi-variable	
	β	P-Value	β	P-Value	β	P-Value	β	P-Value	β	P-Value	β	P-Value
Age	-0.3	<0.01	-0.29	<0.01	-0.014	0.76	-0.13	0.03	-0.28	<0.01	-0.31	<0.01
Gender	-2.3	0.23	-	-	0.47	0.6	-	-	-2.8	0.07	-	-
E	5.6	0.3	-	-	-5.8	0.07	-7.3	0.02	11.4	0.03	-	-
A	-8.6	0.12	-	-	6	0.05	7.8	0.03	-14.6	<0.01	-	-
E'	0.9	0.02	-	-	0.1	0.68	-	-	0.8	0.04	-	-
LV EF	0.12	0.36	-	-	-0.19	0.18	-	-	0.21	0.1	-	-
LV mass index	-0.07	0.3	-	-	0.04	0.29	0.06	0.16	-0.11	0.11	-	-
LV GLS*	0.89	<0.01	0.54	<0.01	-0.08	0.63	-	-	0.97	<0.01	0.9	<0.01
24h MAP	-0.12	0.23	-	-	0.03	0.76	-	-	-0.14	0.17	-	-

*LVGLS from MRI feature tracking

Table 7.5: Coefficient of variation of strain measurements

		LV GLS	LA reservoir strain	LA contractile train	LA conduit strain
Echo	**Inter-Observer**	8.6±6.5	11.5±6.1	9.7±7.7	15.8±8.4
	Intra-Observer	6.6±4.8	6.4±3.0	9.0±4.8	8.9±10.0
MRI	**Inter-Observer**	6.3±6.0	12.0±11.2	10.0±13.0	17.3±9.5
	Intra-Observer	5.5±3.9	9.8±9.3	10.8±11.7	17.4±5.6

Figure 7.1: Correlation analysis of LA and LV strain by STE

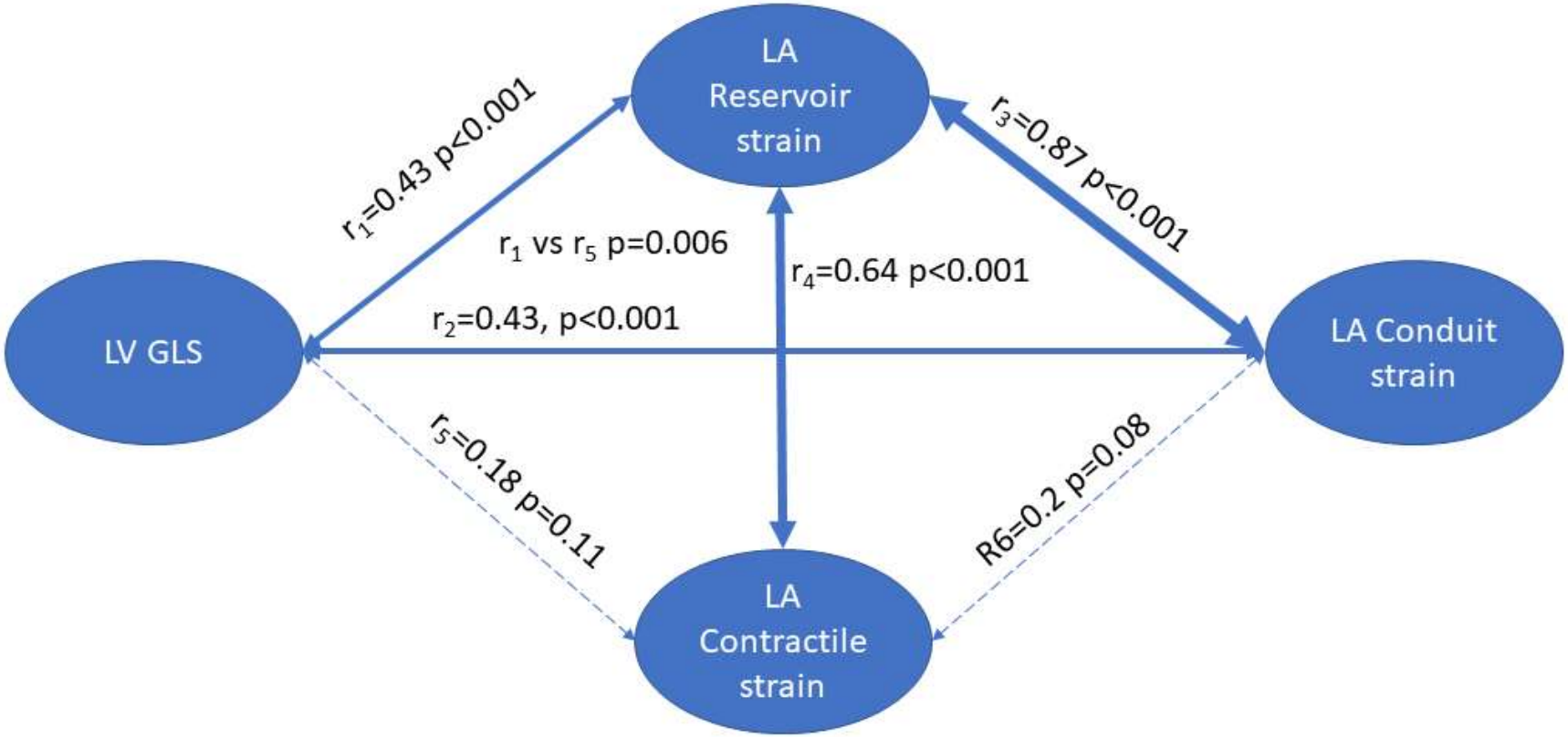

Figure 7.2: Correlation analysis of LA and LV strain by FT

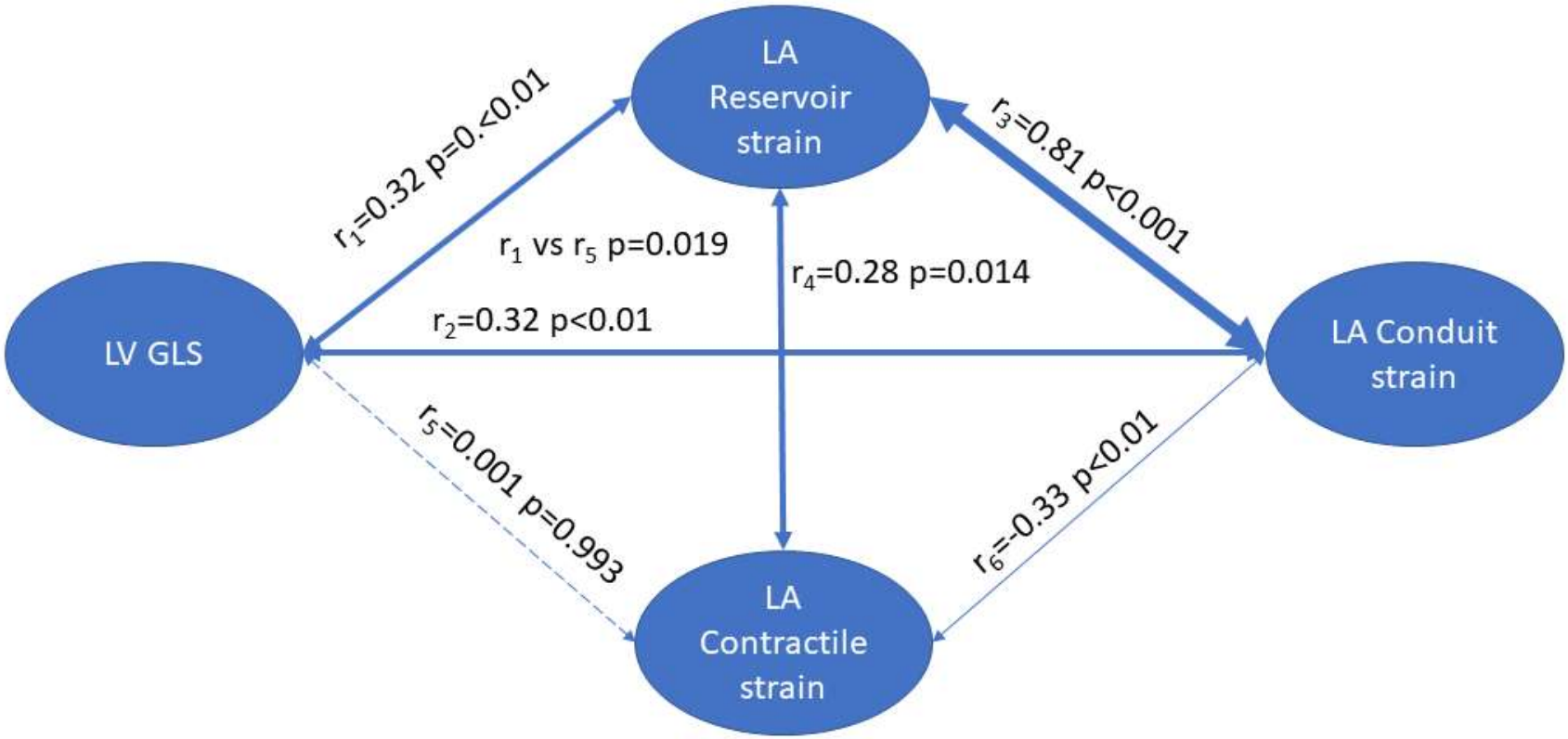

Figure 7.3: Dependency of strain and framerate

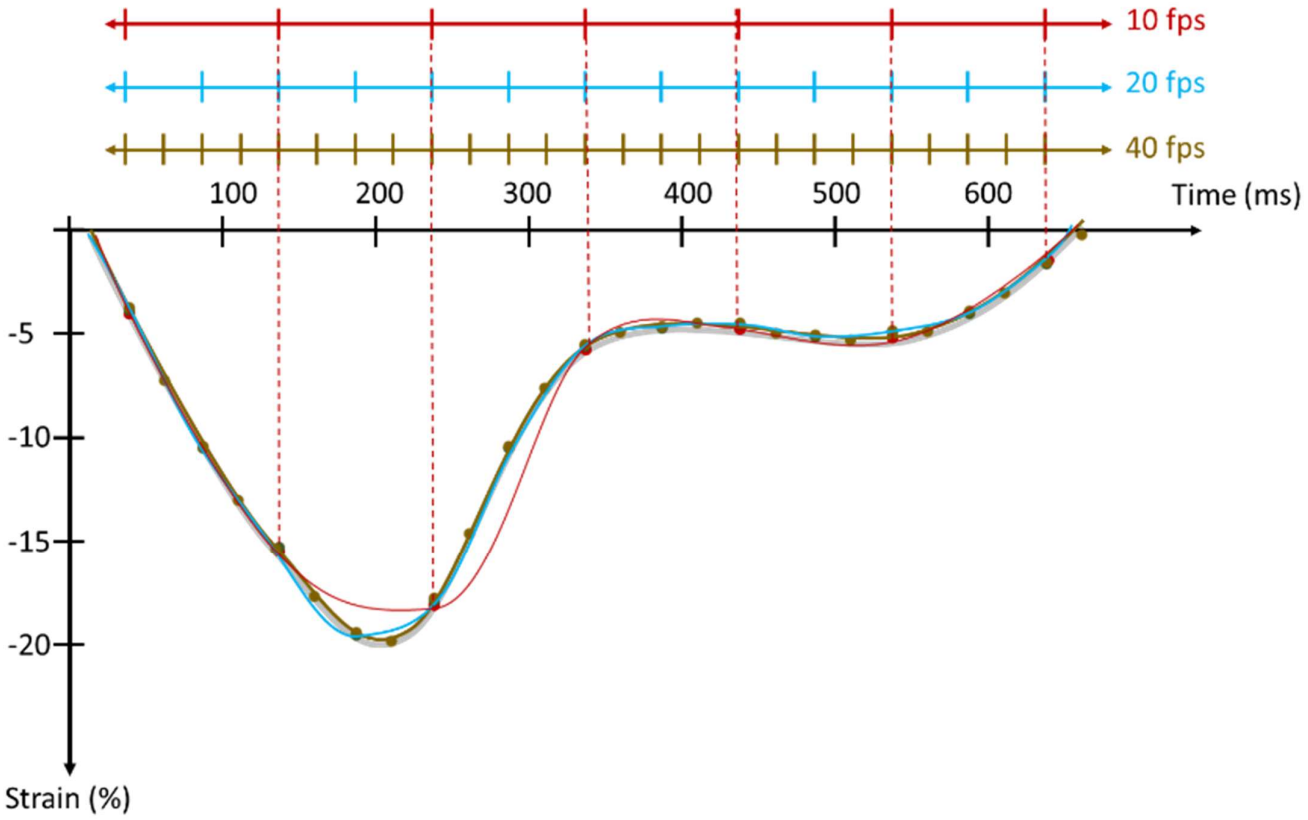

Chapter 8

Difference between Office and 24 hr BP on Cardiac Function and Anatomy

Abstract

Aim: The aim of this study was to test the hypothesis that ABP is better than seated OBP in the reflection of cardiac function and anatomy.

Background: HTN is the most common modifiable cause of death from CVD, which afflicts an estimated 30% of the world's population, half of whom are unaware they have the disease. There are many methods to estimate afterload BP in the literature. The invasive BP method has been accepted as the gold standard and is highly correlated to cardiac function in animal models. However, OBP is the most widely used method, being assumed to be the 'standard' for high BP diagnosis in many institutions. This study hypothesises that conventional seated BP is worse than ABP in the reflection of cardiac function and anatomy

Method: A total of 108 participants aged 57.3±9.2 with 54% males were included in this study. Each participant's OBP and ABP were measured. Participants also underwent echocardiography and MRI scanning for cardiac function and anatomy.

Results: There were no significant differences in systolic, diastolic, and mean arterial blood pressure (SBP, DBP, and MAP) between the two methods of BP measurement except for pulse pressure (PP), if adjusted for age, sex, and risk factors. However, PP was the highest intra-class correlation, 0.74 (0.61, 0.82), among the measures. ABP was proven to be more associated with LV mass index compared to OBP. Only ambulatory and office DBP were associated with LV systolic function. Office DBP was exclusively associated with LV diastolic function.

Conclusion: Although the vast majority of BP used in the literature is OBP, several studies have suggested that 24-hour ABP should replace OBP as the primary method for HTN assessment. However, this study has pointed out that each component had its own values; 24-hour ABP better describes the chronic response of cardiac muscles to elevated afterload pressure, while OBP is more related to instantaneous LV function

I. Introduction

HTN is the most common modifiable cause of death from CVD, which afflicts an estimated 30% of the world's population, half of whom are unaware they have the disease [1, 285]. The invasive BP measurement has been the gold standard. However, there are many non-invasive methods to estimate BP in the literature and in clinical practice. OBP is the most widely used method, which is assumed to be the 'standard' for high BP diagnosis in many institutions [9]. The majority of studies in epidemiology [10, 11] used BP measured by OBP in their studies as a risk factor. However, recently, ambulatory 24-hour BP (ABP) has been reported to be a better predictor for prognosis of hypertensive end-organ damage [12, 13], cardiovascular events [14-16], and all-cause mortality [17].

The benefits of OBP are that it is quick and easy to use. However, it has drawbacks. The main drawbacks are measurement at a single time point and frequent variations in measurement methods [18, 19]. These factors would, in turn, impact on the management of HTN. So far, in the US, evaluation for white-coat HTN is the only indication for ABP that Medicare reimburses [286]. British HTN guidelines [11] suggest that ABP should be considered prior to starting any therapy. Recent guidelines and publications have also emphasised the predictive values of ABP over other BP methods [11, 287]. Nevertheless, whether ABP should replace OBP in clinical practice and the association of each BP index to cardiac anatomy and function are still contentious. Several studies have reported a closer association between ABP and LV mass index or LV diastolic function compared

to OBP [95]. However, those studies had several limitations: (1) only SBP and DBP were assessed; (2) they used LV mass derived from echocardiography and not from gold standard methods (MRI) — errors as small as a few millimetres can result in large errors in calculated LV mass by echocardiography; and (3) they concentrated only on the association between different BP values and LV anatomy or LV diastolic function. To the best of the author's knowledge, a single study that assesses the association between different BP measures and both LV anatomy/function using both echocardiography and MRI has not been conducted. The main aim of this study is to fill that gap.

II. Method

Study population: This study is a sub-study of an ongoing LOWCBP study [218]. Briefly, the inclusion criteria were: 1) adult participants on stable antihypertensive therapy; 2) 1–3 hypertensive drugs to lower BP; and 3) seated OBP being ≤ 140/90 mmHg; and 4) seated central SBP (CSBP) ≥ +0.5SD of age- and gender-specific normal values. Seated OBP was measured three times and the average was used for the analysis. ABP was also collected during awake and sleep time. This sub-study used a population recruited in the Royal Hobart Hospital, Tasmania, Australia.

Echocardiography: Transthoracic echocardiograms were performed using commercially available ultrasound systems from Vivid E9 (GE Medical, and Milwaukee, WI, USA). Each participant first underwent an extensive standard assessment of cardiac anatomy and cardiac function according to clinical protocols with one ultrasound system. Acquisition was obtained at the highest possible frame rate with optimisation of image

depth and sector width. Multiple consecutive cardiac cycles of the three standard apical views (A4C, A2C, and ALAX) were acquired and digitally stored as raw data for offline analysis. LV end-diastolic and end-systolic volumes were measured using the biplane method of disks. The baseline assessment included standard 2D, M-mode, colour Doppler, pulse and continuous wave Doppler, and tissue Doppler imaging using standard parasternal, apical, subcostal and suprasternal windows [275]. Echocardiographic images were analysed using EchoPAC PC software (GE Ultrasound version 112, Waukesha, Wisconsin).

Magnetic Resonance Imaging: CMR images were obtained with a 1.5-T MRI scanner with a phased array cardiac coil. An ECG-gated breath-hold LV vertical long axis (2 chamber) and horizontal long axis (4 chamber) images were used to identify the cardiac short axis. The whole heart was imaged in the short axis plane, from the LV apex to base including both atria, using 14 to 20, 10-mm slice SSFP cines without interslice gap, with 50 frames per cardiac cycle, matrix 256 x 256, and field of view (FOV) 350–400. All images were acquired during 10- to 15-second breath holds and stored digitally for offline analysis of cardiac volumes, mass and function. All CMR scans were performed by the same experienced operator [275]. Echocardiographic images were analysed using commercialised software (QMass and Qstrain, Medis, Leiden, the Netherlands).

Statistical analysis: Continuous variables are presented as mean ± standard deviation (SD). Categorical variables are expressed as percentages. Normality was evaluated using the Kolmogorov-Smirnov test. Pearson's correlation was used to express correlation

coefficients between variables. Intra-class correlation (ICC) was used to assess the concordant between the different methods. Two-way t-test or Wilcoxon signed rank test was used to compare two variables. Linear regression analysis was used to examine the associations between BP and LV indexes. Statistical analyses were performed using a standard statistical software package (SPSS software 22.0, SPSS Inc., Chicago, IL, USA). Statistical significance was defined by $p< 0.05$.

III. Results

Patient demographic and imaging parameters are seen in **Table 8.1**. The 108 participants included 58 men, 10 patients with diabetes mellitus, 51 with a family history of coronary artery disease (CAD), and 39 with a history of smoking. Overall, they had normal cardiac function. BP measures are summarised in **Table 8.2**. No differences were found in SBP, DBP, and mean arterial pressure (MAP) between the two methods. However, pulse pressure (PP) was statistically significantly higher with OBP than ABP.

Correlation analyses indicated that 24-hour ABP was superior to OBP in the association with LV mass index (**Table 8.3**). Indeed, ambulatory SBP, DBP, and MAP significantly correlated with LV mass index ($r= 0.45$, 0.52 and 0.53, respectively), whereas only office DBP (O-DBP) was weakly associated with LV mass index ($r=0.22$). Strength of association between LVGLS and DBP or MAP was similar between ABP and OBP (ABP: $r=-0.31$, and -0.25; OBP: $r=-0.3$, and -0.23 respectively). Interestingly, O-DBP was correlated with LVEF but ABP was not.

In multivariable models (**Table 8.4**), all 24-hour ABP (i.e. SBP, DBP, PP, and MAP) were independently associated with LV mass index (β from 0.26 to 0.4) after adjustment for age, sex, smoking history, diabetes, and family history of CAD, whereas independent determinants for LVGLS were ambulatory and office DBP (β =-0.21, and -0.22, $p<0.05$). Only O-DBP and O-MAP remained significantly associated with LVE.

Finally, the associations of awake or sleeping BP on the heart were assessed (**Table 8.5)**. In univariable analyses, awake and sleeping BP shared similar strength of associations with LV mass index with awake BP being slightly higher in number. These associations remained significant after adjusting for age, sex, smoking history, diabetes, and family history of CAD (**Table 8.6)**. Only awake DBP was independently associated with LVGLS.

IV. Discussion

The study has found associations between different components of BP and cardiac function and anatomy. 24-hour ABP was superior to OBP in explaining variations in the LV mass index. LV function, otherwise, was more associated with OBP rather than ABP. In addition, DBP had stronger correlations with anatomy and function and 24-hour MAP was the strongest correlation with cardiac activities. No significant differences between awake and sleeping BPs were observed in the effects on cardiac anatomy and function. To the best of the author's knowledge, this is the first study to compare the associations of BP and cardiac assessments with MRI including gold standard LV mass and LVEF, and LVGLS.

Stronger association between LV mass and 24-hour ABP: As the results indicated, there were limited agreements between the 24-hour BP and OBP. The 24-hour ABPs had significant associations with the LV mass index but OBP did not, except for O-DBP. The advantage of 24-hour ABP is that it overcomes the variability from instantaneous physiological changes and even some measurement errors. Although human physiology changes continuously every second, BP should revolve around a certain level, which works as averaged afterload to the heart. ABP is useful for detecting cumulative abnormality of the cardiac system, ignoring instantaneous effect. Since LVH results from a cumulative process, it is no doubt that the LV mass index and 24-hour ABP have a strong association, compared to OBP. Stronger correlation between the LV mass index and 24-hour ABP were reported in the literature [288-290]. However, all of these studies used an echocardiographic LV mass index, following guidelines for HTN management [244], and LV mass by echocardiography has marginal accuracy and is very sensitive to measurement error. Due to cubic equation, a millimetre difference may yield a large difference in LV mass. LV mass by MRI is agreed to be the gold standard with high accuracy and reproducibility. High correlation between the LV mass index and 24-hour ABP, compared to OBP, was confirmed by MRI in this study. The superiority of 24-hour ABP over OBP was enhanced in the multivariable model. Different components of 24-hour ABP were all significantly associated with the LV mass index, while none of the components of OBP was significant. Therefore, 24-hour ABP is best for assessing cumulated progress of end-organ damage in HTN.

Associations between OBP and LA function: Compared to the LV anatomy, LV function normally does not reflect the cumulative effect of afterload over a period and is rather affected by instantaneous physiological status including afterload. In this study, OBP had better association with LV function measured by MRI. This is sensible because, unlike 24-hour ABP, OBP is just a snapshot of BP at a certain time point in time. As well, LV function (not LV anatomy) by cardiac MRI is only a snapshot of cardiac activity at a specific point in time. This study reported a contrary result to some previous ones [291, 292]. In those studies, OBP failed to be significant related to LV dysfunction, and 24-hour sleep ABP outweighed awake ABP in the association with LVGLS. However, the differences may lie in the population and modality: 1) the majority of participants in previous studies had LV dysfunction; and 2) the majority were assessed by echocardiography. MRI yields a more accurate LVEF than echocardiography.

Interestingly, LV systolic function was more associated with DBP, which agreed with recent studies [292]. Several large studies have suggested DBP interpretation should consider age [293-296]. Age is one of the known confounders. DBP remained significantly associated after adjusting for age. DBP may better reflect peripheral resistance than SBP because it is more stable than SBP during daily activities [292]. In this study, 24-hour ambulatory and office DBPs had a similar effect on LVGLS. The difference in beta coefficient is relatively small. In the study by Kim et al. [292], 24-hour ABP was superior to OBP in simple correlation analysis with LVGLS. The extent of

association was different between the LVH and non-LVH group. Therefore, the percentage of patients with LVH may be attributed to the difference between the results.

24-hour awake and sleep ABP: Between 24-hour ABP components, awake and sleeping 24-hour ABPs had similar explanatory value for the variation of LV mass index, except for 24-hour awake PP. 24-hour awake DBP was more strongly associated with LV mass index and LVGLS, compared to 24-hour sleep DBP in both uni- and multivariable regression. In fact, this study has shown that 24-hour awake ABP provided more explanatory information than 24-hour sleep ABP, although sleep 24-hour ABP was prone to be more strongly associated with all-cause mortality [17, 297] and cardiovascular events [298-300]. Sleep ABP was reported to be more related to microalbuminuria [292], which is known as an early marker of target organ damage in HTN [301]. This study did not examine microalbuminuria test to confirm their findings.

Limitation: This study should be interpreted in the context of the following limitations. Zhang et al. reported that OBP failed to be significantly related to LV E/e', but not 24-hour ABP [291]. However, this study did not assess the association between LV diastolic function and BP. In addition, the recruited population in this study had high central blood pressure, which differs from published studies. The majority of current studies on this topic have focused on diabetic or high OBP. This has caused difficulties for direct comparison with previous studies.

V. Conclusion

Although the vast majority of BP used in the literature was OBP, several studies suggested that 24-hour ABP should replace OBP as the primary method for HTN assessment. However, this study has pointed out that each component has its own values. 24-hour ABP better describes the chronic response of cardiac muscles to elevated afterload pressure, while OBP is more related to instantaneous LV function.

Table 8.1: Patient demographic and Imaging parameters

Variable	Value
N	108
Age, years	57.3±9.2
Male, n (%)	58 (54%)
Height, cm	170±10
Weight, kg	85±16
BSA, kg/m^2	1.99± 0.22
Smoked, n (%)	39 (36.1)
Family History of CAD, n (%)	51 (47.2)
Diabetes, n (%)	10 (9.2)
MRI	
LVEF (%)	57.4±7.5
LV GLS (%)	20.8±2.6
LV mass index, g/m^2	53.1±10.4

Table 8.2: Concordance between ABP and OBP

	Ambulatory 24h	Office	P-value	Pearson's correlation
SBP	128.2±11.5	129.4 ±11.0	0.338	0.42
DBP	78.4±8.2	79.8±8.1	0.09	0.47
PP	48.4±8.3	51.0±9.5	<0.01	0.59
MAP	95.4±8.1	95.8±8.5	0.56	0.41

Table 8.3: Correlation analyses

	O-SBP	24h A-SBP	O -DBP	24h A-DBP	O -PP	24h A-PP	O -MAP	24h A-MAP
LV mass index	0.18	0.45**	0.22*	0.52**	0.019	0.11	0.23	0.53**
LVGLS (MRI)	-0.62	-0.13	-0.3**	-0.31**	0.19	0.12	-0.23*	-0.25**
LVEF (MRI)	-0.089	0.067	-0.34**	-0.16	-0.19*	0.25**	-0.27	-0.072

A-: Ambulatory, O -: Office *p<0.05. **p<0.01

Table 8.4: Multi-variable linear regression analyses between BP and LV indexes.

	LV Anatomy		LV systolic function			
	LV mass index		LV GLS		LVEF	
	β	P-value	β	P-value	β	P-value
24h Ambulatory SBP	0.40	<0.01	-0.09	0.32	0.121	0.28
Office SBP	0.16	0.06	-0.05	0.57	-0.08	0.44
24h Ambulatory DBP	0.39	<0.01	-0.21	0.04	-0.021	0.85
Office DBP	0.09	0.32	-0.22	0.02	-0.28	0.005
24h Ambulatory PP	0.26	<0.01	0.05	0.63	0.18	0.08
Office PP	0.12	0.18	0.13	0.2	0.15	0.15
24h Ambulatory MAP	0.42	<0.01	-0.17	0.09	0.04	0.7
Office MAP	0.13	0.13	-0.17	0.08	-0.21	0.03

Each of the models were adjusted for age, sex, smoking, family history of coronary heart disease, and diabetes mellitus

Table 8.5: Correlation analyses

	24h awake-SBP	24h Sleep-SBP	24h awake - DBP	24h Sleep-DBP	24h awake-PP	24h Sleep-PP	24h awake - MAP	24h Sleep-MAP
LV mass index	0.42**	0.39**	0.48**	0.43**	0.08	0.21*	0.5**	0.42**
LVGLS (MRI)	-0.11	-0.11	-0.3**	-0.16	0.15	-0.02	-0.24*	-0.14
LVEF (MRI)	0.072	0.44	-0.16	-0.08	0.25**	0.18	-0.07	-0.03

*p<0.05. **p<0.01

Table 8.6: Multi-variable linear regression between awake and sleep ABP and LV indexes.

	LV mass index		LV GLS		LVEF	
	β	**P-value**	**β**	**P-value**	**β**	**P-value**
24h Awake SBP	**0.38**	**<0.01**	-0.09	0.35	0.11	0.28
24h Sleep SBP	**0.32**	**<0.01**	-0.021	0.83	0.12	0.25
24h Awake DBP	**0.36**	**<0.01**	**-0.22**	**0.03**	-0.021	0.85
24h Sleep DBP	**0.27**	**<0.01**	-0.021	0.84	0.05	0.61
24h Awake PP	**0.25**	**<0.01**	0.06	0.52	0.17	0.09
24h Sleep PP	**0.27**	**<0.01**	-0.014	0.88	0.15	0.14
24h Awake MAP	**0.4**	**<0.01**	-0.17	0.08	0.09	0.41
24h Sleep MAP	**0.31**	**<0.01**	-0.02	0.83	0.09	0.7

Each of the models were adjusted for age, sex, smoked, family history of coronary heart disease, and diabetes mellitus.

Chapter 9

General discussion and future directions

I. Background

HTN is the major modifiable risk factor of cardiovascular events. Good BP control is the key for HHD management. OBP is the most widely used method for BP measurement. Several studies have found that 24-hour ABP has better prognosis of CVD, compared to OBP. This thesis step-by-step has seeked to find an association between different BPs with different aspects of cardiac activity by using advanced cardiac imaging. Steps included were: 1) seek potential appropriate techniques to reflect cardiac activities with high accuracy in the literature; 2) define normal ranges or validate the techniques if the work has not been systematically done; 3) assess the association between cardiac activities or function derived by these methods or with conventional variables to define independent variables that add more information to the studies; and 4) evaluate the association between OBP and ABP with these advanced cardiac variables to define which afterload is better in HTN management.

II. Summary of major findings

First, strains by different methods of tissue tracking were similar to each other, although those by MRI tagging were somewhat lower than those by other methods. The range of myocardial strain among normal people with STE was similar to those with FT (**Chapter 2**).

Second, T1 mapping is a novel technique for tissue characterisation, which is beneficial in different diseases. A systematic review and meta-analysis were performed to evaluate the use of T1 mapping in different conditions. Although

it was feasible in many diseases, T1 mapping technique has limited discrimination of HHD from the normal (**Chapter 3**).

Third, strain by tissue has been proven to be reliable with high intra-class coefficient and coefficient of variation. Ventricular strains were more reproducible than atrial strains. Strains by FT were similarly reproducible as those by STE. However, all strain values had good to excellent intra-class correlation, which opens the door for their broader applications in the future (**Chapter 5**).

Fourth, volumes derived by strain analyses had better agreement with the gold standard than conventional echocardiographic method of discs. Volumes by FT were the most concordant with those by MRI, followed by those by STE. However, significant differences were observed between volumes by strain and MRI-derived gold standard volumes. The results suggest that the volumes by strain are not ready to replace the gold standard (**Chapter 6**).

Fifth, LA contractile function has been demonstrated to be independent of other atrial phasic function and LV function. LA reservoir and conduit function were closely associated with LV function. Therefore, LA strains did not add much information except for contractile strain (**Chapter 7**).

Sixth, 24-hour ABPs, but not OBPs, were closely related to the progression of LV hypertrophy because they were averaged values, reflecting more accurate overload to the LV. OBP did reflect LV diastolic function. Both BPs shared the same association with LV SBP (**Chapter 8**).

III. Strength and limitations

To my knowledge, this is the first study in the literature to systematically define, validate novel imaging methods, and apply HHD. This is also the first study to show the association between afterload and gold standard LV mass, advanced systolic and diastolic parameters.

The main limitations of this study have been discussed in each relevant chapter and are as follows:

1. The meta-analyses are limited by variations in the original studies and publication bias, although the study followed standard approaches to detect this. Likewise, the constituent observational studies may be limited by biases in the recruitment process.
2. In the systematic reviews, it has been assumed that all of the measurements were performed by experts, but the levels of expertise among the individuals who conducted the measurements are uncertain.
3. The study used both MRI and echocardiographic variables for the analysis. However, MRI and echocardiography were scanned in different days. Physiological changes may have caused biases in the study's results, although the difference was relatively small (16 days).
4. Although LOWCBP is a multi-institutional study, at this stage the study has only run analyses for the population in Tasmania.

IV. Factors affecting successful implementation of new advanced imaging techniques in clinical settings

1. Accuracy: Accuracy is one of the first consideration for a novel technique. Validation against gold standard is always the first step for any novel imaging technique. In this study, T1 mapping and tissue tracking were validated techniques that got reported in literature. A recent meta-analysis has shown a moderate to excellent correlation between myocardial fibrosis found by histologic biopsy and ECV and native T1 by T1 mapping, pooled correlation coefficient homogenously reached 0.88 (0.85, 0.91) and 0.66 (0.5, 0.87), respectively[302]. Histologic biopsy is the best method so far for tissue characterization in post-mortem, but not in vivo studies. T1 mapping should be a good alternative option which enables to assess the development of myocardial fibrosis.

   Regarding tissue motion tracking, a number of validations against sonomicrometry were reported in literature with high correlation (ICC around 0.9)[303, 304]. Although all of them were animal studies, tissue motion tracking was considered as an accurate technique.

2. Precision: a precise technique means it allows the distinguishing between diseased condition from normal condition. T1 mapping detects myocardial fibrosis based on changes in magnetic characteristics of intra- and extra-cellular space. If the magnetic characteristic of diseased cardiac tissues imitates that of normal healthy tissues, the precision

become low, and in consequences, there is an overlap in value of ECV or native T1. In this thesis, despite high accuracy, I demonstrated that T1 mapping failed to separate a hypertensive from a healthy heart in chapter 2. Hence, it explained why T1 mapping was not used in the following chapters. In fact, hypertension is a risk factor and it has a wide range of conditions, depends on chronicity and severity. T1 mapping can detect both physiological adaptations to increased blood pressure or disease, so an overlap in ECV or native T1 may be found in several diseases including HTN.

Strain, otherwise, is the earliest market of cardiac dysfunction. Low strain reflects cardiac dysfunction and there is no upper limit for strain values. According to the meta-analysis in chapter 3, RV and LVGLS below 20% would be an indicator for cardiac dysfunction.

3. Reproducibility: Inter- and intra-reproducibility are also vital factors for novel techniques to be widely used. High variable or low reliable techniques could not be feasible for clinical use. Instead, as shown in the previous chapters, both ventricular and atrial strains had adequate reproducibility for clinical use.
4. Availability: In this thesis, two novel techniques were introduced: T1 mapping and tissue motion tracking. While T1 mapping was complex, requiring higher skills and expenses, tissue motion tracking was more user-friendly and allows retrospective studies. In addition, T1 mapping required a considerable upgrade of software and sequences. Therefore,

the integration of T1 mapping in clinical settings is slow. On the other hand, tissue motion tracking, otherwise, can be applied on current standard MRI or echo images. This creates new possibilities for clinical use of this technique in the near future.

V. Future directions

We have been witnessing a fast development in cardiac imaging techniques for a decade and the trend is not showing any sign of slowing down. Framerate of MRI is increasing, reaching the limit of real-time acquisition. Novel techniques such as susceptibility weighted imaging and diffusion tensor imaging are in a queue to be applied in cardiac imaging. Echocardiography has been on the right track with the launch of high-resolution and moderate framerate 3D echo. Handheld echocardiography also enables basic assessment of cardiac function with low expense for HTN management and prevention, in line with BP controlling. These potential projects may contribute to early treatment of HHD. Regarding the ongoing LOWCBP study, the availability of follow-up data enables longitudinal studies to find changes of cardiac function overtime. In addition, strain analysis is useful to assess the role of LA function in HHD during HTN progression. 3D strain would be an interesting topic for this study. HTN is always a central topic of interest to many researchers because of its popularity. Application of novel techniques to this disease seems not to be on a wrong track.

References

1. Arredondo, A. and R. Aviles, *Hypertension and its effects on the economy of the health system for patients and society: suggestions for developing countries.* Am J Hypertens, 2014. **27**(4): p. 635-6.
2. Organization, W.H., *A global brief on hypertension: silent killer, global public health crisis.* World, 2015.
3. Arno, P.S. and D. Viola, *Hypertension treatment at the crossroads: a role for economics?* American journal of hypertension, 2013. **26**(11): p. 1257-1259.
4. Kannel, W.B., et al., *Prevalence, incidence, prognosis, and predisposing conditions for atrial fibrillation: population-based estimates.* Am J Cardiol, 1998. **82**(8A): p. 2N-9N.
5. Drazner, M.H., *The progression of hypertensive heart disease.* Circulation, 2011. **123**(3): p. 327-34.
6. Levy, D., et al., *The progression from hypertension to congestive heart failure.* JAMA, 1996. **275**(20): p. 1557-62.
7. Levy, D., et al., *Prognostic implications of echocardiographically determined left ventricular mass in the Framingham Heart Study.* New England Journal of Medicine, 1990. **322**(22): p. 1561-1566.
8. Black, H.R. and W. Elliott, *Hypertension: a companion to Braunwald's heart disease*. 2006: Elsevier Health Sciences.
9. Chobanian, A.V., et al., *Seventh report of the Joint National Committee on Prevention, Detection, Evaluation, and Treatment of High Blood Pressure.* Hypertension, 2003. **42**(6): p. 1206-52.
10. Vasan, R.S., et al., *Impact of high-normal blood pressure on the risk of cardiovascular disease.* N Engl J Med, 2001. **345**(18): p. 1291-7.
11. in *Hypertension: The Clinical Management of Primary Hypertension in Adults: Update of Clinical Guidelines 18 and 34*. 2011: London.
12. Kario, K., et al., *Nocturnal fall of blood pressure and silent cerebrovascular damage in elderly hypertensive patients. Advanced silent cerebrovascular damage in extreme dippers.* Hypertension, 1996. **27**(1): p. 130-5.
13. Mancia, G. and G. Parati, *Ambulatory blood pressure monitoring and organ damage.* Hypertension, 2000. **36**(5): p. 894-900.
14. Staessen, J.A., et al., *Predicting cardiovascular risk using conventional vs ambulatory blood pressure in older patients with systolic hypertension.* Jama, 1999. **282**(6): p. 539-546.
15. Eguchi, K., et al., *Ambulatory blood pressure is a better marker than clinic blood pressure in predicting cardiovascular events in patients with/without type 2 diabetes.* American journal of hypertension, 2008. **21**(4): p. 443-450.
16. Zhang, Y., et al., *Association of left ventricular diastolic dysfunction with 24-h aortic ambulatory blood pressure: the SAFAR study.* J Hum Hypertens, 2015. **29**(7): p. 442-8.
17. Hansen, T.W., et al., *Ambulatory blood pressure and mortality: a population-based study.* Hypertension, 2005. **45**(4): p. 499-504.

18. Eguchi, K., et al., *How many clinic BP readings are needed to predict cardiovascular events as accurately as ambulatory BP monitoring?* Journal of human hypertension, 2014. **28**(12): p. 731.
19. Mancia, G., et al., *2013 ESH/ESC guidelines for the management of arterial hypertension: the Task Force for the Management of Arterial Hypertension of the European Society of Hypertension (ESH) and of the European Society of Cardiology (ESC).* Blood pressure, 2013. **22**(4): p. 193-278.
20. Devereux, R.B. and N. Reichek, *Echocardiographic determination of left ventricular mass in man. Anatomic validation of the method.* Circulation, 1977. **55**(4): p. 613-8.
21. Negishi, K., et al., *Practical guidance in echocardiographic assessment of global longitudinal strain.* JACC: Cardiovascular Imaging, 2015. **8**(4): p. 489-492.
22. Lang, R.M., et al., *Recommendations for Cardiac Chamber Quantification by Echocardiography in Adults: An Update from the American Society of Echocardiography and the European Association of Cardiovascular Imaging.* European Heart Journal-Cardiovascular Imaging, 2015. **16**(3): p. 233-271.
23. Janardhanan, R. and C.M. Kramer, *Imaging in hypertensive heart disease.* Expert Rev Cardiovasc Ther, 2011. **9**(2): p. 199-209.
24. Agabiti-Rosei, E., M.L. Muiesan, and M. Salvetti, *Evaluation of subclinical target organ damage for risk assessment and treatment in the hypertensive patients: left ventricular hypertrophy.* J Am Soc Nephrol, 2006. **17**(4 Suppl 2): p. S104-8.
25. Salcedo, E.E., K. Gockowski, and R.C. Tarazi, *Left ventricular mass and wall thickness in hypertension. Comparison of M mode and two dimensional echocardiography in two experimental models.* Am J Cardiol, 1979. **44**(5): p. 936-40.
26. Wong, R.C., et al., *Echocardiographic left ventricular mass in a multiethnic Southeast Asian population: proposed new gender and age-specific norms.* Echocardiography, 2008. **25**(8): p. 805-11.
27. Rudolph, A., et al., *Noninvasive detection of fibrosis applying contrast-enhanced cardiac magnetic resonance in different forms of left ventricular hypertrophy relation to remodeling.* J Am Coll Cardiol, 2009. **53**(3): p. 284-91.
28. Rodriguez, C.J., et al., *Left Ventricular Mass and Ventricular Remodeling Among Hispanic Subgroups Compared With Non-Hispanic Blacks and Whites MESA (Multi-Ethnic Study of Atherosclerosis).* Journal of the American College of Cardiology, 2010. **55**(3): p. 234-242.
29. Natori, S., et al., *Cardiovascular function in multi-ethnic study of atherosclerosis: Normal values by age, sex, and ethnicity.* American Journal of Roentgenology, 2006. **186**(6): p. S357-S365.
30. Armstrong, A.C., et al., *LV Mass Assessed by Echocardiography and CMR, Cardiovascular Outcomes, and Medical Practice.* Jacc-Cardiovascular Imaging, 2012. **5**(8): p. 837-848.
31. Hoey, E.T., et al., *The role of imaging in hypertensive heart disease.* Int J Angiol, 2014. **23**(2): p. 85-92.

32. Echocardiographic Normal Ranges Meta-Analysis of the Left Heart, C., *Ethnic-Specific Normative Reference Values for Echocardiographic LA and LV Size, LV Mass, and Systolic Function: The EchoNoRMAL Study.* JACC Cardiovasc Imaging, 2015. **8**(6): p. 656-65.
33. Kuhl, H.P., et al., *High-resolution transthoracic real-time three-dimensional echocardiography - Quantitation of cardiac volumes and function using semi-automatic border detection and comparison with cardiac magnetic resonance imaging.* Journal of the American College of Cardiology, 2004. **43**(11): p. 2083-2090.
34. Soriano, B.D., et al., *Matrix-array 3-dimensional echocardiographic assessment of volumes, mass, and ejection fraction in young pediatric patients with a functional single ventricle: a comparison study with cardiac magnetic resonance.* Circulation, 2008. **117**(14): p. 1842-8.
35. Shimada, Y.J. and T. Shiota, *Meta-Analysis of Accuracy of Left Ventricular Mass Measurement by Three-Dimensional Echocardiography.* American Journal of Cardiology, 2012. **110**(3): p. 445-452.
36. Oe, H., et al., *Comparison of accurate measurement of left ventricular mass in patients with hypertrophied hearts by real-time three-dimensional echocardiography versus magnetic resonance imaging.* Am J Cardiol, 2005. **95**(10): p. 1263-7.
37. Altmann, K., et al., *Comparison of three-dimensional echocardiographic assessment of volume, mass, and function in children with functionally single left ventricles with two-dimensional echocardiography and magnetic resonance imaging.* Am J Cardiol, 1997. **80**(8): p. 1060-5.
38. Barkhausen, J., et al., *MR evaluation of ventricular function: true fast imaging with steady-state precession versus fast low-angle shot cine MR imaging: feasibility study.* Radiology, 2001. **219**(1): p. 264-9.
39. Janik, M., et al., *Effects of papillary muscles and trabeculae on left ventricular quantification: increased impact of methodological variability in patients with left ventricular hypertrophy.* J Hypertens, 2008. **26**(8): p. 1677-85.
40. Kirschbaum, S., et al., *Accurate automatic papillary muscle identification for quantitative left ventricle mass measurements in cardiac magnetic resonance imaging.* Acad Radiol, 2008. **15**(10): p. 1227-33.
41. Vogel-Claussen, J., et al., *Left ventricular papillary muscle mass: relationship to left ventricular mass and volumes by magnetic resonance imaging.* J Comput Assist Tomogr, 2006. **30**(3): p. 426-32.
42. Steen, H., et al., *Is magnetic resonance imaging the'reference standard'for cardiac functional assessment? Factors influencing measurement of left ventricular mass and volumes.* Clinical Research in Cardiology, 2007. **96**(10): p. 743-751.
43. Nagueh, S.F., et al., *Doppler tissue imaging: a noninvasive technique for evaluation of left ventricular relaxation and estimation of filling pressures.* J Am Coll Cardiol, 1997. **30**(6): p. 1527-33.
44. Hillis, G.S., et al., *Noninvasive estimation of left ventricular filling pressure by E/e ' is a powerful predictor of survival after acute myocardial infarction.* Journal of the American College of Cardiology, 2004. **43**(3): p. 360-367.

45. Oh, J.K., J.B. Seward, and A.J. Tajik, *The echo manual*. 2006: Lippincott Williams & Wilkins.
46. Milan, A., et al., *Left atrial enlargement in essential hypertension: role in the assessment of subclinical hypertensive heart disease.* Blood Press, 2012. **21**(2): p. 88-96.
47. Di Tullio, M.R., et al., *Left atrial size and the risk of ischemic stroke in an ethnically mixed population.* Stroke, 1999. **30**(10): p. 2019-2024.
48. Barnes, M.E., et al., *Left atrial volume in the prediction of first ischemic stroke in an elderly cohort without atrial fibrillation.* Mayo Clinic Proceedings, 2004. **79**(8): p. 1008-1014.
49. Gerdts, E., et al., *Left atrial size and risk of major cardiovascular events during antihypertensive treatment - Losartan intervention for endpoint reduction in hypertension trial.* Hypertension, 2007. **49**(2): p. 311-316.
50. Nagarajarao, H.S., et al., *The predictive value of left atrial size for incident ischemic stroke and all-cause mortality in African Americans: the Atherosclerosis Risk in Communities (ARIC) Study.* Stroke, 2008. **39**(10): p. 2701-6.
51. Liebson, P.R., et al., *Echocardiographic Correlates of Left-Ventricular Structure among 844 Mildly Hypertensive Men and Women in the Treatment of Mild Hypertension Study (Tomhs).* Circulation, 1993. **87**(2): p. 476-486.
52. Alam, M., et al., *Usefulness of speckle tracking echocardiography in hypertensive crisis and the effect of medical treatment.* Am J Cardiol, 2013. **112**(2): p. 260-5.
53. Galderisi, M., et al., *Differences of myocardial systolic deformation and correlates of diastolic function in competitive rowers and young hypertensives: a speckle-tracking echocardiography study.* J Am Soc Echocardiogr, 2010. **23**(11): p. 1190-8.
54. Leitman, M., et al., *Two-dimensional strain-a novel software for real-time quantitative echocardiographic assessment of myocardial function.* J Am Soc Echocardiogr, 2004. **17**(10): p. 1021-9.
55. Reisner, S.A., et al., *Global longitudinal strain: a novel index of left ventricular systolic function.* J Am Soc Echocardiogr, 2004. **17**(6): p. 630-3.
56. Blessberger, H. and T. Binder, *NON-invasive imaging: Two dimensional speckle tracking echocardiography: basic principles.* Heart, 2010. **96**(9): p. 716-22.
57. Delgado, V., et al., *Relation Between Global Left Ventricular Longitudinal Strain Assessed with Novel Automated Function Imaging and Biplane Left Ventricular Ejection Fraction in Patients with Coronary Artery Disease.* Journal of the American Society of Echocardiography, 2008. **21**(11): p. 1244-1250.
58. Narayanan, A., et al., *Cardiac mechanics in mild hypertensive heart disease: a speckle-strain imaging study.* Circ Cardiovasc Imaging, 2009. **2**(5): p. 382-90.
59. Attili, A.K., et al., *Quantification in cardiac MRI: advances in image acquisition and processing.* International Journal of Cardiovascular Imaging, 2010. **26**: p. 27-40.

60. Harrild, D.M., et al., *Comparison of cardiac MRI tissue tracking and myocardial tagging for assessment of regional ventricular strain.* Int J Cardiovasc Imaging, 2012. **28**(8): p. 2009-18.
61. Heermann, P., et al., *Biventricular myocardial strain analysis in patients with arrhythmogenic right ventricular cardiomyopathy (ARVC) using cardiovascular magnetic resonance feature tracking.* Journal of Cardiovascular Magnetic Resonance, 2014. **16**(1).
62. Heiberg, J., et al., *Structural and functional alterations of the right ventricle are common in adults operated for ventricular septal defect as toddlers.* European Heart Journal-Cardiovascular Imaging, 2015. **16**(5): p. 483-489.
63. Ceelen, F., et al., *Effect of atrial fibrillation ablation on myocardial function: insights from cardiac magnetic resonance feature tracking analysis.* International Journal of Cardiovascular Imaging, 2013. **29**(8): p. 1807-1817.
64. Charles, R., et al., *CMR left atrial characterization in Cushing's syndrome: A feature tracking study.* Journal of Cardiovascular Magnetic Resonance, 2015. **17**.
65. Ciuffo, L.A., et al., *Assessment of left atrial systolic dyssynchrony in paroxysmal atrial fibrillation and heart failure using cardiac magnetic resonance imaging: MESA study.* Journal of Cardiovascular Magnetic Resonance, 2015. **17**.
66. Evin, M., et al., *Left atrium dysfunction by CMR in aortic valve stenosis.* Journal of Cardiovascular Magnetic Resonance, 2015. **17**.
67. Habibi, M., et al., *Association of CMR-measured la function with heart failure development: Results from the MESA study.* JACC: Cardiovascular Imaging, 2014. **7**(6): p. 570-579.
68. Habibi, M., et al., *Association of left atrial function and left atrial enhancement in patients with atrial fibrillation: cardiac magnetic resonance study.* Circ Cardiovasc Imaging, 2015. **8**(2): p. e002769.
69. Imai, M., et al., *Multi-ethnic study of atherosclerosis: Association between left atrial function using tissue tracking from cine mr imaging and myocardial fibrosis.* Radiology, 2014. **273**(3): p. 703-713.
70. Imai, M., et al., *Association between left atrial function using multimodality tissue tracking from cine MRI and myocardial scar in the multi-ethnic study of atherosclerosis (MESA).* Journal of Cardiovascular Magnetic Resonance, 2013. **15**: p. 413.
71. Kowallick, J.T., et al., *Quantification of left atrial strain and strain rate using cardiovascular magnetic resonance myocardial feature tracking.* Journal of Cardiovascular Magnetic Resonance, 2015. **17**.
72. Kowallick, J.T., et al., *Quantification of left atrial strain and strain rate using Cardiovascular Magnetic Resonance myocardial feature tracking: A feasibility study.* Journal of Cardiovascular Magnetic Resonance, 2014. **16**(1).
73. Kowallick, J.T., et al., *Quantification of atrial dynamics using cardiovascular magnetic resonance: Inter-study reproducibility.* Journal of Cardiovascular Magnetic Resonance, 2015.
74. Kutty, S., et al., *Abnormal right atrial performance in surgically repaired tetralogy of fallot: German competence network for congenital heart defects*

investigators. Journal of the American College of Cardiology, 2015. **65**(10): p. A1292.
75. Raissuni, Z., et al., *Functional left atrial CMR parameters are early predictors of left atrial alterations in hypertension and strongly associated with lv remodeling.* Journal of Cardiovascular Magnetic Resonance, 2015. **17**.
76. Shang, Q., et al., *Assessment of ventriculo-vascular properties in repaired coarctation using cardiac MRI derived aortic, left atrial and left ventricular strain.* Journal of the American College of Cardiology, 2015. **65**(10): p. A1291.
77. Smith, K., et al., *Cardiac MRI strain analysis demonstrates systemic right ventricular dysfunction late after atrial switch procedure despite normal ejection fraction.* Journal of Cardiovascular Magnetic Resonance, 2010. **12**: p. 99-100.
78. Zareian, M., et al., *Left atrial structure and functional quantitation using cardiovascular magnetic resonance and multimodality tissue tracking: Validation and reproducibility assessment.* Journal of Cardiovascular Magnetic Resonance, 2015.
79. Sado, D., et al., *Equilibrium contrast cardiovascular magnetic resonance shows increased interstitial expansion in the systemic right ventricle of adults late after Mustard or Senning surgery for transposition of the great arteries.* Journal of Cardiovascular Magnetic Resonance, 2012. **14**(S1): p. O58.
80. Poindron, V., et al. *T1 mapping cardiac magnetic resonance imaging frequently detects subclinical diffuse myocardial fibrosis in systemic sclerosis patients*. in *Seminars in arthritis and rheumatism*. 2019. Elsevier.
81. Diao, K.-y., et al., *Histologic validation of myocardial fibrosis measured by T1 mapping: a systematic review and meta-analysis.* Journal of Cardiovascular Magnetic Resonance, 2017. **18**(1): p. 92.
82. Ferreira, V.M., et al., *T(1) mapping for the diagnosis of acute myocarditis using CMR: comparison to T2-weighted and late gadolinium enhanced imaging.* JACC Cardiovasc Imaging, 2013. **6**(10): p. 1048-58.
83. Chin, C.W.L., et al., *High-sensitivity troponin i concentrations are a marker of an advanced hypertrophic response and adverse outcomes in patients with aortic stenosis.* European Heart Journal, 2014. **35**(34): p. 2312-2321.
84. Dabir, D., et al., *Age-gender normal values of native and post-contrast myocardial T1 relaxation times (lambda) on 1.5T and 3T using MOLLI: A multicenter, single vendor cardiovascular magnetic resonance study.* Journal of Cardiovascular Magnetic Resonance, 2014. **16**.
85. Piechnik, S.K., et al., *Normal variation of magnetic resonance T1 relaxation times in the human population at 1.5 T using ShMOLLI.* J Cardiovasc Magn Reson, 2013. **15**: p. 13.
86. Sado, D.M., et al., *Identification and assessment of anderson-fabry disease by cardiovascular magnetic resonance noncontrast myocardial T1 mapping.* Circulation: Cardiovascular Imaging, 2013. **6**(3): p. 392-398.
87. Bull, S.C., et al., *Myocardial perfusion, strain and pre-contrast T1 values in moderate asymptomatic aortic stenosis.* Heart, 2013. **99**: p. A89.
88. Banypersad, S.M., et al., *T1 mapping and survival in systemic light-chain amyloidosis.* Eur Heart J, 2015. **36**(4): p. 244-51.

89. Dass, S., et al., *Myocardial tissue characterization using magnetic resonance noncontrast T1 mapping in hypertrophic and dilated cardiomyopathy.* Circulation: Cardiovascular Imaging, 2012. **5**(6): p. 726-733.
90. Edwards, N.C., et al., *Diffuse left ventricular interstitial fibrosis is associated with sub-clinical myocardial dysfunction in Alström Syndrome: An observational study.* Orphanet Journal of Rare Diseases, 2015. **10**(1).
91. Edwards, N.C., et al., *Quantification of left ventricular interstitial fibrosis in asymptomatic chronic primary degenerative mitral regurgitation.* Circulation: Cardiovascular Imaging, 2014. **7**(6): p. 946-953.
92. Florian, A., et al., *Myocardial fibrosis imaging based on T1-mapping and extracellular volume fraction (ECV) measurement in muscular dystrophy patients: diagnostic value compared with conventional late gadolinium enhancement (LGE) imaging.* Eur Heart J Cardiovasc Imaging, 2014. **15**(9): p. 1004-12.
93. Chen, Y.Y., et al., *Extracellular volume fraction in coronary chronic total occlusion patients.* International Journal of Cardiovascular Imaging, 2015. **31**(6): p. 1211-1221.
94. Chen, Z., et al., *Focal but not diffuse myocardial fibrosis burden quantification using cardiac magnetic resonance imaging predicts left ventricular reverse modeling following cardiac resynchronization therapy.* J Cardiovasc Electrophysiol, 2015.
95. Kim, B.K., et al., *Revised definition of predicted left ventricular mass using ambulatory blood pressure in healthy Korean adults.* Clinical hypertension, 2017. **23**(1): p. 8.
96. Puntmann, V.O., et al., *T1 Mapping in Characterizing Myocardial Disease: A Comprehensive Review.* Circ Res, 2016. **119**(2): p. 277-99.
97. Moon, J.C., et al., *Myocardial T1 mapping and extracellular volume quantification: a Society for Cardiovascular Magnetic Resonance (SCMR) and CMR Working Group of the European Society of Cardiology consensus statement.* J Cardiovasc Magn Reson, 2013. **15**: p. 92.
98. Moher, D., et al., *Preferred reporting items for systematic reviews and meta-analyses: the PRISMA statement.* Ann Intern Med, 2009. **151**(4): p. 264-9, W64.
99. Cohen, J., *Statistical power analysis for the behavioral sciences*. 2nd ed.. ed. 1988: Hillsdale, N.J. : L. Erlbaum Associates.
100. aus dem Siepen, F., et al., *T1 mapping in dilated cardiomyopathy with cardiac magnetic resonance: quantification of diffuse myocardial fibrosis and comparison with endomyocardial biopsy.* Eur Heart J Cardiovasc Imaging, 2015. **16**(2): p. 210-6.
101. Bull, S., et al., *Human non-contrast T1 values and correlation with histology in diffuse fibrosis.* Heart, 2013. **99**(13): p. 932-7.
102. Carrick, D., et al., *Pathophysiology of LV Remodeling in Survivors of STEMI Inflammation, Remote Myocardium, and Prognosis.* JACC: Cardiovascular Imaging, 2015. **8**(7): p. 779-789.

103. Chin, C.W.L., et al., *Optimization and comparison of myocardial T1 techniques at 3T in patients with aortic stenosis.* European Heart Journal Cardiovascular Imaging, 2014. **15**(5): p. 556-565.
104. Dabir, D., et al., *Reference values for healthy human myocardium using a T1 mapping methodology: results from the International T1 Multicenter cardiovascular magnetic resonance study.* J Cardiovasc Magn Reson, 2014. **16**: p. 69.
105. Doltra, A., et al., *Potential change of diffuse myocardial fibrosis in patients undergoing renal denervation: Preliminary results of a prospective cardiac magnetic resonance study.* European Heart Journal, 2014. **35**: p. 1190.
106. Edwards, N.C., et al., *Diffuse interstitial fibrosis and myocardial dysfunction in early chronic kidney disease.* Am J Cardiol, 2015. **115**(9): p. 1311-7.
107. Ertel, A., et al., *Increased myocardial extracellular volume in active idiopathic systemic capillary leak syndrome.* J Cardiovasc Magn Reson, 2015. **17**(1): p. 76.
108. Ferreira, V.M., et al., *Native T1-mapping displays the extent and non-ischemic patterns of injury in acute myocarditis without the need for contrast agents.* Journal of Cardiovascular Magnetic Resonance, 2014. **16**.
109. Ferreira, V.M., et al., *Non-contrast T1-mapping detects acute myocardial edema with high diagnostic accuracy: A comparison to T2-weighted cardiovascular magnetic resonance.* Journal of Cardiovascular Magnetic Resonance, 2012. **14**(1).
110. Fontana, M., et al., *Native T1 mapping in transthyretin amyloidosis.* JACC Cardiovasc Imaging, 2014. **7**(2): p. 157-65.
111. Fontana, M., et al., *Prognostic value of late gadolinium enhancement cardiovascular magnetic resonance in cardiac amyloidosis.* Circulation, 2015. **132**(16): p. 1570-1579.
112. Fontana, M., et al., *Comparison of T1 mapping techniques for ECV quantification. Histological validation and reproducibility of ShMOLLI versus multibreath-hold T1 quantification equilibrium contrast CMR.* J Cardiovasc Magn Reson, 2012. **14**: p. 88.
113. Hinojar, R., et al., *T1 Mapping in Discrimination of Hypertrophic Phenotypes: Hypertensive Heart Disease and Hypertrophic Cardiomyopathy: Findings From the International T1 Multicenter Cardiovascular Magnetic Resonance Study.* Circ Cardiovasc Imaging, 2015. **8**(12).
114. Hong, Y.J., et al., *Extracellular volume fraction in dilated cardiomyopathy patients without obvious late gadolinium enhancement: comparison with healthy control subjects.* Int J Cardiovasc Imaging, 2015. **31 Suppl 1**: p. 115-22.
115. Jellis, C., et al., *Association of imaging markers of myocardial fibrosis with metabolic and functional disturbances in early diabetic cardiomyopathy: A multi-modality study.* European Heart Journal, 2011. **32**: p. 505.
116. Jellis, C.L., et al., *Biomarker and imaging responses to spironolactone in subclinical diabetic cardiomyopathy.* Eur Heart J Cardiovasc Imaging, 2014. **15**(7): p. 776-86.

117. Karamitsos, T.D., et al., *Noncontrast T1 mapping for the diagnosis of cardiac amyloidosis.* JACC Cardiovasc Imaging, 2013. **6**(4): p. 488-97.
118. Kato, S., et al., *Left ventricular native T1 time and the risk of atrial fibrillation recurrence after pulmonary vein isolation in patients with paroxysmal atrial fibrillation.* International Journal of Cardiology, 2016. **203**: p. 848-854.
119. Kawel, N., et al., *T1 mapping of the myocardium: intra-individual assessment of post-contrast T1 time evolution and extracellular volume fraction at 3T for Gd-DTPA and Gd-BOPTA.* J Cardiovasc Magn Reson, 2012. **14**: p. 26.
120. Kawel-Boehm, N., et al., *In-vivo assessment of normal T1 values of the right-ventricular myocardium by cardiac MRI.* International Journal of Cardiovascular Imaging, 2014. **30**(2): p. 323-328.
121. Kellman, P., et al., *Extracellular volume fraction mapping in the myocardium, part 2: initial clinical experience.* J Cardiovasc Magn Reson, 2012. **14**: p. 64.
122. Kuruvilla, S., et al., *Increased extracellular volume and altered mechanics are associated with LVH in hypertensive heart disease, not hypertension alone.* JACC Cardiovasc Imaging, 2015. **8**(2): p. 172-80.
123. Lee, S.P., et al., *Assessment of diffuse myocardial fibrosis by using MR imaging in asymptomatic patients with aortic stenosis.* Radiology, 2015. **274**(2): p. 359-369.
124. Liu, C.Y., et al., *Reference values of myocardial structure, function, and tissue composition by cardiac magnetic resonance in healthy African-Americans at 3T and their relations to serologic and cardiovascular risk factors.* Am J Cardiol, 2014. **114**(5): p. 789-95.
125. Liu, S., et al., *Diffuse myocardial fibrosis evaluation using cardiac magnetic resonance T1 mapping: sample size considerations for clinical trials.* J Cardiovasc Magn Reson, 2012. **14**: p. 90.
126. Luetkens, J.A., et al., *Acute myocarditis: multiparametric cardiac MR imaging.* Radiology, 2014. **273**(2): p. 383-92.
127. Luetkens, J.A., et al., *Incremental value of quantitative CMR including parametric mapping for the diagnosis of acute myocarditis.* Eur Heart J Cardiovasc Imaging, 2016. **17**(2): p. 154-61.
128. Mordi, I., et al., *T1 and T2 mapping for early diagnosis of dilated non-ischaemic cardiomyopathy in middle-aged patients and differentiation from normal physiological adaptation.* Eur Heart J Cardiovasc Imaging, 2015.
129. Ntusi, N.A.B., et al., *Diffuse myocardial fibrosis and inflammation in rheumatoid arthritis: Insights from CMR T1 Mapping.* JACC: Cardiovascular Imaging, 2015. **8**(5): p. 526-536.
130. Puntmann, V.O., et al., *Native myocardial T1 mapping by cardiovascular magnetic resonance imaging in subclinical cardiomyopathy in patients with systemic lupus erythematosus.* Circulation: Cardiovascular Imaging, 2013. **6**(2): p. 295-301.
131. Puntmann, V.O., et al., *Aortic stiffness and interstitial myocardial fibrosis by native t1 are independently associated with left ventricular remodeling in patients with dilated cardiomyopathy.* Hypertension, 2014. **64**(4): p. 762-768.

132. Puntmann, V.O., et al., *Native T1 mapping in differentiation of normal myocardium from diffuse disease in hypertrophic and dilated cardiomyopathy.* JACC Cardiovasc Imaging, 2013. **6**(4): p. 475-84.
133. Reiter, U., et al., *Normal diastolic and systolic myocardial T1 values at 1.5-T MR imaging: Correlations and blood normalization.* Radiology, 2014. **271**(2): p. 365-372.
134. Sado, D.M., et al., *Noncontrast myocardial T<inf>1</inf> mapping using cardiovascular magnetic resonance for iron overload.* Journal of Magnetic Resonance Imaging, 2015. **41**(6): p. 1505-1511.
135. Singh, A., et al., *Myocardial T1 and extracellular volume fraction measurement in asymptomatic patients with aortic stenosis: reproducibility and comparison with age-matched controls.* Eur Heart J Cardiovasc Imaging, 2015. **16**(7): p. 763-70.
136. Soslow, J.H., et al., *Increased myocardial native T1 and extracellular volume in patients with Duchenne muscular dystrophy.* J Cardiovasc Magn Reson, 2016. **18**(1): p. 5.
137. Tessa, C., et al., *Myocardial T1 and T2 mapping in diastolic and systolic phase.* International Journal of Cardiovascular Imaging, 2015. **31**(5): p. 1001-1010.
138. Treibel, T.A., et al., *Extracellular volume quantification in isolated hypertension - changes at the detectable limits?* J Cardiovasc Magn Reson, 2015. **17**(1): p. 74.
139. van Ooij, P., et al., *4D flow MRI and T1 -Mapping: Assessment of altered cardiac hemodynamics and extracellular volume fraction in hypertrophic cardiomyopathy.* J Magn Reson Imaging, 2016. **43**(1): p. 107-14.
140. von Knobelsdorff-Brenkenhoff, F., et al., *Myocardial T1 and T2 mapping at 3 T: reference values, influencing factors and implications.* J Cardiovasc Magn Reson, 2013. **15**: p. 53.
141. Zhang, Y., et al., *Myocardial T2 mapping by cardiovascular magnetic resonance reveals subclinical myocardial inflammation in patients with systemic lupus erythematosus.* International Journal of Cardiovascular Imaging, 2015. **31**(2): p. 389-397.
142. Azarisman, S.M., et al., *Characterisation of Myocardial Injury via T1 Mapping in Early Reperfused Myocardial Infarction and its Relationship with Global and Regional Diastolic Dysfunction.* Heart Lung Circ, 2016. **25**(11): p. 1094-1106.
143. Chin, C.W., et al., *Myocardial Fibrosis and Cardiac Decompensation in Aortic Stenosis.* JACC Cardiovasc Imaging, 2016.
144. Claridge, S., et al., *Substrate-dependent risk stratification for implantable cardioverter defibrillator therapies using cardiac magnetic resonance imaging: The importance of T1 mapping in nonischemic patients.* J Cardiovasc Electrophysiol, 2017. **28**(7): p. 785-795.
145. Duca, F., et al., *Interstitial Fibrosis, Functional Status, and Outcomes in Heart Failure With Preserved Ejection Fraction: Insights From a Prospective Cardiac Magnetic Resonance Imaging Study.* Circ Cardiovasc Imaging, 2016. **9**(12).

146. Gallego-Delgado, M., et al., *Extracellular Volume Detects Amyloidotic Cardiomyopathy and Correlates With Neurological Impairment in Transthyretin-familial Amyloidosis.* Rev Esp Cardiol (Engl Ed), 2016. **69**(10): p. 923-930.
147. Gao, X., et al., *Native Magnetic Resonance T1-Mapping Identifies Diffuse Myocardial Injury in Hypothyroidism.* PLoS One, 2016. **11**(3): p. e0151266.
148. Gormeli, C.A., et al., *The evaluation of non-ischemic dilated cardiomyopathy with T1 mapping and ECV methods using 3T cardiac MRI.* Radiol Med, 2017. **122**(2): p. 106-112.
149. Homsi, R., et al., *Left Ventricular Myocardial Fibrosis, Atrophy, and Impaired Contractility in Patients With Pulmonary Arterial Hypertension and a Preserved Left Ventricular Function: A Cardiac Magnetic Resonance Study.* J Thorac Imaging, 2017. **32**(1): p. 36-42.
150. Inui, K., et al., *Superiority of the extracellular volume fraction over the myocardial T1 value for the assessment of myocardial fibrosis in patients with non-ischemic cardiomyopathy.* Magnetic Resonance Imaging, 2016. **34**(8): p. 1141-1145.
151. Luetkens, J.A., et al., *Feature-tracking myocardial strain analysis in acute myocarditis: diagnostic value and association with myocardial oedema.* Eur Radiol, 2017.
152. Mahmod, M., et al., *Adenosine stress native T1 mapping in severe aortic stenosis: evidence for a role of the intravascular compartment on myocardial T1 values.* Journal of cardiovascular magnetic resonance : official journal of the Society for Cardiovascular Magnetic Resonance, 2014. **16**: p. 92.
153. Mazurkiewicz, L., et al., *Biventricular mechanics in prediction of severe myocardial fibrosis in patients with dilated cardiomyopathy: CMR study.* Eur J Radiol, 2017. **91**: p. 71-81.
154. Mordi, I.R., et al., *Comprehensive Echocardiographic and Cardiac Magnetic Resonance Evaluation Differentiates Among Heart Failure With Preserved Ejection Fraction Patients, Hypertensive Patients, and Healthy Control Subjects.* JACC Cardiovasc Imaging, 2017.
155. Nakamori, S., et al., *Native T1 Mapping and Extracellular Volume Mapping for the Assessment of Diffuse Myocardial Fibrosis in Dilated Cardiomyopathy.* JACC Cardiovasc Imaging, 2017.
156. Rodrigues, J.C., et al., *ECG strain pattern in hypertension is associated with myocardial cellular expansion and diffuse interstitial fibrosis: a multi-parametric cardiac magnetic resonance study.* Eur Heart J Cardiovasc Imaging, 2017. **18**(4): p. 441-450.
157. Rutherford, E., et al., *Defining myocardial tissue abnormalities in end-stage renal failure with cardiac magnetic resonance imaging using native T1 mapping.* Kidney Int, 2016. **90**(4): p. 845-52.
158. Shang, Y., et al., *Assessment of Diabetic Cardiomyopathy by Cardiovascular Magnetic Resonance T1 Mapping: Correlation with Left-Ventricular Diastolic Dysfunction and Diabetic Duration.* J Diabetes Res, 2017. **2017**: p. 9584278.
159. Messroghli, D.R., et al., *Modified Look-Locker inversion recovery (MOLLI) for high-resolution T1 mapping of the heart.* Magnetic Resonance in Medicine: An

Official Journal of the International Society for Magnetic Resonance in Medicine, 2004. **52**(1): p. 141-146.
160. McDiarmid, A.K., et al., *The effect of changes to MOLLI scheme on T1 mapping and extra cellular volume calculation in healthy volunteers with 3 tesla cardiovascular magnetic resonance imaging.* Quantitative Imaging in Medicine and Surgery, 2015. **5**(4): p. 503-510.
161. Brant, W.E. and C.A. Helms, *Fundamentals of diagnostic radiology*. 2012: Lippincott Williams & Wilkins.
162. Luetkens, J.A., et al., *Feature-tracking myocardial strain analysis in acute myocarditis: diagnostic value and association with myocardial oedema.* Eur Radiol, 2017. **27**(11): p. 4661-4671.
163. Nakamori, S., et al., *Native T1 Mapping and Extracellular Volume Mapping for the Assessment of Diffuse Myocardial Fibrosis in Dilated Cardiomyopathy.* JACC Cardiovasc Imaging, 2018. **11**(1): p. 48-59.
164. Inui, K., et al., *Superiority of the extracellular volume fraction over the myocardial T1 value for the assessment of myocardial fibrosis in patients with non-ischemic cardiomyopathy.* Magn Reson Imaging, 2016. **34**(8): p. 1141-5.
165. Negishi, K., et al., *Independent and incremental value of deformation indices for prediction of trastuzumab-induced cardiotoxicity.* J Am Soc Echocardiogr, 2013. **26**(5): p. 493-8.
166. Negishi, K., et al., *Use of speckle strain to assess left ventricular responses to cardiotoxic chemotherapy and cardioprotection.* Eur Heart J Cardiovasc Imaging, 2014. **15**(3): p. 324-31.
167. Attili, A.K., et al., *Quantification in cardiac MRI: advances in image acquisition and processing.* Int J Cardiovasc Imaging, 2010. **26 Suppl 1**(S1): p. 27-40.
168. Harrild, D.M., et al., *Comparison of cardiac MRI tissue tracking and myocardial tagging for assessment of regional ventricular strain.* International Journal of Cardiovascular Imaging, 2012. **28**(8): p. 2009-2018.
169. Kempny, A., et al., *Quantification of biventricular myocardial function using cardiac magnetic resonance feature tracking, endocardial border delineation and echocardiographic speckle tracking in patients with repaired tetralogy of fallot and healthy controls.* Journal of Cardiovascular Magnetic Resonance, 2012: p. 32.
170. Morton, G., et al., *Inter-study reproducibility of cardiovascular magnetic resonance myocardial feature tracking.* Journal of Cardiovascular Magnetic Resonance, 2012. **14**(1).
171. Ohyama, Y., et al., *Comparison of strain measurement from multimodality tissue tracking with strain-encoding MRI and harmonic phase MRI in pulmonary hypertension.* International Journal of Cardiology, 2015. **182**: p. 342-348.
172. Padiyath, A., et al., *Echocardiography and cardiac magnetic resonance-based feature tracking in the assessment of myocardial mechanics in tetralogy of fallot: An intermodality comparison.* Echocardiography, 2013. **30**(2): p. 203-210.

173. Schuster, A., et al., *Cardiovascular magnetic resonance myocardial feature tracking detects quantitative wall motion during dobutamine stress.* Journal of Cardiovascular Magnetic Resonance, 2011. **13**(1).
174. Schuster, A., et al., *The intra-observer reproducibility of cardiovascular magnetic resonance myocardial feature tracking strain assessment is independent of field strength.* Journal of Cardiovascular Magnetic Resonance, 2013. **15**: p. 12.
175. Schuster, A., et al., *Cardiovascular magnetic resonance feature-tracking assessment of myocardial mechanics: Intervendor agreement and considerations regarding reproducibility.* Clinical Radiology, 2015.
176. Jeung, M.Y., et al., *Myocardial tagging with MR imaging: overview of normal and pathologic findings.* Radiographics, 2012. **32**(5): p. 1381-98.
177. Andre, F., et al., *Age- and gender-related normal left ventricular deformation assessed by cardiovascular magnetic resonance feature tracking.* Journal of Cardiovascular Magnetic Resonance, 2015. **17**(1).
178. Augustine, D., et al., *Global and regional left ventricular myocardial deformation measures by magnetic resonance feature tracking in healthy volunteers: Comparison with tagging and relevance of gender.* Journal of Cardiovascular Magnetic Resonance, 2013. **15**(1).
179. Moher, D., et al., *Preferred reporting items for systematic reviews and meta-analyses: the PRISMA Statement.* Open Med, 2009. **3**(3): p. e123-30.
180. Morton, G., et al., *Inter-study reproducibility of cardiovascular magnetic resonance myocardial feature tracking.* Journal of Cardiovascular Magnetic Resonance, 2012. **14**.
181. Schuster, A., et al., *Cardiovascular magnetic resonance feature-tracking assessment of myocardial mechanics: Intervendor agreement and considerations regarding reproducibility.* Clinical Radiology, 2015. **70**(9): p. 989-998.
182. Yingchoncharoen, T., et al., *Normal ranges of left ventricular strain: a meta-analysis.* Journal of the American Society of Echocardiography : official publication of the American Society of Echocardiography, 2013. **26**(2): p. 185-191.
183. Moody, W.E., et al., *Comparison of magnetic resonance feature tracking for systolic and diastolic strain and strain rate calculation with spatial modulation of magnetization imaging analysis.* Journal of Magnetic Resonance Imaging, 2015. **41**(4): p. 1000-1012.
184. Hor, K.N., et al., *Comparison of Magnetic Resonance Feature Tracking for Strain Calculation With Harmonic Phase Imaging Analysis.* JACC: Cardiovascular Imaging, 2010. **3**(2): p. 144-151.
185. Aletras, A.H., et al., *DENSE: displacement encoding with stimulated echoes in cardiac functional MRI.* J Magn Reson, 1999. **137**(1): p. 247-52.
186. Kim, D., et al., *Myocardial Tissue Tracking with Two-dimensional Cine Displacement-encoded MR Imaging: Development and Initial Evaluation.* Radiology, 2004. **230**(3): p. 862-871.
187. Mangion, K., et al., *Myocardial strain in healthy adults across a broad age range as revealed by cardiac magnetic resonance imaging at 1.5 and 3.0T:*

Associations of myocardial strain with myocardial region, age, and sex. J Magn Reson Imaging, 2016.
188. Osman, N.F., et al., *Imaging longitudinal cardiac strain on short-axis images using strain-encoded MRI.* Magnetic Resonance in Medicine, 2001. **46**(2): p. 324-334.
189. Yang, H., et al., *Improvement in Strain Concordance between Two Major Vendors after the Strain Standardization Initiative.* Journal of the American Society of Echocardiography, 2015. **28**(6): p. 642-+.
190. Li, P., et al., *Quantification of left ventricular mechanics using vector-velocity imaging, a novel feature tracking algorithm, applied to echocardiography and cardiac magnetic resonance imaging.* Chinese Medical Journal, 2012. **125**(15): p. 2719-2727.
191. Kutty, S., et al., *Reduced global longitudinal and radial strain with normal left ventricular ejection fraction late after effective repair of aortic coarctation - A CMR feature tracking study.* Journal of Cardiovascular Magnetic Resonance, 2012. **14**.
192. Orwat, S., et al., *Cardiac magnetic resonance feature tracking: A novel method of assessing myocardial strain. Comparison with echocardiographic speckle tracking in healthy volunteers and in patients with left ventricular hypertrophy.* Kardiologia Polska, 2014. **72**(4): p. 363-371.
193. Wu, L.N., et al., *Feature tracking compared with tissue tagging measurements of segmental strain by cardiovascular magnetic resonance.* Journal of Cardiovascular Magnetic Resonance, 2014. **16**.
194. Nucifora, G., et al., *Systolic and diastolic myocardial mechanics in hypertrophic cardiomyopathy and their link to the extent of hypertrophy, replacement fibrosis and interstitial fibrosis.* Int J Cardiovasc Imaging, 2015.
195. Taylor, R.J., et al., *Myocardial strain measurement with feature-tracking cardiovascular magnetic resonance: normal values.* Eur Heart J Cardiovasc Imaging, 2015. **16**(8): p. 871-81.
196. Orwat, S., et al., *Cardiac magnetic resonance feature tracking: a novel method to assess myocardial strain. Comparison with echocardiographic speckle tracking in healthy volunteers and in patients with left ventricular hypertrophy.* Kardiol Pol, 2014. **72**(4): p. 363-71.
197. Taylor, R.J., et al., *Myocardial strain measurement with feature-tracking cardiovascular magnetic resonance: Normal values.* European Heart Journal Cardiovascular Imaging, 2015. **16**(8): p. 871-881.
198. Neizel, M., et al., *Strain-encoded (SENC) magnetic resonance imaging to evaluate regional heterogeneity of myocardial strain in healthy volunteers: Comparison with conventional tagging.* Journal of Magnetic Resonance Imaging, 2009. **29**(1): p. 99-105.
199. Gupta, A., et al., *Effect of spironolactone on diastolic function in hypertensive left ventricular hypertrophy.* Journal of Human Hypertension, 2015. **29**(4): p. 241-246.
200. Doerner, J.M., et al., *Caffeine and taurine containing energy drink increases left ventricular contractility in healthy volunteers.* International Journal of Cardiovascular Imaging, 2015. **31**(3): p. 595-601.

201. Lawton, J.S., et al., *Magnetic resonance imaging detects significant sex differences in human myocardial strain.* BioMedical Engineering Online, 2011. **10**.
202. Moore, C.C., et al., *Three-dimensional systolic strain patterns in the normal human left ventricle: Characterization with tagged MR imaging.* Radiology, 2000. **214**(2): p. 453-466.
203. Ahmed, M.I., et al., *Relation of torsion and myocardial strains to LV ejection fraction in hypertension.* JACC: Cardiovascular Imaging, 2012. **5**(3): p. 273-281.
204. Wehner, G.J., et al., *2D cine DENSE with low encoding frequencies accurately quantifies cardiac mechanics with improved image characteristics.* Journal of Cardiovascular Magnetic Resonance, 2015. **17**(1).
205. Kar, J., et al., *Three-dimensional regional strain computation method with Displacement ENcoding with Stimulated Echoes (DENSE) in non-ischemic, non-valvular dilated cardiomyopathy patients and healthy subjects validated by tagged MRI.* Journal of Magnetic Resonance Imaging, 2015. **41**(2): p. 386-396.
206. Feng, L., et al., *Numerical and in vivo validation of fast cine displacement-encoded with stimulated echoes (DENSE) MRI for quantification of regional cardiac function.* Magnetic Resonance in Medicine, 2009. **62**(3): p. 682-690.
207. Young, A.A., et al., *Generalized spatiotemporal myocardial strain analysis for DENSE and SPAMM imaging.* Magnetic Resonance in Medicine, 2012. **67**(6): p. 1590-1599.
208. Sigfridsson, A., et al., *Single-breath-hold multiple-slice DENSE MRI.* Magnetic Resonance in Medicine, 2010. **63**(5): p. 1411-1414.
209. Hamdan, A., et al., *Strain-encoded MRI to evaluate normal left ventricular function and timing of contraction at 3.0 tesla.* Journal of Magnetic Resonance Imaging, 2009. **29**(4): p. 799-808.
210. Korosoglou, G., et al., *Real-time fast strain-encoded magnetic resonance imaging to evaluate regional myocardial function at 3.0 Tesla: Comparison to conventional tagging.* Journal of Magnetic Resonance Imaging, 2008. **27**(5): p. 1012-1018.
211. Korosoglou, G., et al., *Left ventricular diastolic function in type 2 diabetes mellitus is associated with myocardial triglyceride content but not with impaired myocardial perfusion reserve.* Journal of Magnetic Resonance Imaging, 2012. **35**(4): p. 804-811.
212. Youssef, A., et al., *Strain-encoding cardiovascular magnetic resonance for assessment of right-ventricular regional function.* Journal of Cardiovascular Magnetic Resonance, 2008. **10**(1).
213. Hamdan, A., et al., *Regional right ventricular function and timing of contraction in healthy volunteers evaluated by strain-encoded MRI.* Journal of Magnetic Resonance Imaging, 2008. **28**(6): p. 1379-1385.
214. Oyama-Manabe, N., et al., *The strain-encoded (SENC) MR imaging for detection of global right ventricular dysfunction in pulmonary hypertension.* International Journal of Cardiovascular Imaging, 2013. **29**(2): p. 371-378.

215. Shehata, M.L., et al., *Real-time single-heartbeat fast strain-encoded imaging of right ventricular regional function: Normal versus chronic pulmonary hypertension.* Magnetic Resonance in Medicine, 2010. **64**(1): p. 98-106.
216. Borenstein, M., Hedges, L. V., Higgins, J. P. T. and Rothstein, H. R., *Introduction to Meta-Analysis*. 2009: John Wiley & Sons, Ltd.
217. Higgins, J.P., et al., *Measuring inconsistency in meta-analyses.* BMJ, 2003. **327**(7414): p. 557-60.
218. Sharman, J.E., et al., *Targeted LOWering of Central Blood Pressure in patients with hypertension: Baseline recruitment, rationale and design of a randomized controlled trial (The LOW CBP study).* Contemp Clin Trials, 2017. **62**: p. 37-42.
219. Cheng, S., et al., *Reproducibility of speckle-tracking-based strain measures of left ventricular function in a community-based study.* J Am Soc Echocardiogr, 2013. **26**(11): p. 1258-1266 e2.
220. Stanton, T., R. Leano, and T.H. Marwick, *Prediction of all-cause mortality from global longitudinal speckle strain: comparison with ejection fraction and wall motion scoring.* Circ Cardiovasc Imaging, 2009. **2**(5): p. 356-64.
221. Hung, C.L., et al., *Longitudinal and circumferential strain rate, left ventricular remodeling, and prognosis after myocardial infarction.* J Am Coll Cardiol, 2010. **56**(22): p. 1812-22.
222. Norisada, K., et al., *Myocardial contractile function in the region of the left ventricular pacing lead predicts the response to cardiac resynchronization therapy assessed by two-dimensional speckle tracking echocardiography.* J Am Soc Echocardiogr, 2010. **23**(2): p. 181-9.
223. Vo, H.Q., T.H. Marwick, and K. Negishi, *MRI-derived myocardial strain measures in normal subjects.* JACC: Cardiovascular Imaging, 2018. **11**(2): p. 196-205.
224. Serri, K., et al., *Global and regional myocardial function quantification by two-dimensional strain: application in hypertrophic cardiomyopathy.* Journal of the American College of Cardiology, 2006. **47**(6): p. 1175-1181.
225. Mavinkurve-Groothuis, A.M., et al., *Interobserver, intraobserver and intrapatient reliability scores of myocardial strain imaging with 2-d echocardiography in patients treated with anthracyclines.* Ultrasound in medicine & biology, 2009. **35**(4): p. 697-704.
226. Oxborough, D., K. George, and K.M. Birch, *Intraobserver reliability of two-dimensional ultrasound derived strain imaging in the assessment of the left ventricle, right ventricle, and left atrium of healthy human hearts.* Echocardiography, 2012. **29**(7): p. 793-802.
227. Rodríguez-Bailón, I., et al., *Left ventricular deformation and two-dimensional echocardiography: temporal and other parameter values in normal subjects.* Revista Española de Cardiología (English Edition), 2010. **63**(10): p. 1195-1199.
228. Serri, K., et al., *Global and regional myocardial function quantification by two-dimensional strain: application in hypertrophic cardiomyopathy.* J Am Coll Cardiol, 2006. **47**(6): p. 1175-81.

229. Schuster, A., et al., *The intra-observer reproducibility of cardiovascular magnetic resonance myocardial feature tracking strain assessment is independent of field strength.* European journal of radiology, 2013. **82**(2): p. 296-301.
230. Lang, R.M., et al., *Recommendations for cardiac chamber quantification by echocardiography in adults: an update from the American Society of Echocardiography and the European Association of Cardiovascular Imaging.* J Am Soc Echocardiogr, 2015. **28**(1): p. 1-39 e14.
231. Puntmann, V.O., et al., *Society for Cardiovascular Magnetic Resonance (SCMR) expert consensus for CMR imaging endpoints in clinical research: part I - analytical validation and clinical qualification.* J Cardiovasc Magn Reson, 2018. **20**(1): p. 67.
232. Badano, L.P., et al., *Standardization of left atrial, right ventricular, and right atrial deformation imaging using two-dimensional speckle tracking echocardiography: a consensus document of the EACVI/ASE/Industry Task Force to standardize deformation imaging.* European Heart Journal-Cardiovascular Imaging, 2018. **19**(6): p. 591-600.
233. Onishi, T., et al., *Global longitudinal strain and global circumferential strain by speckle-tracking echocardiography and feature-tracking cardiac magnetic resonance imaging: comparison with left ventricular ejection fraction.* Journal of the American Society of Echocardiography, 2015. **28**(5): p. 587-596.
234. Schuster, A., et al., *Cardiovascular magnetic resonance feature-tracking assessment of myocardial mechanics: Intervendor agreement and considerations regarding reproducibility.* Clinical radiology, 2015. **70**(9): p. 989-998.
235. Singh, G.K., et al., *Accuracy and reproducibility of strain by speckle tracking in pediatric subjects with normal heart and single ventricular physiology: a two-dimensional speckle-tracking echocardiography and magnetic resonance imaging correlative study.* Journal of the American Society of Echocardiography, 2010. **23**(11): p. 1143-1152.
236. Sjøli, B., et al., *Diagnostic capability and reproducibility of strain by Doppler and by speckle tracking in patients with acute myocardial infarction.* JACC: Cardiovascular Imaging, 2009. **2**(1): p. 24-33.
237. Leischik, R., B. Dworrak, and K. Hensel, *Intraobserver and interobserver reproducibility for radial, circumferential and longitudinal strain echocardiography.* The open cardiovascular medicine journal, 2014. **8**: p. 102.
238. Schuster, A., et al., *Cardiovascular magnetic resonance myocardial feature tracking detects quantitative wall motion during dobutamine stress.* Journal of Cardiovascular Magnetic Resonance, 2011. **13**(1): p. 58.
239. Morton, G., et al., *Inter-study reproducibility of cardiovascular magnetic resonance myocardial feature tracking.* J Cardiovasc Magn Reson, 2012. **14**: p. 43.
240. Donal, E., et al., *Importance of ventricular longitudinal function in chronic heart failure.* European Journal of Echocardiography, 2011. **12**(8): p. 619-627.

241. Rausch, K., et al., *Reproducibility of global left atrial strain and strain rate between novice and expert using multi-vendor analysis software.* The international journal of cardiovascular imaging, 2018: p. 1-8.
242. Orwat, S., et al., *Cardiac magnetic resonance feature tracking–a novel method to assess myocardial strain: Comparison with echocardiographic speckle tracking in healthy volunteers and in patients with left ventricular hypertrophy.* Kardiologia Polska (Polish Heart Journal), 2014. **72**(4): p. 363-371.
243. Hor, K.N., et al., *Magnetic resonance derived myocardial strain assessment using feature tracking.* Journal of visualized experiments: JoVE, 2011(48).
244. Marwick, T.H., et al., *Recommendations on the use of echocardiography in adult hypertension: a report from the European Association of Cardiovascular Imaging (EACVI) and the American Society of Echocardiography (ASE)dagger.* Eur Heart J Cardiovasc Imaging, 2015. **16**(6): p. 577-605.
245. Puntmann, V.O., et al., *Society for Cardiovascular Magnetic Resonance (SCMR) expert consensus for CMR imaging endpoints in clinical research: part I-analytical validation and clinical qualification.* Journal of Cardiovascular Magnetic Resonance, 2018. **20**(1): p. 67.
246. Negishi, K., et al., *What is the primary source of discordance in strain measurement between vendors: imaging or analysis?* Ultrasound in medicine & biology, 2013. **39**(4): p. 714-720.
247. Negishi, K., et al., *Use of speckle strain to assess left ventricular responses to cardiotoxic chemotherapy and cardioprotection.* European Heart Journal–Cardiovascular Imaging, 2013. **15**(3): p. 324-331.
248. Pathan, F., et al., *Normal ranges of left atrial strain by speckle-tracking echocardiography: a systematic review and meta-analysis.* Journal of the American Society of Echocardiography, 2017. **30**(1): p. 59-70. e8.
249. Nesser, H.-J., et al., *Quantification of left ventricular volumes using three-dimensional echocardiographic speckle tracking: comparison with MRI.* European heart journal, 2009. **30**(13): p. 1565-1573.
250. Nishikage, T., et al., *Quantitative assessment of left ventricular volume and ejection fraction using two-dimensional speckle tracking echocardiography.* European Journal of Echocardiography, 2008. **10**(1): p. 82-88.
251. Bhan, A., et al., *High frequency speckle tracking echocardiography in the assessment of left ventricular function after murine myocardial infarction.* American Journal of Physiology-Heart and Circulatory Physiology, 2014.
252. Jacobs, L.D., et al., *Rapid online quantification of left ventricular volume from real-time three-dimensional echocardiographic data.* Eur Heart J, 2006. **27**(4): p. 460-8.
253. Meunier, J., *Tissue motion assessment from 3D echographic speckle tracking.* Phys Med Biol, 1998. **43**(5): p. 1241-54.
254. Chen, X., et al., *3-D correlation-based speckle tracking.* Ultrason Imaging, 2005. **27**(1): p. 21-36.
255. Di Bella, G., et al., *Semiautomatic quantification of left ventricular function by two-dimensional feature tracking imaging echocardiography. A comparison study with cardiac magnetic resonance imaging.* Echocardiography, 2010. **27**(7): p. 791-797.

256. Hoit, B.D. and M. Gabel, *Influence of left ventricular dysfunction on the role of atrial contraction: an echocardiographic-hemodynamic study in dogs.* J Am Coll Cardiol, 2000. **36**(5): p. 1713-9.
257. Couttenye, M.M., et al., *Relaxation properties of mammalian atrial muscle.* Circ Res, 1981. **48**(3): p. 352-6.
258. Suga, H., *Importance of atrial compliance in cardiac performance.* Circ Res, 1974. **35**(1): p. 39-43.
259. Thomas, L., et al., *Compensatory changes in atrial volumes with normal aging: is atrial enlargement inevitable?* Journal of the American College of Cardiology, 2002. **40**(9): p. 1630-1635.
260. Ramkumar, S., et al., *Association of the Active and Passive Components of Left Atrial Deformation with Left Ventricular Function.* J Am Soc Echocardiogr, 2017. **30**(7): p. 659-666.
261. Rosca, M., et al., *Left atrial function: pathophysiology, echocardiographic assessment, and clinical applications.* Heart, 2011. **97**(23): p. 1982-9.
262. Posina, K., et al., *Relationship of phasic left atrial volume and emptying function to left ventricular filling pressure: a cardiovascular magnetic resonance study.* J Cardiovasc Magn Reson, 2013. **15**: p. 99.
263. Rahimtoola, S.H., et al., *Chronic ischemic left ventricular dysfunction: from pathophysiology to imaging and its integration into clinical practice.* JACC: Cardiovascular Imaging, 2008. **1**(4): p. 536-555.
264. Cameli, M., et al., *Novel echocardiographic techniques to assess left atrial size, anatomy and function.* Cardiovasc Ultrasound, 2012. **10**: p. 4.
265. Vianna-Pinton, R., et al., *Two-dimensional speckle-tracking echocardiography of the left atrium: feasibility and regional contraction and relaxation differences in normal subjects.* J Am Soc Echocardiogr, 2009. **22**(3): p. 299-305.
266. Vo, H., T. Marwick, and K. Negishi, *MRI-Derived Myocardial Strain Measures in Normal Subjects.* JACC. Cardiovascular imaging, 2018. **11**(2 Pt 1): p. 196.
267. von Roeder, M., et al., *Influence of Left Atrial Function on Exercise Capacity and Left Ventricular Function in Patients With Heart Failure and Preserved Ejection Fraction.* Circ Cardiovasc Imaging, 2017. **10**(4).
268. Kuppahally, S.S., et al., *Left atrial strain and strain rate in patients with paroxysmal and persistent atrial fibrillation: relationship to left atrial structural remodeling detected by delayed enhancement-MRI.* Circulation: Cardiovascular Imaging, 2010: p. CIRCIMAGING. 109.865683.
269. Ersbøll, M., et al., *The prognostic value of left atrial peak reservoir strain in acute myocardial infarction is dependent on left ventricular longitudinal function and left atrial size.* Circulation: Cardiovascular Imaging, 2012: p. CIRCIMAGING. 112.978296.
270. Cameli, M., et al., *Feasibility and reference values of left atrial longitudinal strain imaging by two-dimensional speckle tracking.* Cardiovasc Ultrasound, 2009. **7**: p. 6.
271. Cameli, M., et al., *Left atrial strain: a new parameter for assessment of left ventricular filling pressure.* Heart Fail Rev, 2016. **21**(1): p. 65-76.

272. Greenberg, B., et al., *The influence of left ventricular filling pressure on atrial contribution to cardiac output.* Am Heart J, 1979. **98**(6): p. 742-51.
273. Kono, T., et al., *Left atrial contribution to ventricular filling during the course of evolving heart failure.* Circulation, 1992. **86**(4): p. 1317-22.
274. Rahimtoola, S.H., et al., *Left atrial transport function in myocardial infarction. Importance of its booster pump function.* Am J Med, 1975. **59**(5): p. 686-94.
275. Lang, R.M., et al., *Recommendations for cardiac chamber quantification by echocardiography in adults: an update from the American Society of Echocardiography and the European Association of Cardiovascular Imaging.* European Heart Journal-Cardiovascular Imaging, 2015. **16**(3): p. 233-271.
276. Negishi, K., et al., *Practical guidance in echocardiographic assessment of global longitudinal strain.* JACC Cardiovasc Imaging, 2015. **8**(4): p. 489-492.
277. Cameli, M., et al., *Speckle tracking analysis: a new tool for left atrial function analysis in systemic hypertension: an overview.* J Cardiovasc Med (Hagerstown), 2016. **17**(5): p. 339-43.
278. Melenovsky, V., et al., *Cardiovascular features of heart failure with preserved ejection fraction versus nonfailing hypertensive left ventricular hypertrophy in the urban Baltimore community: the role of atrial remodeling/dysfunction.* Journal of the American College of Cardiology, 2007. **49**(2): p. 198-207.
279. Shao, C., et al., *Independent prognostic value of left atrial function by two-dimensional speckle tracking imaging in patients with non-ST-segment-elevation acute myocardial infarction.* BMC cardiovascular disorders, 2015. **15**(1): p. 145.
280. Kurt, M., et al., *Left atrial function in diastolic heart failure.* Circ Cardiovasc Imaging, 2009. **2**(1): p. 10-5.
281. Morris, D.A., et al., *Left atrial systolic and diastolic dysfunction in heart failure with normal left ventricular ejection fraction.* Journal of the American Society of Echocardiography, 2011. **24**(6): p. 651-662.
282. Ribeiras, R., *Left atrial function and left ventricular diastolic dysfunction-Just the marionette and its master?* Revista portuguesa de cardiologia: orgao oficial da Sociedade Portuguesa de Cardiologia= Portuguese journal of cardiology: an official journal of the Portuguese Society of Cardiology, 2018. **37**(10): p. 831.
283. Pathan, F., et al., *Use of Atrial Strain to Predict Atrial Fibrillation After Cerebral Ischemia.* JACC Cardiovasc Imaging, 2018. **11**(11): p. 1557-1565.
284. Negishi, K., et al., *Role of temporal resolution in selection of the appropriate strain technique for evaluation of subclinical myocardial dysfunction.* Echocardiography, 2012. **29**(3): p. 334-9.
285. Ezzati, M., et al., *Selected major risk factors and global and regional burden of disease.* Lancet, 2002. **360**(9343): p. 1347-60.
286. Drawz, P.E., M. Abdalla, and M. Rahman, *Blood pressure measurement: clinic, home, ambulatory, and beyond.* Am J Kidney Dis, 2012. **60**(3): p. 449-62.
287. Ogihara, T., et al., *The Japanese Society of Hypertension Guidelines for the Management of Hypertension (JSH 2009).* Hypertens Res, 2009. **32**(1): p. 3-107.

288. Wijkman, M., et al., *Ambulatory systolic blood pressure predicts left ventricular mass in type 2 diabetes, independent of central systolic blood pressure.* Blood Press Monit, 2012. **17**(4): p. 139-44.
289. Weber, T., et al., *Relationship Between 24-Hour Ambulatory Central Systolic Blood Pressure and Left Ventricular Mass: A Prospective Multicenter Study.* Hypertension, 2017. **70**(6): p. 1157-1164.
290. Lim, P.O., P.T. Donnan, and T.M. MacDonald, *Blood pressure determinants of left ventricular wall thickness and mass index in hypertension: comparing office, ambulatory and exercise blood pressures.* J Hum Hypertens, 2001. **15**(9): p. 627-33.
291. Zhang, Y., et al., *Association of left ventricular diastolic dysfunction with 24-h aortic ambulatory blood pressure: the SAFAR study.* Journal of human hypertension, 2015. **29**(7): p. 442.
292. Kim, D., et al., *Impact of ambulatory blood pressure on early cardiac and renal dysfunction in hypertensive patients without clinically apparent target organ damage.* Yonsei medical journal, 2018. **59**(2): p. 265-272.
293. Khattar, R.S., et al., *Effect of aging on the prognostic significance of ambulatory systolic, diastolic, and pulse pressure in essential hypertension.* Circulation, 2001. **104**(7): p. 783-789.
294. Kannel, W.B., T. Gordon, and M.J. Schwartz, *Systolic versus diastolic blood pressure and risk of coronary heart disease. The Framingham study.* Am J Cardiol, 1971. **27**(4): p. 335-46.
295. Khattar, R.S., et al., *Effect of aging on the prognostic significance of ambulatory systolic, diastolic, and pulse pressure in essential hypertension.* Circulation, 2001. **104**(7): p. 783-9.
296. Franklin, S.S., et al., *Hemodynamic patterns of age-related changes in blood pressure. The Framingham Heart Study.* Circulation, 1997. **96**(1): p. 308-15.
297. Banegas, J.R., et al., *Relationship between clinic and ambulatory blood-pressure measurements and mortality.* New England Journal of Medicine, 2018. **378**(16): p. 1509-1520.
298. Shen, J., et al., *Comparison of ambulatory blood pressure and clinic blood pressure in relation to cardiovascular diseases in diabetic patients.* Medicine (Baltimore), 2017. **96**(33): p. e7807.
299. Fagard, R.H. and H. Celis, *Prognostic significance of various characteristics of out-of-the-office blood pressure.* Journal of hypertension, 2004. **22**(9): p. 1663-1666.
300. Boggia, J., et al., *Prognostic accuracy of day versus night ambulatory blood pressure: a cohort study.* Lancet, 2007. **370**(9594): p. 1219-29.
301. Pontremoli, R., et al., *Microalbuminuria is an early marker of target organ damage in essential hypertension.* American journal of hypertension, 1998. **11**(4): p. 430-438.
302. Diao, K.Y., et al., *Histologic validation of myocardial fibrosis measured by T1 mapping: a systematic review and meta-analysis.* J Cardiovasc Magn Reson, 2016. **18**(1): p. 92.
303. Amzulescu, M.S., et al., *Head-to-Head Comparison of Global and Regional Two-Dimensional Speckle Tracking Strain Versus Cardiac Magnetic*

Resonance Tagging in a Multicenter Validation Study. Circ Cardiovasc Imaging, 2017. **10**(11).
304. Hodzic, A., et al., *Accuracy of speckle tracking in the context of stress echocardiography in short axis view: An in vitro validation study.* PLoS One, 2018. **13**(3): p. e0193805.